

# **NITROGEN CYCLING IN COASTAL PERMEABLE SEDIMENTS FROM EUTROPHIED REGIONS**



**Hannah Marchant**



# **Nitrogen cycling in coastal permeable sediments from eutrophied regions**

**Dissertation**

Zur Erlangung des Grades eines  
Doktors der Naturwissenschaften - Dr. rer. nat. -

dem Fachbereich Geowissenschaften  
der Universität Bremen

**Hannah Marchant**

**Bremen, December 2013**

Die vorliegende Arbeit wurde in der Zeit von March 2010 bis December 2013 am Max Planck Institut für Marine Mikrobiologie in Bremen angefertigt.

1. Gutachter: Prof Dr. Marcel M.M. Kuypers
2. Gutachter: PD Dr. Christian Winter

Datum des Promotionskolloquiums: 27 März 2014

# Contents

<b>Summary</b>	<b>1</b>
<b>Zusammenfassung</b>	<b>3</b>
<b>Chapter I</b>	<b>5</b>
General Introduction	5
Aims and Outline	30
<b>Chapter II</b>	<b>43</b>
Anammox, denitrification and dissimilatory nitrate reduction to ammonium in the East China Sea sediment	
<b>Chapter III</b>	<b>87</b>
The fate of nitrate in intertidal permeable sediments	
<b>Chapter IV</b>	<b>115</b>
N-loss due to coupled nitrification-denitrification in subtidal permeable sediments	
<b>Chapter V</b>	<b>155</b>
Stimulation and inhibition of aerobic denitrification in intertidal permeable sediments	
<b>Chapter VI</b>	<b>173</b>
High nitrous oxide emissions from eutrophied coastal sands	
<b>Chapter VII</b>	<b>215</b>
The impact of ocean acidification on nitrogen cycling in coastal permeable sediments	
<b>Chapter VIII</b>	<b>235</b>
Going with the flow: Why we cannot neglect the importance of the coastal sand filter in the anthropocene	
<b>Chapter IX – Outlook</b>	<b>261</b>
<b>List of publications</b>	<b>271</b>
<b>Acknowledgements</b>	<b>273</b>



## Summary

Coastal seas and the biogeochemical transformations that take place within them, have the potential to buffer the ocean from anthropogenic pollution such as fixed nitrogen (N). The benthos in most coastal zones is comprised of sandy permeable sediments, however, for many years these sediments were neglected in studies of benthic N-transformations - as they were assumed to be a desert in terms of microbial activity. In fact, advective flows, driven by water movement across sediment topography, enhance the supply of oxygen, organic nutrients and inorganic nutrients such as nitrate into permeable sediments. These flows render permeable sediments hotspots of microbial activity and turnover.

The aim of this thesis was to describe and quantify N-cycling processes and their interactions within permeable coastal sediments in eutrophied regions. Denitrification, the reduction of nitrate to dinitrogen gas, removes fixed nitrogen from permeable sediments and thus plays a crucial role in mediating the harmful effects of eutrophication. Despite the importance of denitrification, so far little is known about how seasonal conditions and physical parameters such as grain size control the extent of denitrification within permeable sediments. Even less is understood about how other processes such as dissimilatory nitrate reduction to ammonium and nitrification interact with denitrification to influence N-loss and N-recycling.

In this thesis, a novel, non-destructive, ex situ approach using  $^{15}\text{N}$ -labelled tracers, was taken to study nitrogen cycling processes. This approach allowed sampling at a high temporal resolution as well as comparison of multiple N-processes within the same sediment. Quantification of the fate of nitrate within intertidal permeable sediments over different seasons, revealed that only half of the nitrate uptake within the sediment is directly lost as  $\text{N}_2$ . Part of the nitrate is instead reduced to ammonium, while intracellular nitrate storage is responsible for the rest of nitrate uptake. Intracellular nitrate storage, mediated by eukaryotes, represented a so far neglected source of N-loss. These results are presented in Chapter III.

Anthropogenic nitrate inputs to coastal seas are not all consumed within the intertidal zone and therefore impact upon subtidal coastal regions such as the German Bight. In the German Bight, we observed high rates of nitrification and denitrification, and strongly coupled nitrification-denitrification. As a result of these processes most of the anthropogenic nitrate introduced in to the German Bight is removed, however high N-losses and high N-turnover are often masked in nutrient budgets. These results are presented in Chapter IV.

The dynamic conditions in permeable sediments are not just responsible for high N-losses, but create fluctuating redox and oxygen conditions. These fluctuations seem to create an environment in which denitrification – traditionally considered an anaerobic process – can occur in the presence of oxygen. In Chapter V, aerobic denitrification is shown to be stimulated within permeable sediments by frequent shifts in oxygen concentrations. Furthermore, when the sediment was not exposed to fluctuations in oxygen for longer time periods the capacity for aerobic denitrification was lost.

The occurrence of aerobic denitrification suggested emission of the potent greenhouse gas nitrous oxide ( $N_2O$ ) might be enhanced in permeable sediments, as nitrous oxide reductase, the enzyme catalyzing  $N_2O$  reduction to  $N_2$ , is highly sensitive to oxygen. In Chapter 6, permeable sediments were shown to be a substantial source of  $N_2O$ , with emissions driven by advective porewater transport, fluctuating oxygen concentrations and specialization of the microbial community. As permeable sediments play such an important role in nitrogen loss and  $N_2O$  emissions, their response to future climate change, namely ocean acidification, was investigated in Chapter 7. While denitrification rates did not change in response to a future, more acidified ocean, coupled nitrification-denitrification was enhanced in response to changing nitrate conditions in the water column, which could exacerbate the predicted changes in the future oceans N-inventory.

The work presented in this thesis highlights that coastal permeable sediments are not only sites of high prokaryotic denitrification rates, but are also hotspots of eukaryotic nitrate reduction, nitrification and  $N_2O$  emissions, all of which are driven by advective flows and the biocatalytic nature of these fascinating sands.



## Zusammenfassung

Biogeochemische Transformationen in Küstengewässern haben das Potential den Eintrag von anthropogenen Schadstoffen in die Ozeane zu puffern. Das Benthos besteht zum größten Teil aus permeablen Sedimenten. Diese sind seit vielen Jahren im Bezug auf benthische Stickstofftransformationen vernachlässigt worden, da sie als Wüsten im Bezug auf mikrobielle Aktivität angesehen wurden. Diese Sedimente werden durch advective Prozesse, unter anderem dem Durchströmen von Topographien, ständig mit Sauerstoff, sowie organischen und anorganischen Nährstoffen versorgt. Durch diesen dynamischen Prozess bilden permeable Sedimente Hotspots mikrobieller Aktivität.

Das Ziel der vorliegenden Arbeit ist die Quantifizierung der im Stickstoffkreislauf beinhalteten Prozesse und ihre Interaktion innerhalb permeabler küstennaher Sedimente in eutrophierten Regionen. Denitrifizierung, die Reduktion von Nitrat zu  $N_2$  gas, entfernt fixierten Stickstoff aus dem Kreislauf und reduziert die Effekte der Eutrophierung. Trotz der enormen Bedeutung der Denitrifizierung sind die saisonalen Effekte und der Einfluss von physikalischen Parametern, wie Korngröße, nur wenig untersucht. Weit weniger sind Zusammenhänge zwischen dissimilatorischer Nitrat-Reduktion zu Ammonium und Nitrifizierung mit Denitrifizierung verstanden, welche N-Verlust und N-Rezyklierung beeinflussen.

In dieser Arbeit wird ein neuer, nicht destruktiver, ex situ Ansatz mit  $^{15}N$ -Tracern vorgestellt und genutzt um die Prozesse des Stickstoffkreislaufes zu untersuchen. Dieser Ansatz ermöglicht sowohl eine hohe zeitliche Auflösung, als auch die Untersuchung verschiedener Stickstoffprozesse im selben Sediment. Dadurch wird die Quantifizierung von Nitratflüssen innerhalb intertidaler permeabler Sedimente über verschiedene saisonale Zeiträume ermöglicht. Nur die Hälfte der Nitrataufnahme geht direkt als  $N_2$  verloren. Nitrat wird außerdem zum Teil zu Ammonium reduziert, aber auch intrazellulär als Nitrat gespeichert. Die interzelluläre Nitrat-Speicherung wird vorwiegend von Eukaryoten geleistet und wurde bisher im Bezug auf die Berechnung des Stickstoffverlustes vernachlässigt. Die Resultate werden in Kapitel 3 vorgestellt.

Nicht der gesamte anthropogene Nitrateintrag wird innerhalb der intertidalen Zone konsumiert, sondern wirkt sich auf die gesamte Deutsche Bucht aus. Hier wurden

hohe Nitrifizierungs- und Denitrifizierungsraten gemessen, die eine starke Kopplung aufweisen. Auf diese Weise wird ein großer Teil der anthropogen eingebrachten Nitratverschmutzung der Deutschen Bucht entfernt. Diese Resultate sind in Kapitel V vorgestellt.

Die dynamischen Prozesse in permeablen Sedimenten sind nicht nur verantwortlich für hohe Stickstoffverluste, sondern erzeugen auch fluktuierende Redoxbedingungen. Diese Variationen erzeugen eine Umwelt in welcher Denitrifizierung – traditionell als anaerober Prozess gesehen – auch unter oxischen Bedingungen stattfinden kann. In Kapitel V wird gezeigt, dass dynamische Sauerstoffkonzentrationen aerobe Denitrifizierung stimulieren. Wenn das Sediment für länger Zeit unter konstanten, nicht fluktuierenden, Bedingungen gehalten wird, kann die Kapazität der aeroben Denitrifizierung durch die Sedimentgemeinschaft verloren gehen.

Die Anwesenheit aerober Denitrifizierung legt den Schluss nahe, dass Emissionen des potenten Treibhausgases Distickstoffmonoxid ( $N_2O$ ) in permeablen Sedimenten verstärkt werden. Die wechselnden Sauerstoffbedingungen beeinflussen die Stickstoffoxidreduktase, welche im hohem Maße sauerstoffempfindlich ist. In Kapitel 6 wird gezeigt, dass permeable Sedimente eine wesentliche  $N_2O$  Quelle sind, dessen Emission durch advektiven porenwasser Transport, fluktuierende Sauerstoffkonzentrationen und Spezialisierung von mikrobiellen Gemeinschaften getrieben wird. Da permeable Sedimente eine solch wichtige Rolle für den Stickstoffverlust und  $N_2O$  Emission spielen, wird der Einfluss des erwarteten Klimawandels, insbesondere der Ozeanversauerung, in Kapitel 7 behandelt. Die Ozeanversauerung wirkt sich zunächst nicht auf die Denitrifizierungsraten aus. Gekoppelte Nitrifizierungs-Denitrifizierungsprozesse werden allerdings durch sich ändernde Nitrat Bedingungen in der Wassersäule verstärkt. Dies könnte die Vorhersage des zukünftigen globalen Stickstoffhaushaltes erschweren.

Diese Arbeit zeigt das küstennahe permeable Sedimente nicht nur Bereiche hoher prokaryotische Denitrifizierung sind, sondern auch Hotspots der eukaryotischen Nitrat reduzierung, Nitrifizierung und  $N_2O$  Emission. All diese Prozesse werden von advektiven Strömungen durch das Sediment und die biokatalytische Natur dieser faszinierenden Sande getrieben.

# Chapter I

## Introduction

*“it is of universal significance for the improvement of human*

*nutrition and so of the greatest benefit to mankind”*

Presentation speech awarding Fritz Haber the Nobel Prize in Chemistry for the synthesis of ammonia from its elements

Man’s ability to synthesise inert N<sub>2</sub> gas into ammonia has radically shaped the world that we live in. The resultant increase in crop production that is supported by anthropogenically sourced reactive nitrogen (N)<sup>\*</sup> is responsible for feeding at least two fifths of the human population (Smil, 2001). However, it is not just fields which we are fertilizing, but the natural ecosystem itself, and the advent of the anthropocene has arguably perturbed the nitrogen cycle more than any other biogeochemical cycle. As early as 1970, Delwiche argued that “of all man’s recent interventions in the cycles of nature, the industrial fixation of nitrogen far exceeds all the others in magnitude”. The consequences of anthropogenic nitrogen fixation include eutrophication, stratospheric ozone loss and global acidification (Gruber and Galloway et al., 2008).

The perturbation is complex and the effect of the ‘nitrogen cascade’ links changes in nitrogen cycling intimately with other element cycles, creating a series of reactions. One atom of nitrogen can for example, sequentially increase atmospheric O<sub>3</sub>, increase fine particulate matter, alter forest productivity and lead to acidification of surface waters, coastal eutrophication and increased N<sub>2</sub>O production; which increases the greenhouse potential of the atmosphere (Galloway et al., 2003). Therefore in the light of increasing N loads, understanding the nitrogen cycle and in particular the loss of 003; Jensen et al., 2008; Holtappels, 2011; Sokoll et al., 2012)**1. Eutrophication of**

---

<sup>\*</sup> *Reactive Nitrogen (N)*

N is a term which spans broad definitions within the literature, as used by the atmospheric chemistry community it refers to all N-O combinations except N<sub>2</sub>O, for example NO<sub>x</sub>, N<sub>2</sub>O<sub>5</sub>, HNO<sub>2</sub>, HNO<sub>3</sub>, and nitrates including organic and halogen nitrates. Generally in literature focused on the biogeochemistry of the nitrogen cycle it includes inorganic reduced and oxidized forms of N and organic compounds such as urea, amines and proteins e.g. all biologically, photochemically and radiatively active N compounds.

### ***1. Eutrophication of coastal seas – The Wadden Sea and East China Sea as examples***

The marine realms most affected by anthropogenic nitrogen fertilization are coastal seas, which act as a buffer between the land and the open oceans. Since the 1860's anthropogenic N creation has increased from 16 to 156 Tg N yr<sup>-1</sup>. Concurrent rises have occurred in N inputs to coastal seas; N from riverine and land drainage has almost doubled (from 28.4 to 48 Tg N yr<sup>-1</sup>) and N inputs from atmospheric deposition have risen 6-fold (from 1.4 to 8 Tg N yr<sup>-1</sup>) (Galloway et al., 2004).

Nitrogen, which has historically been the limiting nutrient in coastal marine ecosystems, is now considered to be their biggest pollution problem (Vitousek et al., 1997), causing environmental problems ranging from eutrophication to shifts in biodiversity and habitat degradation (Rabalais, 2002). Furthermore, enhanced algal blooms result in the accumulation of particulate organic matter in bottom waters, which enhances microbial activity and consequently increases consumption of dissolved oxygen. This results in hypoxic and anoxic zones in bottom waters, especially in semi-enclosed basins such as the Gulf of Mexico, the Chesapeake Bay, Long Island Sound, Florida Bay, the Baltic Sea, the Adriatic Sea, and many other coastal areas (Diaz and Rosenberg, 1995; Diaz and Rosenberg, 2008).

The Wadden Sea is one such eutrophied coastal sea. Representing the largest tidal flat system in the temperate world, stretching along the Dutch, German and Danish North Sea coast (Reise et al., 2010), the Wadden acts as a catchment area for much of Northern Europe, covering some 230,000 km<sup>2</sup>; much of which is highly industrialized or agronomized and in which >100 million people live. N-loads from rivers such as the Rhine, Elbe, Weser and Ems dominate N-inputs into the Wadden, which are in the range of 640-820 kt N year<sup>-1</sup>. However the Wadden Sea was not always eutrophied; like many coastal seas since the industrial revolution, N loads from rivers have increased by a factor of eight and atmospheric N deposition has doubled (van Beusekom, 2005).



Fig. 1 Former seagrass fishery on the Dutch Coast. © Historische Vereniging Wieringen

This has changed the ecosystem beyond recognition. Today the Wadden Sea is dominated by structureless sand flats which are inhabited by green algae, polychaetes and invasive invertebrate species. Pelagic primary production now occurs primarily in the water column, at high rates throughout the year. During spring, pelagic primary production is dominated by intense diatom blooms, whereas between May and June primary production is characterized by longer, more stable *Phaeocystis* blooms (Loebl et al., 2007). The organic material produced by this primary production is quickly remineralized within the sandy sediments that cover the seafloor. Therefore, although for much of the year the water column may be autotrophic, the Wadden Sea is heterotrophic in nature (van Beusekom et al., 1999).

In the past, a complex 3D structured habitat existed in the Wadden Sea, in which seagrass was the main source of primary production (Fig. 1) and structure was provided by native oyster banks and reef forming polychaetes (Lotze et al., 2005). The decline of seagrass indicates poor ecosystem health, which can largely be attributed to the direct and indirect effects of eutrophication (Burkholder et al., 2007 and references therein).

The effects of eutrophication can also be seen in the coastal seas of China. The East China Sea (ECS), which is one of the largest continental shelves in the world, is fed by the Changjiang estuary, in which fixed nitrogen concentrations have risen exponentially since the 1960's, as a result of anthropogenic activities (Wang, 2006; Zhou et al., 2008). Eutrophication has therefore become a severe problem; increases in the standing stock of phytoplankton have occurred, as have observations of hypoxic events (although few reports have focused on the area). In fact, Chen et al. (2007), estimated that seasonal deoxygenation events might create one of the largest hypoxic areas in the world in the ECS. Coupled to enhanced primary productivity, there has been a decrease in the relative abundance of diatoms in the ECS, and a shift to a dinoflagellate dominated community, the result of which has been an increase in the occurrence and scale of harmful algal blooms (Zhou et al., 2008).

While coastal seas are increasingly affected by anthropogenic N inputs, concurrent rises have not been observed in the open oceans. The main source of anthropogenic N to open oceans is atmospheric deposition rather than riverine inputs (Galloway et al., 2004); in other words, based on nutrient measurements, N inputs from rivers, industrial and sewage wastes and groundwater do not reach the open oceans. This indicates that coastal seas act as a buffer, protecting the open ocean from the impact of anthropogenically derived N, mostly as a result of denitrification within coastal sediments (Gruber and Galloway, 2008). N-loss through denitrification also acts to mediate the effects of eutrophication within coastal seas themselves. Therefore to enable us to understand how coastal ecosystems function and will respond to continuing anthropogenic change, it is important to extend our knowledge of the balance, extent and controllers of N-cycling within coastal seas.

## ***2. Sandy sediments – biocatalysts for biogeochemical cycling***

Coarse grained relict sediments cover 58-70 % of the continental shelves (Emery, 1968); however, little is known about N-cycling within them. Most studies of benthic

sediments have focused on fine grained sediments. These muddy sediments are often rich in organic carbon and characterized by a stable redox zonation with depth, which is reflected in the composition and function of the microbial community (Jørgensen, 1977; Froelich et al., 1979; Sorensen et al., 1979; Canfield et al., 1993; Thamdrup et al., 1994). This zonation is a result of respiring microbes preferentially using the most thermodynamically favourable electron acceptors as they diffuse through the sediment (Sorensen and Jørgensen, 1987; Jørgensen and Revsbech, 1989). Electron acceptor limitation in sediments means that microbes first respire oxygen in the surface, followed by nitrate, manganese (IV), iron (III), and sulfate before finally switching to fermentation and methanogenesis at depth. As a result of high microbial activity and the slow speed of diffusion, the zones where oxygen and nitrate respiration occur are no more than a few millimetres thick in fine grained, muddy sediments (Canfield et al., 1993).

In contrast, coarse grained, sandy sediments have relatively high permeabilities. This results in advective pore-water flow which removes the transport limitations that control microbial activity in diffusive sediments. Advective pore water transport is caused by variations in pressure gradients as unidirectional or oscillating bottom water flows are deflected by rippled sediment topography (Huettel and Gust, 1992; Precht and Huettel, 2003). Wave pumping, groundwater seepage, gas bubble emergence, fluid venting, temperature and salinity gradients, as well as bioirrigation, can all also lead to porewater flow (Huettel and Webster, 2001). Of these, bioirrigation - in which the fauna induced flushing of benthic burrows significantly enhances the exchange of chemical compounds - is the only process which is not directly dependent on the hydrodynamics of the bottom water (Meysman et al., 2007; Volkenborn et al., 2010).

Advective transport of pore water transport accelerates solute and particle transport into the sediment by more than three orders of magnitude compared to diffusion (Huettel et al., 2003), and can lead to solute transport as deep as 10 cm (Huettel and Gust, 1992; Huettel et al., 1996). As a result, particulate matter, is effectively filtered in permeable sands even when it is at low concentrations in the water column and furthermore compounds are efficiently transported in and out of the

sediment (Huettel et al., 1996). Advective flow means that permeable sediments have redox zones which are flow oriented and unidirectionally coupled, these redox zones are unstable and can change with tide, wind direction, movement of the sediment and wave activity (Fig. 2).

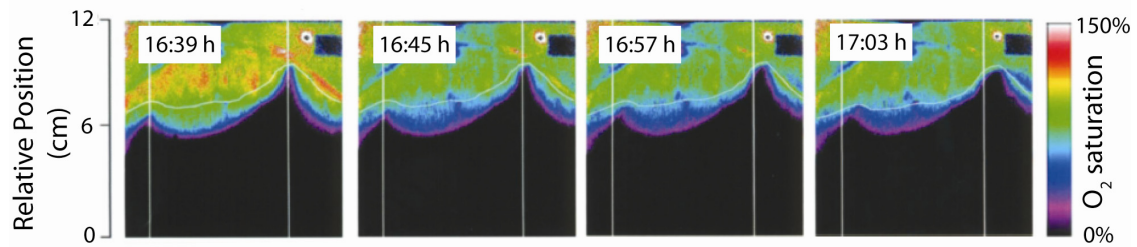


Fig. 2. Planar optode images showing the oxygen distribution around ripples measured *in situ* at Helgoland. Increased penetration of oxygen can be seen where the ripple obstructs bottom water flows, causing high and low pressure. At the same time the ripple itself is moving horizontally in the direction of the flow (adapted from Cook et al., 2007)

Traditionally, permeable sediments have been neglected in studies of biogeochemical cycling. This was a consequence of a number of early misapprehensions when dealing with sands. Firstly, standard measurements indicate that coarse grained sediments are typically organic matter poor (Keil et al., 1994), therefore they were considered to have little microbial activity. On the contrary, the low organic matter content of these sediments is a result of high turnover and an active and diverse microbial community (Boudreau et al., 2001). Secondly, coarse grained sediments appear to have lower cell counts than muddy sediments. This was assumed to result from decreased surface area, lower organic matter content and high predation pressure (Rusch et al., 2003). In fact it was a consequence of methodological problems which did not remove the firmly attached microbes from sand grains. Using methods modified for sands, the first extensive description of the microbial community structure of coastal sandy sediment revealed that cell counts are  $10^9$ , the same order of magnitude as fine grained, cohesive sediments (Musat et al., 2006). Finally, classical measurements of porewater concentrations of electron acceptors and donors are inappropriate within sands when the flow is not considered. Traditional core incubations, where oxygen and



solutes are supplied to sediment by diffusion indicated that remineralization and denitrification were low in sandy sediments. Recent applications of slurry and percolation techniques revealed that oxic respiration (de Beer et al., 2005) and denitrification rates (Gao et al., 2012), are increased by a factor of 10 in sandy sediments compared to diffusive techniques.

The importance of sandy sediments is now increasingly recognized, especially their possible contribution to the removal of N-inputs in coastal seas. This is because the biocatalytic nature of permeable sediments in coastal eutrophied regions filters and removes large amounts of N inputs. Furthermore they act as a reactor for the remineralization of the large amounts of organic matter produced by enhanced primary production. Yet the extent to which coastal permeable sediments can continue to remove N in the face of growing loads is unknown. There is a substantial lack of knowledge about the regulation of microbial processes and their contribution to global budgets of carbon and nitrogen turnover in coastal permeable sediments.

There is still a scarcity of studies available which take advective porewater flow into account, especially in the subtidal where most permeable sediments are found (Fig. 3). Of those studies that have been carried out, most are restricted to only a few sites around the world, which are easily accessible and where sampling and *in-situ* measurements are facilitated, for example, the temperate intertidal sand flats of the Wadden Sea (Huettel and Rusch, 2000; de Beer et al., 2005; Billerbeck et al., 2006a; Werner et al., 2006; Jansen et al., 2009; Gao et al., 2012). At many sites, in particular in the subtidal, measurements of biogeochemical cycling are severely restricted by methodological limitations. *In situ* rate measurements require equipment which does not disturb bottom flow. Microsensors have been deployed successfully in this aspect (e.g. Werner et al., 2006)), however strong bottom currents and ripple migration are often problematic for these sensitive pieces of equipment. When studying N-cycling, microsensors are also limited in their application, although constant improvements in NO<sub>x</sub> biosensors and N<sub>2</sub>O sensors may change this in the future. Benthic chambers, in which porewater flow is simulated with stirring plates, have also been deployed in

permeable sediments and allow for bulk flux measurements (Janssen et al., 2005). However, the flow patterns generated within these chambers are still far from resembling natural advective flows, and flux measurements often obscure details of processes such as coupled nitrification-denitrification. Therefore biogeochemical measurements within permeable sediments often require laboratory incubations of sediment cores, which are percolated with seawater to simulate advective flow (de Beer et al., 2005). Microsensors can then be used to follow processes such as oxygen consumption. However in the case of N-cycling, for example denitrification rate measurements, destructive sampling is often required. This limits the amount of samples which can be taken and the temporal resolution of measurements.

The focus of this thesis is to gain a better understanding of the role benthic sandy sediments in N-cycling, both in the intertidal and subtidal. As historically, little is known about this topic, the following section aims to summarize the current knowledge of benthic N-cycling in sandy sediments by contrasting them to muddy sediments.

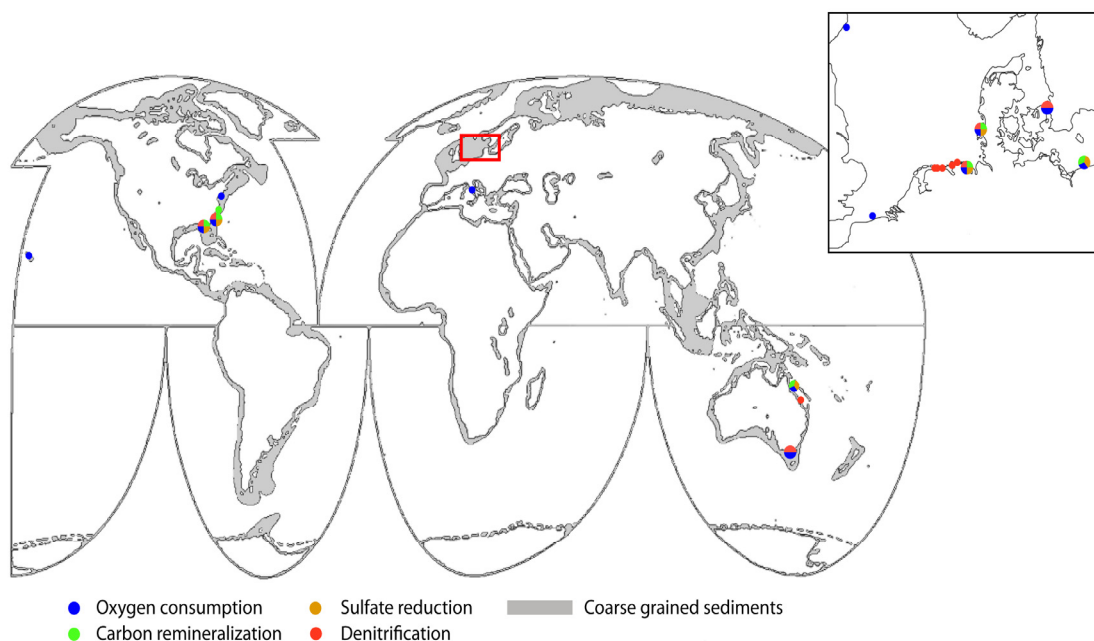


Fig 3. The global distribution of coarse grained permeable sediments on continental shelves (adapted from (Emery, 1968)). Marked are the areas where studies have taken into account the permeable nature of sediments and experiments were designed accordingly. The inlay represents the North Sea, including the Wadden Sea, where the vast majority of research has been done.

### **3. Nitrogen cycling in sediments**

“While some consider the N-cycle to be fiendishly complicated, I prefer to think of it as deliciously complex.” L. Codispoti

Nitrogen is an integral component of many biomolecules, including nucleic acids, amino acids and chlorophylls and is therefore essential to all living organisms. Additionally it is used in many respiratory energy metabolisms by specialized prokaryotes (recent evidence also points to a large contingent of eukaryotes carrying out nitrogen based respirations). Therefore the availability of nitrogen is a major constraint on biological productivity in the biosphere (Gruber and Galloway, 2008). The availability of nitrogen in the environment is controlled by assimilation and dissimilation of different forms of nitrogen, much of which is microbially mediated. There is an eight electron difference between the most oxidized inorganic form of nitrogen (nitrate,  $\text{NO}_3^-$ ) and the most reduced (ammonium,  $\text{NH}_4^+$ ), which allows for numerous microbial redox metabolisms (Fig. 4). The oxidation and reduction of different inorganic N compounds, and their interactions drive the biogeochemical cycle of N in the ocean.

Not all of the processes shown in Fig. 4 are redox metabolisms. For example, biological nitrogen fixation (BNF) is the key process by which microbes fix relatively inert dinitrogen gas ( $\text{N}_2$ ) into biologically available ammonium ( $\text{NH}_4^+$ ). BNF in the ocean provides more fixed N to the environment (177 Tg) than either anthropogenic sources (156 Tg) or N-fixation on land (107 Tg) (Galloway et al., 2004; Grosskopf et al., 2012). Whereas, the majority of marine N-fixation takes place in open ocean pelagic systems; only 15 Tg of N-fixation occurs in benthic systems (Galloway et al., 2004) where it is associated mainly with macrophytes and vegetated sediments such as salt marshes, coral reefs, seagrass and mangroves (Patriqui and Knowles, 1972; Wiebe et al., 1975; Zuberer and Silver, 1978; Wilkinson and Fay, 1979)

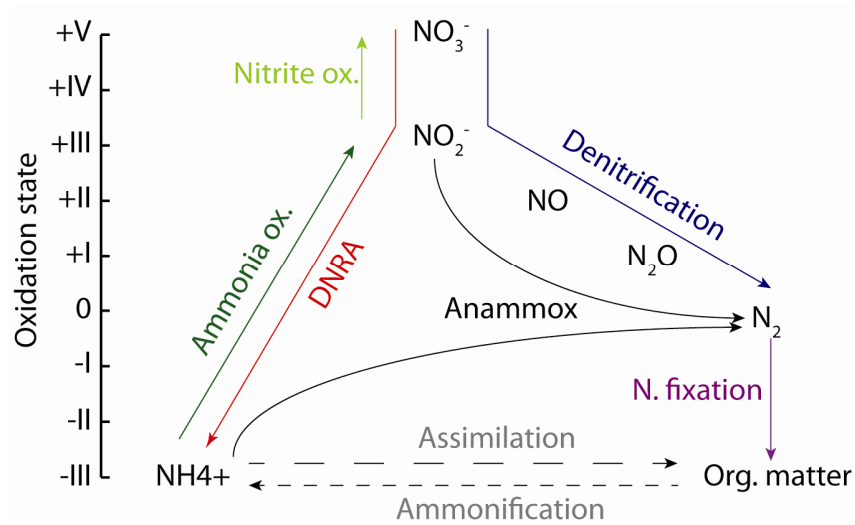


Fig. 4. A simplified overview of the processes that make up the marine nitrogen cycle showing the oxidation state of the various nitrogen compounds involved

### 3.1 Denitrification

Denitrification is the sequential microbial reduction of nitrate via nitrite, nitric oxide and nitrous oxide to  $\text{N}_2$ , at which point N is lost from the pool of reactive nitrogen in the environment. Denitrification can refer both to heterotrophic metabolism, where organic matter is the electron donor, or chemolithotrophic metabolisms; where the reduction of nitrate can be coupled to the oxidation of reduced sulfur and iron compounds (Baalsrud and Baalsrud, 1954; Straub et al., 1996). Denitrification is traditionally seen as an anaerobic process and in the classical view of the redox cascade, nitrate, if available, is the first electron acceptor used preferentially when oxygen is depleted from a system (Froelich et al., 1979). To date all isolated denitrifiers are facultative anaerobes and the ability to denitrify is not constrained to one particular phylogenetic group (Shapleigh, 2011). Therefore organisms which can denitrify are ubiquitous in the marine realm, however denitrification activity is generally restricted to anoxic or micro-oxic habitats.

Benthic N<sub>2</sub> loss in sediments has mainly been attributed to shelf sediments, which account for 50–70% of fixed oceanic N loss in current budgets (Christensen et al., 1987; Codispoti et al., 2001). Moreover, in a modeling study Middleburg et al. (1996) suggested that N-loss from slope and abyssal sediments may exceed that of shelf sediments. The only study to experimentally investigate denitrification in deep ocean sediments found that denitrification was indeed similar to that of muddy shelf sediments (Glud et al., 2009). Increasingly however, the extent of N-loss from shelf sediments appears to be underestimated in current budgets. Most previous research has been carried out on muddy, diffusively controlled sediments and have neglected sandy sediments.

Some of the highest potential denitrification rates in the marine environment have been measured in sandy, permeable sediments from the eutrophied Wadden Sea (Cook et al., 2006; Gao et al., 2010; Gao et al., 2012). These result from the advective supply of nitrate and organic matter to the sediment, and also the competitive advantage that denitrifiers gain as facultative anaerobes in an environment where oxygen fluctuates frequently. It has long been hypothesized that coastal seas buffer the open ocean from riverine run-off of N, and there is now growing evidence that this may be mediated by benthic denitrification in sandy sediments. For example, at least a third of the N-inputs the Wadden Sea are removed by benthic denitrification in sandy sediments (Deek et al., 2012; Gao et al., 2012).

### *3.1.1 Aerobic denitrification*

Denitrification is generally regarded as an anaerobic process (Zumft, 1997), however as long as 25 years ago Lloyd et al. (1987) asserted that the persistence of bacterial denitrification under aerobic conditions was “the rule rather than the exception”. Since that time numerous laboratory studies have shown that some denitrifiers have the ability to reduce NO<sub>x</sub> in the presence of oxygen (Robertson and Kuenen, 1984; Lloyd et al., 1987; Bonin and Gilewicz, 1991; Robertson et al., 1995; Kim et al., 2008). Still, the existence of aerobic denitrification is debated; on an enzymatic

level, oxygen inactivates one of the copper centres ( $\text{Cu}_2$ ) within nitrous oxide reductase (*NosZ*) (Pomowski et al., 2011), the enzyme required for the final step in denitrification. Furthermore, several regulatory systems in well known denitrifiers are shut down by the presence of oxygen (Chen and Strous, 2013) and oxygen can inhibit nitrate transport into the cell (Moir and Wood, 2001).

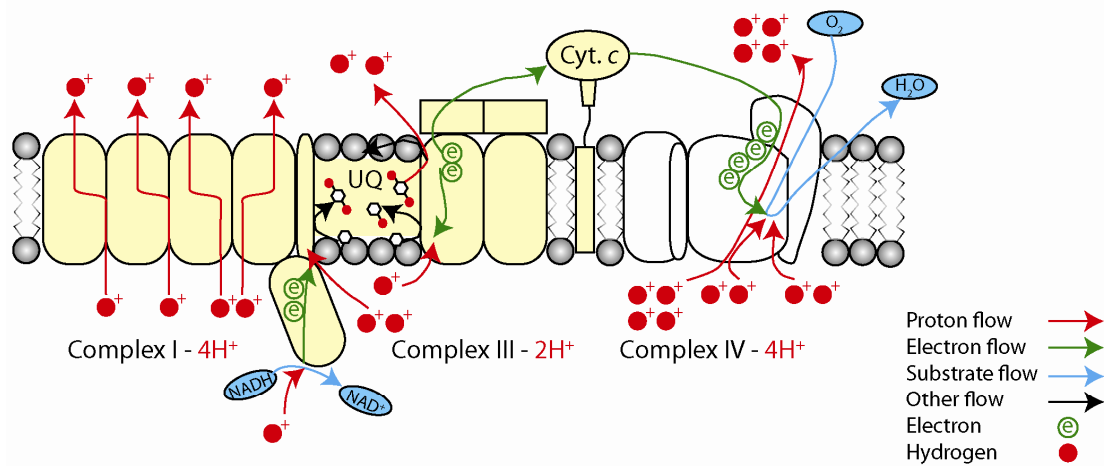
From a bioenergetic perspective aerobic denitrification is unfavourable when oxygen is present. Aerobic respiration translocates 10 protons per electron pair transduced, while denitrification translocates 6 at most. Denitrifiers also require additional enzyme complexes to aerobic organisms and are therefore limited by the space that these must occupy in the membrane and periplasm (Chen and Strous, 2013).

When frequent oscillations occur between oxic and anoxic conditions the bioenergetic restraints of co-respiration of oxygen and denitrification are relaxed and co-expression of the two pathways can become profitable (Chen and Strous, 2013). The cost and time involved in microorganisms rebuilding their respiratory chains if oxygen concentrations are fluctuating rapidly can be prohibitive. Instead facultative denitrifiers are hypothesized to direct electron flow simultaneously to denitrifying enzymes as well as to  $\text{O}_2$ . (Robertson and Kuenen, 1988; Huang and Tseng, 2001; Chen et al., 2003). Using a single hybrid electron transport chain makes it feasible for denitrification enzymes to take care of any overflow in the electron flow, while preferentially using the aerobic pathway (Fig. 4) (Chen and Strous, 2013).

Aerobic denitrification has been identified in situations where frequent fluctuations in oxygen occur such as natural samples artificially exposed to oxic-anoxic phases in the laboratory, wastewater treatment plants and sandy sediments (Patureau et al., 1994; Frette et al., 1997; Patureau et al., 2000; Rao et al., 2008; Gao et al., 2010). Although initial investigations have identified aerobic denitrification in both intertidal (Gao et al., 2010) and subtidal sandy sediments (Rao et al., 2008), it is not known whether oxygen and nitrate are co-metabolised by single organisms or whether separate populations respire oxygen and nitrate simultaneously (Gao et al., 2010). Furthermore, while Gao et al. (2010) used a combination of stirred slurries and core

incubations, debate still exists as to whether denitrification is truly occurring aerobically or whether it is localised within anoxic microsites. Permeable intertidal sandy sediments are an ideal location to further investigate these questions.

a. 10 protons pumped per  $2e^-$



b. 6 protons pumped per  $2e^-$

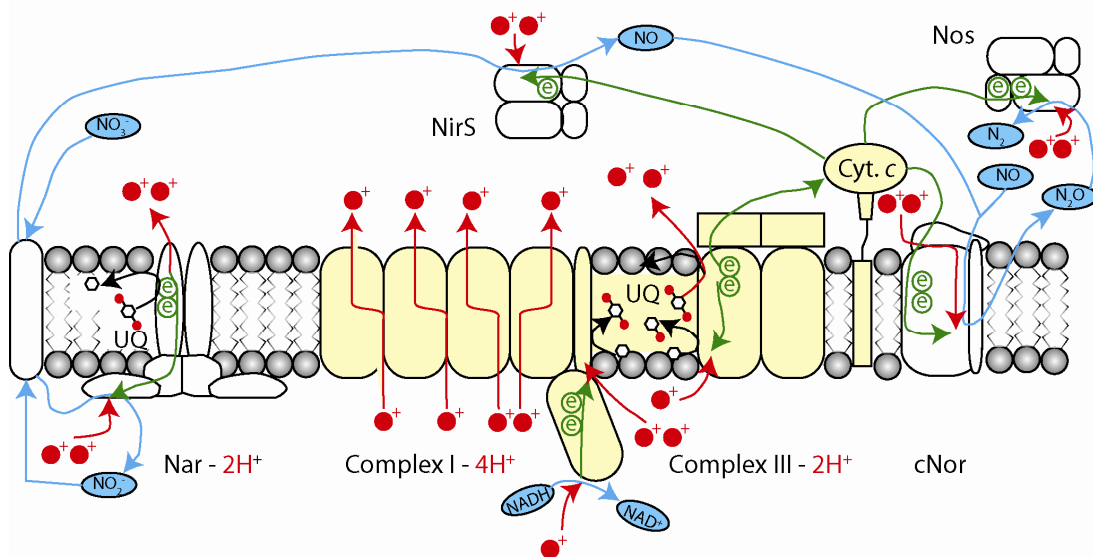


Fig. 4. Shared modules of a) the oxygen respiratory chain and b) the denitrification respiratory chain (shown in yellow). Denitrification modules can in effect be "plugged in" to the four core modules under some conditions (see text), allowing aerobic denitrification to occur even though it less favourable from a bioenergetic point of view (adapted from Chen et al., 2003)).

### 3.2 Anammox

Anammox is the chemolithoautotrophic process by which  $N_2$  is formed from the anaerobic oxidation of ammonium with nitrite and is carried out by a monophyletic group of bacteria within the phylum Planctomycetes (Strous et al., 1999). Discovered first in a wastewater treatment plant (Mulder et al., 1995; Van De Graaf et al., 1997), the environmental occurrence of anammox has been most widely reported from OMZ's (Lam and Kuypers, 2011), however anammox also occurs in benthic sediments (Thamdrup and Dalsgaard, 2002; Sokoll et al., 2012).

Anammox rates in sediments vary ( $0.08 - 11 \text{ nmol cm}^{-3} \text{ h}^{-1}$ ) and can contribute anything from 0 – 79% of total N-loss from benthic environment (Dalsgaard et al., 2005). The relative importance of anammox appears to increase as overlying water depth increases. The correlation between water depth and the importance of anammox has been hypothesized to result from decreasing flux and reactivity of organic matter with depth (Song et al., 2013), although in some deep sediments denitrification is still the dominant N-loss process (Glud et al., 2009). As the absolute rate of  $N_2$  production generally decreases with increasing water depth and anammox is currently estimated to contribute 28 % to benthic N-loss (Trimmer and Engstrom, 2011).

Other factors which could control the balance between denitrification and anammox are competition for  $NO_x$ , the presence of manganese oxides, and sediment stability. In shallow sediments where ammonium is plentiful, denitrifiers seem to be able to outcompete anammox bacteria for nitrite (Trimmer and Engstrom, 2011). In manganese rich sediments, which have consistently high N-loss from anammox, manganese reducing bacteria may outcompete denitrifiers for electron donors (Dalsgaard and Thamdrup, 2002), although there is no direct evidence for this.

Anammox has been shown to be insignificant to N-loss in sandy sediments from both the Wadden Sea, Germany and Port Phillip, Australia (Evrard et al., 2012; Gao et al., 2012). In these environments where variable redox conditions are common and organic matter inputs are often high, relatively slow growing autotrophic anammox



bacteria (which have doubling times between 7 – 22 days (Kartal et al., 2013)), seem to be outcompeted by fast-growing, facultative denitrifiers.

### 3.3 DNRA

Dissimilatory nitrate reduction to ammonium (DNRA) is responsible for consumption of  $\text{NO}_x$  within sediment but produces  $\text{NH}_4^+$  rather than  $\text{N}_2$  or  $\text{N}_2\text{O}$ . Therefore DNRA does not contribute to N-loss. Instead, N is recycled to the environment by DNRA where it can sustain further primary production or nitrification (King and Nedwell, 1987), and further enhances eutrophication. Many microorganisms can perform DNRA, including heterotrophic and chemoautotrophic prokaryotes (Canfield et al., 2005) as well as a diverse range of eukaryotic microorganisms including diatoms (Kamp et al., 2011).

Far fewer studies of benthic DNRA have been carried out in comparison to those on benthic denitrification. Of these benthic DNRA studies, most have been carried out in estuaries and fjords (e.g. (An and Gardner, 2002; Dong et al., 2011)). Nonetheless, a few reports of DNRA exist from subtidal continental shelf sediments from the Atlantic (Trimmer and Nicholls, 2009), the Baltic (Jantti and Hietanen, 2012) and also from sediments underlying OMZ's (Bohlen et al., 2011). DNRA rates in these studies ranges from  $0.02 - 13 \text{ mmol N m}^{-2} \text{ d}^{-1}$  and can contribute 0 – 99 % of nitrate reduction. No known studies on DNRA have been carried out in permeable sediments.

The importance of DNRA relative to denitrification is believed to be controlled by the ratio of electron donors relative to  $\text{NO}_3^-$ . At high C: $\text{NO}_3^-$  ratios DNRA is favoured; despite having a lower energy yield than denitrification, it consumes less nitrate per C (Tiedje, 1988; Kelso et al., 1997; Strohm et al., 2007). Furthermore under conditions of increased temperature and low  $\text{NO}_3^-$  concentrations,  $\text{NO}_3^-$  ammonifiers can scavenge  $\text{NO}_3^-$  more efficiently, and, coupled to gaining more energy per mole thermodynamically, this allows DNRA to compete more successfully with the denitrifying community (Porubsky et al., 2009; Dong et al., 2011). Therefore in permeable sediments where substrate concentrations tend to reflect those in the

overlying water due to pore water advection, it seems that the extent of DNRA in comparison to denitrification would also be dependent on ratio of C:NO<sub>3</sub><sup>-</sup> in the water column.

DNRA can link the sulfur and N cycles when both H<sub>2</sub>S and NO<sub>3</sub><sup>-</sup> are present in sediments, as some organisms that mediate DNRA are chemoautotrophs, using NO<sub>3</sub><sup>-</sup> as the electron acceptor for anaerobic H<sub>2</sub>S oxidation (Otte et al., 1999; Sayama, 2001). This linkage can even occur when NO<sub>3</sub><sup>-</sup> rich surface sediments and H<sub>2</sub>S rich deep sediments are separated, as species such as *Thioploca* and *Beggiatoa* can vertically migrate between the zones (Zopfi et al., 2001; Preisler et al., 2007). Electric coupling within the sediment can also mediate a similar process (Marzocchi et al., 2012).

So far there is little evidence of chemoautotrophic DNRA in permeable sediments, due to the unidirectional nature of most advective flows it seems unlikely that sulfide and nitrate might overlap. Therefore spatially separated surface NO<sub>3</sub><sup>-</sup> zones and deep H<sub>2</sub>S rich zones would have to be linked. Substantial populations of large motile sulfur bacteria are rare in permeable sands and electrical coupling is not assumed to be of importance in high energy environments, therefore these two mechanisms are unlikely. A link between spatially separated pools of nitrate and sulfide within permeable sediments might however be provided by motile meiofauna from sandy sediments which form consortia with microbial symbionts or store nitrate (Hentschel et al., 1999; Kleiner et al., 2012).

### 3.4 Nitrification

#### 3.4.1 Autotrophic nitrification

Nitrification is the autotrophic two step process by which ammonium is first oxidized to nitrite then to nitrate, thereby connecting the most reduced with the most oxidized components in the nitrogen cycle. These reactions are carried out by two functionally distinct groups of microbes, the majority of which are descendants of a common photosynthetic ancestor and, so far, no organism has been identified which can mediate

both reactions (Teske et al., 1994). Ammonia oxidation is carried out by  *$\beta$ -proteobacteria*,  *$\gamma$ -proteobacteria* and Archaea, known respectively as AOB's and AOA's (Konneke et al., 2005; Molina et al., 2007), while nitrite oxidation is carried out by proteobacteria described collectively as NOB's. Research into nitrification has often focused on ammonia oxidation, as it has been considered the rate limiting step in the process and therefore the diversity and distribution of NOB's are less well described (Füssel et al., 2011).

As nitrification requires oxygen as a terminal electron acceptor, it is restricted to the oxic and micro-oxic parts of sediment, therefore oxygen concentrations and oxygen penetration depths are often the main factors controlling the process (Henriksen and Kemp, 1988). In muddy stratified sediments this regularly represents only the top few millimetres of sediment, where nitrifiers can comprise one of the main sinks of oxygen even though they must compete with heterotrophs (Ward, 2008). The ammonium required for nitrification is generally supplied by diffusion from deeper anoxic sediment layers and therefore the extent of processes such as denitrification, DNRA, or other heterotrophic remineralization can also regulate nitrification (Grundmanis and Murray, 1982).

Measurements of nitrification have revealed that the two-step process is ubiquitous and substantial in many types of sediments. In contrast to denitrification, active and substantial nitrification was identified in sandy sediments as early as the 1980's (Henriksen and Kemp, 1988; Ward, 2008). Areal rates in sandy sediments have a tendency to be slightly lower, however none of these measurements have taken advective flows into account. The application of advective flows are likely to change our view of nitrification in sandy permeable sediments to the same extent that they did denitrification. Nitrification under non-advective conditions relies on the diffusive supply of oxygen from the water column above and the diffusive supply of ammonium from below as well as any ammonium supplied from aerobic heterotrophy. In contrast, in permeable sediments where advective flow occurs, the supply of oxygen is greater, which would increase the area in which nitrification can take place, but ammonium

might be more limited as it is unlikely to be supplied by denitrification which would in effect happen “downstream” (Cook et al., 2006). Therefore in the oxic part of permeable sediments, nitrification might be more tightly coupled to aerobic denitrification, which would supply ammonium through remineralization of organic matter, without competing for oxygen as would be the case with other heterotrophs.

#### *3.4.2 Heterotrophic nitrification*

In general nitrifiers are considered obligate chemolithoautotrophs, however research in to their heterotrophic abilities is starting to receive more attention, especially amongst NOB's. However, it is extremely difficult to differentiate between lithotrophic and heterotrophic nitrifiers (Lam and Kuypers, 2011). Autotrophic nitrification is relatively inefficient energetically, as it requires the oxidation of about 35 mol of  $\text{NH}_4^+$  to support the fixation of a single mole of  $\text{CO}_2$  (Baas-Becking and Parks, 1927). Hence, it has been suggested that heterotrophic nitrifiers should be more common, Nevertheless, the energetics for heterotrophic nitrifiers are even unfavourable, and thus, no reports of substantial heterotrophic nitrification exist for the marine environment (Stouthamer et al., 1997). Furthermore, of those heterotrophic nitrifiers which have been identified, many can oxidize ammonia but do so without energy conservation (Robertson et al., 1989)

### 3.5 Nitrous oxide production

$\text{N}_2\text{O}$  is a potent greenhouse gas which has a potential warming factor 310 times higher than carbon dioxide (Stein and Yung, 2003), and is the most important present day contributor to ozone-depletion (Ravishankara et al., 2009). Since the beginning of the industrial revolution the atmospheric inventory of  $\text{N}_2\text{O}$  has risen significantly from 270 ppb to 314 ppb, however estimates of global sources and sinks of  $\text{N}_2\text{O}$  vary widely as observations are limited (Seitzinger et al., 2000; Houghton J.T., 2001; Bange, 2006). Early compilations of oceanic  $\text{N}_2\text{O}$  sources focused on open water column studies (Law

and Owens, 1990; Codispoti, 1992), and more recent estimates have included estuaries, shelves and coastal upwelling (Bange, 2006), however the production of  $N_2O$  in these studies is mainly attributed to pelagic nitrification. Marine sediments are generally considered unimportant as an  $N_2O$  source, and are frequently cited as a sink, although studies are rare (Jørgensen et al., 1984; Kieseckamp et al., 1991; Usui et al., 2001). Where emissions of  $N_2O$  from benthic denitrification have been recorded, rates are very low or decrease to zero in fully saline sediments (Kieseckamp et al., 1991; Middelburg et al., 1995).

Both nitrification and denitrification can be sources of  $N_2O$ . Nitrifiers including AOB and NOB are capable of a process termed nitrifier-denitrification, in which they reduce  $NO_2^-$  to  $N_2O$  and  $N_2$  via denitrifying enzymes using hydrogen, hydroxylamine, or organic compounds (Stueben et al., 1992; Bock et al., 1995). This often occurs under low oxygen conditions and can release substantial amounts of  $N_2O$  (Bock et al., 1988; Dundee and Hopkins, 2001; Shaw et al., 2006). It has been suggested that nitrifier-denitrification could contribute as much  $N_2O$  to the atmosphere as heterotrophic denitrification in marine ecosystems (Cantera and Stein, 2007). Ammonia oxidation itself can also be responsible for the formation of  $N_2O$ , although the exact biochemical pathway is not clear. Other than nitrifier-denitrification, the ammonia oxidation intermediates of hydroxylamine and nitric oxide may also provide routes to  $N_2O$  formation (Ostrom et al., 2000). What is clear is that  $N_2O$  production during nitrification seems to be enhanced at low  $O_2$  concentrations (Firestone and Tiedje, 1979; Codispoti, 2010).

No investigations of  $N_2O$  production have been carried out in permeable sediments using suitable methodology; however  $N_2O$  emissions from permeable sediments are likely. The enzyme that catalyses  $N_2O$  reduction to  $N_2$  (nitrous oxide reductase), is more susceptible to oxygen inhibition and slower to be induced relative to the other denitrification enzymes (Dendooven and Anderson, 1994; Naqvi et al., 2000). Therefore the changing environmental conditions (i.e. switches from oxic to anoxic) found in permeable sediments could lead to greater  $N_2O$  production during

denitrification, furthermore advection may lead to greater N<sub>2</sub>O transport to the water column from the sediment

### 3.6 Studying the nitrogen cycle in sediments

Different approaches can be taken when trying to resolve the nitrogen cycle in sediments. Molecular approaches, which aim to identify and quantify the abundance of microbes and link them to activity, are one possible direction. Such efforts can often be hampered; firstly, DNA and RNA extraction is more problematic in sediments than in water column samples; secondly, visualization of microbes which are firmly attached to sand grains requires sonication procedures which are often inefficient and thirdly, due to the ubiquity of facultative denitrifiers across phylogenetic groupings, it is hard to develop targeted probes with which to identify them. Molecular methods have been successfully applied in sediments in the past however, for example; by measuring the abundance of *nirS*, a biomarker for the nitrate reductase functional gene in both denitrifiers and anammox bacteria and linking the results to activity measurements, Sokoll et al. (2012) could show that anammox increased in sediments in correlation with water and sediment depth in the Arabian Sea .

In the work carried out in this dissertation, I mainly used an approach which relied on activity measurements within sediment that was collected *in situ* and packed into sediment columns. This allowed us to carry out multiple measurements, as well as manipulate environmental conditions such as oxygen concentrations. To do this we had to be able to measure the different processes which were occurring within the sediment, including denitrification, anammox, DNRA and nitrification. Measuring the concentrations of the end products of these reactions is often problematic, especially if they co-occur or if ammonium is produced by remineralization. N<sub>2</sub> measurements themselves pose further challenges; background N<sub>2</sub> concentrations are very high in seawater in equilibrium with the atmosphere (around 500 μM) and excess N<sub>2</sub>

equilibrates easily with air. Therefore, measuring small changes in concentrations of  $N_2$  is difficult.

As such, we applied methods that take advantage of nitrogen stable isotopes. The  $^{15}N$  stable isotope is of low abundance in the natural environment (0.366%), and therefore provides a powerful tool to trace different pathways in the N-cycle (Holtappels, 2011). The most well cited initial use of  $^{15}NO_3^-$  - which assumed random isotope pairing by denitrification of uniformly mixed  $NO_x$  species - was by Nielsen (1992). Nielsen used the Isotope Pairing Method (commonly referred to as the IPM or IPT), to determine total denitrification after addition of  $^{15}NO_3^-$  as well as to separate out the contribution to denitrification of  $NO_x$  diffusing from the overlying water and  $NO_x$  from benthic nitrification. Since this initial application, the power of the IPM in disentangling the nitrogen cycle has been demonstrated numerous times and improvements to the IPM now allow us to determine DNRA, anammox and nitrification (e.g. Thamdrup and Dalsgaard, 2002; Risgaard-Petersen et al., 2003; Jensen et al., 2008; Holtappels, 2011; Sokoll et al., 2012). That is not to say, however, that existing IPT methods and calculations are already suitable for a given environment or experimental set-up. Constant vigilance and revisions to the method based on environmental and experimental conditions are essential to correctly determine N-cycling activity.

#### **4. *The study sites***

##### **4.1 The Wadden Sea**

The Wadden Sea, where the majority of the work in this thesis was carried out, is a UNESCO world heritage site, dominated, like most coastal seas by permeable sandy sediments (Fig. 3). Despite the large increase in N-inputs to the Wadden Sea in the past century, there has seemingly not been a concurrent rise in N exported to the open ocean. This is attributed to benthic denitrification in the permeable sands, which occurs at some of highest rates ever recorded in the marine environment (Gao et al., 2012).

The high denitrification rates measured within the permeable sands of the Wadden Sea ( $207 \pm 30 \mu\text{mol m}^{-2} \text{h}^{-1}$ ) show little seasonal or spatial variation. When integrated over the entire intertidal and subtidal areas of the Wadden Sea, denitrification account for N-losses comprising more than 30% of the annual N-inputs to the Wadden Sea (Gao et al., 2012).

In the Wadden Sea high denitrification rates are mirrored by high oxygen consumption and remineralization rates, which are stimulated by the influx of oxygen and organic material (de Beer et al., 2005). Mineralization rates in the top 15 cm of the sediment have been estimated to range from 38 (winter) to 280  $\text{mmol C m}^{-2} \text{d}^{-1}$  (summer), most of which is aerobic remineralization (sulfate reduction was estimated to contribute 3 to 25% to total mineralization, depending on the season) (Billerbeck et al., 2006b).

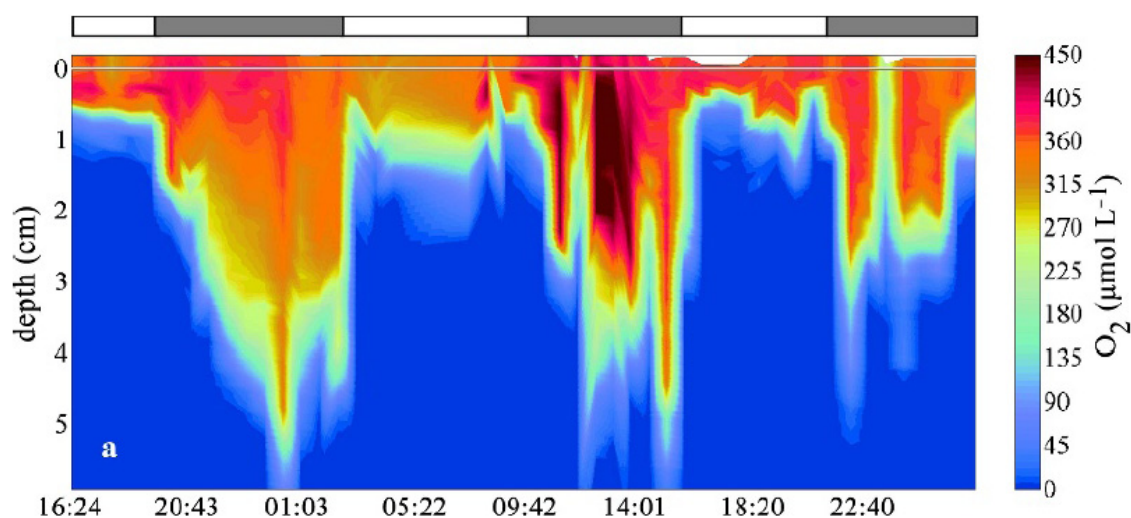


Fig. 8 Oxygen penetration depths over 3 tidal cycles at an intertidal flat from the Wadden Sea. Grey and white bars indicate inundation and exposure periods respectively (taken from (Werner et al., 2006))

Much of the work in this thesis is carried out at an intertidal sand flat in the back barrier area of Spiekeroog Island in the East Frisian Wadden Sea, Germany. The intertidal flat has been shown to consist of three regions, the upper flat, the slope between the upper flat and the low water line and the low water line. The upper flat,



where this work is focused, consists of well sorted silicate sand in the upper 15 cm, with a permeability of  $7.2 - 9.5 \times 10^{-12}$ , a porosity of .35 and a mean grain size of 176mm (Billerbeck et al., 2006a; Billerbeck et al., 2006b). At high tide the flat is covered by 1.5 – 2 m of seawater for 6-8 h and is exposed to air for 6-8 h during low tide, dependent on tidal range. Due to the high permeability of the sand, water is flushed advectively through the sediment on two distinct temporal and spatial scales. During inundation, boundary flows force water into troughs on the rippled surface, filtering organic particles and nutrients, which are then degraded and returned to the overlying water promptly at the ripple peak. Porewater flows in the sediment can transport oxygen to depths of 6 cm (Fig. 8). Referred to as “skin circulation” this process occurs at spatial scales in the order of centimeters and temporal scales of minutes to hours.

#### 4.2 The German Bight

The German Bight is the shallow shelf sea area of the North Sea with depths mainly around 20 m, but extending to 40 m in the glacially formed Elbe Rinne (Budeus, 1989), It is bounded by the Jutland peninsula to the East, Dogger Bank in the North and the coasts of Germany and the Netherlands to the south (Fig. 5).

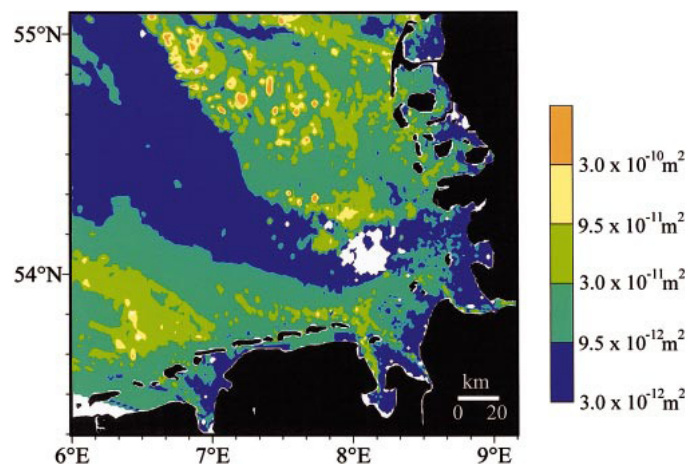


Fig. 5 Contour plot of the permeabilities of the German Bight (taken from Janssen et al., 2005). Permeabilities in excess of  $10^{-12} \text{ m}^{-2}$ , permit pore-water advection (i.e. all coloured areas on the map). The Wadden Sea is the area fringed by the barrier islands around the coastal region.

The Bight is a transition region between the freshwaters of the Elbe, Weser and Ems, the Wadden Sea and North Sea water. It is strongly tidally influenced, with tidal currents of up to  $2.5 \text{ m s}^{-1}$  at the surface and up to  $0.6 \text{ m s}^{-1}$  1 m above the seafloor (Antia et al., 1995; Sündermann, 1997). Nutrient inputs lead to high pelagic primary productivity in the German Bight (around  $400 \text{ g C m}^{-2} \text{ yr}^{-1}$  (Rick et al., 2006)). Benthic primary production has rarely been measured in the German Bight, even though enough light reaches the seafloor to support it. Those few studies which have been carried out suggest that microphytobenthos is an important part of ecosystem but so far no attempt has been made to quantify the benthic contribution to primary production (Reiss et al., 2007). It has been estimated previously that that 80% of the primary production is remineralized within the water column and only 20% within the sediment (van Beusekom and Diel-Christiansen, 2009). However, remineralization within the sediment is likely to have been underestimated as benthic remineralization estimates are based only on muddy sediments, which are likely to have weaker benthic-pelagic coupling than sands.

There are three major nitrate sources for the German Bight, the largest is the influx across the western border ( $270 - 990 \text{ kt N yr}^{-1}$ ), which results from the circulation of Atlantic and Central North Sea Water (Beddig et al., 1997; Paetsch et al., 2010). Almost equaling the oceanic source are inputs from riverine and atmospheric sources ( $256 \text{ kt N yr}^{-1}$  and  $29 \text{ kt N yr}^{-1}$  respectively), which are mainly anthropogenic in nature (van Beusekom, 2005; Paetsch et al., 2010).

Reports of nitrate fluxes into and out of the German Bight remain scarce, but of those surveys carried out, it appears that nitrate fluxes out of the Bight are in the same order of magnitude as fluxes in (Beddig et al., 1997), however at the same time, intense internal turnover of N occurs (Paetsch et al., 2010). For example, recycled nitrate is estimated to contribute up to 50% of phytoplankton N demand (Lohse et al., 1993). Therefore the German Bight has the capacity to be a site of substantial N-loss without changes in the N-inventory being immediately apparent. Some evidence for this is given in Dähnke et al. (2010), whose study of stable isotope composition suggests that that

the nitrate leaving the German Bight is derived from nitrification, possibly within the sediments, rather than riverine sources.

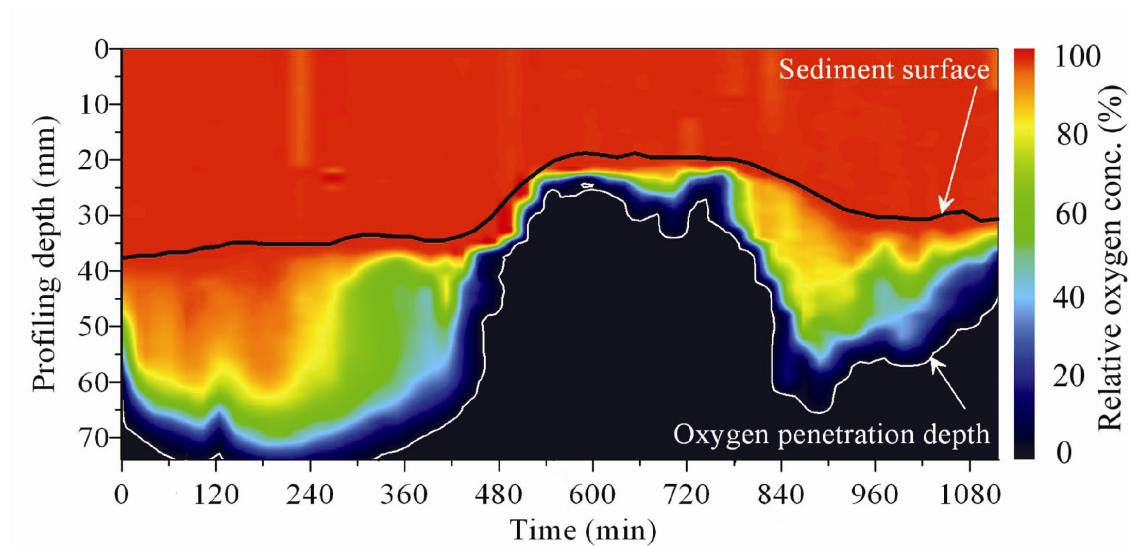


Fig. 6. Oxygen penetration depths measure *in situ* at a medium sand station in the German Bight near Spiekeroog. Sediment surface height changes over time as a result of sand migration (adapted from Janssen, 2004).

The German Bight is also dominated by sandy sediments (Fig. 5), 60% of which have permeabilities within the range where significant porewater advection is expected to occur (Janssen et al., 2005). Little is known about the biogeochemical cycling in these permeable sediments and the extent of benthic-pelagic coupling, other than that oxygen penetration depths remain high (Fig. 6), as do benthic remineralization rates (Janssen et al., 2005). So far no studies of nitrogen cycling have been carried out using suitable methodology in the permeable subtidal sediments of the German Bight.

## ***Aims and outline***

Previous studies have identified coastal intertidal permeable sediments as sites of extensive N-loss through denitrification. However, given the apparent importance which permeable sediments may have in mediating the effects of eutrophication, N-cycling within sands is still desperately understudied. Overall this thesis aimed to characterize the factors controlling denitrification in permeable sands, whether they be seasonal, influenced by advective dynamics or related to sediment characteristics. Furthermore, it aimed to move beyond denitrification measurements and to gain a more holistic picture of how permeable sediments work by investigating other N-cycling pathways and players and the interactions between them. Finally, in the face of global change, it is no longer appropriate to just describe systems, therefore this thesis also aimed to begin understanding how permeable sediments might influence global change in the form of nitrous oxide emissions, but also how global change, in the form of ocean acidification may influence coastal permeable sediments.

The thesis starts in the East China Sea in Chapter 2, an environment which is extensively eutrophied, but which is dominated by diffusive sediments. Here we used standard methodological approaches to extricate details of the complicated interactions among different benthic nitrogen transformations and their relationships to sediment organic matter content.

Chapter 3 returns to permeable sediments and the Wadden Sea, where the vast majority of permeable sediment research has been carried out. Previous research had had left an intriguing conundrum, namely that denitrification could only account for half of the nitrate being consumed; nothing was known about the fate of the other half. To understand the fate of nitrate, I mainly used an ex-situ approach with freshly collected sediment. By adapting previous percolation methods I was able to gain information on high temporal scales with a great degree of control over substrate amendments, oxygen conditions and measurement possibilities. Eventually, after detailed studies in different seasons I was able to follow nitrate transformations within the sediment. This led to

some surprising conclusions about the importance of eukaryotes to N-loss in intertidal permeable environments and how seasonal organic and inorganic nutrient inputs influence sediment N-cycling.

Most coastal permeable sediments are however, not intertidal. Subtidal areas are much larger and therefore have a greater potential to mediate many of the effects of eutrophication. One such environment is the German Bight, where, in Chapter 4 we used the methods developed in Chapter 3 to start investigating nitrogen cycling in subtidal sediments. In contrast to the intertidal we were able to test a range of sediment permeabilities, which allowed us to begin relating how sediment characteristics control organic matter inputs, which in turn regulate denitrification. Furthermore, for the first time we were able to observe high rates of nitrification and show how coupled nitrification-denitrification within permeable sediments can explain previous nutrient observations from within the German Bight.

These larger scale studies improved our insights into the role that permeable sediments play in N-loss. However, while carrying them out we had observed an intriguing phenomenon within the sediment; aerobic denitrification (which was identified in permeable sediments previously) changed in magnitude depending on how we treated the sediment. Hence, Chapter 5 details the amazingly adaptable response of denitrification to different oxygen exposure regimes. While the occurrence of aerobic denitrification enhances the capacity for N-loss within permeable sediments, it also has a dark side, namely, enhanced production of the greenhouse gas nitrous oxide. We found that permeable sediments represent a significant source of N<sub>2</sub>O to the atmosphere, not just because of aerobic denitrification, but also due to transport by advective flow and the specialist denitrifying communities which exist in permeable sediments due to transient oxygen and nutrient supply (Chapter 6).

Global change is also going to impact upon permeable sediments, which might be strongly influenced by changes in the water column due to advective porewater transport. One such change is ocean acidification; while the majority of ocean acidification research focuses on changes in carbon cycling and calcification, previous

studies have shown that it might also impact N-cycling by inhibiting nitrification. Almost nothing was known about the response within benthic systems however and nothing about permeable sediments. Within Chapter 7, I investigated whether N-loss in permeable sediments would be effected by future ocean  $p\text{CO}_2$  conditions and found that while denitrification itself might not be directly effected; decreases in water column nitrate availability enhance the degree of coupled nitrification-denitrification within the sediment. This leads to a positive feedback in which even less nitrate is returned to the water column, with implications for future nutrient ratios and primary production.

Chapter 8 provides a review highlighting our opinions of how the conditions within eutrophied permeable sediments influence the microbial communities and biogeochemical cycling within them. We review the knowledge we have gained from past studies both in permeable sediments and wastewater treatment and look at how in the future we should go about increasing our understanding of these fascinating natural bioreactors.

## References

An, S.M., and Gardner, W.S. (2002) Dissimilatory nitrate reduction to ammonium (DNRA) as a nitrogen link, versus denitrification as a sink in a shallow estuary (Laguna Madre/Baffin Bay, Texas). *Marine Ecology Progress Series* **237**: 41-50.

Antia, E.E., Flemming, B.W., and Wefer, G. (1995) Calm-weather spring and neap tidal current characteristics in a shoreface connected ridge complex in the German Bight (Southern North Sea). *Geo-Marine Letters* **15**: 30-36.

Baalsrud, K., and Baalsrud, K. (1954) Studies on thiobacillus denitrificans. *Archiv fur Mikrobiologie* **20**: 34-62.

Baas-Becking, L.G.M., and Parks, G.S. (1927) Energy relations in the metabolism of autotrophic bacteria. *Physiological Reviews* **7**: 85-106.

Bange, H.W. (2006) Nitrous oxide and methane in European coastal waters. *Estuarine, Coastal and Shelf Science* **70**: 361-374.

Beddig, S., Brockmann, U., Dannecker, W., Korner, D., Pohlmann, T., Puls, W. et al. (1997) Nitrogen fluxes in the German Bight. *Marine Pollution Bulletin* **34**: 382-394.

Billerbeck, M., Werner, U., Bosselmann, K., Walpersdorf, E., and Huettel, M. (2006a) Nutrient release from an exposed intertidal sand flat. *Marine Ecology-Progress Series* **316**: 35-51.

Billerbeck, M., Werner, U., Polerecky, L., Walpersdorf, E., de Beer, D., and Huettel, M. (2006b) Surficial and deep pore water circulation governs spatial and temporal scales of nutrient recycling in intertidal sand flat sediment. *Marine Ecology-Progress Series* **326**: 61-76.

Bock, E., Wilderer, P.A., and Freitag, A. (1988) Growth of nitrobacter in the absence of dissolved oxygen. *Water Research* **22**: 245-250.

Bock, E., Schmidt, I., Stuvan, R., and Zart, D. (1995) Nitrogen loss caused by denitrifying nitrosomonas cells using ammonium or hydrogen as electron donors and nitrite as electron acceptor. *Archives of Microbiology* **163**: 16-20.

Bohlen, L., Dale, A.W., Sommer, S., Mosch, T., Hensen, C., Noffke, A. et al. (2011) Benthic nitrogen cycling traversing the Peruvian oxygen minimum zone. *Geochimica Et Cosmochimica Acta* **75**: 6094-6111.

Bonin, P., and Gilewicz, M. (1991) A direct demonstration of co-respiration of oxygen and nitrogen oxides by *Pseudomonas nautica* - some spectral and kinetic properties of the respiratory components *Fems Microbiology Letters* **80**: 183-188.

Boudreau, B.P., Huettel, M., Forster, S., Jahnke, R.A., McLachlan, A., Middelburg, J.J. et al. (2001) Permeable marine sediments: Overturning an old paradigm. *Eos, Transactions American Geophysical Union* **82**: 133-136.

Budeus, G. (1989) Frontal Variability in the German Bight. *Scientia Marina* **53**.

Burkholder, J.M., Tomasko, D.A., and Touchette, B.W. (2007) Seagrasses and eutrophication. *Journal of Experimental Marine Biology and Ecology* **350**: 46-72.

Canfield, D.E., Thamdrup, B., and Kristensen, E. (2005) *Aquatic Geomicrobiology*: Elsevier Academic Press.

Canfield, D.E., Jørgensen, B.B., Fossing, H., Glud, R., Gundersen, J., Ramsing, N.B. et al. (1993) Pathways of organic-carbon oxidation in 3 continental-margin sediments. *Marine Geology* **113**: 27-40.

Cantera, J.J.L., and Stein, L.Y. (2007) Molecular diversity of nitrite reductase genes (nirK) in nitrifying bacteria. *Environmental Microbiology* **9**: 765-776.

Chen, C.C., Gong, G.C., and Shiah, F.K. (2007) Hypoxia in the East China Sea: one of the largest coastal low-oxygen areas in the world. *Mar Environ Res* **64**: 399-408.

Chen, F., Xia, Q., and Ju, L.K. (2003) Aerobic denitrification of *Pseudomonas aeruginosa* monitored by online NAD(P)H fluorescence. *Applied and Environmental Microbiology* **69**: 6715-6722.

Chen, J.W., and Strous, M. (2013) Denitrification and aerobic respiration, hybrid electron transport chains and co-evolution. *Biochimica Et Biophysica Acta-Bioenergetics* **1827**: 136-144.

Christensen, J.P., Smethie, W.M., and Devol, A.H. (1987) Benthic Nutrient Regeneration and Denitrification on the Washington Continental-Shelf. *Deep-Sea Research Part a-Oceanographic Research Papers* **34**: 1027-1047.

Codispoti, L.A. (2010) Interesting Times for Marine N<sub>2</sub>O. *Science* **327**: 1339-1340.

Codispoti, L.A., Brandes, J.A., Christensen, J.P., Devol, A.H., Naqvi, S.W.A., Paerl, H.W., and Yoshinari, T. (2001) The oceanic fixed nitrogen and nitrous oxide budgets: Moving targets as we enter the anthropocene? *Scientia Marina* **65**: 85-105.

Codispoti, L.A., J.W. Elkins, T. Yosinari, G.E. Friederich, C.M. Sakamoto and T.T. Packard. (1992) On the nitrous oxide flux from productive regions that contain low oxygen waters. In *Oceanography of the Indian Ocean*. Desai, B.N. (ed). New Delhi: Oxford and IBH, pp. 271-284.

Cook, P.L.M., Wenzhofer, F., Glud, R.N., Janssen, F., and Huettel, M. (2007) Benthic solute exchange and carbon mineralization in two shallow subtidal sandy sediments: Effect of advective pore-water exchange. *Limnology and Oceanography* **52**: 1943-1963.

Cook, P.L.M., Wenzhofer, F., Rysgaard, S., Galaktionov, O.S., Meysman, F.J.R., Eyre, B.D. et al. (2006) Quantification of denitrification in permeable sediments: Insights from a two-dimensional simulation analysis and experimental data. *Limnology and Oceanography-Methods* **4**: 294-307.

Dähnke, K., Emeis, K., Johannsen, A., and Nagel, B. (2010) Stable isotope composition and turnover of nitrate in the German Bight. *Marine Ecology Progress Series* **408**: 7-U26.

Dalsgaard, T., and Thamdrup, B. (2002) Factors controlling anaerobic ammonium oxidation with nitrite in marine sediments. *Applied and Environmental Microbiology* **68**: 3802-3808.

Dalsgaard, T., Thamdrup, B., and Canfield, D.E. (2005) Anaerobic ammonium oxidation (anammox) in the marine environment. *Research in Microbiology* **156**: 457-464.

de Beer, D., Wenzhofer, F., Ferdelman, T.G., Boehme, S.E., Huettel, M., van Beusekom, J.E.E. et al. (2005) Transport and mineralization rates in North Sea sandy intertidal sediments, Sylt-Romo Basin, Wadden Sea. *Limnology and Oceanography* **50**: 113-127.

Deek, A., Emeis, K., and van Beusekom, J. (2012) Nitrogen removal in coastal sediments of the German Wadden Sea. *Biogeochemistry* **108**: 467-483.

Dendooven, L., and Anderson, J.M. (1994) Dynamics of reduction enzymes involved in the denitrification process in pasture soil. *Soil Biology and Biochemistry* **26**: 1501-1506.

Diaz, R.J., and Rosenberg, R. (1995) Marine benthic hypoxia: A review of its ecological effects and the behavioural responses of benthic macrofauna. In *Oceanography and Marine Biology - an Annual Review, Vol 33*, pp. 245-303.

Diaz, R.J., and Rosenberg, R. (2008) Spreading dead zones and consequences for marine ecosystems. *Science* **321**: 926-929.

Dong, L.F., Sobey, M.N., Smith, C.J., Rusmana, I., Phillips, W., Stott, A. et al. (2011) Dissimilatory reduction of nitrate to ammonium, not denitrification or anammox, dominates benthic nitrate reduction in tropical estuaries. *Limnology and Oceanography* **56**: 279-291.

Dundee, L., and Hopkins, D.W. (2001) Different sensitivities to oxygen of nitrous oxide production by *Nitrosomonas europaea* and *Nitrosolobus multiformis*. *Soil Biology & Biochemistry* **33**: 1563-1565.

Emery, K.O. (1968) Relict sediments on continental shelves of world. *AAPG Bulletin* **52**: 445-464.



Evrard, V., Glud, R., and Cook, P.M. (2012) The kinetics of denitrification in permeable sediments. *Biogeochemistry*: 1-10.

Firestone, M.K., and Tiedje, J.M. (1979) Temporal Change in Nitrous Oxide and Dinitrogen from Denitrification Following Onset of Anaerobiosis. *Appl. Environ. Microbiol.* **38**: 673-679.

Frette, L., Gejlsbjerg, B., and Westermann, P. (1997) Aerobic denitrifiers isolated from an alternating activated sludge system. *Fems Microbiology Ecology* **24**: 363-370.

Froelich, P.N., Klinkhammer, G.P., Bender, M.L., Luedtke, N.A., Heath, G.R., Cullen, D. et al. (1979) Early oxidation of organic matter in pelagic sediments of the eastern equatorial Atlantic: suboxic diagenesis. *Geochimica et Cosmochimica Acta* **43**: 1075-1090.

Füssel, J., Lam, P., Lavik, G., Jensen, M.M., Holtappels, M., Gunter, M., and Kuypers, M.M.M. (2011) Nitrite oxidation in the Namibian oxygen minimum zone. *ISME J* **6**: 1200-1209.

Galloway, J.N., Dentener, F.J., Capone, D.G., Boyer, E.W., Howarth, R.W., Seitzinger, S.P. et al. (2004) Nitrogen Cycles: Past, Present, and Future. *Biogeochemistry* **70**: 153-226.

Gao, H., Schreiber, F., Collins, G., Jensen, M.M., Kostka, J.E., Lavik, G. et al. (2010) Aerobic denitrification in permeable Wadden Sea sediments. *Isme Journal* **4**: 417-426.

Gao, H., Matyka, M., Liu, B., Khalili, A., Kostka, J.E., Collins, G. et al. (2012) Intensive and extensive nitrogen loss from intertidal permeable sediments of the Wadden Sea. *Limnology and Oceanography* **57**: 185-198.

Glud, R.N., Thamdrup, B., Stahl, H., Wenzhoefer, F., Glud, A., Nomaki, H. et al. (2009) Nitrogen cycling in a deep ocean margin sediment (Sagami Bay, Japan). *Limnology and Oceanography* **54**: 723-734.

Grosskopf, T., Mohr, W., Baustian, T., Schunck, H., Gill, D., Kuypers, M.M.M. et al. (2012) Doubling of marine dinitrogen-fixation rates based on direct measurements. *Nature* **488**: 361-364.

Gruber, N., and Galloway, J.N. (2008) An Earth-system perspective of the global nitrogen cycle. *Nature* **451**: 293-296.

Grundmanis, V., and Murray, J.W. (1982) Aerobic respiration in pelagic marine-sediments. *Geochimica Et Cosmochimica Acta* **46**: 1101-1120.

Henriksen, K., and Kemp, W.M. (1988) Nitrification in estuarine and coastal marine sediments. *Scope* **33**: 207-249.

Hentschel, U., Berger, E.C., Bright, M., Felbeck, H., and Ott, J.A. (1999) Metabolism of nitrogen and sulfur in ectosymbiotic bacteria of marine nematodes (Nematoda, Stilbonematinae). *Marine Ecology Progress Series* **183**: 149-158.

Holtappels, M., Lavik, G., Jensen, M. M., and Kuypers, M. M. M. (2011) <sup>15</sup>N-Labeling Experiments to Dissect the Contributions of Heterotrophic Denitrification and Anammox to Nitrogen Removal in the OMZ Waters of the Ocean, p. 223-251. In *Methods in Enzymology*. Klotz, M.G. (ed).

Houghton J.T., D.Y., Griggs D.J., Noguier M., van der Linden P.J., Xiaosu D. (2001) Climate Change 2001: The Scientific Basis. . In *IPCC Third Assessment Report: Climate Change 2001 Cambridge University Press, Cambridge*.

Huang, H.K., and Tseng, S.K. (2001) Nitrate reduction by *Citrobacter diversus* under aerobic environment. *Applied Microbiology and Biotechnology* **55**: 90-94.

Huettel, M., and Gust, G. (1992) Impact of bioroughness on interfacial solute exchange in permeable sediments. *Marine Ecology Progress Series* **89**: 253-267.

Huettel, M., and Rusch, A. (2000) Transport and degradation of phytoplankton in permeable sediment. *Limnology and Oceanography* **45**: 534-549.

Huettel, M., and Webster, I. (2001) Porewater flow in permeable sediments. In *The benthic boundary layer*. Boudreau, B.P., and Jørgensen, B.B. (eds): Oxford Univ. Press., pp. 144-179.

Huettel, M., Ziebis, W., and Forster, S. (1996) Flow-induced uptake of particulate matter in permeable sediments. *Limnology and Oceanography* **41**: 309-322.

Huettel, M., Røy, H., Precht, E., and Ehrenhauss, S. (2003) Hydrodynamical impact on biogeochemical processes in aquatic sediments. *Hydrobiologia* **494**: 231-236.

Jansen, S., Walpersdorf, E., Werner, U., Billerbeck, M., Bottcher, M.E., and de Beer, D. (2009) Functioning of intertidal flats inferred from temporal and spatial dynamics of O<sub>2</sub>, H<sub>2</sub>S and pH in their surface sediment. *Ocean Dynamics* **59**: 317-332.

Janssen, F. (2004) Sediment surface topographies and bottom water flow: an in situ case-study on the fundamentals of pore-water advection. *Doctoral thesis: Pore water advection and organic matter mineralization in North Sea shelf sands*: 117-154.

Janssen, F., Huettel, M., and Witte, U. (2005) Pore-water advection and solute fluxes in permeable marine sediments (II): Benthic respiration at three sandy sites with different permeabilities (German Bight, North Sea). *Limnology and Oceanography* **50**: 779-792.

Jantti, H., and Hietanen, S. (2012) The Effects of Hypoxia on Sediment Nitrogen Cycling in the Baltic Sea. *Ambio* **41**: 161-169.

Jensen, M.M., Kuypers, M.M.M., Lavik, G., and Thamdrup, B. (2008) Rates and regulation of anaerobic ammonium oxidation and denitrification in the Black Sea. *Limnology and Oceanography* **53**: 23-36.

Jørgensen, B.B. (1977) The Sulfur Cycle of a Coastal Marine Sediment (Limfjorden, Denmark). *Limnology and Oceanography* **22**: 814-832.

Jørgensen, B.B., and Revsbech, N.P. (1989) Oxygen-Uptake, Bacterial Distribution, and Carbon-Nitrogen-Sulfur Cycling in Sediments from the Baltic Sea North-Sea Transition. *Ophelia* **31**: 29-49.

Jørgensen, K., Jensen, H., and Sørensen, J. (1984) Nitrous oxide production from nitrification and denitrification in marine sediment at low oxygen concentrations. *Canadian Journal of Microbiology* **30**: 1073-1078.

Kamp, A., de Beer, D., Nitsch, J.L., Lavik, G., and Stief, P. (2011) Diatoms respire nitrate to survive dark and anoxic conditions. *Proceedings of the National Academy of Sciences* **108**: 5649-5654.

Kartal, B., de Almeida, N.M., Maalcke, W.J., Op den Camp, H.J.M., Jetten, M.S.M., and Keltjens, J.T. (2013) How to make a living from anaerobic ammonium oxidation. *FEMS Microbiology Reviews* **37**: 428-461.

Keil, R.G., Tsamakis, E., Fuh, C.B., Giddings, J.C., and Hedges, J.I. (1994) Mineralogical and Textural Controls on the Organic Composition of Coastal Marine-

Sediments - Hydrodynamic Separation Using Splitt-Fractionation. *Geochimica Et Cosmochimica Acta* **58**: 879-893.

Kelso, B.H.L., Smith, R.V., Laughlin, R.J., and Lennox, S.D. (1997) Dissimilatory nitrate reduction in anaerobic sediments leading to river nitrite accumulation. *Applied and Environmental Microbiology* **63**: 4679-4685.

Kieskamp, W.M., Lohse, L., Epping, E., and Helder, W. (1991) Seasonal-variation in denitrification rates and nitrous oxide fluxes in intertidal sediments of the western Wadden Sea. *Marine Ecology-Progress Series* **72**: 145-151.

Kim, M., Jeong, S.-Y., Yoon, S.J., Cho, S.J., Kim, Y.H., Kim, M.J. et al. (2008) Aerobic Denitrification of *Pseudomonas putida* AD-21 at Different C/N Ratios. *Journal of Bioscience and Bioengineering* **106**: 498-502.

King, D., and Nedwell, D.B. (1987) The adaptation of the nitrate-reducing bacterial communities in estuarine sediments in response to overlying nitrate load. *Fems Microbiology Ecology* **45**: 15-20.

Kleiner, M., Wentrup, C., Lott, C., Teeling, H., Wetzel, S., Young, J. et al. (2012) Metaproteomics of a gutless marine worm and its symbiotic microbial community reveal unusual pathways for carbon and energy use. *Proceedings of the National Academy of Sciences* **109**: 1173-1182.

Konneke, M., Bernhard, A.E., de la Torre, J.R., Walker, C.B., Waterbury, J.B., and Stahl, D.A. (2005) Isolation of an autotrophic ammonia-oxidizing marine archaeon. *Nature* **437**: 543-546.

Lam, P., and Kuypers, M.M.M. (2011) Microbial Nitrogen Cycling Processes in Oxygen Minimum Zones. In *Annual Review of Marine Science, Vol 3*, pp. 317-345.

Law, C.S., and Owens, N.J.P. (1990) Denitrification and nitrous oxide in the North Sea. *Netherlands Journal of Sea Research* **25**: 65-74.

Lloyd, D., Boddy, L., and Davies, K.J.P. (1987) Persistence of bacterial denitrification capacity under aerobic condition - the rule rather than the exception. *Fems Microbiology Ecology* **45**: 185-190.

Loebl, M., Dolch, T., and van Beusekom, J.E.E. (2007) Annual dynamics of pelagic primary production and respiration in a shallow coastal basin. *Journal of Sea Research* **58**: 269-282.

Lohse, L., Malschaert, J.F.P., Slomp, C.P., Helder, W., and van Raaphorst, W. (1993) Nitrogen cycling in North Sea sediments: interaction of denitrification and nitrification in offshore and coastal areas. *Marine Ecology-Progress Series* **101**: 283-283.

Lotze, H., Reise, K., Worm, B., van Beusekom, J., Busch, M., Ehlers, A. et al. (2005) Human transformations of the Wadden Sea ecosystem through time: a synthesis. *Helgoland Marine Research* **59**: 84-95.

Marzocchi, U., Revsbech, N.P., Nielsen, L.P., and Risgaard-Petersen, N. (2012) Distant electric coupling between nitrate reduction and sulphide oxidation investigated by an improved nitrate microscale biosensor. In *EGU*. Vienna, Austria.

Meysman, F.J.R., Galaktionov, O.S., Cook, P.L.M., Janssen, F., Huettel, M., and Middelburg, J.J. (2007) Quantifying biologically and physically induced flow and tracer dynamics in permeable sediments. *Biogeosciences* **4**: 627-646.

Middelburg, J., Klaver, G., Nieuwenhuize, J., Markusse, R., Vlug, T., and Nat, F. (1995) Nitrous oxide emissions from estuarine intertidal sediments. *Hydrobiologia* **311**: 43-55.

Middelburg, J.J., Soetaert, K., Herman, P.M.J., and Heip, C.H.R. (1996) Denitrification in marine sediments: A model study. *Global Biogeochemical Cycles* **10**: 661-673.

Moir, J.W.B., and Wood, N.J. (2001) Nitrate and nitrite transport in bacteria. *Cellular and Molecular Life Sciences* **58**: 215-224.

Molina, V., Ulloa, O., Farias, L., Urrutia, H., Ramirez, S., Junier, P., and Witzel, K.-P. (2007) Ammonia-oxidizing beta-Proteobacteria from the oxygen minimum zone off northern Chile. *Applied and Environmental Microbiology* **73**: 3547-3555.

Mulder, A., Vandegraaf, A.A., Robertson, L.A., and Kuenen, J.G. (1995) Anaerobic ammonium oxidation discovered in a denitrifying fluidized bed reactor. *Fems Microbiology Ecology* **16**: 177-183.

Musat, N., Werner, U., Knittel, K., Kolb, S., Dodenhof, T., van Beusekom, J.E.E. et al. (2006) Microbial community structure of sandy intertidal sediments in the North Sea, Sylt-Romo Basin, Wadden Sea. *Systematic and Applied Microbiology* **29**: 333-348.

Naqvi, S.W.A., Jayakumar, D.A., Narvekar, P.V., Naik, H., Sarma, V.V.S.S., D'Souza, W. et al. (2000) Increased marine production of N<sub>2</sub>O due to intensifying anoxia on the Indian continental shelf. *Nature* **408**: 346-349.

Nielsen, L.P. (1992) Denitrification in Sediment Determined from Nitrogen Isotope Pairing. *Fems Microbiology Ecology* **86**: 357-362.

Ostrom, N.E., Russ, M.E., Popp, B., Rust, T.M., and Karl, D.M. (2000) Mechanisms of nitrous oxide production in the subtropical North Pacific based on determinations of the isotopic abundances of nitrous oxide and di-oxygen. *Chemosphere - Global Change Science* **2**: 281-290.

Otte, S., Kuenen, J.G., Nielsen, L.P., Paerl, H.W., Zopfi, J., Schulz, H.N. et al. (1999) Nitrogen, carbon, and sulfur metabolism in natural Thioploca samples. *Applied and Environmental Microbiology* **65**: 3148-3157.

Paetsch, J., Serna, A., Daehnke, K., Schlarbaum, T., Johannsen, A., and Emeis, K.-C. (2010) Nitrogen cycling in the German Bight (SE North Sea) - Clues from modelling stable nitrogen isotopes. *Continental Shelf Research* **30**: 203-213.

Patriqui, D., and Knowles, R. (1972) Nitrogen fixation in rhizosphere of marine angiosperms. *Marine Biology* **16**: 49-&.

Patureau, D., Davison, J., Bernet, N., and Moletta, R. (1994) Denitrification under various aeration conditions in *Comamonas* sp. strain SGLY2. *Fems Microbiology Ecology* **14**: 71-78.

Patureau, D., Zumstein, E., Delgenes, J.P., and Moletta, R. (2000) Aerobic denitrifiers isolated from diverse natural and managed ecosystems. *Microbial Ecology* **39**: 145-152.

Pomowski, A., Zumft, W.G., Kroneck, P.M.H., and Einsle, O. (2011) N<sub>2</sub>O binding at a [4Cu:2S] copper-sulphur cluster in nitrous oxide reductase. *Nature* **477**: 234-U143.

Porubsky, W.P., Weston, N.B., and Joye, S.B. (2009) Benthic metabolism and the fate of dissolved inorganic nitrogen in intertidal sediments. *Estuarine Coastal and Shelf Science* **83**: 392-402.

Precht, E., and Huettel, M. (2003) Advective pore-water exchange driven by surface gravity waves and its ecological implications. *Limnology and Oceanography* **48**: 1674-1684.

Preisler, A., de Beer, D., Lichtschlag, A., Lavik, G., Boetius, A., and Jørgensen, B.B. (2007) Biological and chemical sulfide oxidation in a Beggiatoa inhabited marine sediment. *Isme Journal* **1**: 341-353.

Rabalais, N.N. (2002) Nitrogen in aquatic ecosystems. *Ambio* **31**: 102-112.

Rao, A.M.F., McCarthy, M.J., Gardner, W.S., and Jahnke, R.A. (2008) Respiration and denitrification in permeable continental shelf deposits on the South Atlantic Bight:  $N_2$ : Ar and isotope pairing measurements in sediment column experiments. *Continental Shelf Research* **28**: 602-613.

Ravishankara, A.R., Daniel, J.S., and Portmann, R.W. (2009) Nitrous Oxide ( $N_2O$ ): The Dominant Ozone-Depleting Substance Emitted in the 21st Century. *Science* **326**: 123-125.

Reise, K., Baptist, M., Burbridge, P., Dankers, N., Fischer, L., Flemming, B. et al. (2010) The Wadden Sea-A universally outstanding tidal wetland. *The Wadden Sea 2010. Common Wadden Sea Secretariat (CWSS); Trilateral Monitoring and Assessment Group: Wilhelmshaven. (Wadden Sea Ecosystem; 29/editors, Harald Marencic and Jaap de Vlas)* **7**.

Reiss, H., Wieking, G., and KrÄ¶ncke, I. (2007) Microphytobenthos of the Dogger Bank: a comparison between shallow and deep areas using phytopigment composition of the sediment. *Marine Biology* **150**: 1061-1071.

Rick, H.J., Rick, S., Tillmann, U., Brockmann, U., Gaertner, U., Duerselen, C., and Suendermann, J. (2006) Primary productivity in the German Bight (1994-1996). *Estuaries and Coasts* **29**: 4-23.

Risgaard-Petersen, N., Nielsen, L.P., Rysgaard, S., Dalsgaard, T., and Meyer, R.L. (2003) Application of the isotope pairing technique in sediments where anammox and denitrification coexist. *Limnology and Oceanography-Methods* **1**: 63-73.

Robertson, L.A., and Kuenen, J.G. (1984) Aerobic denitrification - a controversy revived. *Archives of Microbiology* **139**: 351-354.

Robertson, L.A., and Kuenen, J.G. (1988) Heterotrophic nitrification in *Thiosphaera pantotropha* - oxygen uptake and enzyme studies. *Journal of General Microbiology* **134**: 857-863.

Robertson, L.A., Dalsgaard, T., Revsbech, N.P., and Kuenen, J.G. (1995) Confirmation of aerobic denitrification in batch cultures, using gas-chromatography and  $N_{15}$  mass spectrometry. *Fems Microbiology Ecology* **18**: 113-119.

Robertson, L.A., Cornelisse, R., Devos, P., Hadjoetomo, R., and Kuenen, J.G. (1989) Aerobic denitrification in various heterotrophic nitrifiers. *Antonie Van Leeuwenhoek Journal of Microbiology* **56**: 289-299.

Rusch, A., Huettel, M., Reimers, C.E., Taghon, G.L., and Fuller, C.M. (2003) Activity and distribution of bacterial populations in Middle Atlantic Bight shelf sands. *Fems Microbiology Ecology* **44**: 89-100.

Sayama, M. (2001) Presence of nitrate-accumulating sulfur bacteria and their influence on nitrogen cycling in a shallow coastal marine sediment. *Applied and Environmental Microbiology* **67**: 3481-3487.

Seitzinger, S.P., Kroeze, C., and Styles, R.V. (2000) Global distribution of N<sub>2</sub>O emissions from aquatic systems: natural emissions and anthropogenic effects. *Chemosphere - Global Change Science* **2**: 267-279.

Shapleigh, J.P. (2011) Oxygen control of nitrogen oxide respiration, focusing on alpha-proteobacteria. *Biochemical Society Transactions* **39**: 179-183.

Shaw, L.J., Nicol, G.W., Smith, Z., Fear, J., Prosser, J.I., and Baggs, E.M. (2006) Nitrosospira spp. can produce nitrous oxide via a nitrifier denitrification pathway. *Environmental Microbiology* **8**: 214-222.

Sokoll, S., Holtappels, M., Lam, P., Collins, G., Schluter, M., Lavik, G., and Kuypers, M.M.M. (2012) Benthic nitrogen loss in the arabian sea off pakistan. *Frontiers in microbiology* **3**: 395-395.

Song, G.D., Liu, S.M., Marchant, H., Kuypers, M.M.M., and Lavik, G. (2013) Anaerobic ammonium oxidation, denitrification and dissimilatory nitrate reduction to ammonium in the East China Sea sediment. *Biogeosciences Discuss.* **10**: 4671-4710.

Sorensen, J., and Jørgensen, B.B. (1987) Early diagenesis in sediments from Danish coastal waters: Microbial activity and Mn-Fe-S geochemistry. *Geochimica et Cosmochimica Acta* **51**: 1583-1590.

Sorensen, J., Jørgensen, B.B., and Revsbech, N.P. (1979) Comparison of oxygen, nitrate, and sulfate respiration in coastal marine sediments. *Microbial Ecology* **5**: 105-115.

Stein, L.Y., and Yung, Y.L. (2003) Production, isotopic composition, and atmospheric fate of biologically produced nitrous oxide. *Annual Review of Earth and Planetary Sciences* **31**: 329-356.

Stouthamer, A.H., deBoer, A.P.N., vanderOost, J., and vanSpanning, R.J.M. (1997) Emerging principles of inorganic nitrogen metabolism in *Paracoccus denitrificans* and related bacteria. *Antonie Van Leeuwenhoek International Journal of General and Molecular Microbiology* **71**: 33-41.

Straub, K.L., Benz, M., Schink, B., and Widdel, F. (1996) Anaerobic, nitrate-dependent microbial oxidation of ferrous iron. *Applied and Environmental Microbiology* **62**: 1458-1460.

Strohm, T.O., Griffin, B., Zumft, W.G., and Schink, B. (2007) Growth Yields in Bacterial Denitrification and Nitrate Ammonification. *Applied and Environmental Microbiology* **73**: 1420-1424.

Strous, M., Fuerst, J.A., Kramer, E.H.M., Logemann, S., Muyzer, G., van de Pas-Schoonen, K.T. et al. (1999) Missing lithotroph identified as new planctomycete. *Nature* **400**: 446-449.

Stueven, R., Vollmer, M., and Bock, E. (1992) The impact of organic matter on nitric oxide formation by *Nitrosomonas europaea*. *Archives of Microbiology* **158**: 439-443.

Sündermann, J. (1997) The PRISMA project: an investigation of processes controlling contaminant fluxes in the German Bight. *Marine Ecology Progress Series* **156**: 239-243.

Teske, A., Alm, E., Regan, J.M., Toze, S., Rittmann, B.E., and Stahl, D.A. (1994) Evolutionary relationships among ammonia oxidizing and nitrite oxidizing bacteria. *Journal of Bacteriology* **176**: 6623-6630.

Thamdrup, B., and Dalsgaard, T. (2002) Production of N<sub>2</sub> through anaerobic ammonium oxidation coupled to nitrate reduction in marine sediments. *Applied and Environmental Microbiology* **68**: 1312-1318.

Thamdrup, B., Fossing, H., and Jørgensen, B.B. (1994) Manganese, iron, and sulfur cycling in a coastal marine sediment, Aarhus bay, Denmark. *Geochimica Et Cosmochimica Acta* **58**: 5115-5129.

Tiedje, J.M. (1988) Ecology of denitrification and dissimilatory nitrate reduction to ammonium. In *Biology of Anaerobic Microorganisms*. Zehnder, A.J.B. (ed). New York, NY, USA: Wiley, pp. 179-244.

Trimmer, M., and Nicholls, J.C. (2009) Production of nitrogen gas via anammox and denitrification in intact sediment cores along a continental shelf to slope transect in the North Atlantic. *Limnology and Oceanography* **54**: 577-589.

Trimmer, M., and Engstrom, P. (2011) Distribution, activity, and ecology of anammox bacteria in aquatic environments. In *Nitrification*, pp. 201-235.

Usui, T., Koike, I., and Ogura, N. (2001) N<sub>2</sub>O Production, Nitrification and Denitrification in an Estuarine Sediment. *Estuarine, Coastal and Shelf Science* **52**: 769-781.

van Beusekom, J.E.E. (2005) A historic perspective on Wadden Sea eutrophication. *Helgoland Marine Research* **59**: 45-54.

van Beusekom, J.E.E., and Diel-Christiansen, S. (2009) Global change and the biogeochemistry of the North Sea: the possible role of phytoplankton and phytoplankton grazing. *International Journal of Earth Sciences* **98**: 269-280.

van Beusekom, J.E.E., Brockmann, U.H., Hesse, K.J., Hickel, W., Poremba, K., and Tillmann, U. (1999) The importance of sediments in the transformation and turnover of nutrients and organic matter in the Wadden Sea and German Bight. *Deutsche Hydrografische Zeitschrift* **51**: 245-266.

Van De Graaf, A.A., De Bruijn, P., Robertson, L.A., Jetten, M.S.M., and Kuenen, J.G. (1997) Metabolic pathway of anaerobic ammonium oxidation on the basis of <sup>15</sup>N studies in a fluidized bed reactor. *Microbiology (Reading)* **143**: 2415-2421.

Vitousek, P.M., Aber, J.D., Howarth, R.W., Likens, G.E., Matson, P.A., Schindler, D.W. et al. (1997) Human alteration of the global nitrogen cycle: Sources and consequences. *Ecological Applications* **7**: 737-750.

Volkenborn, N., Polerecky, L., Wetthey, D.S., and Woodin, S.A. (2010) Oscillatory porewater bioadvection in marine sediments induced by hydraulic activities of *Arenicola marina*. *Limnology and Oceanography* **55**: 1231-1247.

Wang, B. (2006) Cultural eutrophication in the Changjiang (Yangtze River) plume: History and perspective. *Estuarine, Coastal and Shelf Science* **69**: 471-477.

Ward, B.B. (2008) Nitrification in marine systems. In *Nitrogen in the Marine Environment*. D.G. Capone, D.A.B., and M.R. Mulholland, a.E.J.C. (eds). Amsterdam: Elsevier Press, pp. 199–262.

Werner, U., Billerbeck, M., Polerecky, L., Franke, U., Huettel, M., van Beusekom, J.E.E., and de Beer, D. (2006) Spatial and temporal patterns of mineralization rates and oxygen distribution in a permeable intertidal sand flat (Sylt, Germany). *Limnology and Oceanography* **51**: 2549-2563.

Wiebe, W.J., Johannes, R.E., and Webb, K.L. (1975) Nitrogen fixation in a coral reef community. *Science* **188**: 257-259.

Wilkinson, C.R., and Fay, P. (1979) Nitrogen fixation in coral reef sponges with symbiotic cyanobacteria. *Nature* **279**: 527-529.

Zhou, M.-j., Shen, Z.-l., and Yu, R.-c. (2008) Responses of a coastal phytoplankton community to increased nutrient input from the Changjiang (Yangtze) River. *Continental Shelf Research* **28**: 1483-1489.

Zopfi, J., Kjaer, T., Nielsen, L.P., and Jørgensen, B.B. (2001) Ecology of *Thioploca* spp.: Nitrate and sulfur storage in relation to chemical microgradients and influence of *Thioploca* spp. on the sedimentary nitrogen cycle. *Applied and Environmental Microbiology* **67**: 5530-5537.

Zuberer, D.A., and Silver, W.S. (1978) Biological dinitrogen fixation (acetylene-reduction) associated with Florida mangroves. *Applied and Environmental Microbiology* **35**: 567-575.

Zumft, W.G. (1997) Cell biology and molecular basis of denitrification. *Microbiology and Molecular Biology Reviews* **61**: 533-616.



## Chapter II

### **Anammox, denitrification and dissimilatory nitrate reduction to ammonium in the East China Sea sediment**

G. D. Song<sup>1</sup>, S. M. Liu<sup>1</sup>, H. K. Marchant<sup>2</sup>, M. M. M. Kuypers<sup>2</sup>, G. Lavik<sup>2</sup>

<sup>1</sup>Key Laboratory of Marine Chemistry Theory and Technology, Ministry of Education, College of Chemistry and Chemical Engineering, Ocean University of China, 238 Songling Road, 266100 Qingdao, China

<sup>2</sup>Max Planck Institute for Marine Microbiology, Celsiusstrasse 1 D-28359 Bremen, Germany}

\*Corresponding author: S. M. Liu ([sumeiliu@ouc.edu.cn](mailto:sumeiliu@ouc.edu.cn))

Contributions to the manuscript:

G.D.S., S.M.L., G.K. designed research. G.D.S., carried out fieldwork., G.D.S., and H.K.M., prepared and measured samples, G.D.S., H.K.M., and G.L., analyzed and interpreted data and G.D.S., S.M.L., G.K., H.K.M and M.M.M.K conceived, wrote and edited the manuscript.

**Published in Biogeosciences; 10, 6851–6864, 2013**

**<http://www.biogeosciences.net/10/6851/2013/bg-10-6851-2013.html>**

### **Acknowledgements**

The authors sincerely thank L. X. Li, and W. D. Zhai, the captain of R/V *Kexue No. 3* and the chief scientist of the NSFC cruise, for their cooperation. L. Xing, H. L. Zhang, D. K. Huang and L. Gu at OUC and ECUN are also thanked for their assistance during the sediment collection; we thank A. R. Sheik in MPI for his help with the manuscript; We also thank T. Kalvelage and J. Füssel from MPI for their help with the N<sub>2</sub> isotope ratio analysis and Z. M. Ning for his help on the sediment organic matter measurement. We thank three reviewers for their constructive comments and suggestions to improve this manuscript. This study is financially supported by the National Science Foundation of China (NSFC: 40925017), the Ministry of Science & Technology of China (No. 2011CB409802), the NSFC 40876054 and China Scholarship Council (No. 2011633021) and the Max Planck Society.

Edited by: K. Küsel

**Abstract**

Benthic nitrogen transformation pathways were investigated in the sediment of the East China Sea (ECS) in June of 2010 using the  $^{15}\text{N}$  isotope pairing technique. Slurry incubations indicated that denitrification, anammox and dissimilatory nitrate reduction to ammonium (DNRA) as well as intracellular nitrate release occurred in the ECS sediments. These four processes did not exist independently, nitrate release therefore diluted the  $^{15}\text{N}$  labeling fraction of  $\text{NO}_3^-$ , and a part of the  $^{15}\text{NH}_4^+$  derived from DNRA also formed  $^{30}\text{N}_2$  via anammox. Therefore current methods of rate calculations led to over and underestimations of anammox and denitrification respectively. Following the procedure outlined in Thamdrup and Dalsgaard (2002), denitrification rates were slightly underestimated by an average 6% without regard to the effect of nitrate release, while this underestimation could be counteracted by the presence of DNRA. On the contrary, anammox rates calculated from  $^{15}\text{NO}_3^-$  experiment were significantly overestimated by 42% without considering nitrate release. In our study, this overestimation could only be compensated 14% by taking DNRA into consideration. In a parallel experiment amended with  $^{15}\text{NH}_4^+ + ^{14}\text{NO}_3^-$ , anammox rates were not significantly influenced by DNRA due to the high background of  $^{15}\text{NH}_4^+$  addition. The significant correlation between potential denitrification rate and sediment organic matter content ( $r=0.68$ ,  $p<0.001$ , Pearson) indicated that denitrification was regulated by organic matter, while, no such correlations were found for anammox and DNRA. The relative contribution of anammox to the total N-loss increased from 13% at the shallowest site near the Changjiang estuary to 50% at the deepest site on the outer shelf, implying the significant role of anammox in benthic nitrogen cycling in the ECS sediments, especially on the outer shelf. N-loss as  $\text{N}_2$  was the main pathway, while DNRA was also an important pathway accounting for 20-31% of benthic nitrate reduction in the ECS. Our study demonstrates the complicated interactions among different benthic nitrogen transformations and the importance of considering denitrification, DNRA, anammox and nitrate release together when designing and interpreting

future studies.

## 1 Introduction

The East China Sea (ECS) is one of the most expansive continental shelf seas, bounded on the west by mainland China and on the east by the western Pacific Ocean island chain (Fig. 1). On the west coast, there is a large freshwater input to the ECS from the Changjiang (Yangtze River) (Beardsley et al., 1985), while on the east outer shelf; the ECS interacts tightly with the Kuroshio, a warm and salty west boundary current. Due to the strong influence of the river input and western boundary current, the ECS exhibits a complex current system, leading to unique nutrient dynamics (Zhang et al., 2007). Nutrient enriched water is restricted to the west inner shelf, where it is influenced by the Changjiang Diluted Water (CDW), while the outer shelf is dominated by the oligotrophic Kuroshio Surface Water (KSW).

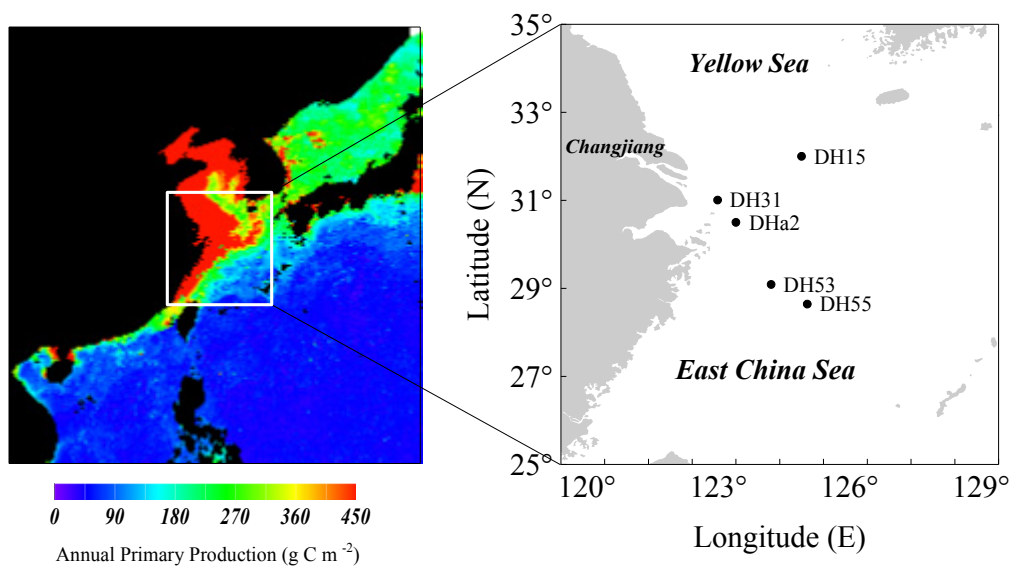


Fig. 1. Sampling locations in the East China Sea. The primary production map is from: [http://marine.rutgers.edu/opp/swf/Production/gif\\_files/PP\\_Month\\_9806B.gif](http://marine.rutgers.edu/opp/swf/Production/gif_files/PP_Month_9806B.gif)

Anthropogenic activities have exponentially increased the fixed nitrogen concentrations in the Changjiang estuary by a factor of 3-5 from the 1960s to the end of the 1990s (Wang, 2006; Zhou et al., 2008). In response to increased nutrients, the phytoplankton standing stock has also increased, as has the occurrence and

scale of harmful algal blooms (Zhou et al., 2008). Consequently, eutrophication has become a severe problem in the Changjiang estuary (Zhang et al., 2007), and hypoxic events in the bottom water off the Changjiang estuary have been reported extensively during the past decade (Zhu et al., 2011). N-loss from sediments via denitrification and anammox is the major N sink on continental shelves (Christensen et al., 1987; Trimmer and Nicholls, 2009); however most studies within the ECS have focused only on benthic nutrient fluxes and nitrous oxide (Aller et al., 1985; Zhang et al., 2010), while benthic N-loss has only been investigated at a tidal flat (Wang, et al., 2006).

Denitrification, anammox and dissimilatory nitrate reduction to ammonium (DNRA) are microbially mediated nitrate reduction pathways. Denitrification, in which nitrate is sequentially reduced to  $N_2$  under anaerobic conditions has been found in numerous anaerobic sediments. Anammox, which represents the reduction of nitrite coupled to ammonia oxidation (Mulder et al., 1995), is generally considered to be less important than denitrification but can also account for up to 60-80% of N-loss in some benthic sediments (Engström et al., 2005; Thamdrup and Dalsgaard, 2002). DNRA is an alternative pathway, by which nitrate is reduced to bio-available ammonium, thus, no fixed N-loss occurs (An and Gardner, 2002; Koike and Hattori, 1978). Progressively over the last few decades, the importance of DNRA in sediment has been recognized (Dong et al., 2011; Gardner et al., 2006; Koike and Hattori, 1978). For example, DNRA was demonstrated to be the dominant pathway of the benthic nitrate reduction in the tropical estuarine sediment (Dong et al., 2011), it has also been demonstrated that DNRA can be performed by fermentative bacteria (Tiedje, 1988). Meanwhile, it has also been shown that both nitrate storing bacteria (Preisler et al., 2007) and diatoms can perform DNRA (Kamp et al., 2011). Therefore it is now recognized that DNRA, and nitrate storage by organisms performing it, are important parts of the benthic nitrogen cycle (Lomstein et al., 1990; Risgaard-Petersen et al., 2006). Denitrification and anammox represent pathways which remove fixed N from marine systems, therefore they can play a role in

reducing eutrophication, and meanwhile DNRA recycles fixed nitrogen which can then be assimilated by primary producers.

Although there have been several reports of the coexistence of anammox, denitrification and DNRA (Bohlen et al., 2011; Dong et al., 2009; Prokopenko et al., 2006; Trimmer and Nicholls, 2009), the contribution of each process in benthic nitrate reduction were not fully studied. The co-occurrence of these processes represented a problem when using the traditional  $^{15}\text{N}$  isotope pairing technique (Kartal et al., 2007; Sokoll et al., 2012), as the presence of DNRA may have influenced the apparent isotope distribution of anammox and denitrification. Briefly,  $^{15}\text{NH}_4^+$  derived from DNRA could have combined with  $^{15}\text{NO}_2^-$  (derived from  $^{15}\text{NO}_3^-$  dissimilatory reduction) via anammox to form  $^{30}\text{N}_2$ , the same product as denitrification (Jensen et al., 2011; Kartal et al., 2007). In the study by Jensen et al (2011), anammox and DNRA was shown to produce  $^{30}\text{N}_2$  in incubations with  $^{15}\text{NO}_2^-$ , however their calculation approach only works in the absence of denitrification. Spott and Stange (2007) developed an approach to calculate anammox and denitrification rates precisely to avoid the influence of DNRA in open steady-state incubation systems. However, our study, as well as the majority of experimental studies of nutrient cycling in marine sediments is carried out in a closed incubation system. Moreover, if nitrate was stored intracellularly by nitrate storing organisms, use of the isotope pairing technique would be further complicated, as this would represent an excess source of  $^{14}\text{NO}_3^-$  (Glud et al., 2009; Sokoll et al., 2012). While aerobic denitrification combined with aerobic ammonium oxidation are further processes which could complicate benthic N-cycling in the permeable sediments (Gao et al., 2010), all of our experiments were carried out under anaerobic conditions so these were not in the scope of this study.

In this study, we investigated the nitrate reduction and N-loss pathways within sediments of the ECS continental shelf in slurry incubations using the  $^{15}\text{N}$  isotope pairing technique. The influence of nitrate release and DNRA on anammox and denitrification calculations was examined quantitatively.

## 2 Materials and methods

### 2.1 Sample collection and preparation

Sediment was collected at five sites from the Changjiang estuary to the outer shelf of the ECS during a cruise on the *R/V Kexue No. 3* from 8 to 22 June, 2010 (Fig. 1 and Table 1). All the sediment samples were collected using a Soutar-type box corer on board; only samples with an undisturbed sediment surface and clear overlying water were used for the subsequent experiments. The bottom water used in the slurry incubations (~2 m above the seafloor) was sampled using Niskin bottles equipped with conductivity, temperature and pressure sensors and stored in 10 L clean polyethylene bottles placed in a seawater bath in dim light. Sediment cores for bulk organic chemical parameters and pore water extraction were collected with large Plexiglas liners (i.d.=9.5 cm, height=60 cm). Sediment cores for the slurry incubation were collected with small Plexiglas liners (i.d.=5 cm, height=30 cm). Sediment cores for chemical and physical parameters were sectioned at 1-cm intervals, frozen for future analysis and subsequently freeze-dried. Water content of sediments was calculated by weight difference before and after drying.

The overlying water above the sediment surface was collected and filtered through 0.45  $\mu\text{m}$  syringe filters, and then poisoned by addition of saturated  $\text{HgCl}_2$  for nutrient analysis with a final  $\text{Hg}^{2+}$  concentration of  $\sim 100 \text{ mg L}^{-1}$ . Sediment cores for pore water extraction were sectioned immediately after collection at 0.5-cm intervals in the upper 5 cm and at 1-cm intervals for the following 15 cm, and at 2-cm intervals for the remainder of the cores. Pore water was extracted using Rhizon Soil Moisture Samplers (19.21.23F Rhizon CSS, Netherlands) (Liu et al., 2011; Seeberg-Elverfeldt et al., 2005). The pore water samples were preserved as described previously.

### 2.2 $^{15}\text{N}$ slurry incubations

$^{15}\text{N}$  tracer sediment slurry incubations, which allow determination of potential rates,

have commonly been used to investigate benthic nitrogen transformations (Dähnke et al., 2012; Risgaard-Petersen et al., 2004; Thamdrup and Dalsgaard, 2002). In this study, slurry incubations were conducted in gastight bags as described by Thamdrup and Dalsgaard (2002) to evaluate the presence of anammox, denitrification and DNRA. Briefly, the cores (i.d.=5 cm) were sectioned into 2-cm slices from the sediment surface down to 8 cm depth, each slice was then mixed with 270 ml He pre-degassed bottom seawater in a gastight plastic bag. The slurries were degassed, and pre-incubated in the dark at room temperature for 24-36 hrs.

After pre-incubation,  $^{15}\text{NH}_4^+$ ,  $^{15}\text{NH}_4^+ + ^{14}\text{NO}_3^-$  and  $^{15}\text{NO}_3^-$  were added to the incubation bags ( $^{15}\text{N}$  atom%, 99.3%, Campro Scientific, Berlin). The experiment amended with  $^{15}\text{NH}_4^+$  was used as a control experiment (denoted as E\_Ctrl), the experiment amended with  $^{15}\text{NH}_4^+ + ^{14}\text{NO}_3^-$  was conducted to confirm the presence of anammox (denoted as E\_Amox) and the experiment amended with  $^{15}\text{NO}_3^-$  was conducted to quantify each process' contribution to nitrate reduction (denoted as E\_Denit) (Table 2). In all experiments, the tracers were amended to a final concentration of 100  $\mu\text{M}$ . After each tracer injection and mixing, subsamples were immediately filled into 6 ml Exetainer vials (Labco Ltd, High Wycombe, UK) with 0.1 ml pre-added saturated  $\text{HgCl}_2$ . The temperature of the incubations was between 18-24 °C at different sites (Table 1). In the following 8-12 h, bags were periodically shaken to ensure that the labeled N compounds were homogeneously distributed and 5 subsamples were withdrawn in each experiment. Exetainer vials containing the subsamples were sealed and stored at room temperature upside down until subsequent  $\text{N}_2$  isotope ratio analysis.

### 2.3 Chemical analysis

The concentrations of  $\text{NH}_4^+$ ,  $\text{NO}_3^-$  and  $\text{NO}_2^-$  in pore water and slurry incubation samples were determined on a segmented flow autoanalyzer (SAN plus, SKALAR) with the standard spectrophotometric methods. The limit of detection for  $\text{NH}_4^+$ ,  $\text{NO}_3^-$  and  $\text{NO}_2^-$  was 0.5  $\mu\text{M}$ , 0.06  $\mu\text{M}$ , 0.01  $\mu\text{M}$ , respectively, with a precision of ~5%.



The sediment organic matter content was expressed as the percent of weight loss on ignition (LOI %), determined by combustion at 550 °C for 4 hours.

Before N<sub>2</sub> analysis, a 1 ml headspace of helium was introduced to the sample and equilibrated after shaking, isotopic compositions of the N<sub>2</sub> gas were determined by gas chromatography-isotope ratio mass spectrometry (GC-IRMS; VG Optima, Manchester, UK) at Max Planck Institute for Marine Microbiology, Bremen and the concentrations of <sup>29</sup>N<sub>2</sub> and <sup>30</sup>N<sub>2</sub> were calculated following Holtappels et al. (2011).

After the measurement of N<sub>2</sub> isotope ratios in the sample from E\_Denit and E\_Amox, 2 ml of remaining sample was filtered into a new 6 ml Exetainer and treated with hypobromite, converting <sup>15</sup>NH<sub>4</sub><sup>+</sup> to <sup>29</sup>N<sub>2</sub> and <sup>30</sup>N<sub>2</sub> (Preisler et al., 2007; Warembourg, 1993), after which the N<sub>2</sub> isotope ratios were measured using the GC-IRMS as described above.

#### 2.4 Rate calculations

The potential rates of anammox, denitrification and DNRA were calculated from the production of <sup>29</sup>N<sub>2</sub>, <sup>30</sup>N<sub>2</sub> and <sup>15</sup>NH<sub>4</sub><sup>+</sup> in the slurry incubation using two methods. The first used the quantification technique of Thamdrup and Dalsgaard (2002).

$$D_{(E\_Denit)} = P_{30} / F_N^2 \quad (1)$$

$$A_{(E\_Denit)} = [P_{29} - 2 \times (1 / F_N - 1) \times P_{30}] / F_N \quad (2)$$

Where,  $D_{(E\_Denit)}$  and  $A_{(E\_Denit)}$  denoted the potential rates of denitrification and anammox in E\_Denit, respectively.  $P_{29}$  and  $P_{30}$  were the production rate of <sup>29</sup>N<sub>2</sub> and <sup>30</sup>N<sub>2</sub> in E\_Denit.  $F_N$  represented the <sup>15</sup>NO<sub>3</sub><sup>-</sup> fraction in E\_Denit, which was determined from the difference in NO<sub>3</sub><sup>-</sup> before and after <sup>15</sup>NO<sub>3</sub><sup>-</sup> addition.

For the experiment of E\_Amox, the potential anammox rate was,

$$A_{(E\_Amox)} = P_{29(E\_Amox)} / F_{A(E\_Amox)} \quad (3)$$

Where,  $A_{(E\_Amox)}$ ,  $P_{29(E\_Amox)}$  and  $F_{A(E\_Amox)}$  represented the total N<sub>2</sub> production by anammox, production of <sup>29</sup>N<sub>2</sub> and <sup>15</sup>NH<sub>4</sub><sup>+</sup> labeling fraction in E\_Amox.

Significant nitrate release and DNRA occurred in our samples (see Sects. 3 and 4), violating the assumptions on which the procedure of Thamdrup and Dalsgaard (2002) was based. Nitrate release from nitrate storing organisms diluted the  $^{15}\text{NO}_3^-$  fraction in E\_Denit, and  $^{15}\text{NH}_4^+$  production via DNRA would combine with  $^{15}\text{NO}_3^-$  to produce  $^{30}\text{N}_2$  through anammox. Therefore we adapted the previous calculation to take this into account.

First, only the effects of nitrate release by nitrate storing organisms were considered. As proposed by Sokoll et al. (2012), we assumed the anammox rate in E\_Denit equaled that from E\_Amox, then the derived  $^{15}\text{NO}_3^-$  fraction ( $F_N^*$ ) could be calculated through Eq. (2) where  $A_{(E\_Denit)}$  was substituted by  $A_{(E\_Amox)}$ .

$$F_N^* = \frac{(P_{29} + 2 \times P_{30}) - \sqrt{(P_{29} + 2 \times P_{30})^2 - 8 \times A_{(E\_Amox)} \times P_{30}}}{2 \times A_{(E\_Amox)}} \quad (4)$$

If  $F_N^*$  is significantly less than  $F_N$ , nitrate release will occur (Sokoll et al., 2012). In this situation, the following calculation would use  $F_N^*$  instead of  $F_N$ ,  $D_{(E\_Denit)}$  and  $A_{(E\_Denit)}$  in Eqs. (1) and (2) would be recalculated and denoted as  $D_{(E\_Denit)}^*$  and  $A_{(E\_Denit)}^*$ . The excess  $^{14}\text{NO}_3^-$  contributed by nitrate release would be calculated according to Sokoll et al. (2012),

$$\text{Excess } ^{14}\text{NO}_3^- = ^{15}\text{NO}_3^- \times (1/F_N^* - 1/F_N) \quad (5)$$

Secondly, the effects of DNRA on the calculation of anammox and denitrification rates were considered. According to the principle of isotope pairing, in E\_Denit, for anammox,

$$A_{29} = A_{(E\_Denit)}^* \times [F_N^* \times (1 - F_A) + F_A \times (1 - F_N^*)] \quad (6)$$

$$A_{30} = A_{(E\_Denit)}^* \times F_N^* \times F_A \quad (7)$$

For denitrification,

$$D_{29} = D_{(E\_Denit)}^* \times 2 \times F_N^* \times (1 - F_N^*) \quad (8)$$

$$D_{30} = D_{(E\_Denit)}^* \times (F_N^*)^2 \quad (9)$$

$$\text{And, } P_{29} = A_{29} + D_{29}, \quad P_{30} = A_{30} + D_{30} \quad (10)$$

Where,  $A_{29}$  and  $A_{30}$  denoted the production of  $^{29}\text{N}_2$  and  $^{30}\text{N}_2$  by anammox.  $D_{29}$  and  $D_{30}$  represented the production of  $^{29}\text{N}_2$  and  $^{30}\text{N}_2$  through denitrification.  $F_A$  represented the fraction of  $^{15}\text{NH}_4^+$  in E\_Denit during the incubation. At each timepoint,  $F_A$  could be calculated by the  $^{15}\text{NH}_4^+$  concentration and total  $\text{NH}_4^+$  concentration.

Here,  $A_{30}$  was the key parameter linking anammox, denitrification and DNRA. By combining Eqs. (6) to (10), we got,

$$A_{30} = \frac{F_A \times [P_{29} \times F_N^* - 2 \times (1 - F_N^*) \times P_{30}]}{F_N^* \times (1 - F_A) - F_A \times (1 - F_N^*)} \quad (11)$$

Then, the revised anammox and denitrification rates could be calculated by Eqs. (7) and (12),

$$D_{(E\_Denit)}^* = [P_{30} - A_{30}] / (F_N^*)^2 \quad (12)$$

Usually,  $F_N^*$  in the anoxic slurry incubations would be constant assuming nitrate release happened only at the beginning as a result of mixing the slurries before subsampling (Sokoll et al., 2012). However, if DNRA occurred,  $F_A$  and  $A_{30}$  would successively increase over time. We have developed a step by step method to quantify the non-linear  $^{30}\text{N}_2$  production via anammox (Song et al., in prep.). However, from the data in present study, we found that  $F_A$  was a semi-linear increase with time, therefore we applied an average  $F_A$  during the incubation instead of the actual  $F_A$  at each time point to calculate anammox rate.

The DNRA rate could be derived from the accumulation rate of  $^{15}\text{NH}_4^+$  in E\_Denit, however, as mentioned above, a part of  $^{15}\text{NH}_4^+$  would form  $^{30}\text{N}_2$  via anammox. Thus,

$$DNRA = (P_{^{15}\text{NH}_4^+} + A_{30}) / F_N^* \quad (13)$$

Where,  $P_{^{15}\text{NH}_4^+}$  was the linear slope of apparent  $^{15}\text{NH}_4^+$  production with time.

DNRA would also influence the anammox rate calculation in E\_Amox as  $^{14}\text{NH}_4^+$  produced by DNRA and remineralization also diluted the  $^{15}\text{NH}_4^+$  fraction. We found

that the fraction of  $^{15}\text{NH}_4^+$  in E\_Amox decreased linearly with time, thus,  $F_{A(E\_Amox)}$  could be replaced by the average value in formula (3).

If we assumed that the denitrification rate in E\_Amox and E\_Denit was equal, then the relative contribution of anammox to the total N-loss in E\_Amox would be,

$$ra = \frac{A_{(E\_Amox)}}{A_{(E\_Amox)} + D_{(E\_Denit)}^*} \quad (14)$$

The production rates of  $^{29}\text{N}_2$ ,  $^{30}\text{N}_2$  and  $^{15}\text{NH}_4^+$  for corrected anammox, denitrification and DNRA rates were calculated from the slope of concentrations versus time. The normality of dependent variable was tested by the Kolmogorov-Smirnov method and standard deviation of the linear rate was derived from the slope standard deviation given by the regression statistic; Pearson correlation was applied to discuss the correlation analysis. The significance level was 0.05. All the statistics were carried out in statistical software (SigmaStat 3.5). To eliminate the discrepancies between in situ bottom water temperature and the incubation temperature, all the rates were corrected to the in situ temperature using the Arrhenius equation assuming average apparent activation energy of  $61 \text{ kJ mol}^{-1}$  for all species (Aller et al., 1985). The average temperature correction factor was 0.7.

### 3 Results

#### 3.1 Water column and sediment characteristics

Bottom seawater and sediment characteristics were investigated at five stations (Table 1). The bottom water  $\text{NO}_3^-$  decreased sharply from the estuary ( $\sim 27 \mu\text{M}$ ) to the outer shelf ( $\sim 2 \mu\text{M}$ ).

Sediment pore water profiles of  $\text{NO}_3^-$  and  $\text{NO}_2^-$  varied from site to site (Fig. 2), as these samples were extracted by Rhizon sampler, any stored nitrate products were excluded in the pore water data. At sites DH31 and DHa2 the nitrate concentration sharply decreased to  $< 0.5 \mu\text{M}$  within the upper 1 cm. Nitrate peaked in the layer from 3 to 5 cm at DHa2 with an average  $\text{NO}_3^-$  concentration of  $13 \mu\text{M}$ , indicating

active nitrification or advection of nitrate rich water into the sediment at this depth. At sites DH53 and DH15, there was a nitrate peak in the upper 2 cm, below this, nitrate concentration sharply declined and was  $<0.5 \mu\text{M}$  below 4 cm. At site DH55,  $\text{NO}_3^-$  mirrored the bottom water concentration then increased to  $67 \mu\text{M}$  at 2 cm, after which it decreased sharply to  $\sim 2 \mu\text{M}$  at 5 cm. A second nitrate peak of  $\sim 10 \mu\text{M}$  was found at 6-7 cm and then decreased to  $<1 \mu\text{M}$  from 7 to 10 cm. The nitrite profile in the pore water was similar to the nitrate but generally one order of magnitude lower in concentration. Pore water  $\text{NH}_4^+$  concentrations generally increased with depth (Fig. 2). Several  $\mu\text{M}$  of ammonium in the upper 0-1 cm of the sediment at most stations indicate that there was a flux of ammonium towards the bottom waters.

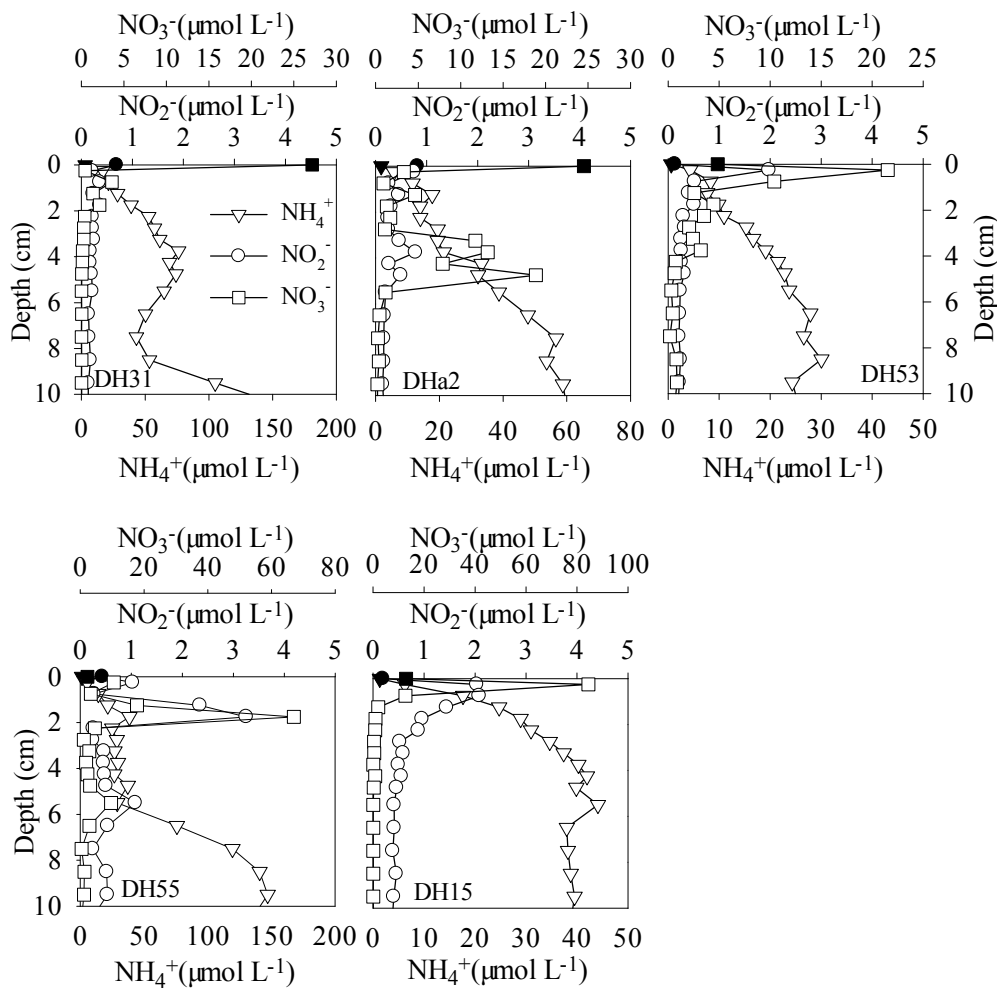


Fig. 2. Pore water profiles of  $\text{NO}_2^-$ ,  $\text{NO}_3^-$  and  $\text{NH}_4^+$  in the East China Sea sediment. The black symbols represent overlying water data.

Table 1 Sampling locations and some general characteristics of bottom water and sediment. The porosity and organic matter content (expressed as LOI%) are the average of the top 8 cm, and data in parentheses represent the variation range.

Station	Latitude (N)	Longitude (E)	Depth (m)	Bottom water Temp. (°C)	Bottom water Salinity (psu)	Bottom water NO <sub>3</sub> <sup>-</sup> (μM)	Sediment type	Porosity	LOI (%)	Incubation temperature (°C)
DH31	30°57.389'	122°33.922'	19.0	19.40	26.40	27.16	Clayey silt	0.78 (0.65-0.88)	6.2 (4.7-7.2)	23.5
DHa2	30°30.077'	122°59.915'	57.8	18.68	34.08	24.51	Silt-clay-sand	0.71 (0.60-0.87)	5.6 (5.0-6.3)	24.0
DH53	29°05.338'	123°48.202'	78.0	19.58	34.36	4.86	Silt-clay-sand	0.74 (0.61-0.87)	5.3 (4.2-6.8)	24.0
DH55	28°38.571'	124°37.672'	86.4	18.72	34.43	2.23	Fine sand	0.54 (0.50-0.61)	3.6 (3.3-3.8)	23.0
DH15	32°00.010'	124°29.794'	41.4	14.70	31.04	13.12	Silty sand	0.62 (0.52-0.75)	3.8 (3.2-4.1)	18.0

Table 2 Slurry incubation approaches performed in this study.

Experiment name	Tracer added	Tracer concentration ( $\mu\text{M}$ )	Isotopes measured	Process targeted
E_Ctrl	$^{15}\text{NH}_4^+$	100	$^{29}\text{N}_2, ^{30}\text{N}_2$	Control experiment
E_Amox	$^{15}\text{NH}_4^+ + ^{14}\text{NO}_3^-$	100+100	$^{29}\text{N}_2, ^{30}\text{N}_2$	Anammox
E_Denit	$^{15}\text{NO}_3^-$	100	$^{29}\text{N}_2, ^{30}\text{N}_2, ^{15}\text{NH}_4^+$	Denitrification and DNRA

### 3.2 $^{15}\text{N}$ slurry incubations

After 24-36 hours pre-incubation in E\_Ctrl,  $\text{NO}_3^-$  was still present in some sediment layers (5~15  $\mu\text{M}$ ), especially in the surface layer (0-2 cm) (Table 3). In those layers with residual  $\text{NO}_3^-$ , significant  $^{29}\text{N}_2$  accumulation was observed (Fig. 3a and Supplementary 1). Although some  $^{30}\text{N}_2$  was observed in a few layers, it was generally one to two magnitudes lower than  $^{29}\text{N}_2$  and not quantitatively important (<1%). Therefore we did not take it into account in later calculations. In the surface layers of DH53 and DH15,  $\text{NO}_3^-$  was not detectable (<1  $\mu\text{M}$ ) after pre-incubation (Table 3), however there was neither measurable  $^{29}\text{N}_2$  nor  $^{30}\text{N}_2$  production ( $p>0.05$ ) during the incubation (Fig. 3b and Supplementary 1). Therefore no coupled nitrification-denitrification in the slurry was observed, and other pathways of anaerobic ammonium oxidation that were of any significance could almost be excluded, e.g.  $\text{MnO}_2$  (Luther et al., 1997) and  $\text{Fe}(\text{OH})_3$  (Yang et al., 2012). This ensured that all the  $^{29}\text{N}_2$  production in E\_Amox was from anammox (see below).

Anammox was observed in E\_Amox incubations:  $^{29}\text{N}_2$  accumulated at all sites over time, while there was no measurable production of  $^{30}\text{N}_2$  (Fig. 3 and Supplementary 1).

Table 3. Nitrate concentration after pre-incubation,  $^{15}\text{NO}_3^-$  labeling fraction ( $F_N$ ) and excess nitrate stored by nitrate storing organisms in each layer. n.d.: not detectable

Station	Layer	$\text{NO}_3^-$ concentration after pre-incubation	$F_N$	Excess nitrate
	(cm)	( $\mu\text{M}$ )	(%)	( $\text{nmol cm}^{-3}$ )
DH31	0-2	15.1	90.7	64
	2-4	9.4	94.2	2.6
	4-6	7.0	95.8	12
	6-8	7.4	95.4	n.d.
DHa2	0-2	9.3	93.9	63
	2-4	8.0	94.2	37
	4-6	6.1	95.8	21
	6-8	9.1	93.4	n.d.
DH53	0-2	0.2	99.2	83
	2-4	0.2	99.2	n.d.
	4-6	0.3	99.1	n.d.
	6-8	0.2	99.2	n.d.
DH55	0-2	10.7	93.2	n.d.
	2-4	1.8	98.8	58
	4-6	1.8	98.8	n.d.
	6-8	2.0	98.8	57
DH15	0-2	0.2	99.2	16
	2-4	0.2	99.1	42
	4-6	0.2	99.1	50
	6-8	0.5	98.9	n.d.



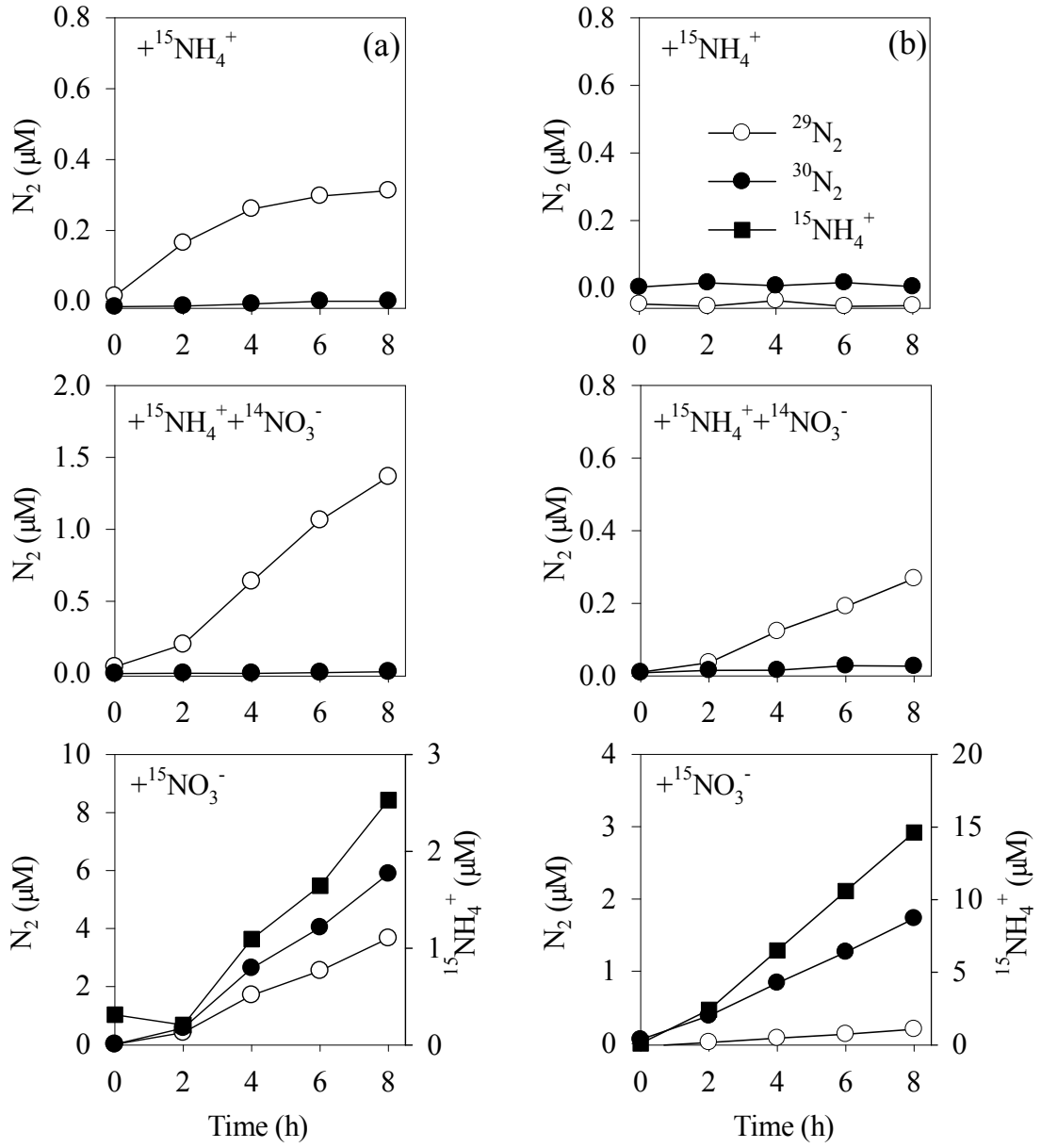


Fig. 3. Production of  $^{29}\text{N}_2$ ,  $^{30}\text{N}_2$  and  $^{15}\text{NH}_4^+$  against time in slurry incubation. (a) DH31 0-2 cm sediment. The residual nitrate was not exhausted after the 24 hrs pre-incubation, thus we observed a slight  $^{29}\text{N}_2$  production before all the nitrate disappeared; (b) DH15 6-8 cm sediment. The nitrate was less than  $1\ \mu\text{M}$  after pre-incubation, hence we did not detect significant  $^{29}\text{N}_2$  production.

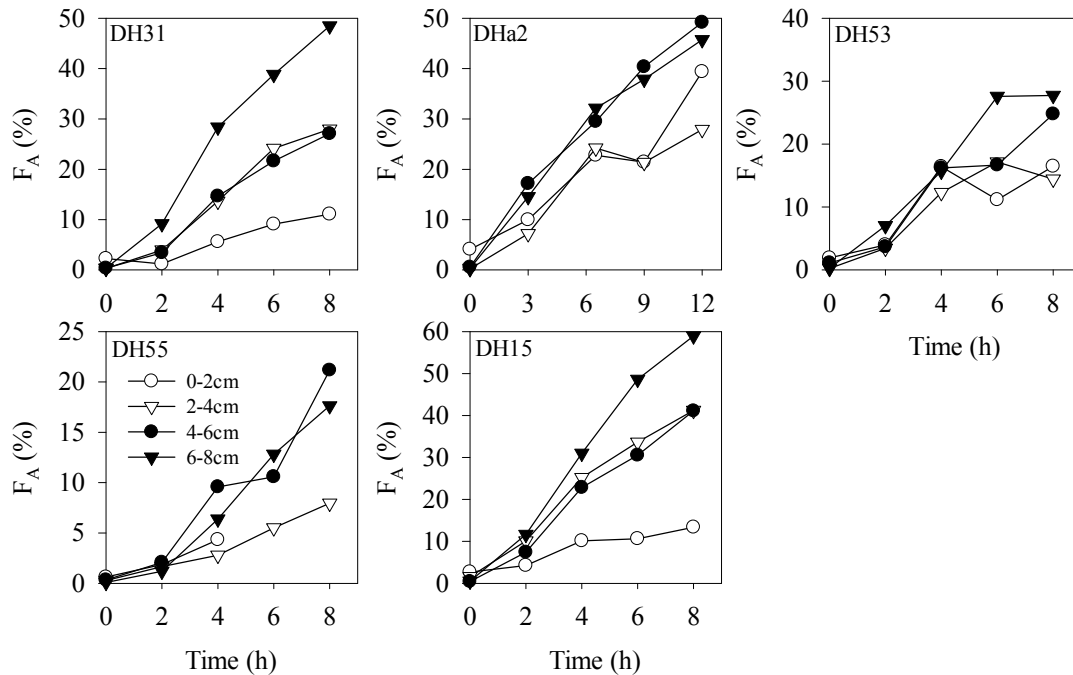


Fig. 4. Time course of  $^{15}\text{NH}_4^+$  fraction ( $F_A$ ) in  $E_{\text{Denit}}$ .

In  $E_{\text{Denit}}$ ,  $^{29}\text{N}_2$  and  $^{30}\text{N}_2$  were produced along with  $^{15}\text{NH}_4^+$  (Fig. 3 and Supplementary 1). This showed that dissimilatory nitrate reduction to ammonium (DNRA) occurred concurrently with anammox and denitrification. Nitrate was not a limiting factor in  $E_{\text{Amox}}$  and  $E_{\text{Denit}}$ . Both  $^{15}\text{NH}_4^+$  and  $F_A$  accumulated linearly over time in all sediment layers ( $r^2 > 0.9$ ,  $p < 0.05$ ) (Figs. 3 and 4). Thus, we used the average  $F_A$  to calculate the  $^{30}\text{N}_2$  production via anammox.

### 3.3 Nitrate storage and release in the sediment

$\text{NO}_3^-$  release occurred at all the sites in the 0-2 cm layer except DH55, at this site  $\text{NO}_3^-$  release was detected in 2-4 cm and 6-8 cm layers. Generally, the decline of  $F_N$

caused by nitrate release ranged from 0.3-10% with an average of 5.1%. The calculated excess  $^{14}\text{NO}_3^-$  ranged from 3 to 83  $\text{nmol cm}^{-3}$  with an average of 42  $\text{nmol cm}^{-3}$  (Table 3).

### 3.4 N-loss and nitrate reduction in slurry incubation

Denitrification rates calculated from the method of Thamdrup and Dalsgaard (2002) ranged from 0.6 to 20  $\text{nmol N cm}^{-3} \text{ h}^{-1}$  and the average denitrification rate showed a decrease from 14  $\text{nmol N cm}^{-3} \text{ h}^{-1}$  at site DH31, close to the coast, to 2.0  $\text{nmol N cm}^{-3} \text{ h}^{-1}$  at site DH55 furthest from the coast (Fig. 5).

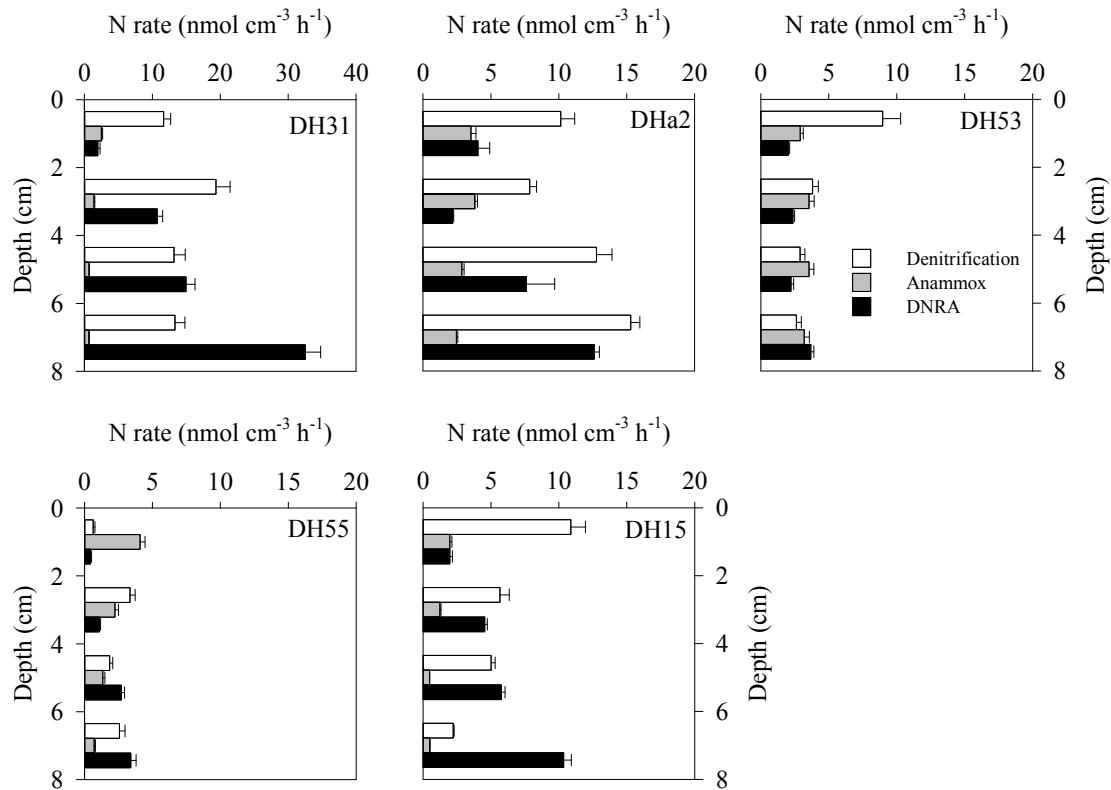


Fig. 5. Vertical distributions of potential denitrification (white bar), anammox (grey bar) and DNRA (black bar) rates in sediment of the ECS from the slurry incubation. The error bar ( $\pm 1$  SE) was calculated from the linear slope standard deviation given by the regression statistic.

Anammox rates from E\_Denit, as calculated using the method of Thamdrup and Dalsgaard (2002) ranged from 0.3 to 4.6  $\text{nmol N cm}^{-3} \text{ h}^{-1}$  with an average of 2.0  $\text{nmol N cm}^{-3} \text{ h}^{-1}$ , after correction for nitrate release and DNRA, the anammox rate in

$E_{\text{Denit}}$  ranged from 0.3 to 3.5  $\text{nmol N cm}^{-3} \text{ h}^{-1}$  with an average of 1.6  $\text{nmol N cm}^{-3} \text{ h}^{-1}$ . Anammox rates were also calculated from the  $E_{\text{Amox}}$  incubation, before the correction by nitrate release and DNRA, anammox ranged from 0.4 to 4.0  $\text{nmol N cm}^{-3} \text{ h}^{-1}$  with an average of 2.1  $\text{nmol N cm}^{-3} \text{ h}^{-1}$ . After correction by DNRA and remineralization, there was a slight increase (~4%). The highest anammox rate was found in the surface layer of site DH55 which was located at the outer shelf of the ECS (Fig. 5).

DNRA rates varied from 0.4 to 33  $\text{nmol N cm}^{-3} \text{ h}^{-1}$  with an average of 6.4  $\text{nmol N cm}^{-3} \text{ h}^{-1}$ . The average DNRA rate decreased from 15  $\text{nmol N cm}^{-3} \text{ h}^{-1}$  at site DH31 to 1.9  $\text{nmol N cm}^{-3} \text{ h}^{-1}$  at site DH55 (Fig. 5).

Denitrification rates decreased with increasing sediment depth at sites DH53 and DH15, while at other sites denitrification rates generally showed a slight increase with increasing sediment depth (Fig. 5). Anammox rates generally decreased with increasing sediment depth at all sites except DH53 (Fig. 5). DNRA rate at all sites generally increased with increasing sediment depth (Fig. 5).

Integrated anammox, denitrification and DNRA potential rates were calculated down to the  $\text{NO}_x^-$  penetration depth where the nitrate+nitrite concentration no longer decreased significantly with sediment depth. The penetration depth of  $\text{NO}_x^-$  at each site was constrained to 3 cm for DH31, 7 cm for DHa2, 5 cm for DH15, 5 cm for DH53 and 8 cm for DH55. All the integrated denitrification, anammox and DNRA rates showed highest values at site DHa2. At all sites except DHa2, integrated denitrification rates generally decreased with the increasing water depth (Fig. 6a). Opposite to this, the depth integrated anammox rates increased by a factor of 2.7 with increasing water depth. Hence, the relative contribution of anammox to the total N-loss exhibited a significant increasing trend with water depth ( $r=0.93$ ,  $p=0.02$ , Pearson), from 13% at site closest to the coast DH31 to 50% at the furthest from the coast, DH55. The contribution of the integrated DNRA rate to the integrated total nitrate reduction rate (sum of DNRA, anammox and denitrification) varied from 23% to 31% with an average of 26% (Fig. 6b).

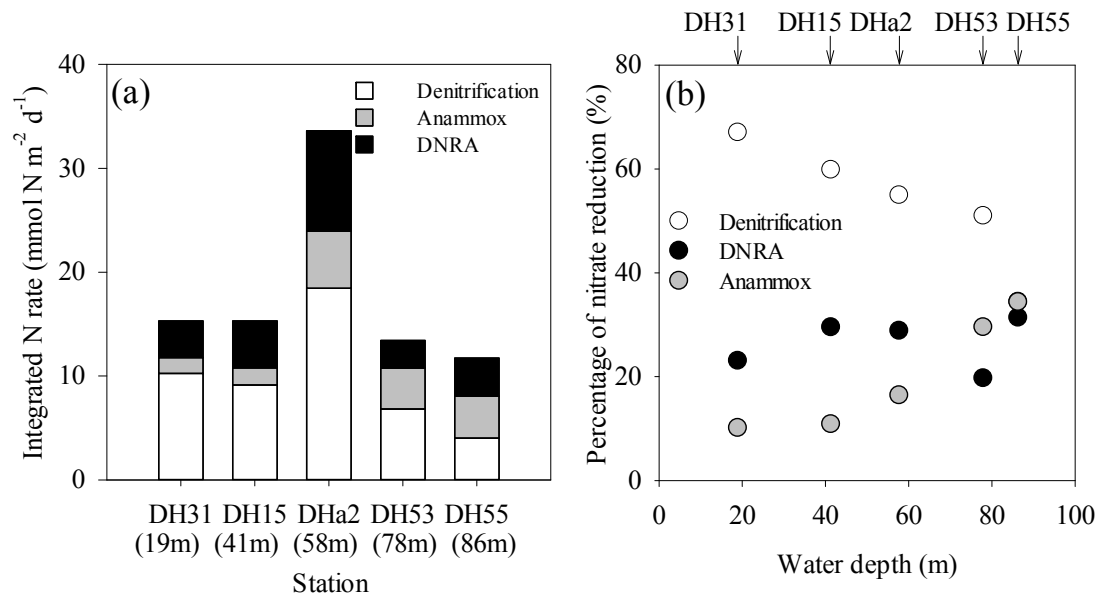


Fig. 6. Total nitrate reduction from denitrification, anammox and DNRA (a) and relative contribution of denitrification, anammox and DNRA as a function of water depth (b).

## 4 Discussion

### 4.1 The influence of nitrate release and DNRA on anammox and denitrification rates calculation with isotope pairing method

Intracellular nitrate storage has been observed in diverse environments (An and Gardner, 2002; Risgaard-Petersen et al., 2006; Thamdrup, 2012), where it was carried out by a diverse range of benthic organisms, such as sulfur oxidizing bacteria (Fossing et al., 1995; Schulz et al., 1999; Sweerts et al., 1990), benthic foraminifera (Glud et al., 2009; Risgaard-Petersen et al., 2006) and diatoms (Lomas and Glibert, 2000; Lomstein et al., 1990). Many of these micro-organisms reduce their intracellular nitrate stores to ammonium (DNRA, Kamp et al., 2011; Otte et al., 1999; Preisler et al., 2007). Therefore the combined effect of intracellular nitrate storage and DNRA on the isotope pairing method calculations needs to be considered.

The influence of nitrate release on benthic N-loss rate calculation was discussed by Sokoll et al. (2012); therefore we will only briefly discuss this here. The equilibrium

and exchange of added labeled  $^{15}\text{NO}_3^-$  with an intracellularly stored  $^{14}\text{NO}_3^-$  pool may be related to nitrate release after addition of  $^{15}\text{NO}_3^-$  and lead to a decrease of  $F_N$  (Dähnke et al., 2012; Sokoll et al., 2012). As a result, our denitrification rates were underestimated according to Eq. (1), while anammox rates were overestimated according to Eq. (2). As  $F_N$  decreased by 0.3-10%, the underestimation of denitrification rates in this study ranged from 0 to 19% with an average of 6% (Fig. 7a). However, the overestimation of anammox rates varied from 10 to 128% with an average of 42% in  $E_{\text{Denit}}$  (Fig. 7d). Excluding four samples for which we could not calculate  $F_N^*$  (for more detailed information see Supplementary material 2), all other anammox rates were consistent from the two experiments (Fig. 8a). Consequently we used Eq. (14) to evaluate the relative contribution of anammox to the total N-loss. So far nitrate storage has not been fully considered in most published benthic anammox rates, thus, the relative contribution of anammox to total N-loss in these studies might be overestimated to some extent when determined from  $^{15}\text{NO}_x^-$  experiments.

Potentially the presence of DNRA would affect the anammox and denitrification rate calculations used in previous isotope pairing technique calculation methods (Holtappels et al., 2011; Nielsen, 1992; Risgaard-Petersen et al., 2003; Thamdrup and Dalsgaard, 2002). Denitrification rates would be overestimated and anammox would be underestimated following the procedure of Thamdrup and Dalsgaard (2002), thus counteracting the influence of nitrate release to some extent. In our study denitrification rates were only slightly overestimated (~1%) if we did not take the measured DNRA into account (Fig. 7b). Combined with the effect of nitrate release, the actual denitrification rate was only underestimated by 2.5% in this study (Fig. 7c), below the coefficient of variation for the experiments (~10%). Contrary to the denitrification rates, anammox rates were underestimated by 16% in  $E_{\text{Denit}}$  without considering DNRA (Fig. 7e). The net effect was that anammox rates would be overestimated by 10% if we followed the calculation procedure of Thamdrup and Dalsgaard (2002) in this study (Fig. 7f). In  $E_{\text{Amox}}$ , anammox rates increased by 4% after DNRA correction (Fig. 8b) since  $F_A$  did not decline significantly

due to the high background of  $^{15}\text{NH}_4^+$  ( $\sim 100 \mu\text{M}$ ). Previous studies had shown the effect of DNRA on denitrification and anammox (Nicholls and Trimmer, 2009; Trimmer et al., 2003), however, they did not quantify the effect. Our correction calculation in this study allows quantification of the extent of the effects of DNRA on denitrification and anammox rates calculation when  $^{15}\text{N}$  isotope pairing method was applied.

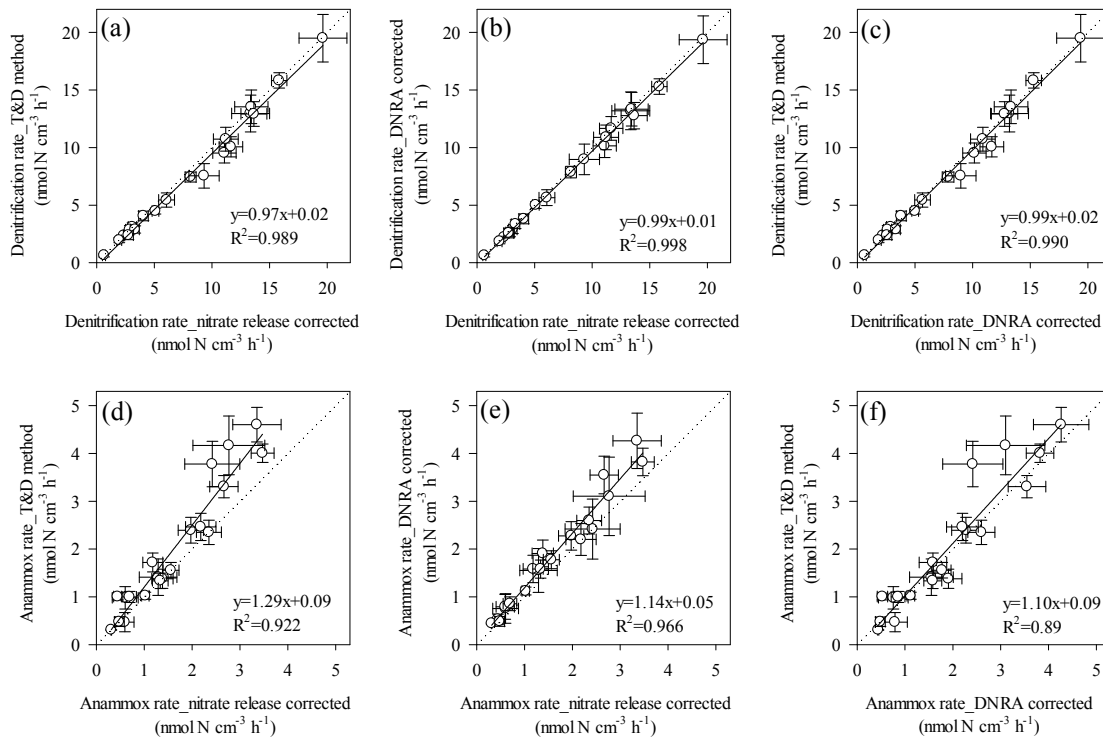


Fig. 7. The influence of nitrate release and DNRA on anammox and denitrification rates in the experiment amended with  $^{15}\text{NO}_3^-$ . T&D method: Thamdrup and Dalsgaard (2002). Nitrate release corrected: the rate calculation corrected by nitrate release. DNRA corrected: after nitrate release correction, the rate calculation was corrected by DNRA. See Sect. 2.4 Rate calculations for more detailed information. The dotted line represents the 1:1 line. The linear regression is shown for the interpretation of different processes effects on the anammox and denitrification rates.

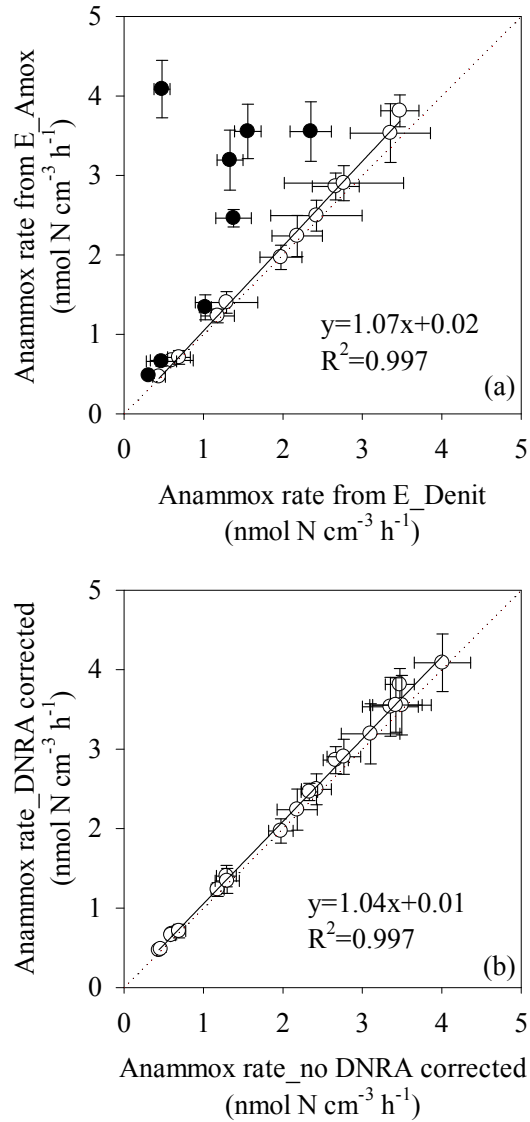


Fig. 8. Comparison of anammox rates from  $E\_Denit$  and  $E\_Amox$  (a) and DNRA effects on the anammox rate in  $E\_Amox$  (b). The black dot represents the anammox rate calculated from  $E\_Denit$  derived from the original  $F_N$  since we can not calculate  $F_N^*$  or  $F_N^* > F_N$  according Eq. (4). The anammox from  $E\_Denit$  is the rate only after nitrate release correction.

#### 4.2 Distribution and regulation of anammox, denitrification and DNRA in ECS sediments

The vertical distribution of potential rates for denitrification, anammox and DNRA may reflect environmental controlling factors in the sediment. In the sediment, nitrate availability in the pore water has usually been considered as a key factor



controlling denitrification rates (Seitzinger, 1990). The decrease of potential denitrification rates with sediment depth at DH53 and DH15 reflected the regulation of denitrification rates by pore water nitrate concentrations (Fig. 2 and Fig. 5). This pattern was consistent with the result of Laverman et al. (2007) and Sokoll et al. (2012). Oxygen is often considered as an inhibitor for denitrification and included in denitrification models (Laverman et al., 2007; Middelburg et al., 1996), but this would only effect the uppermost mm in cohesive sediments (Glud et al., 2008; Lohse et al., 1996). Moreover, denitrification and anammox seem to be less effected by oxygen in non-cohesive sediments and waters with regular intrusions of oxygen (Gao et al., 2010; Kalvelage et al., 2011). As we did not measure oxygen penetration in our incubation sediments, we can only speculate if i.e. the lower denitrification rate in 0-2 cm layer at sandy site DH55 (Fig. 5) could be a reflection of oxygen inhibition on denitrification or organic matter limitation due to oxic respiration.

The availability of organic carbon was also a key factor regulating heterotrophic denitrification. A positive correlation between potential volumetric denitrification rate and organic matter (LOI %) ( $r=0.68$ ,  $p<0.001$ , Pearson), indicated that organic matter content was an important environmental regulator of denitrification. Meanwhile, the integrated denitrification rate also decreased from the shallow coastal site to the outer shelf site except DHa2 (Fig. 6a), agreeing well with the distribution of primary production and/or organic carbon export in the ECS (Gong et al., 2003).

Ammonium concentrations in the pore waters were not limiting for anammox activity at our study (Fig. 2). The decreasing pattern of potential anammox rates at four sites in this study may imply that pore water nitrate and/or nitrite regulated anammox rates (Fig. 2 and Fig. 5). Availability of nitrate and/or nitrite as electron acceptors is considered an important factor controlling anammox (Dalsgaard et al., 2005). Nitrite could be derived from nitrification or nitrate reduction as the first step of denitrification and DNRA in the sediment. Besides, it has been demonstrated that

anammox bacteria could also perform dissimilatory nitrate reduction alone (Kartal et al., 2007). Here, relatively high anammox rates corresponded well with the elevated  $\text{NO}_3^-$  and/or  $\text{NO}_2^-$  concentrations in the surface 2 cm layer; this was very consistent with results from the Arabian Sea sediments off Pakistan (Sokoll et al., 2012). However, similar to denitrification, previous studies of anammox rates from slurry incubation also exhibited a large vertical variation at different sites (Gihring et al., 2010; Neubacher et al., 2012; Thamdrup and Dalsgaard, 2002). There was no correlation between volumetric anammox rate and sediment organic matter content ( $r=0.32$ ,  $p=0.17$ , Pearson), implying that the anammox activity was not directly limited by the availability of organic matter in the ECS sediments.

No correlation between DNRA rate and sediment organic matter content was found ( $r=0.06$ ,  $p=0.81$ , Pearson). The increase of DNRA rate with sediment depth (Fig. 5) suggested the deeper sediment layer was more favorable for DNRA, consistent with previous studies (Stief et al., 2010). This could be due to the lower ratio between electron acceptor and donor (Tiedje, 1988). It has also been reported that DNRA showed significantly higher rates in oxic conditions compared to hypoxic conditions (Roberts et al., 2012). Furthermore, it has been argued that potential DNRA rates might result from a stimulation of DNRA bacteria by high concentrations of added nitrate since they rarely obtain nitrate in normal conditions (Binnerup et al., 1992). Considering that the DNRA rates systematically increased with depth in our study and were highest at depths without in situ nitrate (Fig. 2 and Fig. 5) the DNRA rates might be more overestimated than the anammox rates which were highest at depths with measurable in situ  $\text{NO}_x^-$  concentrations (Fig. 2 and Fig. 5).

Table 4. DNRA rates reported from other marine sediment. The data in parentheses represent the range.

Location	Depth (m)	DNRA (mmol N m <sup>-2</sup> d <sup>-1</sup> )	DNRA% <sup>a</sup>	Reference
Tama estuary		13 (3.6-20) <sup>b</sup>	55 (43-73)	Nishio et al., 1982, 1983
Gullmar fjord	30	0.03 <sup>b</sup>		Enoksson and Samuelsson, 1987
Mokbaai, Netherlands	0	16 <sup>c</sup>	33	Goeyens et al., 1987
Randers Fjord	<2	1.5 (0.62-3.0)	85 (79-93)	Bonin, 1996
Two French lagoons	0	0.16 (0.07-0.31)	66 (23-99)	Rysgaard et al., 1996
Thau lagoon, France	8.5	0.4-161 <sup>c</sup>	98	Gilbert et al., 1997
Gulf of Fos, Marseilles	5.5 (2-10)	1.8 (0.3-6.8) <sup>c</sup>	55 (0-93)	Bonin et al., 1998
Horsens Fjord trout cage	3-9	~2.2 (0.01-6.8)	53 (25-85)	Christensen et al., 2000
Fringing marsh-aquifer ecotone		66 (21-147) <sup>c</sup>	37 (5-77)	Tobias et al., 2001
Texas six estuaries	0-3	0.37 (0-2.4)	24 (0.4-68)	An and Gardner, 2002; Gardner et al., 2006
Kanholmsfjärden	~95	0.8 <sup>b</sup>	97	Karlson et al., 2005
Colne estuary		2.6 (0.1-7.7)	43 (11-60)	Dong et al., 2009
North Atlantic continental shelf	75 (50-100)	0.02-0.1 <sup>d</sup>	<0.2%	Trimmer and Nicholls, 2009
Plum Island Sound estuary		2.1 (0.1-7.4)	43 (29-51)	Koop-Jakobsen and Giblin, 2010
Peruvian OMZ	470 (78-1005)	1.2 (0-2.9)	33 (0-72)	Bohlen et al., 2011
Three tropical estuaries		2.0 (0-27)	81 (69-91)	Dong et al., 2011
Baltic Sea	69 (58-83)	0.3 (0.01-1.1)	52 (17-92)	Jäntti and Hietanen, 2012
Norsminde Fjord estuary	0.5		0-20%	Binnerup et al. 1992; Rysgaard et al., 1993
Skagerrak	695		<2%	Dalsgaard and Thamdrup, 2002
Washington margin	2000-3000	<0.02	<10%	Engström et al., 2009
East China Sea shelf	55 (19-86)	4.8 (2.6-9.7)	26 (20-31)	This study

a. percentage of DNRA in total nitrate reduction (denitrification+anammox+DNRA)

b. the rate is calculated by combination of <sup>15</sup>NO<sub>3</sub><sup>-</sup> method and mass balance, others were obtained by direct <sup>15</sup>NO<sub>3</sub><sup>-</sup> method.

c. the rate was measured by slurry incubation;

d. the unit is μmol N m<sup>-2</sup> d<sup>-1</sup>

### 4.3 Biogeochemical significance of anammox, denitrification and DNRA in the ECS sediments

Pore water  $\text{NO}_x^-$  penetrated in the sediment down to 8 cm (Fig. 2). As our slurry incubations were performed with a resolution of 2 cm, we integrated the potential rates down to the nitrate penetration depth obtained from the pore water profiles to obtain a full understanding of each process in the sediment. However, it should be noted that the low vertical resolution of nitrate profile might cause some over- or underestimation of nitrate penetration depth, and consequently the relative contribution of each process in total nitrate reduction.

The average relative contribution of anammox to total N-loss was 28% in our study, which demonstrated that anammox was an important pathway for fixed nitrogen removal in the ECS sediments. This value was in the range of literature values reported for continental shelves sediments and was also similar to the global average value of 23% in a recent compilation of Trimmer and Engström (2011). Meanwhile, the increase of relative contribution of anammox to total N-loss with water depth also agreed well with the general pattern observed from continental shelves (Thamdrup 2012; Trimmer and Engström, 2011). It was suggested that the increase of the relative contribution of anammox with depth was mainly due to a more significant decrease of denitrification rate than anammox (Trimmer and Engström, 2011). In our study, except at site DHa2, integrated denitrification rates decreased from the shallow estuarine site to the deep outer shelf site, while anammox rates increased and DNRA showed small spatial variation (Fig. 6a). As a result, the percentage of anammox in total nitrate reduction increased with distance from the coast and water depth (Fig. 6b). From this we can infer that in the shallow coastal area, denitrification was the predominant pathway for N-loss. While anammox contributed up to ~50% of the N-loss on the deeper part of the shelf (Fig. 6). This pattern was also a reflection of organic matter availability controlling denitrification. Indeed, organic matter content declined with water depth and

distance from the coast in the ECS (Kao et al., 2003).

DNRA has been widely reported in marine sediments but varies in extent (Table 4). Our integrated DNRA rates were in the same range as reported for Colne estuary (Dong et al., 2009); however, they were significantly higher than those from the Atlantic continental shelf (Trimmer and Nicholls, 2009) and Baltic Sea (Jääntti and Hietanen, 2012). Unlike denitrification and anammox, there is no N-loss through DNRA. As a result, fixed nitrogen was still preserved in the system and could then be further used to sustain primary production (Gardner et al., 2006). Thus, competition between N-loss and DNRA determined the fate of benthic nitrate. Benthic N-loss via anammox and denitrification was the principal fate of nitrate, which accounted for ~75% in nitrate reduction in the ECS sediments significantly decreasing the dissolved inorganic nitrogen concentrations and alleviating eutrophication risks. However, the DNRA contribution of 23-31% of the nitrate reduction is significant for retaining nutrient nitrogen in the system. Combined with the decomposition of settling organic matter, benthic DNRA would lead to enhanced oxygen consumption, contributing to the development of hypoxia in the Changjiang estuary.

## 5 Conclusions

We have shown the coexistence of anammox, denitrification and DNRA using a modification of the  $^{15}\text{N}$  isotope pairing method in the ECS sediments also taking nitrate release by nitrate storing organisms into account. Our calculation demonstrated that nitrate release and DNRA had opposite effects on the denitrification rate calculation, but were of minor importance in most of our experiments due to high label additions ( $\sim 100 \mu\text{M}$ ). On the contrary, calculated anammox rates were more sensitive to nitrate release with an average overestimation of 42% in experiments with  $^{15}\text{NO}_3^-$  (E\_Denit). Within experiments amended with  $^{15}\text{NH}_4^+ + ^{14}\text{NO}_3^-$ , where nitrate release had no effect on  $F_{\text{N}}$ , anammox rate was not significantly influenced by DNRA (4%). Thus, we recommended that anammox rates should be calculated from the experiment amended with  $^{15}\text{NH}_4^+ + ^{14}\text{NO}_3^-$  and not  $^{15}\text{NO}_3^-$ .

The denitrification rates decreased with increasing water depth, increasing distance to the coast and decreasing organic matter content. In contrast the integrated anammox rates increased with water depth, leading to an enhanced importance of anammox to benthic N-loss from ~13% in the coastal area to ~50% on the outer shelf.

DNRA was also an important pathway accounting for up to 30% of benthic nitrate reduction in the ECS sediments. The transformation from nitrate to ammonium via DNRA could prolong the residence time of fixed nitrogen. Consequently, eutrophication and seasonal hypoxia in the bottom water off the Changjiang estuary could potentially be enhanced by DNRA.

### **Supplementary material is included with this manuscript**

### **References**

Aller, R. C., Mackin, J. E., Ullman, W. J., Wang, C. H., Tsai, S. M., Jin, J. C., Sui, Y. N., and Hong J. Z.: Early chemical diagenesis, sediment-water solute exchange, and storage of reactive organic matter near the mouth of the Changjiang, East China Sea, *Cont. Shelf. Res.*, 4, 227–251, 1985.

An, S. and Gardner, W. S.: Dissimilatory nitrate reduction to ammonium (DNRA) as a nitrogen link, versus denitrification as a sink in a shallow estuary (Laguna Madre/Baffin Bay, Texas), *Mar. Ecol.-Prog. Ser.*, 237, 41–50, 2002.

Beardsley, R. C., Limeburner, R., Yu, H., and Cannon, G. A.: Discharge of the Changjiang (Yangtze River) into the East China Sea, *Cont. Shelf. Res.*, 4, 57–76, 1985.

Binnerup, S. J., Jensen, K., Revsbech, N. P., Jensen, M. H., and Sørensen, J.: Denitrification, dissimilatory reduction of nitrate to ammonium, and nitrification in a bioturbated estuarine sediment as measured with <sup>15</sup>N and microsensor techniques, *Appl. Environ. Microb.*, 58, 303–313, 1992.

Bohlen, L., Dale, A., Sommer, S., Mosch, T., Hensen, C., Noffke, A., Scholz, F., and Wallmann, K.: Benthic nitrogen cycling traversing the Peruvian oxygen minimum zone, *Geochim. Cosmochim. Ac.*, 75, 6094–6111, 2011.

Bonin, P.: Anaerobic nitrate reduction to ammonium in two strains isolated from coastal marine sediment: a dissimilatory pathway, *FEMS Microbiol. Ecol.*, 19, 27–38, 1996.

Bonin, P., Omnes, P., and Chalamet, A.: Simultaneous occurrence of denitrification and nitrate ammonification in sediments of the French Mediterranean Coast, *Hydrobiologia*, 389, 169–182, 1998.

Christensen, J. P., Murray, J.W., Devol, A. H., and Codispoti, L. A.: Denitrification in continental shelf sediments has major impact on the oceanic nitrogen budget, *Global Biogeochem. Cy.*, 1, 97–116, 1987.

Christensen, P. B., Rysgaard, S., Sloth, N. P., Dalsgaard, T., and Schwærter, S.: Sediment mineralization, nutrient fluxes, denitrification and dissimilatory nitrate reduction to ammonium in an estuarine fjord with sea cage trout farms, *Aquat. Microb. Ecol.*, 21, 73–84, 2000.

Dähnke, K., Moneta, A., Veuger, B., Soetaert, K., and Middelburg, J. J.: Balance of assimilative and dissimilative nitrogen processes in a diatom-rich tidal flat sediment, *Biogeosciences*, 9, 4059–4070, doi:10.5194/bg-9-4059-2012, 2012.

Dalsgaard, T. and Thamdrup, B.: Factors controlling anaerobic ammonium oxidation with nitrite in marine sediments, *Appl. Environ. Microb.*, 68, 3802–3808, 2002.

Dalsgaard, T., Thamdrup, B., and Canfield, D. E.: Anaerobic ammonium oxidation (anammox) in the marine environment, *Res. Microbiol.*, 156, 457–464, 2005.

Dong, L. F., Smith, C. J., Papaspyrou, S., Stott, A., Osborn, A. M., and Nedwell, D. B.: Changes in Benthic Denitrification, Nitrate Ammonification, and Anammox Process Rates and Nitrate and Nitrite Reductase Gene Abundances along an Estuarine Nutrient Gradient (the Colne Estuary, United Kingdom), *Appl. Environ. Microb.*, 75, 3171–3179, 2009.

Dong, L. F., Sobey, M. N., Smith, C. J., Rusmana, I., Phillips, W., Stott, A., Osborn, A. M., and Nedwell, D. B.: Dissimilatory reduction of nitrate to ammonium, not denitrification or anammox, dominates benthic nitrate reduction in tropical estuaries, *Limnol. Oceanogr.*, 56, 279–291, 2011.

Engström, P., Dalsgaard, T., Hulth, S., and Aller, R. C.: Anaerobic ammonium oxidation by nitrite (anammox): implications for N<sub>2</sub> production in coastal marine sediments, *Geochim. Cosmochim. Ac.*, 69, 2057–2065, 2005.

Engström, P., Penton, C. R., and Devol, A. H.: Anaerobic ammonium oxidation in deep-sea sediments off the Washington margin, *Limnol. Oceanogr.*, 54, 1643–1652, 2009.

Enoksson, V. and Samuelsson, M. O.: Nitrification and dissimilatory ammonium production and their effects on nitrogen flux over the sediment-water interface in bioturbated coastal sediments, *Mar. Ecol.-Prog. Ser.*, 36, 181–189, 1987.

Fossing, H., Gallardo, V. A., Jørgensen, B. B., Hüttel, M., Nielsen, L. P., Schulz, H., Canfield, D. E., Forster, S., Glud, R. N., Gundersen, J. K., Kuver, J., Ramsing, N. B., Teske, A., Thamdrup, B., and Ulloa, O.: Concentration and transport of nitrate by the mat-forming sulphur bacterium *Thioploca*, *Nature*, 374, 713–715, 1995.

Gao, H., Schreiber, F., Collins, G., Jensen, M. M., Kostka, J. E., Lavik, G., de Beer, D., Zhou, H. Y., and Kuypers, M. M. M.: Aerobic denitrification in permeable Wadden Sea sediments, *ISME J.*, 4, 417–426, 2010.

Gardner, W. S., McCarthy, M. J., An, S., Sobolev, D., Sell, K. S., and Brock, D.: Nitrogen fixation and dissimilatory nitrate reduction to ammonium (DNRA) support nitrogen dynamics in Texas estuaries, *Limnol. Oceanogr.*, 51, 558–568, 2006.

Gihring, T. M., Lavik, G., Kuypers, M. M. M., and Kostka, J. E.: Direct determination of nitrogen cycling rates and pathways in Arctic fjord sediments (Svalbard, Norway), *Limnol. Oceanogr.*, 55, 740–752, 2010.

Gilbert, F., Souchu, P., Bianchi, M., and Bonin, P.: Influence of shellfish farming activities on nitrification, nitrate reduction to ammonium and denitrification at the water-sediment interface of the Thau lagoon, France, *Mar. Ecol.-Prog. Ser.*, 151, 143–153, 1997.

Glud, R. N.: Oxygen dynamics of marine sediments, *Mar. Biol. Res.*, 4, 243–289, 2008.

Glud, R. N., Thamdrup, B., Stahl, H., Wenzhoefer, F., Glud, A., Nomaki, H., Oguri, K., Revsbech, N. P., and Kitazato, H.: Nitrogen cycling in a deep ocean margin sediment (Sagami Bay, Japan), *Limnol. Oceanogr.*, 54, 723–734, 2009.

Goeyens, L., De Vries, R. T. P., Bakker, J. F., and Helder, W.: An experiment on the relative importance of denitrification, nitrate reduction and ammonification in coastal marine sediment, *Neth. J. Sea Res.*, 21, 171–175, 1987.

Gong, G. C., Wen, Y. H., Wang, B. W., and Liu, G. J.: Seasonal variation of chlorophyll a concentration, primary production and environmental conditions in the subtropical East China Sea, *Deep-Sea. Res. Pt. II*, 50, 1219–1236, 2003.

Holtappels, M., Lavik, G., Jensen, M. M., Kuypers, M. M. M.: <sup>15</sup>N labelling experiments to dissect the contributions of heterotrophic denitrification and anammox to nitrogen removal in the OMZ waters of the ocean, in: *Methods in Enzymology: Research on Nitrification and Related Processes*, 486, Part A, edited by: Klotz, M., Elsevier Academic Press Inc., San Diego, 223–251, 2011.

Jäntti, H. and Hietanen, S.: The Effects of Hypoxia on Sediment Nitrogen Cycling in the Baltic Sea, *AMBIO*, 41, 161–169, 2012.

Jensen, M. M., Lam, P., Revsbech, N. P., Nagel, B., Gaye, B., Jetten, M. S. M., and Kuypers, M. M. M.: Intensive nitrogen loss over the Omani Shelf due to anammox coupled with dissimilatory nitrite reduction to ammonium, *ISME J.*, 5, 1660–1670, 2011.

Kalvelage, T., Jensen, M. M., Contreras, S., Revsbech, N. P., Lam, P., Günter, M., LaRoche, J., Lavik, G., and Kuypers, M. M. M.: Oxygen sensitivity of anammox and coupled N-cycle processes in oxygen minimum zones, *PLoS One*, 6, e29299, doi:10.1371/journal.pone.0029299, 2011.



Kamp, A., de Beer, D., Nitsch, J. L., Lavik, G., and Stief, P.: Diatoms respire nitrate to survive dark and anoxic conditions, *P. Natl. Acad. Sci. USA*, 108, 5649–5654, 2011.

Kao, S. J., Lin, F. J., and Liu, K. K.: Organic carbon and nitrogen contents and their isotopic compositions in surficial sediments from the East China Sea shelf and the southern Okinawa Trough, *Deep-Sea. Res. Pt. II*, 50, 1203–1217, 2003.

Karlson, K., Hulth, S., Ringdahl, K., and Rosenberg, R.: Experimental recolonisation of Baltic Sea reduced sediments: survival of benthic macrofauna and effects on nutrient cycling, *Mar. Ecol.-Prog. Ser.*, 294, 35–49, 2005.

Kartal, B., Kuypers, M. M. M., Lavik, G., Schalk, J., Op den Camp, H. J. M., Jetten, M. S. M., and Strous, M.: Anammox bacteria disguised as denitrifiers: nitrate reduction to dinitrogen gas via nitrite and ammonium, *Environ. Microbiol.*, 9, 635–642, 2007.

Koike, I. and Hattori, A.: Denitrification and ammonia formation in anaerobic coastal sediments, *Appl. Environ. Microb.*, 35, 278–282, 1978.

Koop-Jakobsen, K. and Giblin, A. E.: The effect of increased nitrate loading on nitrate reduction via denitrification and DNRA in salt marsh sediments, *Limnol. Oceanogr.*, 55, 789–802, 2010.

Laverman, A. M., Meile, C., Van Cappellen, P., and Wieringa, E. B. A.: Vertical distribution of denitrification in an estuarine sediment: integrating sediment flowthrough reactor experiments and microprofiling via reactive transport modeling, *Appl. Environ. Microb.*, 73, 40–47, 2007.

Liu, S. M., Li, L.W., and Zhang, Z. N.: Inventory of nutrients in the Bohai, *Cont. Shelf. Res.*, 31, 1790–1797, 2011.

Lohse, L., Epping, E. H. G., Helder, W., and Van Raaphorst, W.: Oxygen pore water profiles in continental shelf sediments of the North Sea: turbulent versus molecular diffusion, *Mar. Ecol.-Prog. Ser.*, 145, 63–75, 1996.

Lomas, M. W. and Glibert, P. M.: Comparisons of nitrate uptake, storage, and reduction in marine diatoms and flagellates, *J. Phycol.*, 36, 903–913, 2000.

Lomstein, E., Jensen, M. H., and Sørensen, J.: Intracellular  $\text{NH}_4^+$  and  $\text{NO}_3^-$  pools associated with deposited phytoplankton in a marine sediment (Aarhus Bight, Denmark), *Mar. Ecol.-Prog. Ser.*, 61, 97–105, 1990.

Luther, G. W., Sundby, B., Lewis, B. L., Brendel, P. J., and Silverberg, N.: Interactions of manganese with the nitrogen cycle: Alternative pathways to dinitrogen, *Geochim. Cosmochim. Ac.*, 61, 4043–4052, 1997.

Middelburg, J. J., Soetaert, K., Herman, P. M. J., and Heip, C. H. R.: Denitrification in marine sediments: A model study, *Global. Biogeochem. Cy.*, 10, 661–673, 1996.

Mulder, A., van de Graaf, A. A., Robertson, L. A., and Kuenen, J. G.: Anaerobic ammonium oxidation discovered in a denitrifying fluidized bed reactor, *FEMS Microbiol. Ecol.*, 16, 177–184, 1995.

Neubacher, E. C., Parker, R. E., and Trimmer, M.: The potential effect of sustained hypoxia on nitrogen cycling in sediment from the southern North Sea: a mesocosm experiment, *Biogeochemistry*, 113, 69–84, 2013.

Nicholls, J. C. and Trimmer, M.: Widespread occurrence of the anammox reaction in estuarine sediments, *Aquat. Microb. Ecol.*, 55, 105–113, 2009.

Nielsen, L. P.: Denitrification in sediment determined from nitrogen isotope pairing, *FEMS Microbiol. Lett.*, 86, 357–362, 1992.

Nishio, T., Koike, I., and Hattori, A.: Denitrification, nitrate reduction, and oxygen consumption in coastal and estuarine sediments, *Appl. Environ. Microb.*, 43, 648–653, 1982.

Nishio, T., Koike, I., and Hattori, A.: Estimates of denitrification and nitrification in coastal and estuarine sediments, *Appl. Environ. Microb.*, 45, 444–450, 1983.

Otte, S., Kuenen, J. G., Nielsen, L. P., Paerl, H.W., Zopfi, J., Schulz, H. N., Teske, A., Strotmann, B., Gallardo, V. A., and Jørgensen, B. B.: Nitrogen, Carbon, and Sulfur Metabolism in Natural *Thioploca* Samples, *Appl. Environ. Microb.*, 65, 3148–3157, 1999.

Preisler, A., de Beer, D., Lichtschlag, A., Lavik, G., Boetius, A., and Jørgensen, B. B.: Biological and chemical sulfide oxidation in a *Beggiatoa* inhabited marine sediment, *ISME J.*, 1, 341–353, 2007.

Prokopenko, M. G., Hammond, D. E., Berelson, W. M., Bernhard, J. M., Stott, L., and Douglas, R.: Nitrogen cycling in the sediments of Santa Barbara basin and Eastern Subtropical North Pacific: Nitrogen isotopes, diagenesis and possible chemosymbiosis between two lithotrophs (*Thioploca* and Anammox) – “riding on a glider”, *Earth Planet. Sc. Lett.*, 242, 186–204, 2006.

Risgaard-Petersen, N., Nielsen, L. P., Rysgaard, S., Dalsgaard, T., and Meyer, R. L.: Application of the isotope pairing technique in sediments where anammox and denitrification coexist, *Limnol. Oceanogr.- Meth.*, 1, 63–73, 2003.

Risgaard-Petersen, N., Meyer, R. L., Schmid, M., Jetten, M. S. M., Enrich-Prast, A., Rysgaard, S., and Revsbech, N. P.: Anaerobic ammonium oxidation in an estuarine sediment, *Aquat. Microb. Ecol.*, 36, 293–304, 2004.

Risgaard-Petersen, N., Langezaal, A. M., Ingvarsdén, S., Schmid, M. C., Jetten, M. S. M., Op den Camp, H. J. M., Derksen, J. W. M., Piña-Ochoa, E., Eriksson, S., Nielsen, L. P., Revsbech, N. P., Cedhagen, T., and van der Zwaan, G. J.: Evidence for complete denitrification in a benthic foraminifer, *Nature*, 443, 93–96, 2006.

Roberts, K. L., Eate, V. M., Eyre, B. D., Holland, D. P., and Cook, P. L. M.: Hypoxic events stimulate nitrogen recycling in a shallow salt-wedge estuary: The Yarra River estuary, Australia, *Limnol. Oceanogr.*, 57, 1427–1442, 2012.

Rysgaard, S., Risgaard-Petersen, N., Nielsen, L. P., and Revsbech, N. P.: Nitrification and denitrification in lake and estuarine sediments measured by the  $^{15}\text{N}$  dilution technique and isotope pairing, *Appl. Environ. Microb.*, 59, 2093–2098, 1993.

Rysgaard, S., Risgaard-Petersen, N., and Sloth, N. P.: Nitrification, denitrification, and nitrate ammonification in sediments of two coastal lagoons in Southern France, *Hydrobiologia*, 329, 133–141, 1996.

Schulz, H. N., Brinkhoff, T., Ferdelman, T. G., Mariné, M. H., Teske, A., and Jørgensen, B. B.: Dense populations of a giant sulphur bacterium in Namibian shelf sediments, *Science*, 284, 493–495, 1999.

Seeberg-Elverfeldt, J., Schlüter, M., Feseker, T., and Kölling, M.: Rhizon sampling of pore waters near the sediment/water interface of aquatic systems, *Limnol. Oceanogr.-Meth.*, 3, 361–371, 2005.

Seitzinger, S. P.: Denitrification in aquatic sediments, in: *Denitrification in Soil and Sediment*, edited by: Revsbech, N. P. and Sørensen, J., Plenum Press, New York, 301–322, 1990.

Sokoll, S., Holtappels, M., Lam, P., Collins, G., Schlüter, M., Lavik, G., and Kuypers, M. M. M.: Benthic nitrogen loss in the Arabian Sea off Pakistan, *Front. Microbiol.*, 3, doi:10.3389/fmicb.2012.00395, 2012.

Song, G. D., Liu, S. M., Kuypers, M. M. M., and Lavik, G.: Application of the isotope pairing technique in sediments where anammox, denitrification and DNRA coexist, in preparation, 2013.

Spott, O. and Stange, C. F.: A new mathematical approach for calculating the contribution of anammox, denitrification and atmosphere to an  $\text{N}_2$  mixture based on a  $^{15}\text{N}$  tracer technique, *Rapid Commun. Mass Sp.*, 21, 2398–2406, 2007.

Stief, P., Behrendt, A., Lavik, G., and de Beer, D.: Combined gel probe and isotope labelling technique for measuring dissimilatory nitrate reduction to ammonium in sediments at millimeter-level resolution, *Appl. Environ. Microb.*, 76, 6239–6247, 2010.

Sweerts, J. P. R. A., de Beer, D., Nielsen, L. P., Verdouw, H., van den Heuvel, J. C., Cohen, Y., and Cappenberg, T. E.: Denitrification by sulphur oxidizing *Beggiatoa* spp. mats on freshwater sediments, *Nature*, 344, 762–763, 1990.

Thamdrup, B.: Novel Pathways and Organisms in Global Nitrogen Cycling, *Annu. Rev. Ecol. Evol. S.*, 43, 407–428, 2012.

Thamdrup, B. and Dalsgaard, T.: Production of  $\text{N}_2$  through anaerobic ammonium oxidation coupled to nitrate reduction in marine sediments, *Appl. Environ. Microb.*, 68, 1312–1318, 2002.

Tiedje, J. M.: Ecology of denitrification and dissimilatory nitrate reduction to ammonium, in: *Biology of anaerobic microorganisms*, edited by: Zehnder, A. J. B., JohnWiley & Sons, Inc., New York, 179–244, 1988.

Tobias, C. R., Anderson, I. C., Canuel, E. A., and Macko, S. A.: Nitrogen cycling through a fringing marsh-aquifer ecotone, *Mar. Ecol.-Prog. Ser.*, 210, 25–39, 2001.

Trimmer, M. and Engström, P.: Distribution, Activity, and Ecology of Anammox Bacteria in Aquatic Environments, in: *Nitrification*, edited by: Ward, B. B. and Arp, D. J., ASM Press, Washington, DC, 201–235, 2011.

Trimmer, M. and Nicholls, J. C.: Production of nitrogen gas via anammox and denitrification in intact sediment cores along a continental shelf to slope transect in the North Atlantic, *Limnol. Oceanogr.*, 54, 577–589, 2009.

Trimmer, M., Nicholls, J. C., and Deflandre, B.: Anaerobic ammonium oxidation measured in sediments along the Thames estuary, United Kingdom, *Appl. Environ. Microb.*, 69, 6447–6454, 2003.

Wang, B. D.: Cultural eutrophication in the Changjiang (Yangtze River) plume: History and perspective, *Estuar. Coast. Shelf. S.*, 69, 471–477, 2006.

Wang, D. Q., Chen, Z. L., Xu, S. Y., Hu, L. Z., and Wang, J.: Denitrification in Chongming east tidal flat sediment, Yangtze estuary, China, *Sci. China Ser. D*, 49, 1090–1097, 2006.

Warembourg, F. R.: Nitrogen fixation in soil and plant systems. in: *Nitrogen Isotope Techniques*, edited by: Knowles, R. and Blackburn, T. H., Academic Press, San Diego, 127–156, 1993.

Yang, W. H., Weber, K. A., and Silver, W. L.: Nitrogen loss from soil through anaerobic ammonium oxidation coupled to iron reduction, *Nat. Geosci.*, 5, 538–541, 2012.

Zhang, G.-L., Zhang, J., Liu, S.-M., Ren, J.-L., and Zhao, Y.-C.: Nitrous oxide in the Changjiang (Yangtze River) Estuary and its adjacent marine area: Riverine input, sediment release and atmospheric fluxes, *Biogeosciences*, 7, 3505–3516, doi:10.5194/bg-7-3505-2010, 2010.

Zhang, J., Liu, S. M., Ren, J. L., Wu, Y., and Zhang, G. L.: Nutrient gradients from the eutrophic Changjiang (Yangtze River) Estuary to the oligotrophic Kuroshio waters and re-evaluation of budgets for the East China Sea Shelf, *Prog. Oceanogr.*, 74, 449–478, 2007.

Zhou, M. J., Shen, Z. L., and Yu, R. C.: Responses of a coastal phytoplankton community to increased nutrient input from the Changjiang (Yangtze) River, *Cont. Shelf. Res.*, 28, 1483–1489, 2008.

Zhu, Z. Y., Zhang, J., Wu, Y., Zhang, Y. Y., Lin, J., and Liu, S. M.: Hypoxia off the Changjiang (Yangtze River) Estuary: Oxygen depletion and organic matter decomposition, *Mar. Chem.*, 125, 108–116, 2011.

## Supplementary Material

### Supplementary discussion about the influence of nitrate release on anammox rate calculation.

The potential rates of anammox could be calculated from the production of  $^{29}\text{N}_2$  and  $^{30}\text{N}_2$  and the labeling  $^{15}\text{NO}_3^-$  fraction ( $F_N$ ) in the slurry incubation with the calculation procedure of Thamdrup and Dalsgaard (2002) as was shown in equation (2) in the text. If nitrate release occurred, then we could use equation (4) to calculate the derived  $^{15}\text{NO}_3^-$  fraction ( $F_N^*$ ).

$$A_{(E\_Denit)} = [P_{29} - 2 \times (1/F_N - 1) \times P_{30}] / F_N \quad (2)$$

$$F_N^* = \frac{(P_{29} + 2 \times P_{30}) - \sqrt{(P_{29} + 2 \times P_{30})^2 - 8 \times A_{(E\_Amox)} \times P_{30}}}{2 \times A_{(E\_Amox)}} \quad (4)$$

Where, denoted the potential rate anammox in  $E\_Denit$ .  $P_{29}$  and  $P_{30}$  were the production rate of  $^{29}\text{N}_2$  and  $^{30}\text{N}_2$  in  $E\_Denit$ , which could be obtained by the linear regression of the  $\text{N}_2$  isotope concentration against time.

This first order derivative of equation (2) could be written as,

$$\frac{dA_{(E\_Denit)}}{dF_N} = \frac{4 \times P_{30} - (P_{29} + 2P_{30}) \times F_N}{F_N^3} = \frac{4 - (r_{29} + 2) \times F_N}{F_N^3 / P_{30}}$$

Where,  $r_{29} = P_{29}/P_{30}$ . Because  $0 < F_N < 1$ , if  $0 < F_N < 4/(r_{29} + 2)$ ,  $\frac{dA_{(E\_Denit)}}{dF_N}$  would

be a positive value and equation (2) would be an increasing function with  $F_N$ . In our study, all the measured  $r_{29} < 2$ , thus  $4/(r_{29} + 2) > 1$ , therefore when  $0 < F_N < 1$ , the anammox rate in  $E\_Denit$  would also decrease with the decreasing of  $F_N$ . Thus, anammox rate would be overestimated if nitrate release was not considered according to equation (2). If nitrate release was very significant and led to the mismatch of potential anammox rate in  $E\_Amox$  and  $E\_Denit$ , then

$(P_{29} + 2 \times P_{30})^2 - 8 \times A_{(E\_Amox)} \times P_{30}$  could probably be less than 0, meaning that equation (4) could not be solved successfully. Maybe this was the case for 4 samples in our study; in these cases we recommended the anammox rates from  $E\_Amox$  as the actual rates, as here nitrate release would have no effect. Besides, in another 4 samples, calculated  $F_N^*$  was higher than  $F_N$ , even more than 100%, these maybe caused by the sediment heterogeneity. In these cases, we used the original  $F_N$  to calculate  $A_{E\_Denit}$ . However, excluding the four samples that we could not calculate  $F_N^*$ , all other anammox rates from the two experiments were consistent (Fig. 8a in the text).

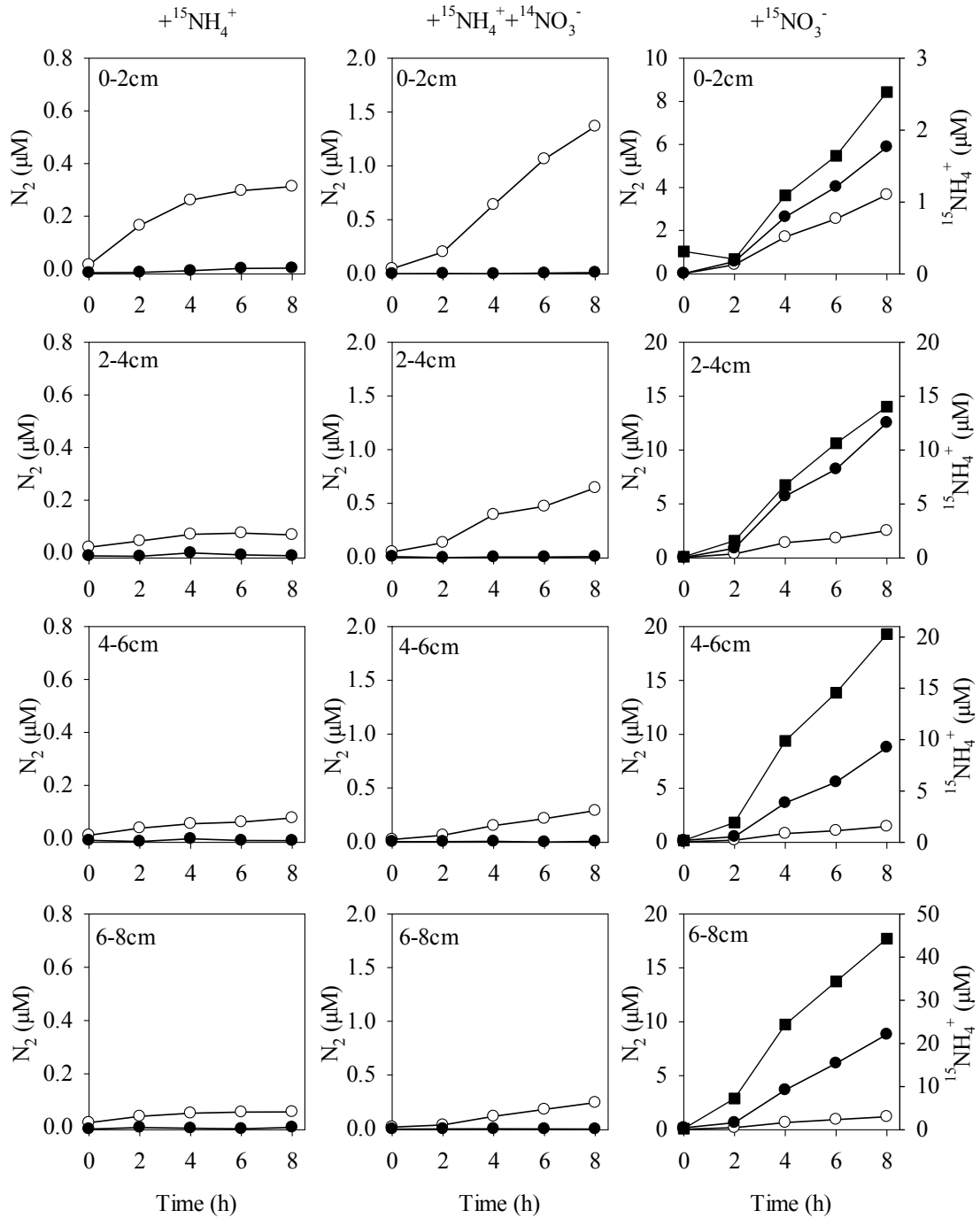


Fig. S1 Production of  $^{29}\text{N}_2$  (open circles),  $^{30}\text{N}_2$  (closed circles) and  $^{15}\text{NH}_4^+$  (closed squares) against time in slurry incubations at DH31.

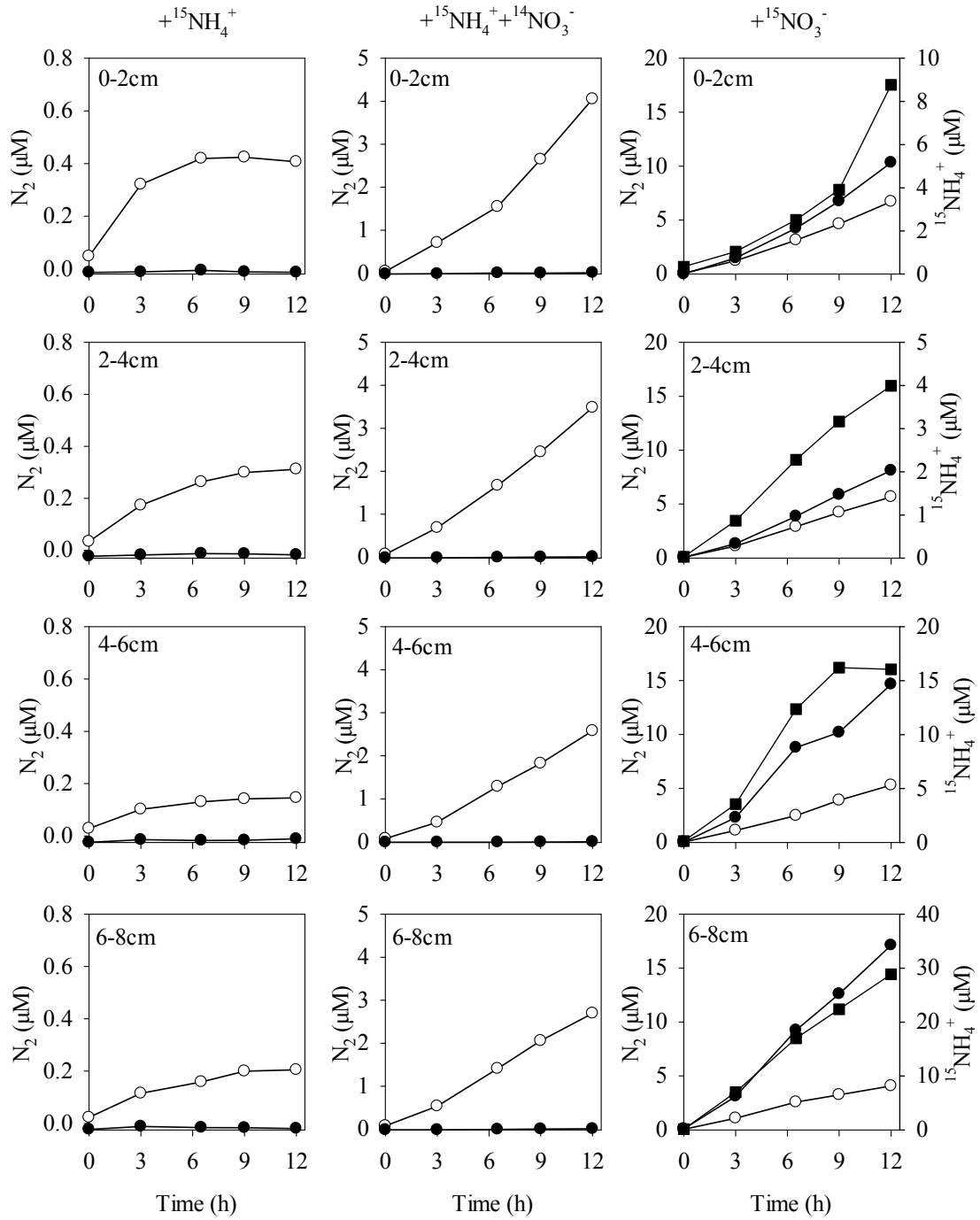


Fig. S2 Production of  $^{29}\text{N}_2$  (open circles),  $^{30}\text{N}_2$  (closed circles) and  $^{15}\text{NH}_4^+$  (closed squares) against time in slurry incubations at DHa2.



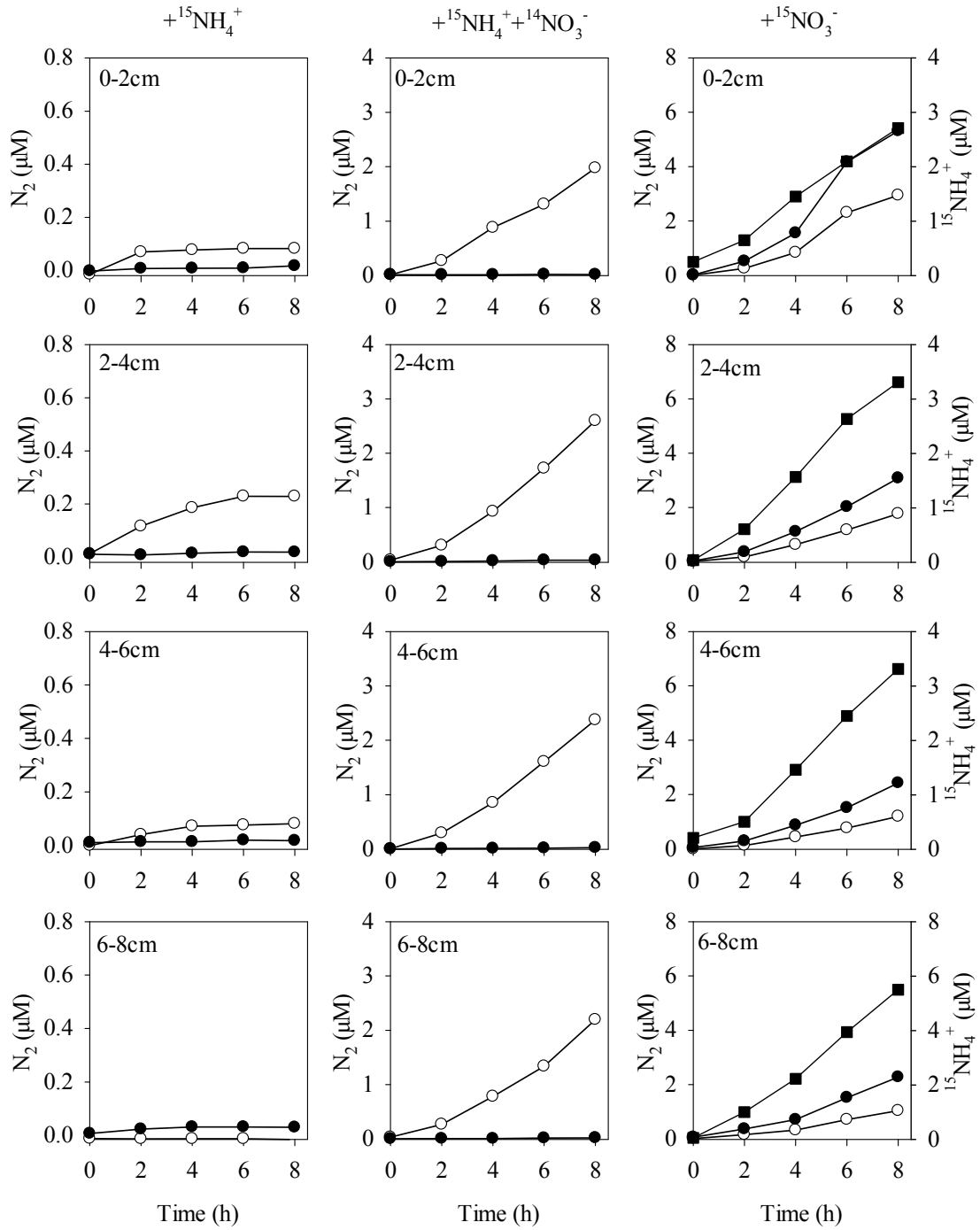


Fig. S3 Production of  $^{29}\text{N}_2$  (open circles),  $^{30}\text{N}_2$  (closed circles) and  $^{15}\text{NH}_4^+$  (closed squares) against time in slurry incubations at DH53.

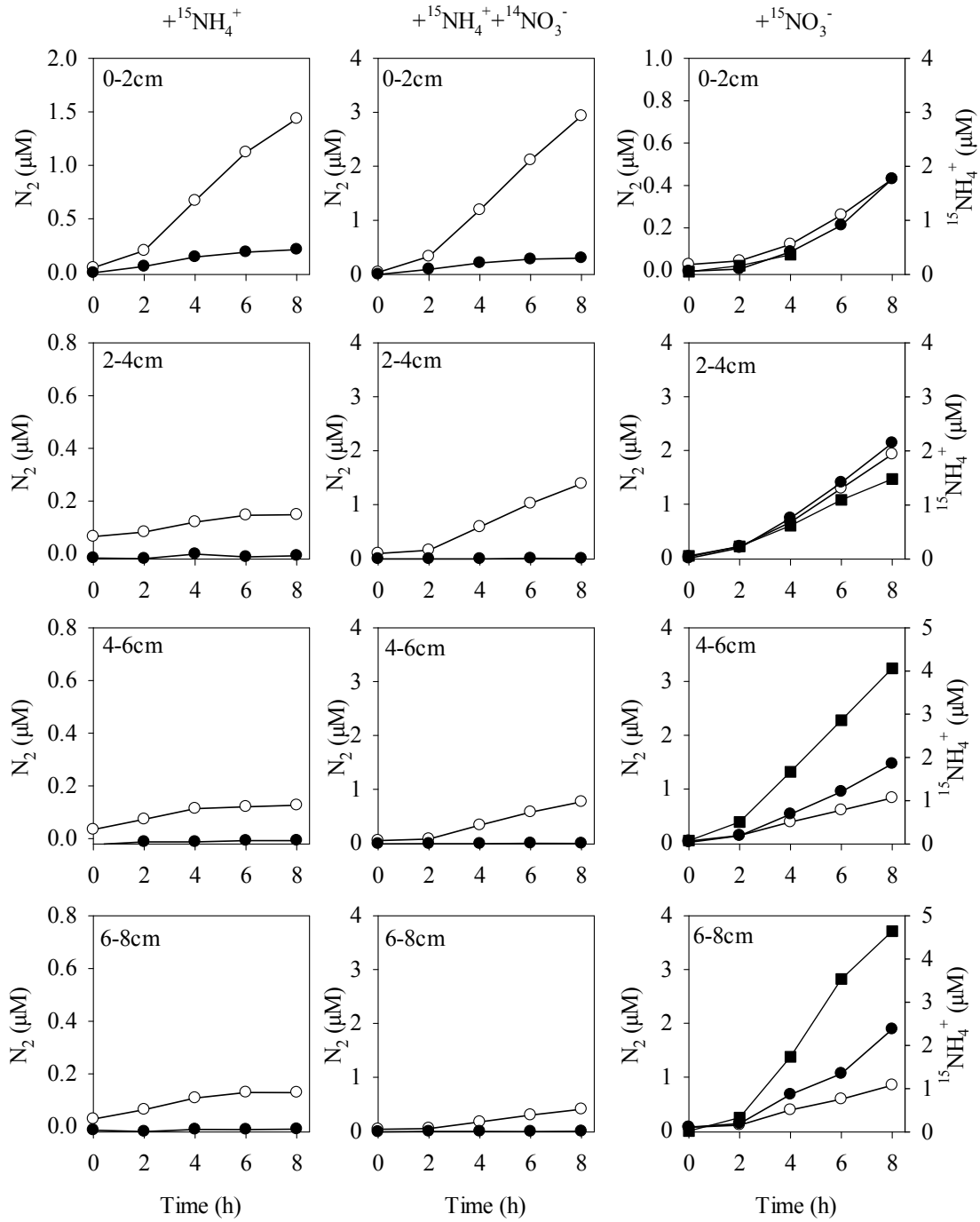


Fig. S4 Production of  $^{29}\text{N}_2$  (open circles),  $^{30}\text{N}_2$  (closed circles) and  $^{15}\text{NH}_4^+$  (closed squares) against time in slurry incubations at DH55.

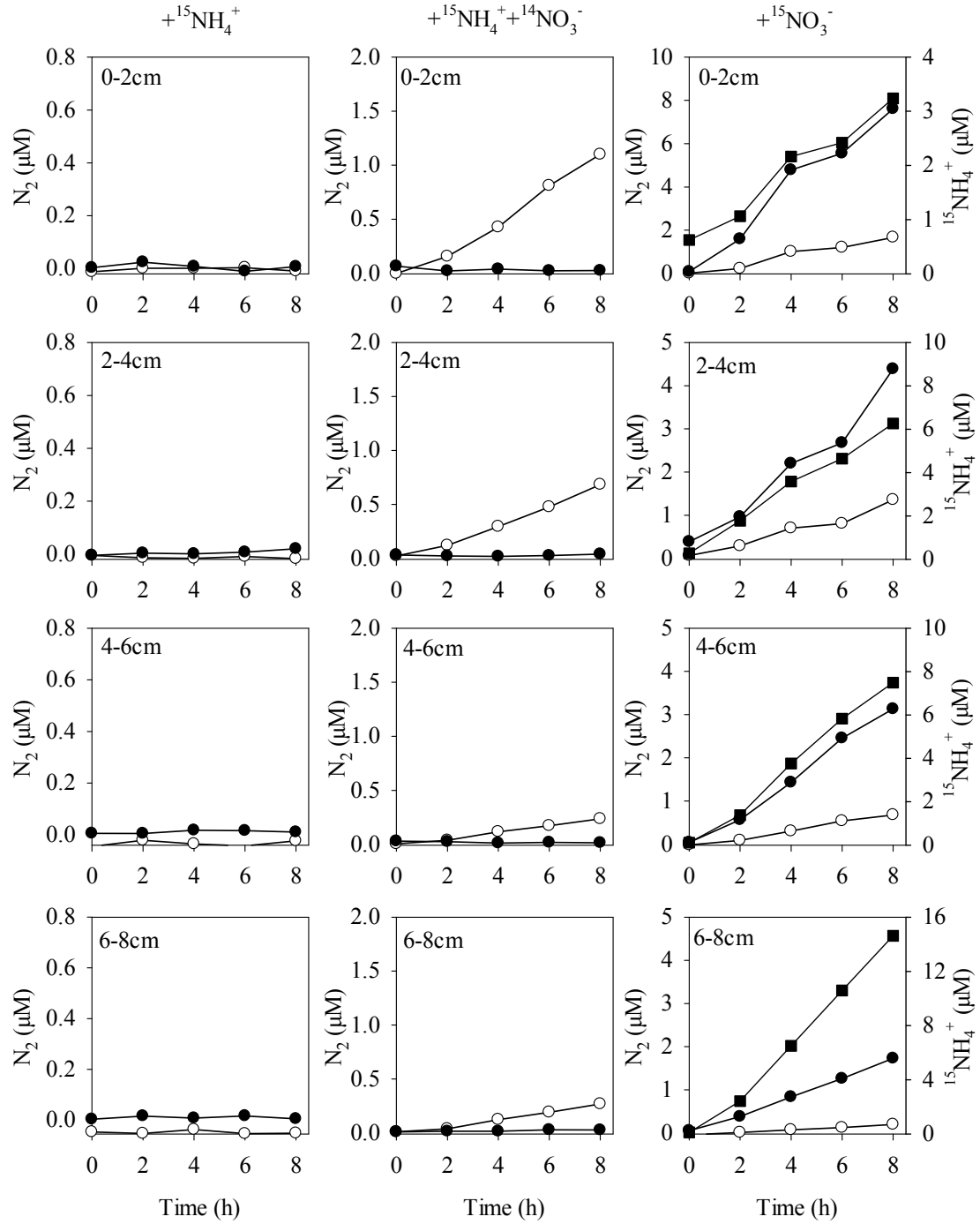


Fig. S5 Production of  $^{29}\text{N}_2$  (open circles),  $^{30}\text{N}_2$  (closed circles) and  $^{15}\text{NH}_4^+$  (closed squares) against time in slurry incubations at DH15.



## Chapter III

### The fate of nitrate in intertidal permeable sediments

Hannah K. Marchant<sup>1\*</sup>, Gaute Lavik<sup>1</sup>, Moritz Holtappels<sup>1</sup>, Marcel M.M. Kuypers<sup>1</sup>

<sup>1</sup>Max Planck Institute for Marine Microbiology, Celsiusstrasse 1, 28359 Bremen, Germany

\* Corresponding author: hmarchan@mpi-bremen.de, tel: +49421-2028630, fax: +49421-2028790

Keywords: nitrate respiration; permeable sediment; nitrogen cycling; DNRA; denitrification; eukaryotes

Contributions to the manuscript:

H.K.M., G.L., and M.M.M.K., designed research. H.K.M carried out fieldwork, performed MIMS and GC-IRMS measurements and data analysis. H.K.M., G.L., M.H., and M.M.M.K., conceived wrote and edited the manuscript

**Submitted to *PLoS One***

### **Acknowledgements**

We thank Theresa Hargesheimer for field support, Gabriele Klockgether, Sarah Kuschnerow and Kim Pohlmann for technical support in the lab and Ole Pfieler for assistance on the ship. This research was funded by the Max Planck Society.

**Abstract**

Coastal zones act as a sink for riverine and atmospheric nitrogen inputs and thereby buffer the open ocean from the effects of anthropogenic activity. Recently, microbial activity in sandy permeable sediments has been identified as a dominant source of N-loss in coastal zones, namely through denitrification. Some of the highest coastal denitrification rates measured so far occur within the intertidal permeable sediments of the eutrophied Wadden Sea. Still, denitrification alone can often account for only half of the substantial nitrate ( $\text{NO}_3^-$ ) consumption. Therefore, to investigate alternative  $\text{NO}_3^-$  sinks such as dissimilatory nitrate reduction to ammonium (DNRA), intracellular nitrate storage by eukaryotes and isotope equilibration effects we carried out  $^{15}\text{NO}_3^-$  amendment experiments. By considering all of these sinks in combination, we could quantify the fate of the  $^{15}\text{NO}_3^-$  added to the sediment. Denitrification was the dominant nitrate sink (50-75%), while DNRA, which recycles N to the environment accounted for 10-20% of  $\text{NO}_3^-$  consumption. Intriguingly, we also observed that between 20 and 40% of  $^{15}\text{NO}_3^-$  added to the incubations entered an intracellular pool of  $\text{NO}_3^-$  and was subsequently respired when nitrate became limiting. Eukaryotes were responsible for a large proportion of intracellular nitrate storage, and it could be shown through inhibition experiments that at least a third of the stored nitrate was subsequently also respired by eukaryotes. The environmental significance of the intracellular nitrate pool was confirmed by *in situ* measurements which revealed that intracellular storage can accumulate nitrate at concentrations six fold higher than the surrounding porewater. This intracellular pool is so far not considered when modeling N-loss from intertidal permeable sediments, however, it can act as a reservoir for nitrate during low tide. Consequently, nitrate respiration supported by intracellular nitrate storage can add an additional 20 % to previous nitrate reduction estimates in intertidal sediments, further increasing their contribution to N-loss.

## Introduction

Human activity has dramatically increased the amount of fixed nitrogen (N) in the environment, to the extent that anthropogenic sources now contribute  $156 \text{ Tg yr}^{-1}$ , almost as much as biological nitrogen fixation in the ocean ( $177 \text{ Tg}$ ), and more than biological  $\text{N}_2$ -fixation on land ( $107 \text{ Tg}$ ) (Galloway et al. 2004; Grosskopf et al. 2012). Worldwide, coastal seas receive a significant amount of this anthropogenic N through riverine run off ( $48 \text{ Tg N yr}^{-1}$ , Boyer et al. 2006), much of which respired to  $\text{N}_2$  within the sediment by benthic denitrification and anammox. The high rates of these processes within shelf sediments mean that they can account for up to 70% of all sedimentary N-loss (Gruber 2004). Therefore coastal seas act as a buffer, protecting the open ocean from the impact of anthropogenically derived N (Gruber and Galloway 2008).

Permeable, coarse grained sediments cover 58-70% of continental shelves and a large part of the coastal zone (Emery 1968). Nonetheless, most studies of N-cycling in coastal seas have focused on muddy diffusively controlled sediments and have neglected sandy sediments, which are highly efficient biocatalytic filters, in which organic matter inputs from the water column are quickly remineralized (Huettel et al. 2003). Moreover, permeable sediments are characterized by some of the highest potential denitrification rates in the marine environment (Cook et al. 2006; Gao et al. 2012) and are sites of aerobic denitrification (Gao et al. 2010; Rao et al. 2008). This is stimulated by advective pore water transport, which is caused by variations in pressure gradients as bottom water currents pass over sediment topography such as ripples. As a result the sediment is supplied with nutrient and oxygen rich water to penetration depths up to 6 cm (De Beer et al. 2005; Huettel and Rusch 2000; Werner et al. 2006).

The Wadden Sea, a UNESCO world heritage site, is one of the worlds largest intertidal ecosystems and is largely characterised by permeable sandy sediments, in which at least a third of extensive anthropogenic N-inputs are removed by microbially mediated processes (Gao et al. 2012). The vast majority of the  $640\text{-}820 \text{ kt N year}^{-1}$  N input enters the Wadden Sea as riverine discharges from rivers including the Rhine, Elbe and Weser, which represent a catchment area for a large part of the European agricultural run-off (Van Beusekom 2005).

Gao et al. (2010), first reported the occurrence of exceptionally high denitrification rates in the Wadden Sea using a combination of percolation techniques and isotope labeling studies.



Despite high rates of denitrification,  $\text{NO}_x$  consumption exceeded  $\text{N}_2$  production by a factor of 2 ( $22 \text{ mmol N m}^{-3}_{\text{sediment}} \text{ h}^{-1}$  compared to  $8 \text{ mmol N m}^{-3}_{\text{sediment}} \text{ h}^{-1}$ ) (Gao et al. 2012; Gao et al. 2010). It seems unlikely that  $\text{NO}_x$  assimilation alone could account for this discrepancy since incubations were run in the dark, reducing the potential for algal uptake of nitrate (Admiraal et al. 1987; Cook et al. 2004; Feuillet-Girard et al. 1997). Indeed, it has been demonstrated that  $^{15}\text{NO}_3^-$  assimilation into organic matter is negligible in sediments incubated in the dark. Instead, nitrate turnover is almost exclusively controlled by dissimilatory process such as denitrification and dissimilatory nitrate reduction to ammonium (DNRA) (Dähnke et al. 2012).

Denitrification is the best studied pathway of nitrate reduction in permeable sediments; whereas the alternative pathway of DNRA has rarely been investigated and has never been tested using percolation techniques. While DNRA consumes  $\text{NO}_x$ , it does not produce  $\text{N}_2$  or  $\text{N}_2\text{O}$  and as such does not contribute to N-loss but rather leads to N-recycling. Therefore, when DNRA is substantial, it can lead to sustained primary production and nitrification (King and Nedwell 1987). Many microorganisms can perform DNRA, including heterotrophic and chemoautotrophic prokaryotes (Canfield et al. 2005). Recently, eukaryotes, namely diatoms have also been shown to carry out DNRA. Diatoms appear to store nitrate in millimolar concentrations as a survival mechanism and are capable of switching from aerobic respiration to nitrate respiration when they are buried within the sediment (Lomstein et al. 1990).

In general, intracellular storage of nitrate appears to be common in permeable intertidal sediments similar to those from this study and represents a significant pool of  $\text{NO}_x$  which is not measurable in the porewater (Garcia-Robledo et al. 2010; Heisterkamp et al. 2012). Intracellular nitrate pools in sands have largely been attributed to diatoms (Lomas and Glibert 2000; Lomstein et al. 1990) while in muddy sediments, foraminifera (Piña-Ochoa et al. 2010) and large vacuolated sulfur bacteria have also been identified storing nitrate at high intracellular concentrations (Fossing et al. 1995; Mchatton et al. 1996; Sayama 2001). Nitrate storage offers an advantage to microorganisms in intertidal permeable systems, where oxygen and nitrate concentrations fluctuate frequently. However, it can also complicate stable isotope studies, as  $^{15}\text{N}$ -label additions to sediment incubations have been observed to cause nitrate release to the porewater (Sokoll et al. 2012; Song et al. 2013), or rapid equilibrations between stored  $^{14}\text{NO}_3^-$  pools and added  $^{15}\text{NO}_3^-$  pools (Dähnke et al. 2012).

Diatoms, both from the water column and the microphytobenthic (MPB) layer can contribute significantly to N-uptake and N-loss in permeable sediments (Grippo et al. 2010). Benthic primary production is enhanced in permeable quartz sands, as they refract light, leading to greater light penetration than in fine grained diffusive sediments (Jahnke et al. 2000). These microphytobenthos are subsequently more likely to be buried within permeable sediments during physical disturbance of the sediment (Böer et al. 2009; Ehrenhauss et al. 2004a). After burial and the onset of anoxic conditions, diatoms have been shown to switch to nitrate respiration (Kamp et al. 2011). So far, the overall contribution of these buried microphytobenthos to nitrogen cycling is not well understood.

Here we used a non-destructive percolation method, which enabled determination of nitrate conversion processes such as denitrification, DNRA and intracellular storage at high resolution in whole core incubations (Fig. 1). Previously, whole core percolation incubations have involved destructive sampling of an entire core for a single time point (e.g. Gao et al., 2012), while multiple or continuous sampling required slurry incubations (e.g. Gao et al., 2010). In this study, the use of whole core incubations directly linked to Membrane Inlet Mass Spectrometry (MIMS) enabled immediate determination of oxygen consumption rates and denitrification rates. Subsequent timing and labeling of further isotope experiments were then fine tuned to provide high resolution data. Thereby we were able assess the fate of nitrate within the sediment by quantifying nitrate reduction to  $N_2$  and  $NH_4^+$  by both eukaryotes and prokaryotes and also determine the role that intracellular nitrate storage plays within permeable sediments.

## **Methods**

### **Sampling site**

The Janssand sand flat (13 km<sup>2</sup>) is located in the back barrier area of Spiekeroog Island in the East Frisian Wadden Sea, Germany. The intertidal flat consists of three regions, the upper flat, the slope between the upper flat and the low water line and the low water line. The upper flat, which is the focus of the this study, consists of well sorted silicate sand in the upper 15 cm, with a permeability of  $7.2 - 9.5 \times 10^{-12}$ , a porosity of .35 and a mean grain size of 176mm (Billerbeck et al. 2006a; Billerbeck et al. 2006b). At high tide the flat is covered by 1.5 – 2 m of

seawater for 6-8 h and is exposed to air for 6-8 h during low tide, dependent on tidal range. The sampling site (53.73515 'N, 007.69913'E) is on the northeastern margin of the flat around 80m upslope from the mean low water line. Due to the high permeability of the sand, water is flushed advectively through the sediment in two distinct temporal and spatial scales. During inundation, boundary flows force water into troughs on the rippled surface, filtering organic particles and nutrients, which are then degraded and returned to the overlying water promptly at the ripple peak. The "skin circulation" of porewater occurs at spatial scales in the order of centimeters and temporal scales of minutes to hours (Billerbeck et al. 2006b).

### **Sample collection**

Sediment sampling for  $^{15}\text{N}$ -labelled incubations was conducted on the upper flat in winter, spring and summer on 1 November 2011, 13 April 2012 and 20 July 2012 respectively. Sediment was collected from the upper 5 cm of the sand flat, placed in a prewashed plastic container and returned to the Max Planck Institute, Bremen. Within 4 hours of collection, homogenized sediment was carefully packed into sediment columns (see below), ensuring no bubbles were present. Sediment cores were then allowed to equilibrate overnight, during which time aerated site seawater was pumped through them on a simulated tidal cycle consisting of a 6 hour period of 30 minutes with pumping (at  $2.5 \text{ ml min}^{-1}$ ), 15 minutes without pumping, followed by 6 hours without additional water supply. All incubations were carried out after 24 hours of equilibration. Homogenization of sediment has previously been shown to have little effect on nitrogen cycling rates, as observed in Gao et al., (2010). Rates obtained from whole cores percolated with nitrate amended seawater were the same as rates obtained from homogenized slurries.

### **Sediment columns**

Columns were constructed of PVC tubing (height 9 cm, I.D. 10.3 cm) and sealed with rubber stoppers. Inflow and outflow ports were provided by boring 0.5 cm I.D. holes through the centre of the rubber stopper, which were fitted with 2 way valves. The internal face of each rubber stopper was milled with radial grooves to create radial pressure and flow through the columns. To prevent sediment from filling the grooves and obstructing flow, they were covered with a fine mesh filter (500 microns, Hydra-BIOS, Germany). Columns and supply seawater were held at 19°C for the entire experiment.

## Incubations

In each season experiments were carried out on 3 replicate sediment columns. Incubations were started by amending 600 ml of aerated site seawater with labeled and unlabeled substrate dependent on the process being investigated (Table 1). Water was then pumped through the core from the bottom using a peristaltic pump at 30 ml min<sup>-1</sup>. Preliminary measurements (data not shown), confirmed that this was more than 1.5 x the volume needed to entirely exchange the porewater within the sediment. After 20 minutes the inflow port was closed using a 2-way valve. A sampling port was connected to the 2-way valve and porewater was then sampled using one of two methods.

**Table 1. Summary of sampling dates, conditions, and <sup>15</sup>N incubation experiments conducted.**

Sampling Date	Substrate Additions ( $\mu\text{M}$ )	Sampling method <sup>a</sup>	Processes Targeted
November 1st 2011	<sup>15</sup> NO <sub>3</sub> <sup>-</sup> (50)	MIMS	O <sub>2</sub> consumption, denitrification
	<sup>15</sup> NO <sub>3</sub> <sup>-</sup> (50)	Exetainers	Denitrification, DNRA
	Unamended	Exetainers	Storage
	<sup>15</sup> NO <sub>3</sub> <sup>-</sup> (50) + 200 $\mu\text{g}$ cyclohexamide*	Exetainers	Denitrification, DNRA
	200 $\mu\text{g}$ cyclohexamide	Exetainers	Storage
April 13rd 2012	<sup>15</sup> NO <sub>3</sub> <sup>-</sup> (50)	MIMS	O <sub>2</sub> consumption, denitrification
	<sup>15</sup> NO <sub>3</sub> <sup>-</sup> (30)	Exetainers	Denitrification, DNRA
	Unamended	Exetainers	Storage
	<sup>15</sup> NO <sub>3</sub> <sup>-</sup> (30) + 200 $\mu\text{g}$ cyclohexamide*	Exetainers	Denitrification, DNRA
	200 $\mu\text{g}$ cyclohexamide	Exetainers	Storage
July 22nd 2012	<sup>15</sup> NH <sub>4</sub> <sup>+</sup> (50) + <sup>14</sup> NO <sub>2</sub> <sup>-</sup> (100) + <sup>14</sup> NO <sub>3</sub> <sup>-</sup> (100) + ATU (86)	Exetainers	Anammox**
	<sup>15</sup> NO <sub>3</sub> <sup>-</sup> (50)	MIMS	O <sub>2</sub> consumption, denitrification
	<sup>15</sup> NO <sub>3</sub> <sup>-</sup> (50)	Exetainers	Denitrification, DNRA
	Unamended	Exetainers	Storage
	<sup>15</sup> NO <sub>3</sub> <sup>-</sup> (50) + 200 $\mu\text{g}$ cyclohexamide* 200 $\mu\text{g}$ cyclohexamide	Exetainers Exetainers	Denitrification, DNRA Storage

<sup>a</sup> For further detail see description in text

\* Before incubation sediment columns were additionally preincubated for 6 hours with porewater containing 200  $\mu\text{g}$  cyclohexamide

\*\* The sediment cores used in this incubation were not used for further incubations

In the first instance the sampling port was connected via a piece of tygon tubing to a membrane inlet mass spectrometer (MIMS; GAM200, IPI). Porewater was pulled through the

membrane from the column at a speed of  $500 \mu\text{l min}^{-1}$  by a peristaltic pump placed downstream of the membrane. This allowed simultaneous online measurements of mass 28 ( $^{14}\text{N}^{14}\text{N}$ ), 29 ( $^{14}\text{N}^{15}\text{N}$ ), 30 ( $^{15}\text{N}^{15}\text{N}$ ), 40 (Ar), and 32 ( $\text{O}_2$ ) and was equivalent to a flow velocity of around  $1 \text{ cm h}^{-1}$ . Oxygen consumption rates,  $^{29}\text{N}_2$  and  $^{30}\text{N}_2$  production rates showed low standard deviation between biological replicates, indicating that this method gives replicable results.

In the second instance, porewater was collected by opening the 2 way valve on the bottom of the column and letting porewater flow directly into 6 ml exetainers (Labco Ltd, High Wycombe, UK), prefilled with  $100 \mu\text{l}$  saturated  $\text{HgCl}_2$ .  $1.5 \text{ ml}$  of porewater was discarded initially at each time point to flush the tubing between the column and the sediment (the total volume sampled was therefore  $90 \text{ ml}$  per incubation, less than half the porewater contained per core and a flow velocity around  $2 - 3 \text{ cm h}^{-1}$ ). In both cases sampled porewater was replaced passively with unamended sea water at the top of the column.

Mass balances were performed on incubations to which  $^{15}\text{NO}_3$  was added and exetainer sampling performed. At the end of the incubation the amount of  $^{15}\text{N}$  present as  $^{15}\text{NO}_3$ ,  $^{15}\text{NO}_2$ ,  $^{15}\text{NH}_4$ ,  $^{15}\text{N}_2\text{O}$ , and  $^{15}\text{N}_2$  was determined.

Furthermore, after the last time point was taken, the entire porewater volume within the sediment column was exchanged for unlabeled water and over 4 hours the accumulation of the same labeled compounds was followed. Following this cores were preincubated with cycloheximide (an inhibitor of eukaryotic protein synthesis, Fuhrman and Mcmanus 1984) for six hours and both incubations were repeated.

In April and July the oxygen concentration of the porewater at each time point was determined in the exetainer immediately after filling using an  $\text{O}_2$  microsensor. Oxygen microsensors were constructed as described in Revsbech (1989). Calibration was performed prior to sampling using a 2 point method, in which the signal was determined in air saturated seawater and  $\text{N}_2$  degassed seawater before correcting for  $\text{O}_2$  solubility based on the ambient water temperature ( $19.2^\circ\text{C}$ ) and salinity (35). There were only small differences between oxygen consumption rates when determined from MIMS or by direct microsensor measurement in exetainers. Therefore, for the samples from winter where no microsensor measurements were available,  $\text{O}_2$  concentrations were determined from the initial MIMS incubation.

### Intracellular nitrate storage determination

Sediment and porewater for the determination of intracellularly stored nitrate was collected on October 24 2013 from the upper sand flat and approximately 5 m downslope. Sediment had been exposed to the air for approximately 120 minutes and 90 minutes respectively. Rhizon samplers (Seeberg-Elverfeldt et al. 2005) were used to directly sample porewater from the top 3 cm of sediment (5 samples per location). Approximately 5 mL of sediment was collected concurrently and added to a 50 mL falcon tube along with 3 mL NaCl solution (adjusted to the *in situ* salinity of 33) and 400  $\mu$ l saturated  $\text{HgCl}_2$  (5 samples per location). All samples were kept on ice and upon return stored at  $-20^\circ\text{C}$  upon return until further analysis. 2 litres of sediment was also collected and upon return packed into a sediment core (as before), whereupon it was supplied with site seawater for 6 hours before being sampled for porewater and sediment. Intracellular nitrate concentrations within the sediment were determined using the method of Stief et al., 2013. Briefly sediment samples were shock-frozen in liquid nitrogen for 5 min, and then heated to  $90^\circ\text{C}$  in a water bath for 10 min, a process which was repeated 3 times.  $\text{NO}_x$  was determined in all samples as detailed below. Diatom abundances within the upper layer of the sediment were estimated using the method described in Ehrenhauss et al. (2004a). Diatoms counts were split into 4 size classes based on morphology and the average biovolume of each size class was determined using the calculations of Hillebrand et al. (1999). Foram abundance was estimated using the method described in Goineau et al. (2011).

### Isotopic and nutrient analyses

2 ml of porewater within each exetainer was replaced with a helium headspace and allowed to equilibrate, subsequently the isotopic N composition of  $\text{N}_2$  and  $\text{N}_2\text{O}$  gas in all exetainers was determined by GC-IRMS (VG Optima, Manchester, UK). Afterwards,  $^{15}\text{NO}_2$  and  $^{15}\text{NO}_3$  concentrations were determined in subsamples of all samples, after conversion to  $\text{N}_2$  by sulfamic acid addition or cadmium reduction/sulfamic acid addition (after  $\text{NO}_2$  removal) respectively (Füssel et al. 2011).  $^{15}\text{NH}_4^+$  was determined in subsamples after oxidation with hypobromite to  $\text{N}_2$  (Preisler et al. 2007; Waremburg 1993)

Concentrations of  $^{45}\text{N}_2\text{O}$ ,  $^{46}\text{N}_2\text{O}$ ,  $^{29}\text{N}_2$  and  $^{30}\text{N}_2$  were calculated from the excess relative to air, explained in detail in Holtappels et al. (2011) and rates were calculated from the slope of

linear regression of  $^{15}\text{N}$ -production as a function of time. Only significant and linear production or consumption of  $^{15}\text{N}$ -species was considered ( $t$ -tests,  $p < 0.05$ ;  $R^2 > 0.75$ ).

Combined nitrate and nitrite ( $\text{NO}_x$ ) concentration within each exetainer was determined by a CLD 60 Chemiluminescence  $\text{NO}/\text{NO}_x$  analyzer (Ecophysics) after reduction to  $\text{NO}$  with acidic vanadium (II) chloride (Braman and Hendrix 1989). Total  $\text{NH}_4^+$  was determined either by flow injection analysis (Hall and Aller 1992) or photometrically (Grasshoff 1999), dependent on whether samples contained  $\text{HgCl}_2$  or were filtered, respectively.

### Rate determinations

Denitrification rates were determined from the production of  $^{29}\text{N}_2$  ( $p^{29}\text{N}_2$ ) and  $^{30}\text{N}_2$  ( $p^{30}\text{N}_2$ ) according to Thamdrup and Dalsgaard (2002):

$$\text{Den} = p^{30}\text{N}_2 (F_{\text{NO}_3}^{15 \text{ prod}})^{-2} \quad (\text{eq 1})$$

Where  $F_{\text{NO}_3}^{15 \text{ prod}}$  is the labeling percentage of nitrate which was calculated from the production of  $^{29}\text{N}_2$  and  $^{30}\text{N}_2$ :

$$F_{\text{NO}_3}^{15 * } = 2 / (p^{29}\text{N}_2 / p^{30}\text{N}_2 + 2) \quad (\text{eq 2})$$

The labeling percentage of nitrate can also be calculated from the initial concentrations of labeled and unlabeled nitrate ( $F_{\text{NO}_3}^{15 \text{ added}}$ )

$$F_{\text{NO}_3}^{15 \text{ added}} = {}^{15}\text{NO}_3^- / ({}^{14}\text{NO}_3^- + {}^{15}\text{NO}_3^-) \quad (\text{eq 3})$$

$F_{\text{NO}_3}^{15 \text{ prod}}$  and  $F_{\text{NO}_3}^{15 \text{ added}}$  can be different from each other if the fraction of labeled nitrate changes during the incubation, therefore we compared the results from both.

DNRA rates were determined from the labeling percentage of nitrate (eq 2) and the production of  $^{15}\text{NH}_4^+$  ( $p^{15} \text{NH}_4^+$ ):

$$\text{DNRA} = p^{15} \text{NH}_4^+ / F_{\text{NO}_3}^{15 \text{ added}} \quad (\text{eq 4})$$

Eukaryotic and prokaryotic rates for all processes were determined by subtracting the rates obtained in the incubation amended with  $^{15}\text{NO}_3^-$  and cyclohexamide ( $\text{Inc}_{\text{cyc}}$ ) from the rates obtained in the incubation amended with only  $^{15}\text{NO}_3^-$  ( $\text{Inc}_1$ )

$$\text{Prokaryotic rate} = (\text{Inc}_{\text{cyc}}) \quad (\text{eq 5})$$

$$\text{Eukaryotic rate} = (\text{Inc}_1) - (\text{Inc}_{\text{cyc}}) \quad (\text{eq 6})$$

## Results

### Oxygen consumption rates

Online Membrane Inlet Mass Spectrometry (MIMS) was used to determine  $\text{O}_2$  respiration rates in parallel to  $^{15}\text{N-N}_2$  production rates (Fig. 1). Oxygen consumption rates (OCR) were highest in winter ( $459 \pm 60 \mu\text{mol L}^{-1} \text{h}^{-1}$ ) and lowest during spring ( $271 \pm 51 \mu\text{mol L}^{-1} \text{h}^{-1}$ ) and summer ( $292 \pm 23 \mu\text{mol L}^{-1} \text{h}^{-1}$ ). Furthermore, the online MIMS data meant that subsequent incubations could be timed to ensure that samples were collected until oxygen was entirely consumed and  $^{15}\text{N-N}_2$  production had ceased.

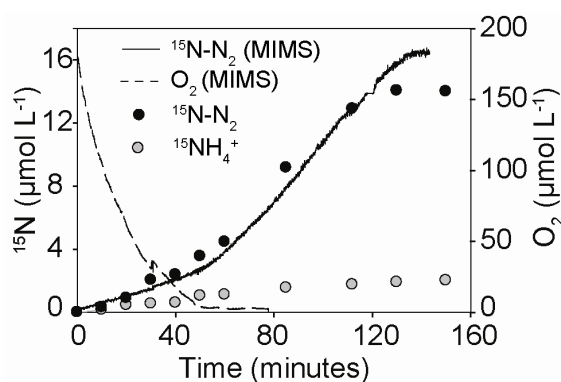


**Figure 1. Comparison of incubation methods.** Incubations were carried out using either membrane inlet mass spectrometry (MIMS) which allowed for continuous online measurements or by discrete porewater sampling into exetainers and subsequent measurement on a GC-IRMS.

### Denitrification rates

Subsequent to the MIMS incubation, production of  $^{15}\text{N-N}_2$  and  $^{15}\text{NH}_4^+$  were determined from  $^{15}\text{NO}_3^-$  amendment experiments in which porewater was subsampled discretely into exetainers and measured by GC-IRMS.  $^{15}\text{N-N}_2$  and  $^{15}\text{NH}_4^+$  concentrations within subsampled porewater revealed that denitrification was the most dominant nitrate sink within the sediment in all seasons (Fig. 2). Aerobic denitrification occurred in all seasons, however rates were 80-90



% lower than the anaerobic denitrification rates, which were measured upon the sediment becoming anoxic. Oxygen consumption rates of individual sediment cores positively correlated with anaerobic denitrification rates. This correlation persisted in all seasons, even though denitrification rates differed seasonally. In winter denitrification rates were  $22.8 \pm 2.9 \text{ mmol N m}^{-3} \text{ sediment h}^{-1}$ , almost double those in spring ( $8.65 \pm 0.6 \text{ mmol N m}^{-3} \text{ sediment h}^{-1}$ ) and summer ( $9.02 \pm 0.9 \text{ mmol N m}^{-3} \text{ sediment h}^{-1}$ ) (Fig. 2). A further set of incubations were carried out on the same sediment, which were amended with  $^{15}\text{NO}_3^-$  and cycloheximide, a eukaryote inhibitor. In these cycloheximide incubations, the only change that could be observed in denitrification rates was during winter, when a slight decrease in rates was observed.

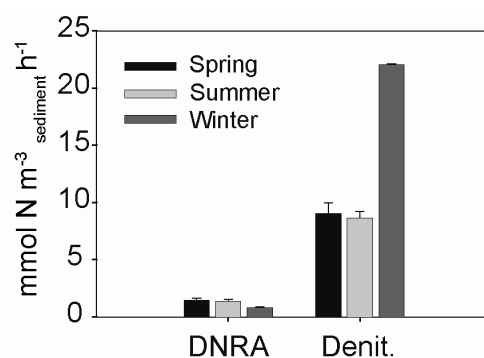


**Figure 2. Rates of nitrogen cycling processes determined over 3 seasons.** Anaerobic dissimilatory nitrate reduction to ammonium (DNRA) and denitrification (Denit.) rates from the incubation amended with  $^{15}\text{NO}_3^-$ . Rates were determined from linear production slopes after oxygen had been consumed. Error bars are SD ( $n = 3$ )

### DNRA rates

DNRA was determined from the production of  $^{15}\text{NH}_4^+$  in the  $^{15}\text{NO}_3^-$  amendment experiments and occurred in all seasons (Fig. 2). DNRA rates were detectable in the presence and absence of oxygen, with oxic rates 50-80% lower than anoxic rates. In the  $^{15}\text{NO}_3^-$  amendment experiment, the only significant seasonal difference in DNRA rates was observed during winter, when rates were lower. However, the subsequent  $^{15}\text{NO}_3^-$  + cycloheximide amendment allowed us to determine the contribution of eukaryotes and prokaryotes to DNRA separately. Prokaryotic DNRA rates were higher in summer, while eukaryotic rates were higher in spring (Fig. 3).

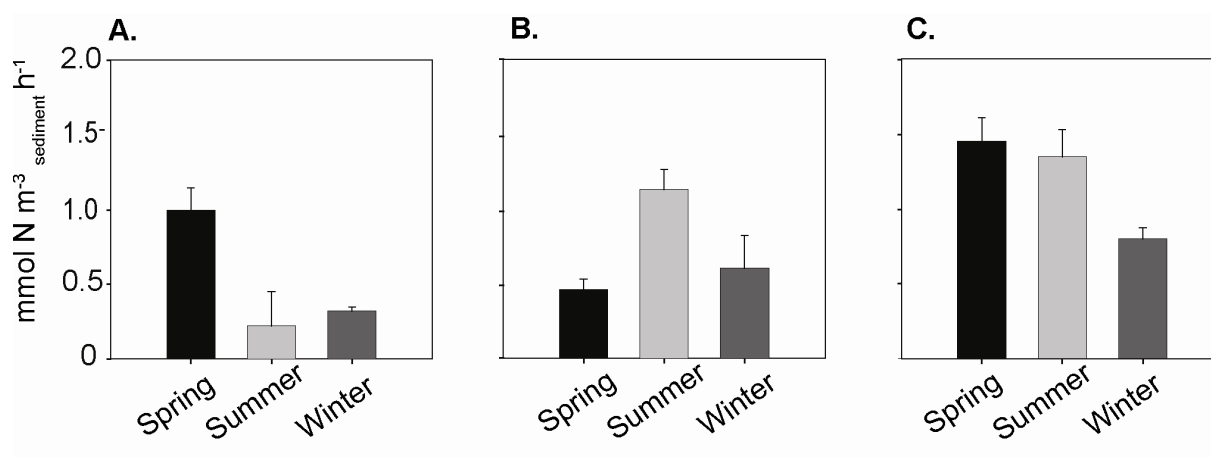


**Figure 3. Seasonal patterns in DNRA rates mediated by the prokaryotic and eukaryotic community.** A) Eukaryotic DNRA rates B) Prokaryotic DNRA rates C) Overall DNRA rates. Total rates were determined from the incubation amended with  $^{15}\text{NO}_3^-$ . Prokaryotic rates were determined after addition of the eukaryote inhibitor cycloheximide. Eukaryotic rates were calculated by subtracting prokaryotic rates from total rates. Error bars are SD (n = 3)

### Anammox rates

Anammox could not be detected from incubations in summer which were amended with  $^{15}\text{NH}_4^+$ ,  $^{14}\text{NO}_2^-$ ,  $^{14}\text{NO}_3^-$  and ATU. Although incubations for anammox were not carried out in spring or winter, the  $^{15}\text{NO}_3^-$  amendment experiment indicated that  $\text{N}_2$  due to anammox was insignificant in these seasons as well. If anammox ( $\text{NH}_4^+ + \text{NO}_2^- \rightarrow \text{N}_2$ ), was occurring to any significant extent then  $^{29}\text{N}_2$  production ( $^{14}\text{NH}_4^+ + ^{15}\text{NO}_2^- \rightarrow ^{29}\text{N}_2$ ) within the incubation would be higher than expected if only denitrification were reducing  $^{14+15}\text{NO}_3^-$ . This would cause the ratio of  $^{29}\text{N}_2$  and  $^{30}\text{N}_2$  produced ( $F_{\text{NO}_3}^{15 \text{ prod}}$ ) to be lower than expected from the  $\text{NO}_3^-$  labeling fraction ( $F_{\text{NO}_3}^{15 \text{ added}}$ ). When  $F_{\text{NO}_3}^{15 \text{ added}}$  was compared to  $F_{\text{NO}_3}^{15 \text{ prod}}$  they did not vary by more than 1.5% at each time point during the anoxic phase of incubations in spring and winter,.

### N-Isotope equilibration

Despite the absence of detectable anammox activity in summer,  $F_{\text{NO}_3}^{15 \text{ prod}}$  was significantly lower than  $F_{\text{NO}_3}^{15 \text{ added}}$  throughout the  $^{15}\text{NO}_3^-$  amendment experiment. The difference in  $F_{\text{NO}_3}^{15 \text{ prod}}$  and  $F_{\text{NO}_3}^{15 \text{ added}}$  was a result of a large initial decrease in the  $^{15}\text{N}$  labeling percentage of  $\text{NO}_3^-$  in the porewater (Fig. 4). Almost 35% of the added  $^{15}\text{NO}_3^-$  was no longer present in the porewater when sampling began, whereas  $^{14}\text{NO}_3^-$  concentrations were higher in the porewater than the  $^{14}\text{NO}_3^-$  concentrations measured in the seawater before it was percolated through the sediment.  $^{14}\text{NO}_3^-$  concentrations continued to increase over time,

appearing to equilibrate with  $^{15}\text{NO}_3^-$ . The decrease in labeling percentage occurred in all three summer replicates and represented an apparent ‘loss’ of around 40% of the added  $^{15}\text{NO}_3^-$  which appears to have been exchanged with  $^{14}\text{NO}_3^-$ .

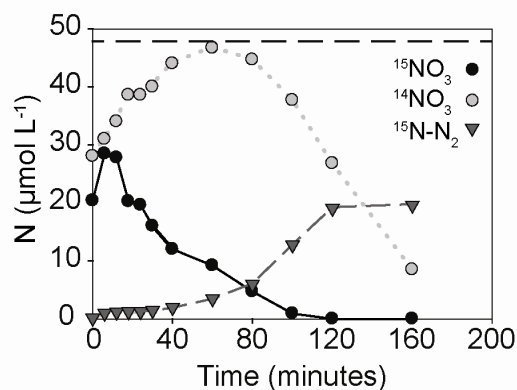


**Figure 4. Exchange of  $^{15}\text{NO}_3^-$  and  $^{14}\text{NO}_3^-$  over time in summer incubations.** The dashed line indicates the initial amount of  $^{15}\text{NO}_3^-$  added to the incubation

### Intracellular nitrate storage

After  $^{15}\text{NO}_3^-$  “loss” due to isotope equilibration effects were taken into account in the  $^{15}\text{NO}_3^-$  amendment experiment, we found that  $^{15}\text{NO}_3^-$  consumption exceeded  $^{15}\text{NH}_4^+$  and  $^{15}\text{N-N}_2$  production. To see whether there had been  $^{15}\text{NO}_3^-$  uptake into the intracellular pool which was not identified by the isotope equilibration analysis, we performed another incubation after all the  $^{15}\text{NO}_3^-$  had been consumed and  $^{15}\text{N-N}_2$  production had ceased in the  $^{15}\text{NO}_3^-$  amendment experiment. In this incubation we exchanged the entire porewater volume within the sediment core with oxic seawater to which no  $^{15}\text{NO}_3^-$  had been added. No  $^{15}\text{NO}_3^-$  or  $^{15}\text{NO}_2^-$  could be detected in the porewater within the first 5 minutes of this incubation. Subsequently, the production of  $^{15}\text{NO}_x$ ,  $^{15}\text{N-N}_2$  and  $^{15}\text{NH}_4^+$  was observed (Fig. 5a).  $^{15}\text{NO}_x$  did accumulate after 10 minutes to low concentrations, but was consumed rapidly. This accumulation of  $^{15}\text{NO}_x$  was too small to account for the overall production of  $^{15}\text{N-N}_2$  and  $^{15}\text{NH}_4^+$  observed during the same time period. Therefore another pool of  $^{15}\text{NO}_x$  must have been present with the sediment, which we attributed to the storage of  $^{15}\text{NO}_3^-$  intracellularly.

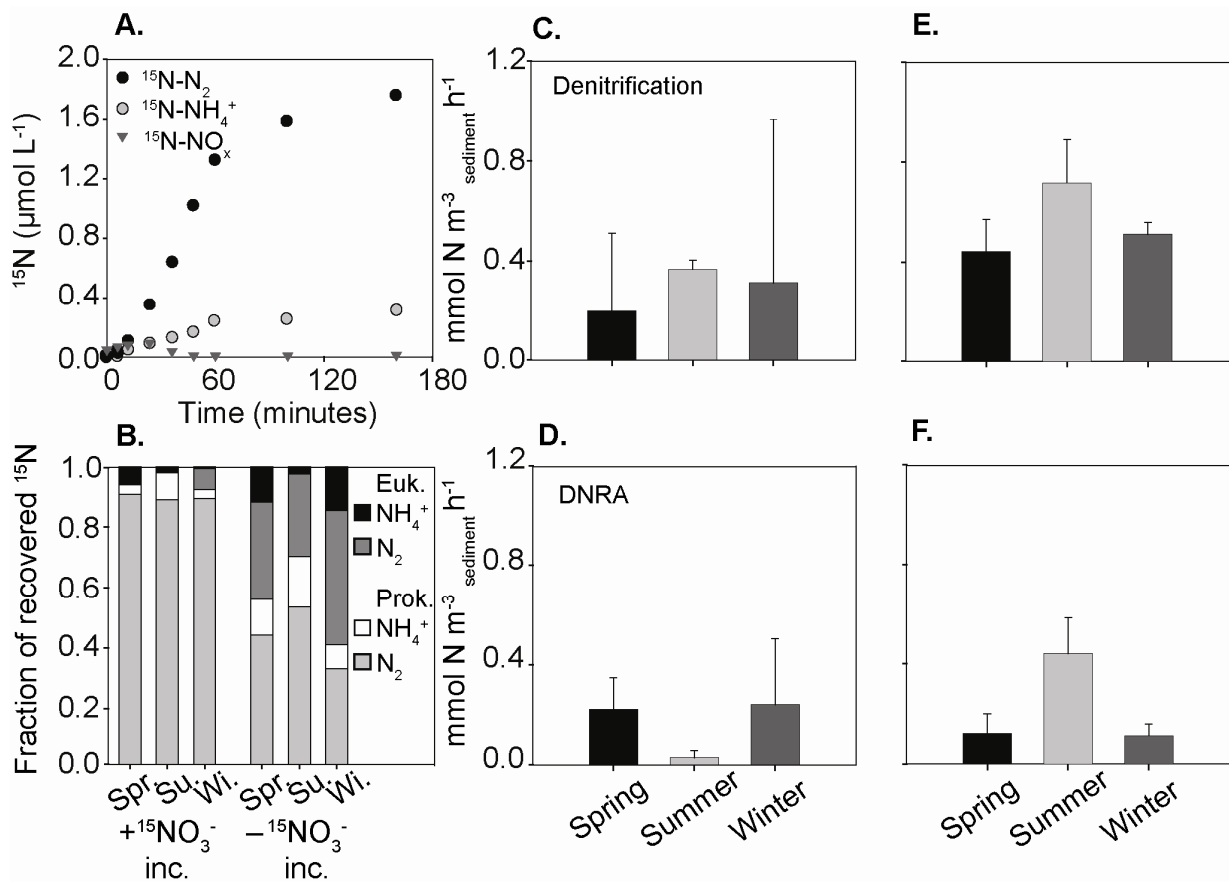


**Figure 5. Respiration of stored intracellular nitrate by eukaryotes and prokaryotes.** A) Example of the appearance of  $^{15}\text{N}$  labeled compounds stored in the sediment during the secondary incubation to which no label was added B) Comparison of the overall fraction of  $^{15}\text{N}$  recovered as either  $\text{N}_2$  or  $\text{NH}_4^+$  in both the primary and secondary incubation and the partitioning between eukaryotes and prokaryotes C) Eukaryotic denitrification rates E) prokaryotic denitrification rates D) eukaryotic DNRA rates F) prokaryotic DNRA rates. Error bars are SD (n = 3).

The denitrification rates supported by intracellularly stored  $^{15}\text{NO}_3^-$  were always higher than the co-occurring DNRA rates (Fig. 5c-f). Overall the storage driven rates of denitrification and DNRA were  $\sim 15\%$  and  $30\%$  respectively when compared to rates determined previously in the  $^{15}\text{NO}_3^-$  amendment experiment. 40% of the storage driven denitrification rates could be attributed to eukaryotes (Fig. 5b,c,d). Prokaryotes were mainly responsible for storage driven DNRA in summer (Fig. 5f), while in spring and winter the contributions of prokaryotes and eukaryotes were similar (Fig. 5b).

### ***In situ* concentrations of intracellular nitrate storage**

To investigate whether intracellular storage of nitrate is relevant within the sediment in the environment, we determined the concentration of nitrate stored intracellularly *in situ* in

early winter 2013. Porewater  $\text{NO}_x$  concentrations were on average  $4.4 \mu\text{mol dm}^{-3}_{\text{sediment}}$  ( $\pm 1.0$ ) 90 minutes after sediment exposure at low tide and  $2.5 \mu\text{mol dm}^{-3}_{\text{sediment}}$  ( $\pm 1.2$ ) 120 minutes after exposure. Concentrations of nitrate stored intracellularly were  $29.5 \mu\text{mol dm}^{-3}_{\text{sediment}}$  ( $\pm 3.5$ ) in the sediment exposed by low tide for 90 minutes, and  $27.5 \mu\text{mol dm}^{-3}_{\text{sediment}}$  ( $\pm 6.6$ ) in sediment exposed for 120 minutes. On average therefore, concentrations of nitrate stored intracellularly were ~6 fold higher than average porewater nitrate concentrations.

To examine whether the eukaryotic community within the sediment was sufficient to account for the observed intracellular nitrate storage, we determined the abundance of diatoms and foraminifera. We found foraminifera at abundances of around  $8 (\pm 4) \text{ cm}^{-3}_{\text{sediment}}$ , these were identified as belonging to the genus *Ammonia*. Diatoms were found in abundances of around  $2.7 \times 10^4 \text{ cm}^{-3}_{\text{sediment}}$ . Four classes of diatoms were identified within the sediment which we described as 1) large pennate, 2) chain forming short pennate, 3) chain forming long pennate and 4) other small. These 4 classes of diatoms comprised 55 % ( $\pm 14$ ), 14 % ( $\pm 9$ ), 25 % ( $\pm 15$ ) and 7 % ( $\pm 7$ ) of the total diatom count, respectively. The average biovolumes of the same 4 classes were  $3700 \mu\text{m}^3 (\pm 1240)$ ,  $930 \mu\text{m}^3 (\pm 420)$ ,  $1200 \mu\text{m}^3 (\pm 250)$  and  $519 \mu\text{m}^3 (\pm 310)$ , respectively. Cell-volume-specific intracellular nitrate concentrations calculated for the average cell volume were therefore  $60 \text{ mmol L}^{-1}$  diatom.

## Discussion

We used a non-destructive percolation method to follow transformations of nitrate within permeable sediments from the intertidal Wadden Sea. By amending seawater with  $^{15}\text{NO}_3^-$  and exchanging it with porewater in a sediment core we could quantify denitrification rates at high temporal resolutions (12 time points over 2-3 hours; Fig. 1). With this method, we observed volumetric denitrification rates ranging from  $8\text{-}23 \text{ mmol N m}^{-3}_{\text{sediment}} \text{ h}^{-1}$ . These rates represent a two to five fold increase in denitrification relative to rates previously reported from the same site (Gao et al., 2012). Gao et al. used whole core incubations percolated to 5cm depth with  $50 \mu\text{mol } ^{15}\text{NO}_3^- \text{ L}^{-1}$  that were subsequently sacrificed at a given time point, and therefore were restricted to at most 5 timepoints per incubation. In their incubations, nitrate appeared to be consumed before 4 time points were sampled, which could have lead to underestimated

denitrification rates. We added the same amount of  $^{15}\text{NO}_3^-$  (30-50  $\mu\text{mol L}^{-1}$ ) as Gao et al., but the higher sampling frequency ensured that rates were determined from linear production slopes. The consistently higher denitrification rates in this study indicate that the high N-loss estimates for the Wadden Sea reported in Gao et al., 2012, (750  $\text{mmol N m}^{-2} \text{yr}^{-1}$ ) might be conservative.

### Denitrification as a nitrate sink

N-loss in the form of  $\text{N}_2$  was the main sink of nitrate in intertidal permeable Wadden Sea sediments. Denitrification was revealed to be the main process by which N-loss occurred, as the combination of  $^{15}\text{NO}_3^-$  incubations, production ratios of  $^{29}\text{N}_2$  and  $^{30}\text{N}_2$ , as well as  $^{15}\text{NH}_4^+$  incubations showed that anammox was insignificant. These results agree well with previous results from this study site, where  $^{15}\text{N}$ -labelling experiments have indicated anammox rates are <1% of denitrification (Gao et al. 2012) and metagenomic analysis has revealed that anammox bacteria are of low abundance (pers. comm. M. Strous).

While denitrification was always the dominant sink of nitrate in the sediment, rates of N-loss differed seasonally. Denitrification rates were double in winter in comparison to spring or summer (Fig. 2). The seasonal changes in denitrification rates could have resulted from seasonal differences in organic matter limitation, nitrate concentrations or the composition of the microbial community (Seitzinger et al. 2006). Our results indicated that nitrate and organic matter may both have played a role within our sediments, we could show that there was a weak positive correlation between denitrification rates and average seasonal water column nitrate concentrations ( $r^2 = 0.67$   $p = <0.01$ ) and a strong positive correlation between denitrification rates and measured oxygen consumption rates ( $r^2 = 0.76$   $p = <0.01$ ).

Oxygen consumption rate (OCR) is a proxy for labile organic matter (OM) (Glud 2008). Thus, the decreased OCR in spring and summer indicates that those seasons had less available labile OM compared to OM in winter. As OM is the substrate for heterotrophic denitrification, it can limit denitrification rates (Trimmer and Nicholls 2009). Therefore lower summer OM availability could have been responsible for the relatively lower spring and summer denitrification rates. Initially this seems surprising, as OM availability in the water column is higher in spring and summer due to increased pelagic primary production. However, previous studies have shown that despite high water column concentrations of dissolved organic carbon

and particulate organic carbon (DOC and POC), summer concentrations of DOC are low in the surface layer of permeable sediments (Chipman et al. 2012; Rusch et al. 2003). This is a result of reduced wind and wave action during summer, which leads to decreased pore water filtration and limits the transport of POC into the sediment. In contrast, during winter, labile DOC distributions in the surface layer of permeable sediments are at their highest (Billerbeck et al. 2006b; Chipman et al. 2012). This is due to high winds, which increase advective porewater flow, thereby enhancing the transport of POC into the surface layer of the sediment, whereupon they are retained by sediment filtration and provide a source of new DOC.

### **DNRA as a nitrate sink**

In the  $^{15}\text{NO}_3^-$  amendment experiment,  $^{15}\text{NO}_3^-$  was reduced to  $^{15}\text{NH}_4^+$  as well as  $^{15}\text{N-N}_2$ , indicating that dissimilatory nitrate reduction to ammonium (DNRA) was occurring (Fig. 1). DNRA was a smaller sink for nitrate than denitrification, with DNRA rates accounting for around 15% of total nitrate reduction rates (DNRA + Denitrification) (Fig. 2). The DNRA rates are comparable to those measured in a diverse range of muddy shelf sediments, including the Baltic sea (Jantti and Hietanen 2012), East China Sea (Song et al. 2013), temperate and tropical estuaries (An and Gardner 2002; Dong et al. 2011; Koop-Jakobsen and Giblin 2010) and fjords (Bonin et al. 1998; Christensen et al. 2000). However, as denitrification rates are so high in the Wadden Sea, the contribution of DNRA to total nitrate reduction was lower than in other continental shelf sediments.

The rate of nitrate reduction to ammonium varied seasonally within the sediment, overall DNRA rates were higher in spring and summer and significantly lower in winter (Fig. 2). However, different seasonal patterns emerged when prokaryotic and eukaryotic DNRA rates were considered separately (Fig 3). Prokaryotic DNRA rates were highest in summer (Fig 3b) while eukaryotic rates were highest in spring (Fig. 3a). The high prokaryotic rates of DNRA in summer agree well with the observations of a number of previous studies and may have resulted from a combination of factors; 1) DNRA increases when the ratio of electron donor to acceptor increases (Christensen et al. 2000; Kelso et al. 1997), as is the case in the Wadden Sea during summer when  $\text{NO}_3^-$  concentrations in the water column are very low in comparison to OM. 2) Based on growth yields, increased summer temperatures and low  $\text{NO}_3^-$  concentrations

have been shown to allow  $\text{NO}_3^-$  ammonifiers to scavenge  $\text{NO}_3^-$  more efficiently, and gain more energy per mole of nitrate than denitrifiers (Strohm et al. 2007). 3) DNRA may also have been more favourable during summer due to enhanced sulfide concentrations in surface sediments at the study site (Al-Raei et al. 2009). High sulfide concentrations can inhibit denitrification, and as such, the presence of high sulfide concentrations have been reported to favour DNRA over heterotrophic denitrification (An and Gardner 2002; Gardner et al. 2006; Sorensen 1978).

The controls upon eukaryotic DNRA are less well defined than those in prokaryotes. We can speculate however, that high eukaryotic DNRA rates in spring resulted from the settling and burial of diatoms after the spring bloom (Ehrenhauss et al. 2004a; Ehrenhauss et al. 2004b; Huettel and Rusch 2000). Upon burial diatoms have been shown to switch to anaerobic respiration as a survival mechanism at the onset of dark and anoxic conditions (Kamp et al. 2011). Eukaryotic nitrate respiration is increasingly reported as an important pathway in the nitrogen cycle (See Thamdrup 2012 for review), and is usually associated with intracellular storage of  $\text{NO}_3^-$  or  $\text{NH}_4^+$  (Lomas and Glibert 2000; Lomstein et al. 1990; Risgaard-Petersen et al. 2006). Therefore, to investigate the potential importance of eukaryote-associated nitrate respiration within Wadden Sea permeable sediments, we looked for evidence of intracellular nitrate storage *in situ*.

#### **Intracellular storage of nitrate *in situ***

To determine how much nitrate is stored *in situ* within permeable Wadden Sea sediments, we compared porewater nitrate concentrations with intracellular nitrate concentrations. This revealed that shortly after low tide, intracellular nitrate concentrations within the sediment were six fold higher than the porewater concentrations. Benthic diatoms and foraminifera were present at the study site and could have been responsible for this storage. Both diatoms and foraminifera are capable of storing nitrate intracellularly to concentrations orders of magnitude higher than the surrounding porewater, in fact laboratory studies have demonstrated that cell volume specific accumulation can be as high as  $450 \text{ mmol L}^{-1}$  in diatoms (Høgslund 2008) and  $570 \text{ mmol L}^{-1}$  in foraminifera (Piña-Ochoa et al. 2010). If we were to assume that only the diatoms that we identified within the sediment were responsible for intracellular nitrate storage, then, based on diatom cell counts and biovolume estimates, this



would make cell specific intracellular nitrate storage in the range of  $60 \text{ mmol L}^{-1}$ , a concentration well within the range identified in laboratory studies.

### **Intracellular storage as a short-term sink of nitrate**

Taken together, the *in situ* intracellular nitrate concentrations and the eukaryote-associated nitrate respiration suggested that in all seasons intracellular nitrate storage may have played an important role in the  $^{15}\text{NO}_3^-$  amendment experiment. This was further supported by a  $^{15}\text{N}$  mass balance, calculated after all the  $^{15}\text{NO}_3^-$  within the incubation had been consumed and denitrification and DNRA had ceased. The mass balance revealed that the production of  $^{15}\text{N-N}_2$  and  $^{15}\text{NH}_4^+$  was insufficient to account for the amount of nitrate consumed; in fact between 20 and 40% of the added  $^{15}\text{NO}_3^-$  was missing from the porewater and might have entered an intracellular pool (Fig. 6). Nitrate uptake into intracellular pools could have occurred actively, but could also have resulted from isotope equilibration effects between the added  $^{15}\text{NO}_3^-$  and pre-existing intracellular  $^{14}\text{NO}_3^-$  pools (as observed in summer; Fig. 4). Similar equilibration effects have recently been observed in sediment incubations carried out with  $^{15}\text{NO}_3^-$  when stores of intracellular nitrate were present (Dähnke et al. 2012; Sokoll et al. 2012).

To investigate whether part of the  $^{15}\text{NO}_3^-$  added to the sediment had been transferred to an intracellular pool, we ran a second incubation using the sediment cores that were previously amended with  $^{15}\text{NO}_3^-$ . In this subsequent experiment, we percolated the sediment core with oxic seawater that had no added  $^{15}\text{NO}_3^-$  and then examined whether  $^{15}\text{N}$ -labelled substrates appeared in the porewater. In the incubation to which no  $^{15}\text{NO}_3^-$  was added, up to 100% of the “missing”  $^{15}\text{N}$  appeared in the porewater as either  $^{15}\text{N-N}_2$  or  $^{15}\text{NH}_4^+$  (Fig. 5a). This indicates that denitrification and DNRA were carried out using a pool of  $^{15}\text{N}$  that had been stored within an intracellular nitrate pool.

When denitrification and DNRA rates were derived from the incubation with no  $^{15}\text{NO}_3^-$  added to the porewater, rates of both processes were much lower than in the  $^{15}\text{NO}_3^-$  amendment experiment, indicating that only a part of the community contributed to the respiration of stored nitrate (Fig. 5c-f). The eukaryote community continued to respire  $^{15}\text{NO}_3^-$  at the same rate as in the  $^{15}\text{NO}_3^-$  amendment experiment, whereas prokaryotic DNRA and denitrification rates dropped by 60% and 97% respectively, when compared to the  $^{15}\text{NO}_3^-$  amendment experiment. This suggests that while eukaryotes were supplied within ample

nitrate from the intracellular pool, prokaryote nitrate respiration was limited, possibly by nitrate leaking out of eukaryotes. As prokaryote denitrification rates dropped so drastically in the incubation where no  $^{15}\text{NO}_3^-$  was added to the porewater, we were able to observe low rates of eukaryotic denitrification of  $^{15}\text{NO}_3^-$ , which had not been apparent before. It is likely that eukaryotic denitrification also occurred in the  $^{15}\text{NO}_3^-$  amendment experiment, however it was masked by the comparatively high prokaryote denitrification rates.

Eukaryotes therefore seem to play an important role in intracellular nitrate storage and subsequent nitrate reduction. However, upon inhibition of the eukaryotic community within the  $^{15}\text{NO}_3^-$  amendment experiment and the incubation to which no  $^{15}\text{NO}_3^-$  was added,  $^{15}\text{N}$  storage decreased, but did not cease entirely (Fig. 6). Can this fraction of stored nitrate therefore be attributed to prokaryotes? Nitrate storage in prokaryotes is mainly known to occur in large vacuolated sulfur bacteria (Fossing et al. 1995), which are not present in substantial numbers in permeable Wadden Sea sediments. Therefore, the intracellular storage of  $^{15}\text{N}$  observed after eukaryote inhibition suggests that we had either failed to completely inhibit the eukaryotic community (in which case, prokaryotic rates of DNRA and denitrification derived from intracellular storage would be overestimated), or that nitrate was stored within the sediment by an unidentified prokaryote.

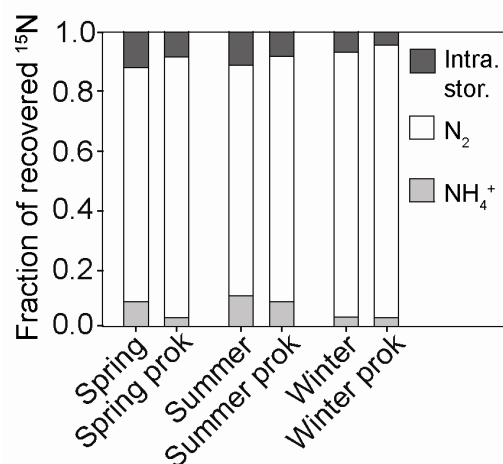
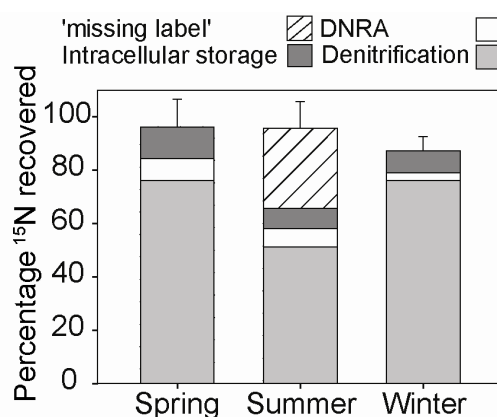


Figure 6. Changes in the partitioning of  $^{15}\text{N}$  recovery before and after addition of a eukaryotic inhibitor.

### Implications for N-loss from permeable sediments

Our results illustrate that the nitrate transformations which take place within intertidal permeable sediments are the result of denitrification, DNRA, intracellular nitrate storage and eukaryotes as well as prokaryotes. When nitrate is advectively transported into permeable sediments during tidal inundation, denitrification is the main process that consumes nitrate, although DNRA and intracellular storage by the eukaryotic community are also significant in determining the fate of nitrate (Fig. 7). The magnitude of each of these processes differs seasonally, seemingly in response to organic matter availability, nitrate availability and the composition and abundance of the eukaryotic community.



**Figure 7. Average percentage of <sup>15</sup>N recovered in various pools.** Denitrification denotes <sup>15</sup>N that was present as <sup>29+30</sup>N<sub>2</sub>, DNRA denotes <sup>15</sup>N that was present as <sup>15</sup>NH<sub>4</sub><sup>+</sup> and intracellular storage represents <sup>15</sup>N which was present as either <sup>29+30</sup>N<sub>2</sub> or <sup>15</sup>NH<sub>4</sub> at the termination of the secondary incubation to which no additional <sup>15</sup>NO<sub>3</sub> was added. The 'missing label' fraction refers to the discrepancy between added <sup>15</sup>NO<sub>3</sub><sup>-</sup>, measured <sup>15</sup>NO<sub>3</sub><sup>-</sup> and <sup>15</sup>N<sub>2</sub> production (shown in Fig. 5). Error bars are overall SD (n = 3)

Intracellular storage of nitrate complicates nitrogen cycling within intertidal sediments, adding a heretofore unconsidered supply of nitrate during low tide. So far, areal N-loss estimates are based on denitrification rates determined during the period where the sand flat is inundated with water and nitrate is advectively transported into the sediment (Gao et al. 2012). During exposure the advectively dominated system undergoes a shift towards a steady, diffusion limited state in which oxygen penetration depth drops significantly (< 1cm) and any remaining porewater nitrate should be consumed within 40-100 minutes, at which point N-loss is assumed to cease. However, intracellular nitrate storage could act as a reservoir, providing a

supply of nitrate to support anaerobic respiration during exposure. In fact, the occurrence of DNRA during exposure has been indicated previously within Wadden Sea intertidal sand flats, where *in situ*  $\text{NH}_4^+$  measurements were higher than would be expected from remineralization alone (Gao et al. 2010).

We calculated the additional N-transformations that may have occurred during exposure, as a result of intracellular nitrate storage, assuming that the *in situ* concentration is always similar to that which we measured during winter 2013 (around  $28 \text{ mmol m}^{-3}_{\text{sediment}}$ ). Average N-loss associated with storage was  $0.84 \text{ mmol m}^{-3}_{\text{sediment}} \text{ h}^{-1}$  and N-recycling by DNRA was  $0.26 \text{ mmol m}^{-3}_{\text{sediment}} \text{ h}^{-1}$ . Over 6 hours of exposure this would represent the reduction of  $6 \text{ mmol N m}^{-3}$  sediment or ~24% of the stored nitrate pool. Integrating these rates over the top 5cm of intertidal Wadden Sea sediments would represent an additional  $0.5 \text{ mmol m}^{-2} \text{ d}^{-1}$  N-loss and  $0.22 \text{ mmol m}^{-2} \text{ d}^{-1}$  N-regeneration by DNRA (assuming the sand flat is exposed for 12 hours daily). Reduction of the stored nitrate pool during the diurnal exposure of the sand flat would therefore add an extra 20% to N-loss estimates on top of that calculated previously for these intertidal sediments ( $2.48 \text{ mmol m}^{-2} \text{ d}^{-1}$  ( $2.48 \text{ mmol m}^{-2} \text{ d}^{-1}$ , Gao et al. 2012)).

The Wadden Sea has previously been identified as a site of N-loss (Gao et al. 2012; Van Beusekom 2001), acting as a sink for high riverine N loads and preventing them from reaching the open ocean, a conclusion strongly supported by this study. Our results indicate that intertidal permeable sediments must also be considered as hotspots of eukaryotic nitrate storage and respiration. Furthermore, while DNRA is of less importance than denitrification in this environment, up to 20 % of the nitrate reduction that occurs in Wadden Sea sediments is as DNRA, recycling fixed N to  $\text{NH}_4^+$  which can then fuel primary production. Previously Gao et al. estimated that 30% of the total annual N input into the Wadden Sea is denitrified within the sediment. The two to five fold higher denitrification rates we have reported here, combined with the additional N-loss during exposure, indicate that this estimate appears to be conservative and that higher N-losses may occur.

## References

Admiraal, W., C. Riauxgobin, and R. Laane. 1987. Interactions of ammonium, nitrate and D-amino acids and L-amino acids in the nitrogen assimilation of 2 species of estuarine benthic diatoms. *Marine Ecology Progress Series* **40**: 267-273.

- Al-Raei, A. M., K. Bosselmann, M. E. Boettcher, B. Hespeneide, and F. Tauber. 2009. Seasonal dynamics of microbial sulfate reduction in temperate intertidal surface sediments: controls by temperature and organic matter. *Ocean Dyn.* **59**: 351-370.
- An, S. M., and W. S. Gardner. 2002. Dissimilatory nitrate reduction to ammonium (DNRA) as a nitrogen link, versus denitrification as a sink in a shallow estuary (Laguna Madre/Baffin Bay, Texas). *Marine Ecology Progress Series* **237**: 41-50.
- Billerbeck, M., U. Werner, K. Bosselmann, E. Walpersdorf, and M. Huettel. 2006a. Nutrient release from an exposed intertidal sand flat. *Mar. Ecol.-Prog. Ser.* **316**: 35-51.
- Billerbeck, M., U. Werner, L. Polerecky, E. Walpersdorf, D. De Beer, and M. Huettel. 2006b. Surficial and deep pore water circulation governs spatial and temporal scales of nutrient recycling in intertidal sand flat sediment. *Mar. Ecol.-Prog. Ser.* **326**: 61-76.
- Böer, S. I., C. Arnosti, J. E. E. Van Beusekom, and A. Boetius. 2009. Temporal variations in microbial activities and carbon turnover in subtidal sandy sediments. *Biogeosciences* **6**: 1149-1165.
- Boyer, E. W., R. W. Howarth, J. N. Galloway, F. J. Dentener, P. A. Green, and C. J. Vörösmarty. 2006. Riverine nitrogen export from the continents to the coasts. *Global Biogeochem. Cycles* **20**: GB1S91.
- Braman, R. S., and S. A. Hendrix. 1989. Nanogram nitrite and nitrate determination in environmental and biological materials by vanadium(III) reduction with chemiluminescence detection. *Analytical Chemistry* **61**: 2715-2718.
- Canfield, D. E., B. Thamdrup, and E. Kristensen. 2005. *Aquatic Geomicrobiology*. Elsevier Academic Press.
- Chipman, L., M. Huettel, and M. Laschet. 2012. Effect of benthic-pelagic coupling on dissolved organic carbon concentrations in permeable sediments and water column in the northeastern Gulf of Mexico. *Continental Shelf Research* **45**: 116-125.
- Christensen, P. B., S. Rysgaard, N. P. Sloth, T. Dalsgaard, and S. Schwaerter. 2000. Sediment mineralization, nutrient fluxes, denitrification and dissimilatory nitrate reduction to ammonium in an estuarine fjord with sea cage trout farms. *Aquatic Microbial Ecology* **21**: 73-84.
- Cook, P. L. M., A. T. Revill, E. C. V. Butler, and B. D. Eyre. 2004. Carbon and nitrogen cycling on intertidal mudflats of a temperate Australian estuary. II. Nitrogen cycling. *Marine Ecology Progress Series* **280**: 39-54.
- Cook, P. L. M. and others 2006. Quantification of denitrification in permeable sediments: Insights from a two-dimensional simulation analysis and experimental data. *Limnology and Oceanography-Methods* **4**: 294-307.
- Dähnke, K., A. Moneta, B. Veuger, K. Soetaert, and J. J. Middelburg. 2012. Balance of assimilative and dissimilative nitrogen processes in a diatom-rich tidal flat sediment. *Biogeosciences* **9**: 4059-4070.
- De Beer, D. and others 2005. Transport and mineralization rates in North Sea sandy intertidal sediments, Sylt-Romo Basin, Wadden Sea. *Limnology and Oceanography* **50**: 113-127.
- Ehrenhauss, S., U. Witte, S. I. Buhning, and M. Huettel. 2004a. Effect of advective pore water transport on distribution and degradation of diatoms in permeable North Sea sediments. *Marine Ecology Progress Series* **271**: 99-111.

- Ehrenhauss, S., U. Witte, F. Janssen, and M. Huettel. 2004b. Decomposition of diatoms and nutrient dynamics in permeable North Sea sediments. *Continental Shelf Research* **24**: 721-737.
- Emery, K. O. 1968. Relict sediments on continental shelves of world. *AAPG Bulletin* **52**: 445-464.
- Feuillet-Girard, M., D. Gouleau, G. Blanchard, and L. Joassard. 1997. Nutrient fluxes on an intertidal mudflat in Marennes-Oleron Bay, and influence of the emersion period. *Aquatic Living Resources* **10**: 49-58.
- Fossing, H. and others 1995. Concentration and transport of nitrate by the mat-forming sulphur bacterium *Thioploca*. *Nature* **374**: 713-715.
- Fuhrman, J. A., and G. B. Mcmanus. 1984. Do bacteria-sized marine eukaryotes consume significant bacterial production. *Science* **224**: 1257-1260.
- Füssel, J. and others 2011. Nitrite oxidation in the Namibian oxygen minimum zone. *ISME J* **6**: 1200-1209.
- Galloway, J. N. and others 2004. Nitrogen Cycles: Past, Present, and Future. *Biogeochemistry* **70**: 153-226.
- Gao, H. and others 2012. Intensive and extensive nitrogen loss from intertidal permeable sediments of the Wadden Sea. *Limnology and Oceanography* **57**: 185-198.
- . 2010. Aerobic denitrification in permeable Wadden Sea sediments. *Isme Journal* **4**: 417-426.
- Garcia-Robledo, E., A. Corzo, S. Papaspyrou, J. L. Jimenez-Arias, and D. Villahermosa. 2010. Freeze-lysable inorganic nutrients in intertidal sediments: dependence on microphytobenthos abundance. *Marine Ecology Progress Series* **403**: 155-163.
- Gardner, W. S., M. J. McCarthy, S. An, D. Sobolev, K. S. Sell, and D. Brock. 2006. Nitrogen fixation and dissimilatory nitrate reduction to ammonium (DNRA) support nitrogen dynamics in Texas estuaries. *Limnology and Oceanography* **51**: 558-568.
- Glud, R. N. 2008. Oxygen dynamics of marine sediments. *Marine Biology Research* **4**: 243-289.
- Goineau, A. and others 2011. Live (stained) benthic foraminifera from the Rhone prodelta (Gulf of Lion, NW Mediterranean): Environmental controls on a river-dominated shelf. *Journal of Sea Research* **65**: 58-75.
- Grasshoff, K., Ehrhardt, K, Kremling, K & Anderson, Lg 1999. Determination of nutrients, p. 159-226. *Methods of seawater analysis*. Wiley.
- Grippo, M. A., J. W. Fleeger, N. N. Rabalais, R. Condrey, and K. R. Carman. 2010. Contribution of phytoplankton and benthic microalgae to inner shelf sediments of the north-central Gulf of Mexico. *Continental Shelf Research* **30**: 456-466.
- Grosskopf, T. and others 2012. Doubling of marine dinitrogen-fixation rates based on direct measurements. *Nature* **488**: 361-364.
- Gruber, N. 2004. The dynamics of the marine nitrogen cycle and its influence on atmospheric CO<sub>2</sub> variation, p. 97–148. *In* M. Follows and T. Oguz [eds.], *The ocean carbon cycle and climate*. Kluwer Academic.
- Gruber, N., and J. N. Galloway. 2008. An Earth-system perspective of the global nitrogen cycle. *Nature* **451**: 293-296.
- Hall, P. O. J., and R. C. Aller. 1992. Rapid, small-volume, flow injection analysis for CO<sub>2</sub> and NH<sub>4</sub><sup>+</sup> in marine and freshwaters. *American Society of Limnology and Oceanography*.
- Heisterkamp, I. M., A. Kamp, A. T. Schramm, D. De Beer, and P. Stief. 2012. Indirect control of the intracellular nitrate pool of intertidal sediment by the polychaete *Hediste diversicolor*. *Marine Ecology Progress Series* **445**: 181-192.

- Hillebrand, H., C. D. Durselen, D. Kirschtel, U. Pollinger, and T. Zohary. 1999. Biovolume calculation for pelagic and benthic microalgae. *Journal of Phycology* **35**: 403-424.
- Høgslund, S. 2008. Nitrate storage as an adaptation to benthic life.
- Holtappels, M., Lavik, G., Jensen, M. M., and Kuypers, M. M. M. 2011. <sup>15</sup>N-Labeling Experiments to Dissect the Contributions of Heterotrophic Denitrification and Anammox to Nitrogen Removal in the OMZ Waters of the Ocean, p. 223-251. *In* M. G. Klotz [ed.], *Methods in Enzymology*.
- Huettel, M., H. Roy, E. Precht, and S. Ehrenhauss. 2003. Hydrodynamical impact on biogeochemical processes in aquatic sediments. *Hydrobiologia* **494**: 231-236.
- Huettel, M., and A. Rusch. 2000. Transport and degradation of phytoplankton in permeable sediment. *Limnology and Oceanography* **45**: 534-549.
- Jahnke, R. A., J. R. Nelson, R. L. Marinelli, and J. E. Eckman. 2000. Benthic flux of biogenic elements on the Southeastern US continental shelf: influence of pore water advective transport and benthic microalgae. *Continental Shelf Research* **20**: 109-127.
- Kamp, A., D. De Beer, J. L. Nitsch, G. Lavik, and P. Stief. 2011. Diatoms respire nitrate to survive dark and anoxic conditions. *Proceedings of the National Academy of Sciences* **108**: 5649-5654.
- Kelso, B. H. L., R. V. Smith, R. J. Laughlin, and S. D. Lennox. 1997. Dissimilatory nitrate reduction in anaerobic sediments leading to river nitrite accumulation. *Applied and Environmental Microbiology* **63**: 4679-4685.
- King, D., and D. B. Nedwell. 1987. The adaptation of the nitrate-reducing bacterial communities in estuarine sediments in response to overlying nitrate load. *Fems Microbiology Ecology* **45**: 15-20.
- Lomas, M. W., and P. M. Glibert. 2000. Comparisons of nitrate uptake, storage, and reduction in marine diatoms and flagellates. *Journal of Phycology* **36**: 903-913.
- Lomstein, E., M. H. Jensen, and J. Sorensen. 1990. Intracellular NH<sub>4</sub><sup>+</sup> and NO<sub>3</sub><sup>-</sup> pools associated with deposited phytoplankton in a marine sediment (Aarhus Bight, Denmark). *Marine Ecology Progress Series* **61**: 97-105.
- Mchatton, S. C., J. P. Barry, H. W. Jannasch, and D. C. Nelson. 1996. High nitrate concentrations in vacuolate, autotrophic marine *Beggiatoa* spp. *Applied and Environmental Microbiology* **62**: 954-958.
- Piña-Ochoa, E. and others 2010. Widespread occurrence of nitrate storage and denitrification among Foraminifera and Gromiida. *Proceedings of the National Academy of Sciences* **107**: 1148-1153.
- Preisler, A., D. De Beer, A. Lichtschlag, G. Lavik, A. Boetius, and B. B. Jørgensen. 2007. Biological and chemical sulfide oxidation in a *Beggiatoa* inhabited marine sediment. *Isme Journal* **1**: 341-353.
- Rao, A. M. F., M. J. Mccarthy, W. S. Gardner, and R. A. Jahnke. 2008. Respiration and denitrification in permeable continental shelf deposits on the South Atlantic Bight: N<sub>2</sub> : Ar and isotope pairing measurements in sediment column experiments. *Continental Shelf Research* **28**: 602-613.
- Revsbech, N. P. 1989. An oxygen microsensor with a guard cathode. *Limnology and Oceanography* **34**.
- Risgaard-Petersen, N. and others 2006. Evidence for complete denitrification in a benthic foraminifer. *Nature* **443**: 93-96.

- Rusch, A., M. Huettel, C. E. Reimers, G. L. Taghon, and C. M. Fuller. 2003. Activity and distribution of bacterial populations in Middle Atlantic Bight shelf sands. *Fems Microbiology Ecology* **44**: 89-100.
- Sayama, M. 2001. Presence of nitrate-accumulating sulfur bacteria and their influence on nitrogen cycling in a shallow coastal marine sediment. *Applied and Environmental Microbiology* **67**: 3481-3487.
- Seeberg-Elverfeldt, J., M. Schluter, T. Feseker, and M. Kolling. 2005. Rhizon sampling of porewaters near the sediment-water interface of aquatic systems. *Limnology and Oceanography-Methods* **3**: 361-371.
- Seitzinger, S. and others 2006. Denitrification across landscapes and waterscapes: a synthesis. *Ecol Appl* **16**: 2064-2090.
- Sokoll, S. and others 2012. Benthic nitrogen loss in the arabian sea off pakistan. *Frontiers in microbiology* **3**: 395-395.
- Song, G. D., S. M. Liu, H. Marchant, M. M. M. Kuypers, and G. Lavik. 2013. Anaerobic ammonium oxidation, denitrification and dissimilatory nitrate reduction to ammonium in the East China Sea sediment. *Biogeosciences Discuss.* **10**: 4671-4710.
- Sorensen, J. 1978. Capacity for denitrification and reduction of nitrate to ammonia in a coastal marine sediment. *Appl Environ Microbiol* **35**: 301-305.
- Strohm, T. O., B. Griffin, W. G. Zumft, and B. Schink. 2007. Growth Yields in Bacterial Denitrification and Nitrate Ammonification. *Applied and Environmental Microbiology* **73**: 1420-1424.
- Thamdrup, B. 2012. New Pathways and Processes in the Global Nitrogen Cycle, p. 407-428. *Annual Review of Ecology, Evolution, and Systematics*, Vol 43. *Annual Review of Ecology Evolution and Systematics*.
- Thamdrup, B., and T. Dalsgaard. 2002. Production of N<sub>2</sub> through anaerobic ammonium oxidation coupled to nitrate reduction in marine sediments. *Applied and Environmental Microbiology* **68**: 1312-1318.
- Trimmer, M., and J. C. Nicholls. 2009. Production of nitrogen gas via anammox and denitrification in intact sediment cores along a continental shelf to slope transect in the North Atlantic. *Limnology and Oceanography* **54**: 577-589.
- Van Beusekom, J. E. E. 2005. A historic perspective on Wadden Sea eutrophication. *Helgoland Marine Research* **59**: 45-54.
- Van Beusekom, J. E. E., H. Fock, F. De Jong, S. Diehl-Christiansen, B. Christiansen. 2001. Wadden Sea Specific Eutrophication Criteria *In* C. W. S. Secretariat [ed.], *Wadden Sea Ecosystem* No. 14.
- Waremburg, F. 1993. Nitrogen fixation in soil and plant systems p. 157–180. *In* B. T. Knowles K [ed.], *Nitrogen Isotopes Techniques*. Academic Press.
- Werner, U. and others 2006. Spatial and temporal patterns of mineralization rates and oxygen distribution in a permeable intertidal sand flat (Sylt, Germany). *Limnology and Oceanography* **51**: 2549-2563.



## Chapter IV

### **N-loss due to coupled nitrification-denitrification in subtidal permeable sediments**

Hannah K. Marchant<sup>1</sup>, Moritz Holtappels<sup>1</sup>, Gaute Lavik<sup>1</sup>, Christian Winter<sup>2</sup>,  
Marcel M.M. Kuypers<sup>1</sup>

<sup>1</sup>Biogeochemistry Department, Max Planck Institute for Marine Microbiology, Bremen, Germany

<sup>2</sup>MARUM—Center for Marine Environmental Sciences, University of Bremen, Leobener Straße, D-28359 Bremen, Germany

Contributions to the manuscript:

H.K.M. and M.M.M.K. designed research. H.K.M and C.W. carried out fieldwork, H.K.M carried out GC-IRMS measurements and data analysis. C.W. performed grain size analysis and provided *in situ* data. H.K.M., and M.H., carried out modeling and areal rate estimates. H.K.M., M.H., G.L. and M.M.M.K., conceived, wrote and edited the manuscript

**In preparation for *Limnology and Oceanography***

### **Acknowledgements**

We sincerely thank cruise leader Thomas Lüdman as well as the captain and crew of the Heincke (He-383). We are grateful to Gabi Klockgether and Sarah Kuschnerow for technical assistance. We also thank Felix Janssen and Soeren Ahmerkamp with whom discussion helped improve the manuscript. This work was financially supported by the Max Planck Society.

### **Abstract**

We investigated oxygen consumption rates and microbial pathways of nitrogen (N) transformation in the sandy permeable sediments of the German Bight (South-East North Sea) using sediment core incubations percolated with  $^{15}\text{N}$ -labelled substrates. In incubations with  $^{15}\text{NH}_4^+$ , production of  $^{15}\text{NO}_2^-$  occurred while the sediment was oxic indicating ammonia oxidation. Similarly,  $^{15}\text{NO}_3^-$  production during  $^{15}\text{NO}_2^-$  incubations indicated nitrite oxidation. Taken together these findings provided evidence of high nitrification rates within the sands of the German Bight. The production of  $^{15}\text{N-N}_2$  upon addition of  $^{15}\text{NO}_3^-$  revealed high denitrification rates within the sediment when it was oxic and anoxic. Denitrification rates were strongly and positively correlated with oxygen consumption rates, suggesting that denitrification is controlled by the availability of organic matter in these sediments. Nitrification and denitrification rates were of the same magnitude and incubations with  $^{15}\text{NH}_4^+$  confirmed that the two processes were closely coupled. Areal rates of N-transformation were estimated by integrating measured volumetric rate over modeled oxygen and nitrate penetration depths. Areal N-loss rates ranged between 118 and 383  $\mu\text{mol N m}^{-2} \text{ h}^{-1}$  for sediments of different permeabilities. When areal rates were extrapolated to areas with similar sediment characteristics in the German Bight, the N-loss was around 400 kt N  $\text{yr}^{-1}$ , which is more than double that previously estimated. At the same time extensive N-regeneration through nitrification occurred (176 kt N  $\text{yr}^{-1}$ ), supporting N-loss by providing an additional source of nitrate, but also masking N-losses in net nutrient budgets.

## Introduction

Shallow coastal seas are subject to high loads of anthropogenic inorganic nitrate inputs from both riverine sources and atmospheric deposition. These inputs cause eutrophication, which has negative impacts on the ecosystem ranging from changes in species composition, increased phytoplankton blooms and bottom water hypoxia (Rabalais, 2002). Eutrophication in shallow coastal seas is alleviated by denitrification, which is stimulated by high nitrate and organic matter (OM) inputs. In fact, a significant proportion of global N-loss has been attributed to heterotrophic denitrification in shallow sediments (Devol et al., 1997; Gruber and Galloway, 2008).

Until recently, benthic nitrogen cycling studies were carried out mainly in muddy sediments. However, 70% of all continental shelves are comprised of coarse grained sandy sediments in which advection can occur (Emery, 1968). Advection transports bottom water into the sediment at velocities up to three orders of magnitude higher than diffusion (Huettel et al., 2003). This supplies the sediment with particulate organic matter and electron acceptors, and furthermore, increases oxygen penetration depths, which oscillate within the sediment dependent on tidal forcing and ripple migration (Huettel et al., 2003; Cook et al., 2007). As a result of advective solute supply, high rates of organic matter mineralization occur in permeable sediments (de Beer et al., 2005), and benthic denitrification rates are amongst the highest in the marine environment (Gao et al., 2010; Gao et al., 2012). Furthermore, variations in oxygen concentrations appear to stimulate the co-occurrence of aerobic and anaerobic processes, for example denitrification, traditionally an anaerobic process has been observed in oxic permeable sediments (Rao et al., 2008; Gao et al., 2010).

Permeable sediments are increasingly recognized as natural bioreactors, and as such, reports of oxygen consumption rates and denitrification rates within them are becoming more frequent. However, few environmental studies have focused on the impact of advection on benthic nitrification and coupled nitrification-denitrification in permeable sediments. As nitrification can provide a secondary nitrate source for denitrification, it can influence the extent of benthic N-loss, or, if not tightly coupled to

denitrification, nitrification can recycle remineralized N to the environment. Benthic nitrification has been measured previously in disparate environments, including permeable sediments, although only under diffusive conditions. These previous reports have shown nitrification rates to be remarkably similar regardless of sediment type (see Henriksen and Kemp, 1988; Ward, 2008 and references therein). Strongly coupled nitrification-denitrification has been predicted in permeable sediments based on isotope pairing studies (Rao et al., 2007, 2008; Gihring et al., 2010), although, a modeling study suggested that advection may have a negative impact on nitrification (Cook et al., 2006). Rates of nitrification and coupled nitrification-denitrification were reduced by a factor of 6 upon the application of advective flows, this was attributed to the decreased supply of  $\text{NH}_4^+$ , the substrate required for nitrification. So far, no direct measurements of ammonia oxidation and nitrite oxidation have been undertaken in permeable sediments under advective conditions.

Although environmental studies into coupled nitrification-denitrification in permeable sediments are still scarce, similar research has been undertaken by the wastewater treatment industry, within which there are many parallels to permeable sediments. Wastewater treatment has taken advantage of the occurrence of coupled nitrification-denitrification in single chamber reactors for many decades (Prakasam and Loehr, 1972; Sharma and Ahlert, 1977); generally, oxygenated, ammonium rich wastewater is percolated or pumped through a permeable medium which is colonized with microbes. Ammonium within the wastewater is nitrified and anoxic conditions are then achieved by increasing the path length of the permeable bed, or intermittently removing the oxygen, whereupon denitrification occurs (Yoo et al., 1999; Guo et al., 2005). In simultaneous nitrification-denitrification reactors, spatial separation of nitrification and denitrification is not required and the two processes occur while the reactor is oxic (Münch et al., 1996; Tait et al., 2013).

The availability of substrates can determine the extent of coupling between nitrification and denitrification. Heterotrophic denitrifiers require organic matter, while nitrification, which is an autotrophic process, does not. Nevertheless, the supply of

organic matter can also determine the amount of ammonium remineralized within the sediment, and therefore organic matter availability can effect both nitrification and denitrification. The availability of substrates such as organic matter in permeable sediments is controlled by the efficiency with which they act as a biocatalytic filter. This efficiency is dependent on grain size, permeability and bottom flow velocity (Yao et al., 1971; Fries and Trowbridge, 2003; Ehrenhauss et al., 2004), however little is known about the relationship between these and organic matter remineralization or biogeochemical N-cycling in the environment. Under advective conditions oxygen uptake within sandy sediments gradually increases with increasing permeability, as does microbial metabolic activity, this is attributed to increased supply and filtering of organic matter (Janssen et al., 2005). Additionally however, the use of sand filters and other media in wastewater treatment has shown that above a certain grain size threshold, total activity drops again (Moore et al., 2001; Li et al., 2013). This results from a combination of the reduced surface available for microbes to grow on and the wash out of organic substrates due to increased advective flow (Stevenson, 1997). So far, it is unknown whether similar effects are seen in sandy sediments with different permeabilities. Investigations into the detailed relationships between permeability and biogeochemical cycling are required to better understand the potential role that sandy sediments play in N-loss especially in eutrophied coastal zones.

The German Bight is one such eutrophied coastal sea which receives extensive anthropogenic nitrate inputs from riverine and atmospheric sources (van Beusekom, 2005; Paetsch et al., 2010). In fact anthropogenic nitrate inputs ( $\sim 290 \text{ kt N yr}^{-1}$ ) almost equal the net influx of nitrate across the western border of the German Bight, which result from Atlantic and Central North Sea Water (Beddig et al., 1997; Paetsch et al., 2010). Due to the anti-clockwise circulation pattern of the North Sea, nitrate export is observed across the northern border of the German Bight. However, fluxes of nitrate out of the German Bight are lower than the combined anthropogenic and advective influxes, indicating that benthic N-loss must occur (Beddig et al., 1997; Paetsch et al., 2010). Furthermore, based upon natural abundance stable isotope signatures of nitrate,

it has been suggested that riverine nitrate inputs are removed before water is exported out of the German Bight and that intense N-recycling occurs through nitrification, possibly within the sediment (Dähnke et al., 2010). Nonetheless, so far no direct measurements of nitrification or denitrification have been undertaken in the subtidal permeable sediments which cover approximately 60% of the German Bight seafloor (Janssen et al., 2005).

We investigated the role of nitrification and denitrification in permeable subtidal sediments of the German Bight using a combination of core percolation and  $^{15}\text{N}$  labeling experiments. These allowed us to measure rates of nitrification, denitrification and their associated  $\text{N}_2\text{O}$  production as well as anammox and DNRA. So far none of these processes have been well constrained in sub-tidal sandy sediments and therefore almost nothing is known about coupled nitrification-denitrification. During a sampling campaign we investigated three different sandy sediments spanning a range of grain sizes and permeabilities. This allowed us to gain insights into the nitrate and oxygen turnover rates in different sandy sediments which were supplied by the same overlying water, and to investigate the importance of organic matter in controlling nitrogen cycling processes.

## **Materials and Methods**

### *Sediment sampling*

Sampling was conducted in the North Sea around Helgoland on board the RV Heincke from 22 June 2012 to 28 June 2012. Sediment was collected in a box corer and the top 5 cm were subsampled on deck, homogenized and filled into PVC cores (height 9 cm, I.D 10.3 cm). Cores were sealed with rubber stoppers fitted with inflow and outflow ports controlled by 2 way valves. Bottom water was collected using a rosette water sampler and incubations were carried out immediately on board at *in situ* temperature.

### *Sediment characteristics*

Sub samples of sediment were collected from box cores, transferred to 50 ml falcon tubes (Sarstedt) and returned to Bremen, Germany. Porosity was calculated from the weight loss of a known volume of sediment after drying and grain size distribution was determined on a Beckman Coulter LS Particle Analyzer at the Center for Marine Environmental Sciences (MARUM), University of Bremen. Permeability of homogenized sediments was measured using the falling head approach and a setup similar to that described in Rocha et al. (2005).

### *Sediment core incubations*

Rates of oxygen consumption, ammonia oxidation, nitrite oxidation, denitrification, dissimilatory nitrate reduction to ammonium (DNRA) and anammox were determined in triplicate from percolated sediment cores. 5 incubations were carried out at each station and are summarized in Table 1. Briefly, bottom seawater was amended with  $^{14}\text{N}$  and  $^{15}\text{N}$  inorganic compounds and aerated before being pumped upwards through the sediment core with a peristaltic pump in a modified version of the percolation method (de Beer et al., 2005) described in more detail in (Marchant et al., 2013). Pumping was continued until the entire porewater volume of the core had been exchanged more than 1.5 times with amended seawater. At this point the inflow port was closed using a 2-way valve and a sampling port was connected to the bottom of the column. Porewater was subsequently collected by opening the 2 way valve and letting porewater flow directly into 6 ml exetainers (Labco Ltd, High Wycombe, UK), prefilled with 100  $\mu\text{l}$  saturated  $\text{HgCl}_2$ . 1.5 ml of porewater was discarded initially at each time point to flush the tubing between the column and the sediment. 12 time points were taken corresponding to 90 ml per incubation, less than half the porewater contained per core and on average creating a flow velocity around 2 – 3  $\text{cm hr}^{-1}$ . Porewater was replaced passively with unamended sea water at the outflow on the top of the column. Exetainers were stored upside down at room temperature until analysis.



### *Oxygen determination*

Oxygen was determined in each exetainer using an O<sub>2</sub> microsensor (response time < 2 s), briefly, exetainers were opened and the microsensor inserted before being closed again. This procedure took less than 5 seconds and did not result in any water loss from the exetainers. Oxygen microsensors were constructed as described in Revsbech (1989) and calibration was performed before and after measurements using a 2 point calibration in air saturated seawater and N<sub>2</sub> degassed seawater.

### *<sup>15</sup>N analyses*

The isotopic N composition of nitrogen and nitrous oxide gas at each time point was determined after replacing 2 ml of water within each exetainer with a helium headspace. Gas from the headspace was injected directly into a GC-IRMS (VG Optima, Manchester, UK), for further details see Holtappels (2011).

<sup>15</sup>NO<sub>2</sub><sup>-</sup> was determined in subsamples after conversion to N<sub>2</sub> by sulfamic acid. <sup>15</sup>NO<sub>3</sub><sup>-</sup> was determined in a further subsample after NO<sub>2</sub><sup>-</sup> removal with sulfamic acid, at which point spongy cadmium was applied to reduce NO<sub>3</sub><sup>-</sup> to NO<sub>2</sub><sup>-</sup>. After one further sulfamic acid treatment, N<sub>2</sub> was measured from a helium headspace using GC-IRMS (Füssel et al., 2011). <sup>15</sup>NH<sub>4</sub><sup>+</sup> was determined in a different set of subsamples after hypobromite reduction to N<sub>2</sub> (Waremburg, 1993; Preisler et al., 2007)

### *Total nitrate, nitrite and ammonium determination*

Combined nitrate and nitrite (NO<sub>x</sub>) concentration within each exetainer was determined by a commercial chemiluminescence NO<sub>x</sub> analyzer after reduction to NO with acidic Vanadium (II) chloride (Braman and Hendrix, 1989). Nitrite was determined after reduction to NO with acidic potassium iodide and nitrate was then calculated by the difference between NO<sub>x</sub> and NO<sub>2</sub><sup>-</sup>. Total NH<sub>4</sub><sup>+</sup> was determined by flow injection analysis (Hall and Aller, 1992).

*Rate calculations*

Denitrification rates were determined from the production of  $^{29}\text{N}_2$  ( $p^{29}\text{N}_2$ ) and  $^{30}\text{N}_2$  ( $p^{30}\text{N}_2$ ) (Thamdrup and Dalsgaard, 2002):

$$\text{Den} = p^{30}\text{N}_2 (F^{15}\text{NO}_3^-)^{-2} \quad (\text{eq 1})$$

Where  $F^{15}\text{NO}_3^-$  is the labeling percentage of nitrate which was calculated from the production of  $^{29}\text{N}_2$  ( $p^{29}\text{N}_2$ ) and  $^{30}\text{N}_2$  ( $p^{30}\text{N}_2$ ) and assuming isotope pairing of denitrification only (Nielsen, 1992):

$$F^{15}\text{NO}_3^- = 2 / (p^{29}\text{N}_2 / p^{30}\text{N}_2 + 2) \quad (\text{eq 2})$$

The labeling percentage of nitrate can also be calculated from the measured concentrations of labeled and unlabeled nitrate ( $F^{15}\text{NO}_3^-$ )

$$F^{15}\text{NO}_3^- = {}^{15}\text{NO}_3^- / ({}^{14}\text{NO}_3^- + {}^{15}\text{NO}_3^-) \quad (\text{eq 3})$$

DNRA rates were determined from the labeling percentage of nitrate (eq 2) and the production of  $^{15}\text{NH}_4^+$  ( $p^{15}\text{NH}_4^+$ ):

$$\text{DNRA} = p^{15}\text{NH}_4^+ / F^{15}\text{NO}_3^- \quad (\text{eq 4})$$

Ammonia oxidation rates were determined from the production of  $^{15}\text{NO}_2^-$ . During ammonia oxidation the pool of  $^{15}\text{NH}_4^+$  can become significantly diluted with  $^{14}\text{NH}_4^+$  formed during remineralization of organic matter. Therefore to avoid rate underestimations we corrected the produced  $^{15}\text{NO}_2^-$  for the labeling percentage of ammonium at each time point (eq 5).

$$\text{NO}_{2\text{tx}} = ({}^{15}\text{NO}_{2\text{tx}} - {}^{15}\text{NO}_{2\text{tx}-1}) / (F_{\text{NH}_4\text{tx}} + F_{\text{NH}_4\text{tx}-1}) / 2 \quad (\text{eq 5})$$

Where tx refers to the time point and  $F_{\text{NH}_4}$  is the labeling percentage of ammonium determined by GC-IRMS. Ammonia oxidation rates were then calculated by the increase of  $\text{NO}_2^-$  over time.

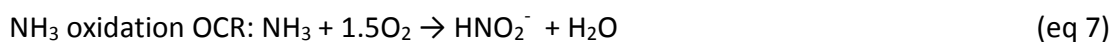
Nitrite oxidation rates were determined from the production of  $^{15}\text{NO}_3^-$  ( $p^{15}\text{NO}_3^-$ ) after addition of  $^{15}\text{NO}_2^-$ . Due to sample limitations we did not correct these rates for changes in labeling percentage.

Assuming Redfield stoichiometry of organic matter, the amount of ammonium released during oxic respiration was compared to ammonia oxidation rates from  $^{15}\text{N}$ -labeling experiments. Briefly, aerobic respiration of organic matter with a redfield stoichiometry would lead to production of  $\text{NH}_4^+$  at a ratio of  $138 \text{ O}_2 / 16 \text{ NH}_4^+$

$$(\text{CH}_2\text{O})_{106}(\text{NH}_3)_{16}\text{H}_3\text{PO}_4 + 138\text{O}_2 + 16\text{H}^+ \rightarrow 106\text{CO}_2 + 16\text{NO}_3^- + 106\text{H}_2\text{O} + \text{H}_3\text{PO}_4$$

(eq 6)

The oxygen consumed by ammonia oxidation and nitrite oxidation was calculated according to



and subtracted from total oxygen consumption rate (OCR) to determine potential heterotrophic OCR:

$$\text{Heterotrophic OCR} = \text{Total OCR} - (\text{NH}_3 \text{ oxidation OCR}) - (\text{NO}_2^- \text{ oxidation OCR}) \quad (\text{eq 9})$$

#### *O<sub>2</sub> and NO<sub>3</sub><sup>-</sup> penetration depths and areal rates*

Porewater concentrations of  $\text{O}_2$  and  $\text{NO}_3^-$  were not measured during this cruise. Instead,  $\text{O}_2$  and  $\text{NO}_3^-$  penetration depths were derived from a transport model published by Elliott and Brooks (1997a; 1997b) which investigated mass transport into permeable sediment as a function of time. The model allows for calculation of an “effective mean mixing depth”, which represents the average length the flow paths of inflowing water in the sediment domain, regardless of the curvature of those flow paths. Therefore the use of effective mean mixing depths accounts for the heterogeneity of transport over time. For stationary ripples with a simplified geometry Elliot and Brooks (1997b) derived an analytical solution to describe the increase of the effective mean mixing depth (D) of a

solute as a function of time (t) after the initial appearance of the solute in the bottom water:

$$D = 3.5/(2\pi) \sqrt{K hm t / \theta} \quad (\text{eq 10})$$

Where K and  $\theta$  are the measured hydraulic conductivity and porosity, respectively. The dynamic hydraulic head (hm) was calculated from measured mean bottom water currents and assumed ripple dimensions (height: 3cm; length: 20cm; similar to observations made during a subsequent cruise in the same region (M. Holtappels pers. comm) using the empirical expression in Elliott and Brooks (1997b).

The effective mean mixing depth of  $O_2$  was determined as follows: the time of  $O_2$  depletion from bottom water entering the pore space was calculated from the initial  $O_2$  concentration in the bottom water divided by the volumetric  $O_2$  consumption rate assuming zero order kinetics. Thereafter the time of depletion was inserted into eq 10 to estimate the effective mean mixing depth of  $O_2$ . The effective mean mixing depth of  $NO_3^-$  was calculated in a similar way. Here, the volumetric rates of nitrification, denitrification and DNRA and their dependence on  $O_2$  concentrations were considered to calculate the time of  $NO_3^-$  depletion and the  $NO_3^-$  mixing depth. To estimate areal rates, the volumetric rates were integrated over the mixing depth of the limiting substrate, i.e.  $O_2$  for  $O_2$  consumption, nitrification, aerobic denitrification and aerobic DNRA, and  $NO_3^-$  for anaerobic denitrification and anaerobic DNRA. Areal rates were extrapolated over 13920 km<sup>2</sup>, the area of the German Bight that exhibits sediment permeabilities in the range of St.1 and St. 2.

**Table 1. Summary of sediment core incubations**

Incubation	Replicates per site	<sup>15</sup> N amendment ( $\mu\text{mol L}^{-1}$ )	<sup>14</sup> N amendment ( $\mu\text{mol L}^{-1}$ )	Other amendment	Processes targeted
<sup>15</sup> NH <sub>4</sub> <sup>+</sup> exp	3	NH <sub>4</sub> <sup>+</sup> (75)	NO <sub>2</sub> <sup>-</sup> (100) + NO <sub>3</sub> <sup>-</sup> (150)	-	Ammonia oxidation
<sup>15</sup> NO <sub>2</sub> <sup>-</sup> exp	3	NO <sub>2</sub> <sup>-</sup> (100)	NO <sub>3</sub> <sup>-</sup> (150)	-	Nitrite oxidation/reduction
<sup>15</sup> NO <sub>3</sub> <sup>-</sup> exp	3	NO <sub>3</sub> <sup>-</sup> (75)	-	-	Denitrification/DNRA
Anammox. exp	2	NH <sub>4</sub> <sup>+</sup> (75)	-	86 $\mu\text{mol L}^{-1}$ ATU*	Anammox
Acet. exp	1	NH <sub>4</sub> <sup>+</sup> (75)	-	10 Pa acetylene**	Anammox

\* Allylthiourea was added to block ammonia oxidation

\*\* Acetylene at this concentration fully inhibits ammonia oxidation, but only partly inhibits anammox (Jensen et al., 2007).

**Table 2. Station locations within the German Bight and water and sediment characteristics**

Site	Latitude	Longitude	Depth (m)	Bottom water temp (°C)	Air Temp (°C)	Salinity	Bottom water NO <sub>3</sub> <sup>-</sup> ( $\mu\text{M}$ )	Porosity	Median grain size ( $\mu\text{m}$ )	Permeability
1	54° 10,16' N	7° 59,70' E	21.0	12.9	14.1	32.1	6	0.36	440	1.87-12
2	54° 10,55' N	7° 57,24' E	23.3	13.2	12.8	31.5	8	0.40	576	8.91-12
3	54° 14,36' N	7° 51,31' E	18.4	12.8	12.6	32.0	7	0.36	429	3.28-11

## Results

### *Sediment characteristics and oxygen consumption rates*

Benthic processes were investigated in permeable sandy sediments at three stations within the German Bight; the stations differed in grain size, porosity and permeability. Median grain size as determined on a particle analyzer ranged from medium sand at St. 1 and St. 3 (440  $\mu\text{m}$  and 429  $\mu\text{m}$ , respectively) to coarse sand at St. 2 and (576  $\mu\text{m}$ ) (Wentworth, 1922). Grain size showed a Gaussian distribution at St. 1, at St. 2 there was an additional fraction of fine sand and St. 3, there was an additional fraction of shell fragments and gravel (> 2mm) (Supp. Fig. 1).; Permeability was lowest and porosity highest at St. 1, St. 2 had intermediate permeability and porosity, and permeability was highest at St. 3, where porosity was lowest (Table 2). The enhanced permeability at St. 3, combined with the additional fraction of shell fragments and gravel led us to conclude that this station was in fact characterized by the coarsest sand and it is referred to as such throughout the text. Oxygen consumption rates differed significantly between each station, the highest rates were observed at St. 2 and the lowest at St. 3 (Fig. 1). Moreover, while oxygen decreased linearly to below 25  $\mu\text{M}$  at St. 1 and 2, an exponential decrease was observed at St. 3 (Fig. 1).

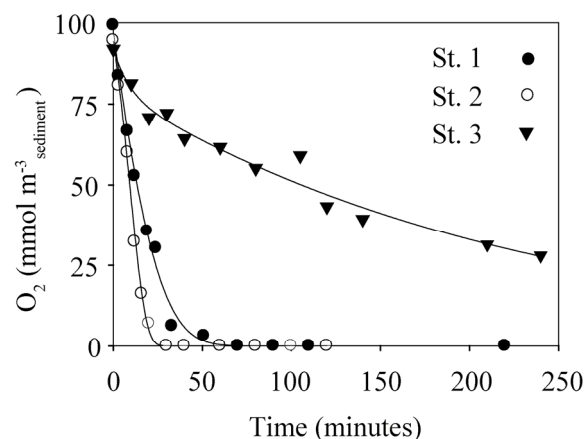


**Fig. 1.** Examples of oxygen consumption profiles measured during the  $^{15}\text{NH}_4^+$  addition experiment at all 3 stations

*Ammonia oxidation*

Ammonia oxidation was determined under oxic conditions from the production of  $^{15}\text{NO}_2^-$  after addition of  $^{15}\text{NH}_4^+$ ,  $^{14}\text{NO}_2^-$  and  $^{14}\text{NO}_3^-$ . Although  $^{14}\text{N}$ -substrates were added to hamper the further oxidation or reduction of  $^{15}\text{NO}_2^-$  by nitrification and denitrification, a small amount of  $^{15}\text{NO}_3^-$  was produced during the incubation and therefore this was added to the  $^{15}\text{NO}_2^-$  concentration. Substantial and linear production of  $^{15}\text{NO}_2^-$  was observed at all three stations ( $^{15}\text{NH}_4^+$  exp.; Supp. Fig. 2). Ammonia oxidation rates were highest at St. 1 and lowest at St. 2 (Fig 2a).

The low apparent ammonia oxidation rates observed at St. 2 coincided with high rates of denitrification and DNRA during oxic conditions (measured in the  $^{15}\text{NO}_3^-$  exp.; Fig. 2a). To investigate whether the low ammonia oxidation rates at St. 2 resulted from tight coupling between nitrification and denitrification, we measured the production of  $^{15}\text{N-N}_2$  in the  $^{15}\text{NH}_4^+$  addition experiment.  $^{15}\text{N-N}_2$  production was very low (<100 nM), as a result of the  $^{14}\text{N}$ -substrate additions. Therefore we could rule out interference from denitrification and DNRA on the ammonia oxidation rates at St. 2

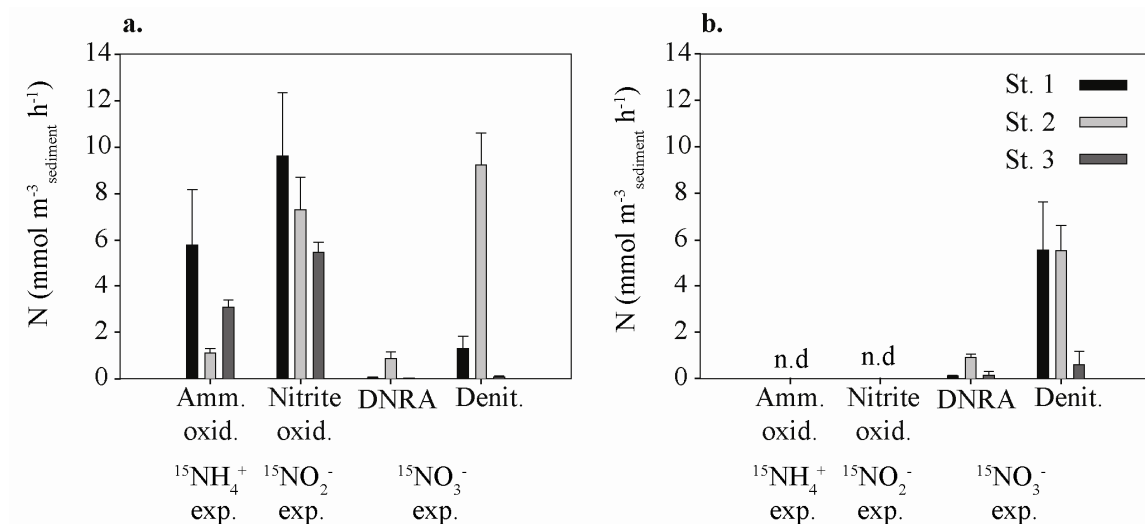


**Fig. 2. Volumetric rates of nitrogen cycling processes at all three stations**, determined from the a) oxic and b) anoxic phase of the incubation. For details of substrate additions see table 1. Error bars are SD, n = 3 (n=2 at St. 3,  $^{15}\text{NO}_3^-$  addition experiment), n.d. = not detected.

*Nitrite oxidation*

Linear production of  $^{15}\text{NO}_3^-$  occurred after addition of  $^{15}\text{NO}_2^-$  at all 3 stations while oxygen was present ( $^{15}\text{NO}_2^-$  exp; Supp. Fig 2). The highest rates of nitrite oxidation were observed at St. 1 and the lowest rates at St. 3. Nitrite oxidation rates were always higher than ammonia oxidation rates (Fig. 2a). There was a weak positive correlation between ammonia oxidation rates measured in the  $^{15}\text{NH}_4^+$  addition exp. and nitrite oxidation rates measured in the  $^{15}\text{NO}_2^-$  addition exp. ( $r^2 = 0.48$   $p = 0.04$ ).

*Denitrification and anammox*

The production of  $^{29+30}\text{N}_2$ , after addition of  $^{15}\text{NO}_3^-$ , occurred at all 3 stations even when oxygen was still present ( $^{15}\text{NO}_3^-$  exp. Supp Fig. 2) (1 replicate of St. 3 was discarded as anaerobic rates were not linear by the time the incubation was terminated). At station St. 1 and St. 3, denitrification rates increased when the sediment became anoxic (Fig. 2). At St. 2, denitrification rates were high while oxygen was still present and did not increase upon anoxia, in fact, they dropped slightly. As a consequence of the high oxic denitrification rates at St. 2,  $\text{NO}_3^-$  concentrations were already low when the sediment became anoxic ( $\sim 10 \mu\text{mol L}^{-1}$ ) and dropped to below detection limit by the time the incubations were terminated. Therefore we assume that anoxic denitrification rates were most likely substrate limited and thus underestimated. Hence when comparing heterotrophic oxygen consumption rates and denitrification rates we used anoxic denitrification rates from St. 1 and St. 3 and oxic rates from St. 2. There was a significant positive correlation between oxygen consumption rates and denitrification rates ( $y = 0.032x + 0.7$   $p = 0.002$   $r^2 = 0.82$  (Fig. 3)).

We investigated possible  $^{15}\text{N-N}_2$  production from anammox by incubating one core from St. 1 and St. 2 by incubating the sediment with  $^{15}\text{NH}_4^+$  as well as 10 Pa of acetylene to block ammonia oxidation (acet. exp). If anammox were occurring  $^{29}\text{N}_2$  should have been produced, however we observed no production of any  $^{15}\text{N}$ -labeled compound. The  $^{15}\text{NO}_3^-$  addition exp. also indicated that anammox was not a significant process within these sediments. In the  $^{15}\text{NO}_3^-$  addition exp.  $^{29}\text{N}_2$  and  $^{30}\text{N}_2$  were produced, which we attributed to denitrification. However part of the  $^{29}\text{N}_2$  pool could also have



been produced by anammox. To investigate whether this was the case we compared the labeling percentage ( $F^{15}\text{NO}_3^-*$ ) based on the produced  $^{29}\text{N}_2$  and  $^{30}\text{N}_2$  at each time point with the labeling percentage ( $F^{15}\text{NO}_3^-$ ) from substrate measurements. There was no difference between these two values; therefore providing no evidence that anammox occurred. Furthermore, in the  $^{15}\text{NH}_4^+$  addition exp. (designed to determine ammonia oxidation rates), the presence of anammox would have been indicated by a decrease of  $^{15}\text{NH}_4^+$  concentrations at anoxic conditions, this was not the case.

One further experiment was carried out to determine the occurrence of anammox - sediment from St. 1 and St. 2 was incubated with  $^{15}\text{NH}_4^+$ ,  $^{14}\text{NO}_2^-$ ,  $^{14}\text{NO}_3^-$  and allythiourea (ATU) and  $^{29}\text{N}_2$  production was measured (anammox. exp). The ability to detect anammox using this incubation relies on the assumption that nitrification is inhibited by ATU. In the case that nitrification is not inhibited,  $^{15}\text{NH}_4^+$  is oxidized to  $^{15}\text{NO}_3^-$  at which point denitrification can also produce  $^{29}\text{N}_2$  and  $^{30}\text{N}_2$ . We added  $86 \mu\text{mol L}^{-1}$  ATU, to block bacterial ammonia oxidation, however ammonia oxidation still occurred, therefore we were unable to use this incubation to determine anammox.

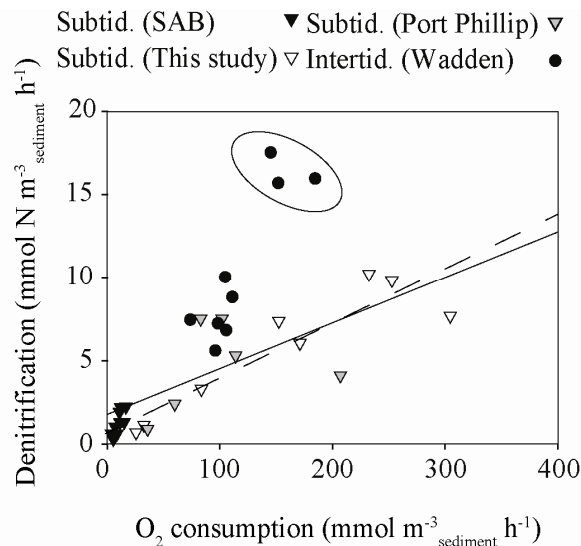


**Fig. 3. The correlation between oxygen consumption rates and denitrification rates in a variety of permeable sediments.** The dashed line represents the linear regression of rates from this study (heterotrophic OCR was used) ( $y = 0.032x + 0.7$   $p = 0.002$   $r^2 = 0.82$ ). The three circled points represent rates measured during winter in the Wadden Sea, when nitrate concentrations in the water column are on average  $70 \mu\text{mol L}^{-1}$ . The solid line represents the linear regression excluding these three data points ( $y = 0.031x + 1.78$   $r^2 = 0.59$   $p < 0.01$ ). The sub-tidal data from the SAB (South Atlantic Bight) are taken from Rao et al. (2007), subtidal (Port Phillip) refers to the data in Evrard et al. (2012) and the intertidal (Wadden) is from Marchant et al. (2013a)

*Coupled nitrification-denitrification*

Coupled nitrification-denitrification was observed in an experiment that was originally planned to assess anammox rates (anammox exp). Due to the apparent failure of ATU to block ammonia oxidation,  $^{15}\text{NH}_4^+$  was sequentially oxidized to  $^{15}\text{NO}_2^-$  then  $^{15}\text{NO}_3^-$ , and  $^{29+30}\text{N}_2$  production began almost immediately (Fig. 4a+b). The sum off all  $^{15}\text{N}$  labeled products increased constantly over the first 60 minutes of the incubation, until  $\text{O}_2$  was depleted, reflecting ammonium oxidation rates which around 50% lower than measured in the ammonium oxidation experiment but nevertheless followed the same trend. The successive increase and decrease of oxidized  $^{15}\text{N}$ -products and the increase of  $^{15}\text{N-N}_2$  (supp. Fig. 3), indicate direct coupling of nitrification and denitrification. Coupled nitrification-denitrification was also indicated in the  $^{15}\text{NO}_3^-$  addition exp. where distinct changes occurred in the labeling percentage of  $\text{NO}_3^-$  ( $\text{F}^{15}\text{NO}_3^*$ ) during the oxic part of the incubation, which suggests that the  $^{15}\text{NO}_3^-$  added at the start of the incubation was constantly diluted by the production of  $^{14}\text{NO}_3^-$  via nitrification.

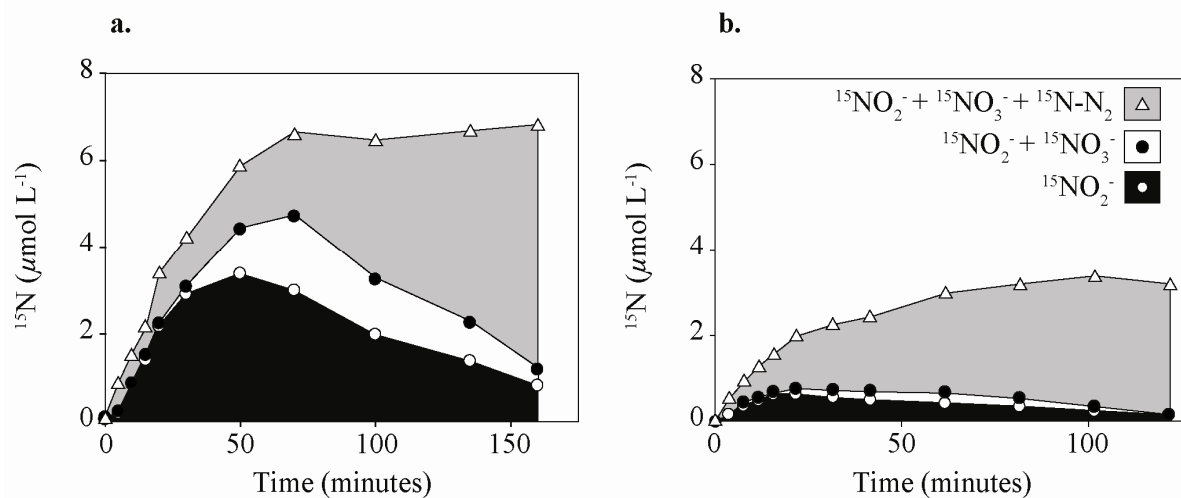


**Fig. 4. Evidence for coupled nitrification-denitrification.** Stacked area plot of the production of  $^{15}\text{N}$ -labeled after  $^{15}\text{NH}_4^+$  and ATU addition. a) Example from St. 1 b) Example from St. 2

*Dissimilatory nitrate reduction to ammonium (DNRA)*

In the  $^{15}\text{NO}_3^-$  addition exp. we also observed the production of  $^{15}\text{NH}_4^+$ , indicative of DNRA, at all 3 stations, even when oxygen was still present, ( $^{15}\text{NO}_3^-$  exp; Supp. Fig. 2).

DNRA rates were low but generally showed similar trends as denitrification, i.e. rates were higher during sediment anoxia at St. 1 and St. 3 and no trend was observed at St. 2 (Fig. 2). Like denitrification rates, DNRA rates also positively correlated to oxygen consumption rates (Supp. Fig. 4).

#### Nitrous oxide ( $N_2O$ ) production

$^{15}N$ - $N_2O$  formation occurred at all three stations when  $^{15}NH_4^+$  and when  $^{15}NO_3^-$  were added to the sediment ( $^{15}NH_4^+$  exp.;  $^{15}NO_3^-$  exp. respectively; Supp Fig. 2). In the  $^{15}NO_3^-$  addition exp.  $^{45+46}N_2O$  production occurred both in the presence and absence of oxygen at St. 1 and St. 3.  $N_2O$  production rates were significantly higher under oxic conditions than anoxic conditions at St. 1, whereas at St. 3 there was no difference between oxic and anoxic  $N_2O$  production rates (Fig. 5). At St. 2,  $N_2O$  was only produced under oxic conditions. Hence, when denitrification rates were compared to  $N_2O$  production rates, the ratio of  $N_2O:N_2$  was higher during the oxic part of the incubation (Fig. 4b). Little to no  $N_2O$  consumption occurred in the denitrification incubations at St. 1 and St. 3, whereas at St. 2, where we observed high aerobic denitrification rates,  $N_2O$  was produced rapidly at the beginning of the incubation and consumed when the sediment became anoxic ( $^{15}NO_3^-$  exp- $N_2O$ ; Supp. Fig 2).

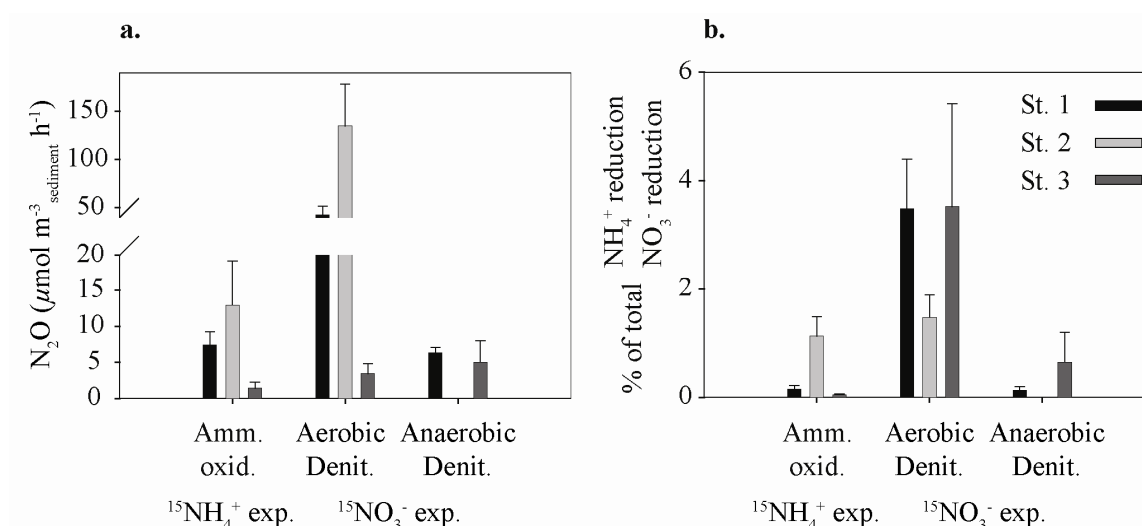


**Fig. 5.  $N_2O$  formation** a) Rates of  $N_2O$  formation from ammonia oxidation and denitrification b) Comparison of  $N_2O$  formation rates against total ammonia oxidation and denitrification rates. Error bars are SD,  $n = 3$  apart from anaerobic rates at St. 2 in the  $^{15}NO_3^-$  addition experiment, where  $n = 2$

### *O<sub>2</sub> and NO<sub>3</sub><sup>-</sup> penetration depths and areal rate estimates*

To integrate volumetric rates into areal rates, the transport model of Elliott and Brooks (1997a; 1997b) was applied. This allowed for the transformation of porewater age into a mean effective mixing depth. The effective mixing depths for O<sub>2</sub> and NO<sub>3</sub><sup>-</sup> were X and Y cm for station 1 and X and Y cm for station 2, respectively (Supp. Fig. 5). The effective mean mixing depths were then used to integrate volumetric rates of oxygen respiration, nitrification, (an)aerobic denitrification and (an)aerobic DNRA over specific depth layers. From this integration we derived areal rates of denitrification (X and Y mmol m<sup>-2</sup> d<sup>-1</sup>), nitrification (X and Y mmol m<sup>-2</sup> d<sup>-1</sup>), DNRA (X and Y mmol m<sup>-2</sup> d<sup>-1</sup>) and oxygen respiration (X and Y mmol m<sup>-2</sup> d<sup>-1</sup>) for station 1 and 2, respectively.

## **Discussion**

### **Permeability and oxygen consumption rates**

Subtidal coastal sediments are often sites of anthropogenically induced eutrophication. As such, it is important to understand how they might remove or recycle anthropogenic N-inputs and act as a buffer between the land and the oceans. Although many studies have investigated muddy subtidal sediments, sandy permeable subtidal sediments - which cover 70% of the continental shelf - have largely been neglected. The few observations of oxygen consumption and denitrification conducted in subtidal sandy sediments have identified high rates of both processes (Gihring et al., 2010; Evrard et al., 2012). However little is known about the relationship between oxygen consumption and denitrification in sands of different permeabilities. Within the German Bight, more than 60% of the sediment ranges between fine and extremely coarse sand, which accordingly vary in permeability (Janssen et al., 2005). Therefore, we investigated sediments at three stations with different permeabilities, ranging from the lowest permeability at which advective transport still occurs (Station 1) (Huettel et al., 2003), intermediate permeability (Station 2) and very high permeability (Station 3). The sediments we studied are representative of almost the entire spectrum of permeability

in German Bight sands; more than 80% of the permeable sediments fall into a range between Station 1 and 2, while < 2% are more permeable than Station 3 (Janssen et al., 2005).

Most permeable sediments have high oxygen consumption rates (OCR) and denitrification rates, which are supported by constant advective supply of organic matter and electron acceptors (de Beer et al., 2005). We observed high OCR's in the German Bight, and also that OCR increased with permeability at Station 1 and 2, results similar to those of Janssen et al. (2005). Interestingly, we found that OCR was comparatively low at station 3, which had very coarse sediment, characterized by high permeability. Decreases in OCR at very high permeabilities have not been observed directly before in permeable sediments. However, it has been demonstrated that in very coarse sediments advection does not enhance the burial of diatoms (Ehrenhauss et al., 2004), indicating that the filtration of organic matter (OM) sources might be less efficient at high permeabilities. Similarly, within bioreactors which utilize permeable media such as sand grains; wash-out, preferential flow paths and reduced surface area can all lead to lower biological activity at high permeabilities/large grain sizes (Stevenson, 1997; Moore et al., 2001). A combination of these three factors may have been responsible for the reduced OCR at Station. 3; first, organic matter may have no longer been filtered effectively by the sediment and instead washed out. Second, transport may have become so high that flow within the sediments followed preferential pathways. Modelling studies have shown that high flows can lead to "dead zones" in the sediment in which no advective flow occurs (Matyka et al., 2008; Narsilio et al., 2009). In these zones, conditions would become diffusion limited, which could explain the non-linear oxygen consumption profile at Station. 3 (Fig. 1). Third, increased grain size would have reduced the surface area available for colonization by microbes, leading to decreases in microbial abundance and thus OCR (Belser, 1979).

## **Aerobic processes**

### **Ammonia oxidation**

Little is known so far about the relationship between nitrification and permeability, however our results indicate found that permeability did not just impact upon OCR, but also affected nitrification within the German Bight. We observed ammonia oxidation occurring within the sediment at all three stations (Fig. 2a). Rates differed between each station; with the highest rates of ammonia oxidation at Station 1, followed by Station 3. Comparatively low ammonia oxidation rates were observed at Station 2, which coincided with high OCR and intermediate grain size. Interestingly, this meant that when ammonia oxidation rates were correlated to permeability they did not show the same trends as OCR. This is to be expected as OCR is generally determined by the amount of labile organic material available, and almost all ammonia oxidisers are autotrophs, requiring CO<sub>2</sub> rather than OM. Instead, an inverse correlation between OCR and ammonia oxidation was observed at Station 1 and Station 2 and could result from the heterotrophic community outcompeting ammonia oxidisers. High OCR indicate a thriving heterotrophic community existed at Station 2, and ammonia oxidizers have been shown to be poor competitors with heterotrophs for resources such as space (Belser, 1979) and oxygen (Henriksen et al. 1993).

The volumetric ammonia oxidation rates are in the upper range of benthic nitrification rates reported so far (see Blackburn and Henriksen, 1983; Ward, 2008 and references therein). Therefore, our high rates are at odds with previous measurements from permeable sediments, that have found comparatively low benthic nitrification rates, however none of these studies were carried out under advective conditions. A modeling study has predicted that benthic nitrification rates might even lower than those previously measured in permeable sediments due to advective transport (Kessler et al., 2012). Kessler et al. (2012), hypothesized that advective porewater flow in permeable sediments should limit the ammonium available to ammonia oxidizers, as ammonium produced in anoxic sediments would be returned directly to the water column rather than be made available to supply ammonia oxidation. Comparison of OCR

and ammonia oxidation rates in our study strongly indicated that enough ammonium would have been produced *in situ* by aerobic remineralization to support the observed rates (Fig. 6). The ammonia oxidation rates we observed therefore indicate that previous reports of nitrification in sandy sediments are more likely to be an underestimation than an overestimation, as rather than cause substrate limitation, advective flows increase oxygen concentrations and oxygen penetration depths, both of which enhance the possibility that nitrification may occur (Lohse et al., 1993; Jensen et al., 1994; Jensen et al., 1996; Gihring et al., 2010)

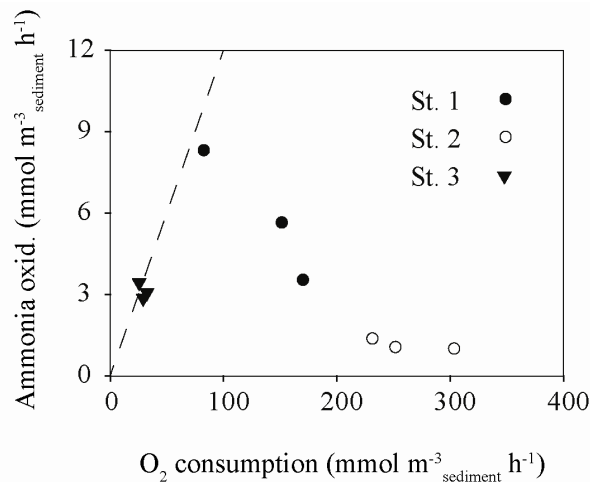


**Fig. 6. Comparison of heterotrophic oxygen consumption rates and ammonia oxidation rates.** The dashed line represents the amount of  $\text{NH}_4^+$  that would have been supplied from remineralization of organic matter by oxygen respiration.

### Nitrite oxidation

Ammonia oxidation is generally considered as the rate limiting step for nitrification (e.g. Ward, 2005) and nitrite oxidation as a separate process is often neglected. Recently, method improvements have enhanced our ability to measure nitrite oxidation as a stand alone process (Füssel et al., 2011). Nonetheless, reports of nitrite oxidation are still rare in the marine environment, especially in benthic settings and no direct measurements exist for permeable sandy sediments.

Our nitrite oxidation rates can only be considered as potential rates, as it is difficult to determine the robustness of the method we used due to the scarcity of

previous measurements. It is possible that we underestimated the rates as the co-occurrence of nitrate reduction and ammonia oxidation during nitrite oxidation would have diluted the  $^{15}\text{NO}_2^-$  pool with  $^{14}\text{NO}_2^-$  and, thus, lowered  $^{15}\text{NO}_3^-$  production. We added high starting concentrations of  $^{15}\text{NO}_2^-$  to minimize the influence of such dilutions, this addition may have stimulated nitrite oxidation, in which case the *in situ* rates would be overestimated. However, no evidence of stimulation of nitrite oxidation by the addition of  $\text{NO}_2^-$  has been observed previously in incubation experiments (Olson, 1981; Ward, 1987; Clark et al., 2008).

Intriguingly the nitrite oxidation rates we measured always exceeded ammonia oxidation rates (Fig. 2). If nitrite oxidation rates were not overestimated, this suggests that ammonia oxidation and nitrite oxidation might be partly uncoupled in these sediments. This could result from the co-occurrence of nitrite oxidation and denitrification, as denitrification would provide a secondary source of nitrite other than ammonia oxidation. A similar uncoupling of the two processes has been observed in suboxic ocean waters where nitrite oxidation and nitrate reduction co-occur (Füssel et al., 2011; Isobe et al., 2012). Our results therefore provide evidence to support the inference from natural abundance stable isotope composition data that intense nitrate/nitrite redox cycling occurs within the sediments of the Bight (Dähnke et al., 2010).

#### **Denitrification and DNRA in the presence of oxygen**

The co-occurrence of aerobic and anaerobic processes in both pelagic and benthic settings is increasingly recognized to occur in environments where conditions are dynamic (Jensen et al., 2007; Gao et al., 2010; Kalvelage et al., 2011). As such, aerobic denitrification has previously been identified in subtidal permeable sediments (Rao et al., 2008), where oxygen penetration depths oscillate with tidal forcing and ripple migration. In depth investigations have also confirmed that both denitrification and DNRA occur while oxygen is still present in intertidal permeable sediments where



additional oxygen fluctuations occur in relation to diurnal tidal cycles (Gao et al., 2010, Marchant; unpublished data).

In our study, denitrification and DNRA both occurred in subtidal sediments while oxygen concentrations were still high ( $\text{NO}_3^-$  exp.; Supp. Fig. 2). Aerobic denitrification rates were 10 and 20 % of the anaerobic rates at Station 1 and Station 3, respectively, and aerobic DNRA rates were 30 and 20% of the anaerobic DNRA rates at Station 1 and Station 3, respectively (Fig. 2). Similar proportions have been measured previously in intertidal sediments (Marchant et al., 2013a). In contrast at Station 2, aerobic denitrification and DNRA rates were of similar proportions to anaerobic denitrification and DNRA rates.

The increased oxic denitrification rates at Station 2 were surprising, since previous observations have always indicated that aerobic denitrification rates are lower in the presence of oxygen. High oxic denitrification rates may have resulted from extreme heterogeneity within the sediment, leading to the co-existence of both fully anoxic and fully oxic micro-environments. However, since the production of  $\text{N}_2$  and the consumption of oxygen were linear, it is unlikely that anoxic microenvironments were extensive from the start of the experiment. Briefly, as the extent of the anoxic sediment increased, a greater proportion of the community would have started to denitrify, resulting in non-linear, increasing rates of  $\text{N}_2$  production. Further, if  $^{15}\text{N}$ - $\text{N}_2$  production only occurred in anoxic microenvironments, the volumetric rates of denitrification within the microenvironments would have to be extremely high to explain the observed rates; such high rates have no precedent. Therefore, we conclude that denitrification was not just occurring in isolated anoxic patches, but rather in oxic sediment as a result of microbial adaptation.

Station 2 had the highest OCR and therefore the sediment community may have experienced changes in oxygen conditions more rapidly than the other two stations. Frequent exposure to fluctuations in oxygen availability has been shown to induce cultures of denitrifiers to constantly express the enzymes needed for denitrification, even while oxygen is present (Robertson and Kuenen, 1988; Patureau et al., 2000; Chen

and Strous, 2013). We can speculate that this resulted in a large part of the denitrifying community continuing to express denitrifying enzymes at all times and as a consequence, high aerobic denitrification rates. The occurrence of denitrification in the presence of oxygen significantly increases the areal estimate of N-loss because the sediment layers over which volumetric denitrification rates are integrated include the oxic layer and are therefore significantly larger (Supp. Fig. 5).

## **Anaerobic processes**

### **Denitrification**

The major N-loss pathway within the permeable subtidal German Bight sediments was anoxic denitrification, which was observed at all 3 stations (Fig. 2). While anammox can significantly contribute to N-loss from sediments (Thamdrup and Dalsgaard, 2002), our combined results from the acetylene addition exp, the  $^{15}\text{NO}_3^-$  addition exp. and the  $^{15}\text{NH}_4^+$  addition exp. indicate that anammox was not substantial. Denitrification rates were strongly correlated to calculated heterotrophic oxygen consumption rates. This correlation is not surprising as OCR are a robust proxy for the amount of labile organic matter in sediments (Glud, 2008) and denitrification is generally a heterotrophic process.

Volumetric denitrification rates at Station 1 and Station 2 were similar to those reported for the intertidal Wadden Sea and the subtidal Port Phillip Bay, Australia, (Evrard et al., 2012; Marchant et al., 2013a), whereas, the lower denitrification rates at Station 3 were comparable to rates obtained from subtidal sandy sediments of the South Atlantic Bight (Rao et al., 2007; Evrard et al., 2012). When volumetric rate data from different permeable sediments, both subtidal, intertidal, eutrophied and oligotrophic is taken together, the strong positive correlation between OCR and denitrification rates persists (Fig. 3), the correlation indicates that denitrification potential was controlled by organic matter availability (Fig. 3). This suggests that the differences observed previously between intertidal and subtidal sandy sediments are not related to the tidal regime itself, but rather to the availability of organic matter

within the sediment. Intriguingly, when water column nitrate concentrations and OCR are both high, denitrification rates increase in a non-linear fashion (circled points, Fig. 3), indicating that nitrate concentrations are a secondary controller of denitrification in permeable sediments.

### **DNRA**

DNRA also occurred at all 3 stations and rates showed many of the same trends as denitrification, for example DNRA rates were also positively correlated to oxygen consumption rates (Supp. Fig 3). DNRA rates were however, lower than denitrification, making up 2, 10 and 17 % of total  $\text{NO}_3^-$  reduction (DNRA + Denitrification), for Station 1, 2 and 3, respectively. This is similar to the contribution of DNRA in intertidal permeable sediments (Marchant et al., 2013a), but lower than in other temperate diffusive sediments (An and Gardner, 2002; Trimmer and Nicholls, 2009; Koop-Jakobsen and Giblin, 2010; Jantti and Hietanen, 2012). The dominance of denitrification over DNRA results in high N-loss and low ammonium release. While this removes fixed N from the German Bight, rather than recycling it, reducing eutrophication, high denitrification rates coupled to advective transport also have the potential to lead to  $\text{N}_2\text{O}$  emissions,

### **$\text{N}_2\text{O}$ production**

Until recently subtidal permeable sediments were not associated with nitrogen cycling and therefore they were rarely considered as a source of  $\text{N}_2\text{O}$ . As understanding of nitrogen cycling in permeable sediments has grown, so has the recognition of their role as significant sources of  $\text{N}_2\text{O}$  (Marchant et al., 2013b). We observed significant  $^{15}\text{N}_2\text{O}$  formation in the  $^{15}\text{NH}_4^+$  exp., only when oxygen was present and therefore concluded that ammonia oxidation was the source. Whereas, in the  $^{15}\text{NO}_3^-$  experiment,  $^{45+46}\text{N}_2\text{O}$  were produced both in the presence and absence of oxygen, indicating  $\text{N}_2\text{O}$  production from oxic and anoxic denitrification (Fig. 5a). The patterns of  $\text{N}_2\text{O}$  formation during denitrification that were observed at St.1 and St. 3 are very similar to those that occur in intertidal sandy sediments, i.e. the ratio between  $\text{N}_2\text{O}$  and  $\text{N}_2$  production was

always higher during the aerobic part of the incubation (Fig. 5b) and N<sub>2</sub>O was not consumed until nitrate became limiting (Supp. Fig. 2). At St. 2 (where we observed the anomalously high aerobic denitrification rates), N<sub>2</sub>O consumption began as soon as the sediment became anaerobic. This further indicates that the denitrifying community at St. 2 was extremely well adapted to changes in oxygen conditions.

N<sub>2</sub>O formation within permeable sediments is closely linked with N<sub>2</sub>O emissions to the water column and subsequently the atmosphere (Marchant et al., 2013b). Therefore the occurrence of N<sub>2</sub>O formation during both ammonia oxidation and denitrification adds to evidence that sandy sediments may play a significant role in global N<sub>2</sub>O emissions.

### **The coupling of nitrification and denitrification in permeable sediments**

The temporal overlap between nitrification and denitrification, combined with the high rates of both processes indicated that coupled nitrification-denitrification might be occurring within the sediment. The sequential ammonia oxidation, nitrite oxidation and denitrification observed within the <sup>15</sup>NH<sub>4</sub><sup>+</sup> and ATU amendment experiment (Fig. 4 and Supp. Fig. 4), strongly indicates that this was indeed the case. We could show that while oxygen was present <sup>15</sup>N built up in the NO<sub>2</sub><sup>-</sup>, NO<sub>3</sub><sup>-</sup> and N<sub>2</sub> pools, whereas upon anoxia, the <sup>15</sup>NO<sub>2</sub><sup>-</sup> and <sup>15</sup>NO<sub>3</sub><sup>-</sup> pools decreased, while the <sup>15</sup>N-N<sub>2</sub> pool continued to increase. As a result, when ammonia oxidation ceased during anoxia, no net gain or loss of label occurred from the combined <sup>15</sup>NO<sub>2</sub><sup>-</sup>, <sup>15</sup>NO<sub>3</sub><sup>-</sup> and <sup>15</sup>N-N<sub>2</sub> pools (Fig. 4).

The 86 μmol L<sup>-1</sup> ATU addition should have inhibited ammonia oxidation in this incubation (which was originally intended to determine anammox rates). At concentrations of 86 μmol L<sup>-1</sup> cultivated ammonia oxidizing bacteria are completely inhibited by ATU (Ginestet et al., 1998). However, in our sediment, ATU appeared to only halve ammonia oxidation rates. Incomplete inhibition of ammonia oxidation by ATU has been observed previously and may be attributed to the presence of ammonia oxidizing archaea (Santoro et al., 2010; Taylor et al., 2010; Santoro and Casciotti, 2011), although we have no evidence this was the case in our study.

In permeable sediments from areas where water-column nitrate concentrations are low, coupled nitrification-denitrification is predicted to be the main pathway of N<sub>2</sub> loss (Gihring et al., 2010). In the German Bight, where water column nitrate concentrations are high, and denitrifiers are supplied with nitrate by advective transport, we did not necessarily expect a close coupling between nitrification and denitrification. Nevertheless, the temporal and spatial overlap of denitrification and nitrification and the rapid oxidation and reduction of <sup>15</sup>N that we observed in the <sup>15</sup>NH<sub>4</sub><sup>+</sup> + ATU experiment indicate a strong coupling between the two processes. As a result of the partial inhibition of ammonia oxidation and the rapid turnover of <sup>15</sup>N we did not directly determine rates of coupled nitrification-denitrification; however the occurrence of the process in the German Bight has the potential to lead to higher N-losses than previously estimated from nitrate fluxes alone.

#### **Areal denitrification and nitrification rates from permeable German Bight sediments**

To estimate the impact of nitrification, denitrification and DNRA on N-loss and N-turnover within the German Bight, we transformed volumetric rates into areal rates. In permeable sediments, flow paths of porewater start and end at the water-sediment-interface, therefore solute penetration depth is both a function of depth and the horizontal plane. To take this into account, the measured volumetric rates were integrated over times and depths corresponding to the curved flow paths as well as the changes in nitrate and oxygen concentration that occur as porewater is advected through the sediment.

To determine nitrate and oxygen concentrations within the sediment along a flow path, we combined the nitrification rates from the <sup>15</sup>NH<sub>4</sub><sup>+</sup> amendment exp. with the oxygen consumption, denitrification and DNRA rates from the <sup>15</sup>NO<sub>3</sub><sup>-</sup> amendment experiments. Two different scenarios were identified for station 1 and 2, respectively (upper panels; Fig. 6). At station 1, under aerobic conditions, nitrification exceeded nitrate removal by denitrification and DNRA. Therefore, nitrate concentrations increased within the sediment until oxygen was entirely consumed. Thereafter,

increased rates of denitrification and DNRA prevail until nitrate is completely respired. At station 2, under aerobic conditions, nitrate removal by denitrification and DNRA exceeded nitrification. Therefore, nitrate concentrations decreased until nitrate was completely consumed. After nitrate was consumed, oxygen still remained for around 12 minutes, during which time nitrate removal via denitrification and DNRA could not proceed at rates greater than nitrification – the only remaining nitrate source.

To determine the sediment depths that nitrification, denitrification and DNRA were integrated over, we had to estimate oxygen and nitrate penetration depths for each station respectively. In order to take the curved porewater flow paths into account, porewater ages and the subsequent concentration of  $O_2$ ,  $NO_3^-$ ,  $NH_4^+$  and  $N_2$  within the sediment were transformed into a “mean effective mixing depth” (Elliott and Brooks (1997a; 1997b). Effective mixing depths of  $O_2$  and  $NO_3^-$  were 2.7 and 4.1 cm for station 1, and 4.3 and 3.9 cm for station 2, respectively (lower panels; Fig. 6). Such  $O_2$  penetration depths are realistic in comparison to *in situ* measurements made during a subsequent cruise to the same region (M. Holtappels pers. comm), providing validation for the Elliot and Brooks model. By combining the effective mean mixing depths with the succession of rates described above, oxygen consumption, nitrification, aerobic denitrification and DNRA rates, and anaerobic denitrification and DNRA rates were integrated over specific depth layers to calculate areal rates.

At St. 1, areal rates of N-loss were lower than nitrification rates, whereas at St. 2, areal rates of N-loss exceeded those of nitrification by a factor of 7, suggesting that although nitrification-denitrification was tightly coupled at both stations, a net uptake of nitrate from bottom waters only occurred at St. 2. Areal denitrification rates (118 and 363  $\mu\text{mol m}^{-2} \text{h}^{-1}$ ), were similar to those in permeable sediments in the intertidal Wadden Sea (207  $\mu\text{mol m}^{-2} \text{h}^{-1}$ , Gao et al., 2010; Gao et al., 2012), while areal nitrification rates (158 and 47  $\mu\text{mol m}^{-2} \text{h}^{-1}$ ), were also in the range of previous areal estimates from continental shelf sediments e.g. 117  $\mu\text{mol m}^{-2} \text{h}^{-1}$  (Laursen and Seitzinger, 2002).

### N-loss and nitrification estimates for the German Bight

The nitrification, denitrification and DNRA rates measured within this study are likely to exhibit seasonal and regional variations dependent on OM and  $\text{NO}_3^-$  concentrations in the bottom water, as well as oxygen respiration rates in the sediment. Nevertheless, we extrapolated the rates of Station 1+2 to the entire area (13920 km<sup>2</sup>) of the German Bight that exhibits similar sediment permeabilities. In this way we could establish an annual net N-loss for the German Bight of 200 kt yr<sup>-1</sup> (Table 3). This flux is comparable to the 140 kt yr<sup>-1</sup> estimated previously using the 3D-ecosystem model ECOHAM (Radach and Patsch, 2007; Paetsch et al., 2010). However, our gross annual N-loss (410 kt yr<sup>-1</sup>) was up to double that of Paetsch et al. who did not include benthic nitrification or DNRA in their model.

**Table 3. Annual nitrification, denitrification, DNRA and net N-loss determined for the permeable sediments of the German Bight.** Rates were extrapolated to an area of 13920 km<sup>2</sup>, which is the area of German Bight sediments falling between the permeability of Station 1 and Station 2.

	Gross nitrate production from nitrification	Gross N-loss from denitrification	Ammonium production by DNRA	Net N-loss	Riverine + atmospheric N inputs recycled within sediment*
	(kt N yr <sup>-1</sup> )				
Station 1	270,7	195,7	4,60	-79,6	97 %
Station 2	81,3	619,8	58,7	479,8	49 %
Scenario a**	176,0	407,8	31,6	200,1	73 %

\* Atmospheric deposition and riverine fluxes were estimated as 29 kt yr<sup>-1</sup> and 256 kt yr<sup>-1</sup> respectively (Dähnke et al., 2010)

\*\* Equal weighting is given to Station 1 and Station 2

The areal rates revealed that nitrification and to a lesser extent DNRA within the permeable sediments of the German Bight, have the capacity to recycle between 49 and 97 % of the riverine and atmospheric nitrate inputs (Table 3). This provides confirmation that significant N-turnover due to nitrification occurs within the German Bight, a concept which has been inferred previously from mass balances and natural abundance stable isotope composition of dissolved nitrate (Dähnke et al., 2010).

Increasingly in the last decade, intertidal permeable sediments such as those in the Wadden Sea (Germany) have been recognized as sites of substantial N-loss (45.6 kt N loss yr<sup>-1</sup>) (Gao et al., 2012). Less is known about permeable sediments from subtidal zones, which cover significantly more of the seafloor than intertidal zones. Here we can conclude that denitrification in subtidal permeable sediments from the German Bight acts as a sink for around 400 kt N yr<sup>-1</sup> and therefore N-losses from the German Bight are up to 10-fold higher than the neighbouring intertidal sediments in the Wadden Sea. Benthic nitrification is also important in these permeable sediments, where, although it is strongly coupled to denitrification, it can regenerate almost as much nitrate as that which is lost as N<sub>2</sub>.

**Supplementary Figures are included with this manuscript**

## References

- An, S.M., and Gardner, W.S. (2002) Dissimilatory nitrate reduction to ammonium (DNRA) as a nitrogen link, versus denitrification as a sink in a shallow estuary (Laguna Madre/Baffin Bay, Texas). *Marine Ecology Progress Series* **237**: 41-50.
- Beddig, S., Brockmann, U., Dannecker, W., Korner, D., Pohlmann, T., Puls, W., Radach, G., Rebers, A., Rick, H.J., Schatzmann, M., Schlunzen, H., and Schulz, M. (1997) Nitrogen fluxes in the German Bight. *Marine Pollution Bulletin* **34**: 382-394.
- Belser, L.W. (1979) Population ecology of denitrifying bacteria. *Annual Review of Microbiology* **33**: 309-333.
- Blackburn, T.H., and Henriksen, K. (1983) Nitrogen cycling in different types of sediments from Danish waters. *Limnology and Oceanography* **28**: 477-493.
- Braman, R.S., and Hendrix, S.A. (1989) Nanogram nitrite and nitrate determination in environmental and biological materials by vanadium(III) reduction with chemiluminescence detection. *Analytical Chemistry* **61**: 2715-2718.
- Chen, J.W., and Strous, M. (2013) Denitrification and aerobic respiration, hybrid electron transport chains and co-evolution. *Biochim Biophys Acta-Bioenerg* **1827**: 136-144.
- Clark, D.R., Rees, A.P., and Joint, I. (2008) Ammonium regeneration and nitrification rates in the oligotrophic Atlantic Ocean: Implications for new production estimates. *Limnology and Oceanography* **53**: 52-62.
- Cook, P.L.M., Wenzhofer, F., Glud, R.N., Janssen, F., and Huettel, M. (2007) Benthic solute exchange and carbon mineralization in two shallow subtidal sandy



sediments: Effect of advective pore-water exchange. *Limnology and Oceanography* **52**: 1943-1963.

Cook, P.L.M., Wenzhofer, F., Rysgaard, S., Galaktionov, O.S., Meysman, F.J.R., Eyre, B.D., Cornwell, J., Huettel, M., and Glud, R.N. (2006) Quantification of denitrification in permeable sediments: Insights from a two-dimensional simulation analysis and experimental data. *Limnology and Oceanography-Methods* **4**: 294-307.

Dähnke, K., Emeis, K., Johannsen, A., and Nagel, B. (2010) Stable isotope composition and turnover of nitrate in the German Bight. *Marine Ecology Progress Series* **408**: 7-U26.

de Beer, D., Wenzhofer, F., Ferdelman, T.G., Boehme, S.E., Huettel, M., van Beusekom, J.E.E., Bottcher, M.E., Musat, N., and Dobilier, N. (2005) Transport and mineralization rates in North Sea sandy intertidal sediments, Sylt-Romo Basin, Wadden Sea. *Limnology and Oceanography* **50**: 113-127.

Devol, A.H., Codispoti, L.A., and Christensen, J.P. (1997) Summer and winter denitrification rates in western Arctic shelf sediments. *Continental Shelf Research* **17**: 1029-&.

Ehrenhauss, S., Witte, U., Buhning, S.I., and Huettel, M. (2004) Effect of advective pore water transport on distribution and degradation of diatoms in permeable North Sea sediments. *Marine Ecology Progress Series* **271**: 99-111.

Elliott, A.H., and Brooks, N.H. (1997a) Transfer of nonsorbing solutes to a streambed with bed forms: Laboratory experiments. *Water Resources Research* **33**: 137-151.

Elliott, A.H., and Brooks, N.H. (1997b) Transfer of nonsorbing solutes to a streambed with bed forms; Theory. *Water Resources Research* **33**: 123-136.

Emery, K.O. (1968) Relict sediments on continental shelves of world. *AAPG Bulletin* **52**: 445-464.

Evrard, V., Glud, R., and Cook, P.M. (2012) The kinetics of denitrification in permeable sediments. *Biogeochemistry*: 1-10.

Fries, J.S., and Trowbridge, J.H. (2003) Flume observations of enhanced fine-particle deposition to permeable sediment beds. *Limnology and Oceanography* **48**: 802-812.

Füssel, J., Lam, P., Lavik, G., Jensen, M.M., Holtappels, M., Gunter, M., and Kuypers, M.M.M. (2011) Nitrite oxidation in the Namibian oxygen minimum zone. *ISME J* **6**: 1200-1209.

Gao, H., Schreiber, F., Collins, G., Jensen, M.M., Kostka, J.E., Lavik, G., de Beer, D., Zhou, H.Y., and Kuypers, M.M.M. (2010) Aerobic denitrification in permeable Wadden Sea sediments. *Isme Journal* **4**: 417-426.

Gao, H., Matyka, M., Liu, B., Khalili, A., Kostka, J.E., Collins, G., Jansen, S., Holtappels, M., Jensen, M.M., Badewien, T.H., Beck, M., Grunwald, M., de Beer, D., Lavik, G., and Kuypers, M.M.M. (2012) Intensive and extensive nitrogen loss from intertidal permeable sediments of the Wadden Sea. *Limnology and Oceanography* **57**: 185-198.

- Gihring, T.M., Canion, A., Riggs, A., Huettel, M., and Kostka, J.E. (2010) Denitrification in shallow, sublittoral Gulf of Mexico permeable sediments. *Limnology and Oceanography* **55**: 43-54.
- Ginestet, P., Audic, J.M., Urbain, V., and Block, J.C. (1998) Estimation of nitrifying bacterial activities by measuring oxygen uptake in the presence of the metabolic inhibitors allylthiourea and azide. *Applied and Environmental Microbiology* **64**: 2266-2268.
- Glud, R.N. (2008) Oxygen dynamics of marine sediments. *Marine Biology Research* **4**: 243-289.
- Gruber, N., and Galloway, J.N. (2008) An Earth-system perspective of the global nitrogen cycle. *Nature* **451**: 293-296.
- Guo, H., Zhou, J., Su, J., and Zhang, Z. (2005) Integration of nitrification and denitrification in airlift bioreactor. *Biochemical Engineering Journal* **23**: 57-62.
- Hall, P.O.J., and Aller, R.C. (1992) *Rapid, small-volume, flow injection analysis for CO<sub>2</sub> and NH<sub>4</sub><sup>+</sup> in marine and freshwaters*. Waco, TX, ETATS-UNIS: American Society of Limnology and Oceanography.
- Henriksen, K., and Kemp, W.M. (1988) Nitrification in estuarine and coastal marine sediments. *Scope* **33**: 207-249.
- Holtappels, M., Lavik, G., Jensen, M. M., and Kuypers, M. M. M. (2011) <sup>15</sup>N-Labeling Experiments to Dissect the Contributions of Heterotrophic Denitrification and Anammox to Nitrogen Removal in the OMZ Waters of the Ocean, p. 223-251. In *Methods in Enzymology*. Klotz, M.G. (ed).
- Huettel, M., Roy, H., Precht, E., and Ehrenhauss, S. (2003) Hydrodynamical impact on biogeochemical processes in aquatic sediments. *Hydrobiologia* **494**: 231-236.
- Isobe, K., Koba, K., Suwa, Y., Ikutani, J., Kuroiwa, M., Fang, Y., Yoh, M., Mo, J., Otsuka, S., and Senoo, K. (2012) Nitrite transformations in an N-saturated forest soil. *Soil Biology and Biochemistry* **52**: 61-63.
- Janssen, F., Huettel, M., and Witte, U. (2005) Pore-water advection and solute fluxes in permeable marine sediments (II): Benthic respiration at three sandy sites with different permeabilities (German Bight, North Sea). *Limnology and Oceanography* **50**: 779-792.
- Jantti, H., and Hietanen, S. (2012) The Effects of Hypoxia on Sediment Nitrogen Cycling in the Baltic Sea. *Ambio* **41**: 161-169.
- Jensen, K., Sloth, N.P., Risgaardpetersen, N., Rysgaard, S., and Revsbech, N.P. (1994) Estimation of nitrification and denitrification from microprofiles of oxygen and nitrate in model systems. *Applied and Environmental Microbiology* **60**: 2094-2100.
- Jensen, K.M., Jensen, M.H., and Kristensen, E. (1996) Nitrification and denitrification in Wadden Sea sediments (Konigshafen, Island of Sylt, Germany) as measured by nitrogen isotope pairing and isotope dilution. *Aquatic Microbial Ecology* **11**: 181-191.
- Jensen, M.M., Thamdrup, B., and Dalsgaard, T. (2007) Effects of specific inhibitors on anammox and denitrification in marine sediments. *Applied and Environmental Microbiology* **73**: 3151-3158.

Kalvelage, T., Jensen, M.M., Contreras, S., Revsbech, N.P., Lam, P., Guenter, M., LaRoche, J., Lavik, G., and Kuypers, M.M.M. (2011) Oxygen Sensitivity of Anammox and Coupled N-Cycle Processes in Oxygen Minimum Zones. *Plos One* **6**.

Kessler, A.J., Glud, R.N., Cardenas, M.B., Larsen, M., Bourke, M.F., and Cook, P.L.M. (2012) Quantifying denitrification in rippled permeable sands through combined flume experiments and modeling. *Limnology and Oceanography* **57**: 1217-1232.

Koop-Jakobsen, K., and Giblin, A.E. (2010) The effect of increased nitrate loading on nitrate reduction via denitrification and DNRA in salt marsh sediments. *Limnology and Oceanography* **55**: 789-802.

Laursen, A.E., and Seitzinger, S.P. (2002) The role of denitrification in nitrogen removal and carbon mineralization in Mid-Atlantic Bight sediments. *Continental Shelf Research* **22**: 1397-1416.

Li, Y., Yu, J.J., Liu, Z.G., and Ma, T. (2013) Estimation and modeling of direct rapid sand filtration for total fecal coliform removal from secondary clarifier effluents. *Water Science and Technology* **65**: 1615-1623.

Lohse, L., Malschaert, J.F.P., Slomp, C.P., Helder, W., and van Raaphorst, W. (1993) Nitrogen cycling in North Sea sediments: interaction of denitrification and nitrification in offshore and coastal areas. *Mar Ecol-Prog Ser* **101**: 283-283.

Marchant, H., Lavik, G., Holtappels, M., and Kuypers, M.M. (2013a) The fate of nitrate in intertidal permeable sediments. *PloS one* **Submitted**.

Marchant, H., Lavik, G., Holtappels, M., Schreiber, F., Vahrenhorst, R., Strous, M., Kuypers, M.M., and Tegetmeyer, H. (2013b) Nitrous oxide emissions from coastal sands due to anthropogenic nitrogen input. *Nature Geoscience* **In revision**.

Matyka, M., Khalili, A., and Koza, Z. (2008) Tortuosity-porosity relation in porous media flow. *Physical Review E* **78**: 026306.

Moore, R., Quarmby, J., and Stephenson, T. (2001) The effects of media size on the performance of biological aerated filters. *Water Research* **35**: 2514-2522.

Münch, E.V., Lant, P., and Keller, J. (1996) Simultaneous nitrification and denitrification in bench-scale sequencing batch reactors. *Water Research* **30**: 277-284.

Narsilio, G.A., Buzzi, O., Fityus, S., Yun, T.S., and Smith, D.W. (2009) Upscaling of Navier-Stokes equations in porous media: Theoretical, numerical and experimental approach. *Computers and Geotechnics* **36**: 1200-1206.

Nielsen, L.P. (1992) Denitrification in Sediment Determined from Nitrogen Isotope Pairing. *Fems Microbiology Ecology* **86**: 357-362.

Olson, R.J. (1981) 15-N tracer studies of the primary nitrite maximum. *Journal of Marine Research* **39**: 203-226.

Paetsch, J., Serna, A., Daehnke, K., Schlarbaum, T., Johannsen, A., and Emeis, K.-C. (2010) Nitrogen cycling in the German Bight (SE North Sea) - Clues from modelling stable nitrogen isotopes. *Continental Shelf Research* **30**: 203-213.

Patureau, D., Zumstein, E., Delgenes, J.P., and Moletta, R. (2000) Aerobic denitrifiers isolated from diverse natural and managed ecosystems. *Microbial Ecology* **39**: 145-152.

Prakasam, T.B.S., and Loehr, R.C. (1972) Microbial nitrification and denitrification in concentrated wastes. *Water Research* **6**: 859-869.

Preisler, A., de Beer, D., Lichtschlag, A., Lavik, G., Boetius, A., and Jørgensen, B.B. (2007) Biological and chemical sulfide oxidation in a Beggiatoa inhabited marine sediment. *Isme Journal* **1**: 341-353.

Rabalais, N.N. (2002) Nitrogen in aquatic ecosystems. *Ambio* **31**: 102-112.

Radach, G., and Patsch, J. (2007) Variability of continental riverine freshwater and nutrient inputs into the North Sea for the years 1977-2000 and its consequences for the assessment of eutrophication. *Estuaries and Coasts* **30**: 66-81.

Rao, A.M.F., McCarthy, M.J., Gardner, W.S., and Jahnke, R.A. (2007) Respiration and denitrification in permeable continental shelf deposits on the South Atlantic Bight: Rates of carbon and nitrogen cycling from sediment column experiments. *Continental Shelf Research* **27**: 1801-1819.

Rao, A.M.F., McCarthy, M.J., Gardner, W.S., and Jahnke, R.A. (2008) Respiration and denitrification in permeable continental shelf deposits on the South Atlantic Bight:  $N_2$ : Ar and isotope pairing measurements in sediment column experiments. *Continental Shelf Research* **28**: 602-613.

Revsbech, N.P. (1989) An oxygen microsensor with a guard cathode. *Limnology and Oceanography* **34**.

Robertson, L.A., and Kuenen, J.G. (1988) Heterotrophic nitrification in *Thiosphaera pantotropha* - oxygen uptake and enzyme studies. *Journal of General Microbiology* **134**: 857-863.

Rocha, C., Forster, S., Koning, E., and Epping, E. (2005) High-resolution permeability determination and two-dimensional porewater flow in sandy sediment. *Limnology and Oceanography-Methods* **3**: 10-23.

Santoro, A.E., and Casciotti, K.L. (2011) Enrichment and characterization of ammonia-oxidizing archaea from the open ocean: phylogeny, physiology and stable isotope fractionation. *ISME J* **5**: 1796-1808.

Santoro, A.E., Casciotti, K.L., and Francis, C.A. (2010) Activity, abundance and diversity of nitrifying archaea and bacteria in the central California Current. *Environ Microbiol* **12**: 1989-2006.

Sharma, B., and Ahlert, R.C. (1977) Nitrification and nitrogen removal. *Water Research* **11**: 897-925.

Stevenson, D.G. (1997) Flow and filtration through granular media—the effect of grain and particle size dispersion. *Water Research* **31**: 310-322.

Tait, D.R., Erler, D.V., Dakers, A., Davison, L., and Eyre, B.D. (2013) Nutrient processing in a novel on-site wastewater treatment system designed for permeable carbonate sand environments. *Ecological Engineering* **57**: 413-421.

Taylor, A.E., Zeglin, L.H., Dooley, S., Myrold, D.D., and Bottomley, P.J. (2010) Evidence for Different Contributions of Archaea and Bacteria to the Ammonia-Oxidizing Potential of Diverse Oregon Soils. *Applied and Environmental Microbiology* **76**: 7691-7698.

Thamdrup, B., and Dalsgaard, T. (2002) Production of  $N_2$  through anaerobic ammonium oxidation coupled to nitrate reduction in marine sediments. *Applied and Environmental Microbiology* **68**: 1312-1318.

Trimmer, M., and Nicholls, J.C. (2009) Production of nitrogen gas via anammox and denitrification in intact sediment cores along a continental shelf to slope transect in the North Atlantic. *Limnology and Oceanography* **54**: 577-589.

van Beusekom, J.E.E. (2005) A historic perspective on Wadden Sea eutrophication. *Helgoland Marine Research* **59**: 45-54.

Ward, B.B. (1987) Nitrogen transformations in the southern-california bight. *Deep-Sea Research Part a-Oceanographic Research Papers* **34**: 785-805.

Ward, B.B. (2005) Temporal variability in nitrification rates and related biogeochemical factors in Monterey Bay, California, USA. *Marine Ecology Progress Series* **292**: 97-109.

Ward, B.B. (2008) Nitrification in marine systems. In *Nitrogen in the Marine Environment*. D.G. Capone, D.A.B., and M.R. Mulholland, a.E.J.C. (eds). Amsterdam: Elsevier Press, pp. Pp. 199–262.

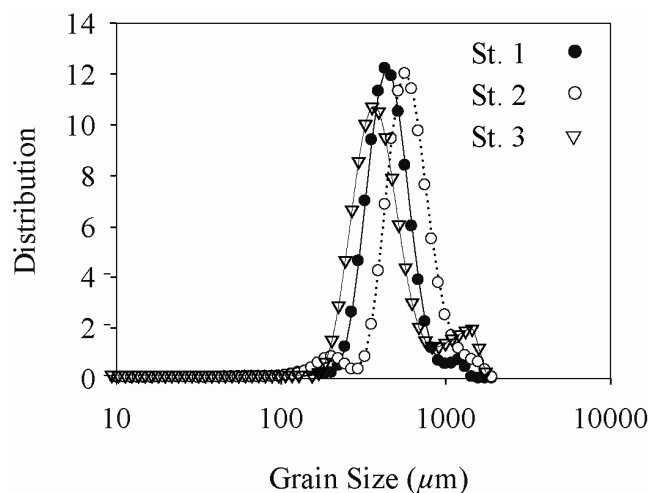
Waremburg, F. (1993) Nitrogen fixation in soil and plant systems In *Nitrogen Isotopes Techniques*. Knowles K, B.T. (ed). New York: Academic Press, pp. 157–180.

Wentworth, C.K. (1922) A scale of grade and class terms for clastic sediments. *Journal of Geology* **30**: 377-392.

Yao, K.-M., Habibian, M.T., and O'Melia, C.R. (1971) Water and waste water filtration. Concepts and applications. *Environmental Science & Technology* **5**: 1105-1112.

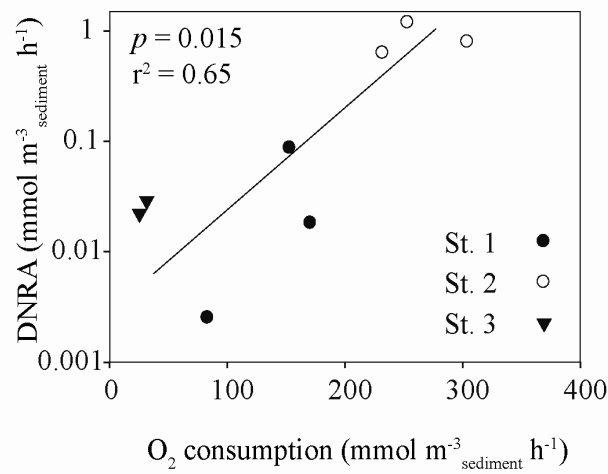
Yoo, H., Ahn, K.-H., Lee, H.-J., Lee, K.-H., Kwak, Y.-J., and Song, K.-G. (1999) Nitrogen removal from synthetic wastewater by simultaneous nitrification and denitrification (SND) via nitrite in an intermittently-aerated reactor. *Water Research* **33**: 145-154.

### Supplementary Figures

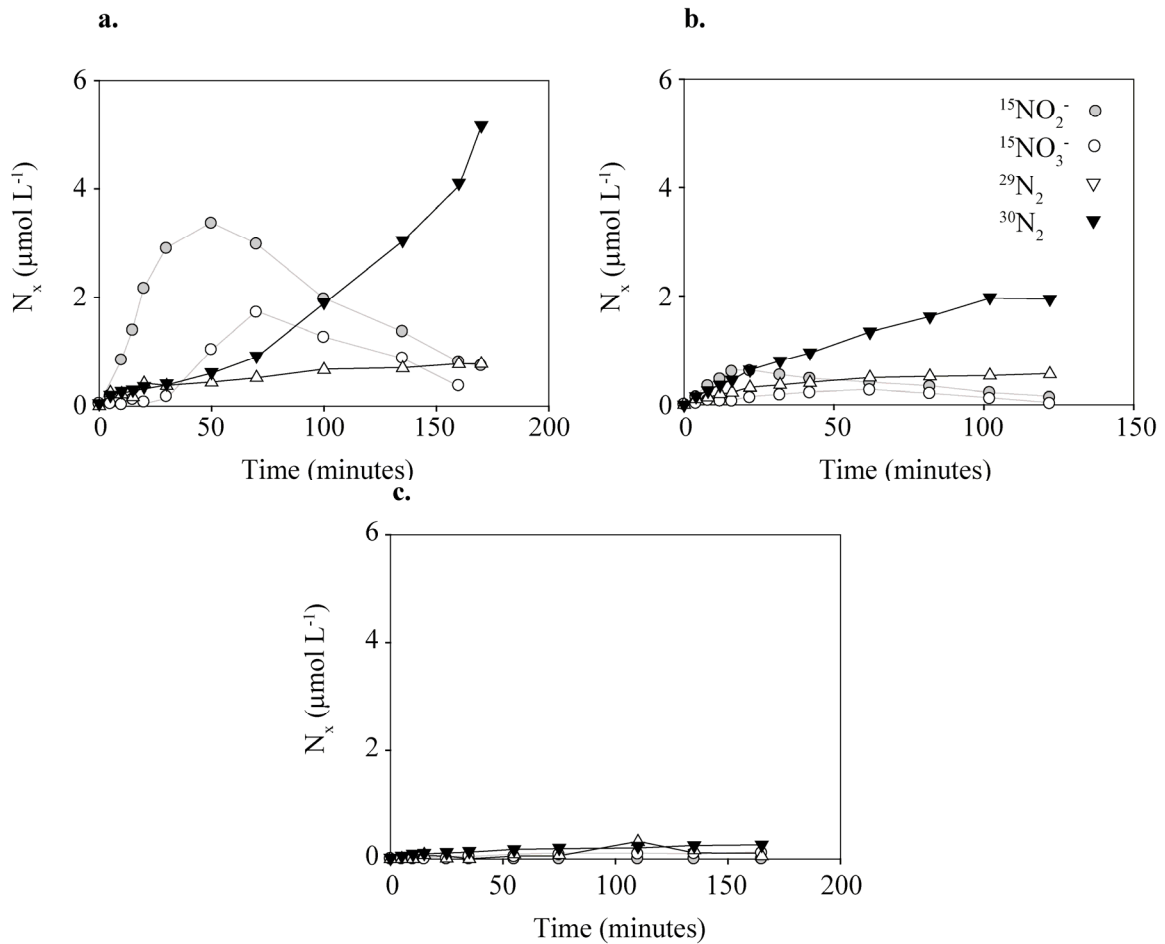


Supp. Fig. 1. Grain size distribution from each station.

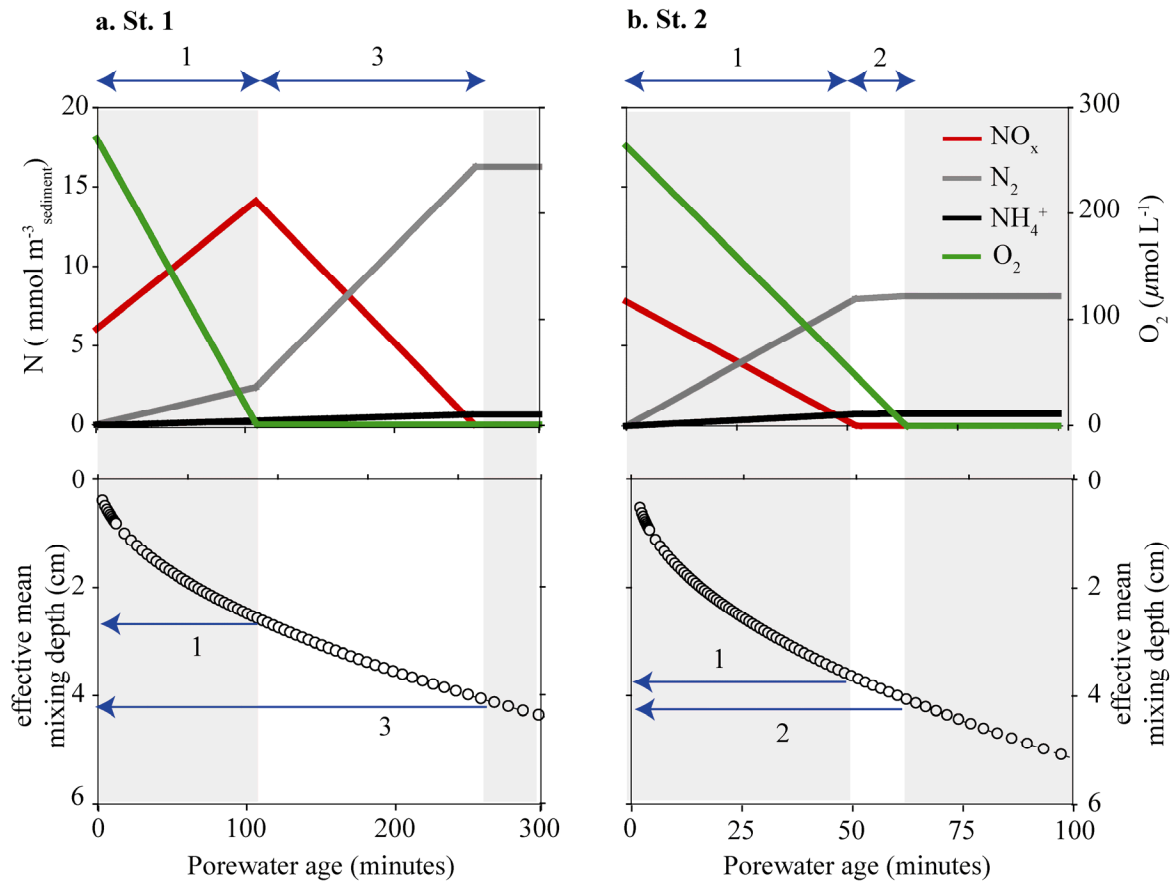




**Supp. Fig. 3. Exponential correlation between heterotrophic oxygen consumption rates DNRA rates** ( $y = 0.0053e^{0.0172x}$   $r^2 = 0.65$   $p = 0.015$ ). Heterotrophic oxygen consumption was determined by subtracting oxygen consumption of ammonia oxidation and nitrite oxidation from total oxygen consumption.



**Supp. Fig. 4. Coupled nitrification-denitrification** after addition of  $^{15}\text{NH}_4^+$  and ATU. a) Example from St. 1 b) Example from St. 2 c) Successful inhibition of ammonia oxidation by 10 Pa acetylene



**Supp. Fig. 5. Modelled concentrations of  $\text{NO}_x$ ,  $\text{N}_2$ ,  $\text{NH}_4^+$  and  $\text{O}_2$  at different porewater ages within the sediment and effective mixing depth of porewater at different ages.** a) at Station 1, where nitrification was high, net production of nitrate occurs while the sediment is oxic (1) and net consumption does not occur until the sediment becomes anoxic (3). (b) at Station 2, where aerobic denitrification and DNRA were high, net consumption of nitrate occurs (1), after 50 minutes, aerobic denitrification and DNRA are limited and can only proceed at the rate of nitrification (2), when the sediment becomes anoxic and the supply of nitrate stops, so do DNRA and denitrification. The lower panels show the output of the Elliot model, which estimates the effective mean mixing depth for a given porewater age. The blue lines and numbers represent the time and depth to which the appropriate rates were integrated for areal estimates.



## Chapter V

### Stimulation and inhibition of aerobic denitrification in intertidal permeable sediments

Hannah K. Marchant<sup>1</sup>, Moritz Holtappels<sup>1</sup>, Soeren Ahmerkamp<sup>1</sup>, Gaute Lavik<sup>1</sup>, Marcel M.M. Kuypers<sup>1</sup>

<sup>1</sup>Max Planck Institute for Marine Microbiology, Celsiusstrasse 1, 28359 Bremen, Germany

\* Corresponding author: hmarchan@mpi-bremen.de, tel: +49421-2028630, fax: +49421-2028790

Keywords: aerobic denitrification; permeable sediment; nitrogen cycling; microsites

Contributions to the manuscript:

H.K.M., G.L., and M.M.M.K., designed research. H.K.M carried out fieldwork, performed MIMS measurements and data analysis. H.K.M., G.L., M.H., and M.M.M.K., conceived wrote and edited the manuscript

**In preparation**

### **Acknowledgements**

We thank Theresa Hargesheimer for field support, Gabriele Klockgether for technical support in the lab and Ole Pfieler for assistance on the ship. This research was funded by the Max Planck Society.

**Abstract**

Aerobic denitrification has been studied in pure cultures and in waste-water treatment plants but little is known about its role in environmental systems. Using an approach comprising short and long term experiments and  $^{15}\text{N}$ -labelling incubations, we investigated the extent and persistence of aerobic denitrification in permeable sediments from an intertidal sand flat in the Wadden Sea (Germany). The response of benthic aerobic denitrification was examined 1) after a 7 week exposure to anoxic or fluctuating porewater oxygen conditions and 2) during short term oscillations between oxic and anoxic conditions. In long term experiments, aerobic denitrification no longer occurred in the sediment supplied with anoxic seawater, although anaerobic denitrification rates had not changed. We were unable to reestablish aerobic denitrification within these sediments, indicating that the denitrifying community was no longer adapted to denitrify in the presence of oxygen. In short term experiments we found evidence that aerobic denitrification can be stimulated by repeated oscillations between oxic and anoxic conditions and could show that this response was not an artifact of the experimental set up. This work demonstrates how aerobic denitrification appears to be an adaptation favored by the environmental niche created in intertidal permeable sediments, where oxygen conditions fluctuate.

## Introduction

Denitrification, the process by which nitrate is sequentially reduced to dinitrogen gas by microbes, has generally been regarded as an anoxic process (Zumft, 1997). Canonically, nitrate is only used by facultative anaerobic organisms as a terminal electron acceptor after dissolved oxygen has been depleted. However, as long as 25 years ago Lloyd et al. (1987) asserted that the persistence of bacterial denitrification under aerobic conditions was “the rule rather than the exception’. The occurrence of aerobic denitrification has been demonstrated in pure cultures of denitrifiers since the 1980’s (Robertson and Kuenen, 1984a; Robertson et al., 1995), however the debate about the ecological significance and even the existence of the process still continues to the present day.

Oxygen is considered to be one of the main environmental inhibitors of denitrification (Zumft, 1997) and classically, N-loss by denitrification is assumed to be restricted to zones where oxygen is below 5  $\mu\text{M}$  (Codispoti et al., 2001). Physiological, bioenergetic and kinetic considerations all provide evidence that denitrification should not occur in the presence of oxygen. On an enzymatic level, oxygen inactivates one of the copper centres ( $\text{Cu}_z$ ) of nitrous oxide reductase (*NosZ*), the enzyme required for the final step in denitrification (Pomowski et al., 2011). Furthermore, several regulatory systems in well known denitrifiers are shut down by the presence of oxygen (Chen and Strous, 2013) and in some organisms, oxygen can even inhibit nitrate transport into the cell (Zumft, 1997; Moir and Wood, 2001).

From a bioenergetic and kinetic perspective, oxygen is a much better electron acceptor than nitrate. Aerobic respiration translocates 10 protons per electron pair transduced compared to 6 during denitrification at most. Furthermore denitrifiers require additional enzyme complexes for respiration in comparison to aerobic organisms and are limited by the space that these must occupy in the membrane and periplasm. Therefore denitrification in the presence of oxygen seems unfavourable on bioenergetic grounds (Chen and Strous, 2013).

Nevertheless, isolates of facultative denitrifiers have frequently been shown to carry out aerobic denitrification in laboratory studies (for a few examples see Robertson and Kuenen, 1984b; Lloyd et al., 1987; Bonin and Gilewicz, 1991; Robertson et al., 1995; Kim et al., 2008). Although it has been suggested that the presence of anaerobic microsites caused by biofilm formation may have allowed denitrification under seemingly oxic conditions in these studies (Robertson and Kuenen, 1984a; Chen and Strous, 2013). This controversy has often overshadowed the investigation of aerobic denitrification. Recently however, more rigorous methodology and interest from the wastewater community (for which aerobic denitrification is of economic value) has led to the firm conclusion that some strains of denitrifiers can, under the correct conditions, denitrify under aerobic conditions (Bonin and Gilewicz, 1991; Patureau et al., 1998; Huang and Tseng, 2001).

A major finding of laboratory studies is that aerobic denitrifiers are often isolated from systems that have alternating oxic-anoxic phases (Patureau et al., 1994; Frette et al., 1997; Patureau et al., 2000). Under these conditions, the bioenergetic restraints of co-respiration of oxygen and denitrification are relaxed and co-expression of the two pathways can become profitable (Chen and Strous, 2013). It has been suggested that it makes little sense for microorganisms to rebuild their respiratory chains dependent on the availability of oxygen when oxygen concentrations are fluctuating rapidly. Instead facultative denitrifiers are able to direct electron flow simultaneously to denitrifying enzymes as well as to O<sub>2</sub> (Robertson and Kuenen, 1988; Huang and Tseng, 2001; Chen et al., 2003). Using a single hybrid electron transport chain, it then becomes feasible that while preferentially using the aerobic pathway, denitrification enzymes could be used to take care of any overflow in the electron flow (Chen and Strous, 2013). Aerobic denitrification therefore seems to become favourable in environments where oxygen concentrations fluctuate.

Despite the identification of an ecological niche in which aerobic denitrification can occur, the environmental significance of the process is still relatively understudied. Permeable sediments represent one environment where aerobic denitrification has

been identified and attributed to the dynamic conditions within the sediment using rigorous methodology (Rao et al., 2007; Gao et al., 2010). Gao et al. for example, used a combination of methods including stirred reactors and microsensors to rule out the presence of anoxic microsites. The dynamic conditions that occur within permeable sediments seem to favour aerobic denitrification. These conditions result from advective porewater flow (Huettel et al., 2003), which leads to rapid oscillations in oxygen and nitrate penetration depths, but also results in high respiration and denitrification rates (de Beer et al., 2005; Cook et al., 2007; Rao et al., 2008; Gao et al., 2012).

We investigated the effect that both frequent and longer term oscillations in oxygen availability have on the capacity for aerobic denitrification within permeable sediments. To do this we collected permeable sediments from the intertidal Wadden Sea and exposed them to different oxygen regimes in the laboratory. Subsequently we observed denitrification using a  $^{15}\text{N}$ -labelling approach coupled to high temporal resolution measurements with a membrane inlet mass spectrometer.

## **Methods**

### *Sampling site*

Sediment was sampled from the Janssand sand flat, which is located in the back barrier area of Spiekeroog Island in the East Frisian Wadden Sea, Germany. The entire flat is inundated with ca. 2m of seawater during high tide before exposure to the air for 6 – 8 h during low tide in a semi diurnal cycle. The sampling site (53.73515 'N, 007.69913'E) was situated in the upper flat, which consists of silicate sands with a mean porosity of 0.35, mean grain size of 176  $\mu\text{m}$  and mean permeability of  $7.2\text{--}9.5 \times 10^{-12} \text{ m}^2$  in the upper 15 cm of sediment (Billerbeck et al., 2006a). The high permeability permits water to be flushed advectively through the sediment in two distinct temporal and spatial scales depending on tidal phase. During inundation, boundary flows cause flushing of the surface sediment layer, at which point oxygen has been shown to penetrate up to depths up to 6cm and additionally organic particles and nutrients are filtered from the water, degraded and promptly returned to the overlying water. This occurs at spatial scales in

the order of centimeters and temporal scales of minutes to hours. During exposure of the flat the upper sediment becomes anoxic and the nutrient-rich pore water from the entire sand flat drains through a thick sediment layer (>50 cm) at a relatively low pore flow velocity (Billerbeck et al., 2006b).

#### *Sediment collection and experimental column set up*

Sediment from the upper 5cm of the sand flat was collected on January 12 2012 at low tide, whereupon it was homogenized and returned to the lab. Less than 4 hours after collection sediment was packed into sediment columns (construction of which has been described in detail in Marchant et al. (2013)).

#### *Confirmation of aerobic denitrification*

To confirm whether aerobic denitrification was occurring within the sediment an incubation was carried out using aerated  $^{15}\text{NO}_3^-$  amended seawater. The entire volume of porewater within the sediment core was exchanged for the aerated  $^{15}\text{NO}_3^-$  amended seawater (enough water was pumped through the core to exchange the entire porewater volume more than 1.5 times). After porewater exchange, the inlet through which the seawater had been pumped into the column was adapted so that seawater could be pumped back out and into a membrane inlet mass spectrometer (MIMS; GAM200, In Process Instruments), at a velocity around  $1\text{cm h}^{-1}$ . MIMS was then used to measure production of  $^{29}\text{N}_2$ ,  $^{30}\text{N}_2$ , Argon and  $\text{O}_2$  concentrations over time. 2 point calibrations for each gas were conducted using air-saturated and He-degassed water before and after the incubation.

#### *Long term experiments*

The long term persistence of aerobic denitrification in the sediment was tested under two different flow regimes using filtered seawater containing  $20\ \mu\text{M NO}_3^-$ . The first regime was designed to mimic the distinct tidal cycle at the Janssand tidal flat. The semi diurnal cycle consisted of two 6 hour “inundation” and “exposure” periods. During “inundation” seawater was pumped in 30 minute on; 15 minute off cycles at a rate of  $2.5\ \text{ml min}^{-1}$ , no pumping occurred during the “exposure” period. In the second flow regime, the column was exposed to the same tidal cycle, however the water supply was

degassed with  $N_2$ , thereby keeping the sediment anoxic constantly. Three sediment columns were assigned to each condition. After 55 days the experiment was terminated and incubations were carried out to determine denitrification rates. The same incubation was carried out as detailed above. Each core was exposed to aerated, labeled seawater only once, except for one of the anoxic cores, to which multiple exposures were carried out, similar to the short term experiment (see below). Subsequently the 2 remaining anoxic replicates were placed on the standard tidal cycle and the capacity for aerobic denitrification was measured again after 4 and 7 days.

### Short-term experiments

A separate set of sediment columns were allowed to equilibrate for 3 days on the simulated tidal cycle. Unfiltered seawater from the study site was supplied via a single aerated reservoir. After three days the incubation described above was carried out. Once all the oxygen had been consumed and  $^{15}N-N_2$  production had ceased in the sediment column, the incubation was repeated. 5 such exposures were conducted, on the fifth no  $^{15}NO_3^-$  was added as a control to ensure that  $^{15}N-N_2$  was not present from previous incubations.

### Results

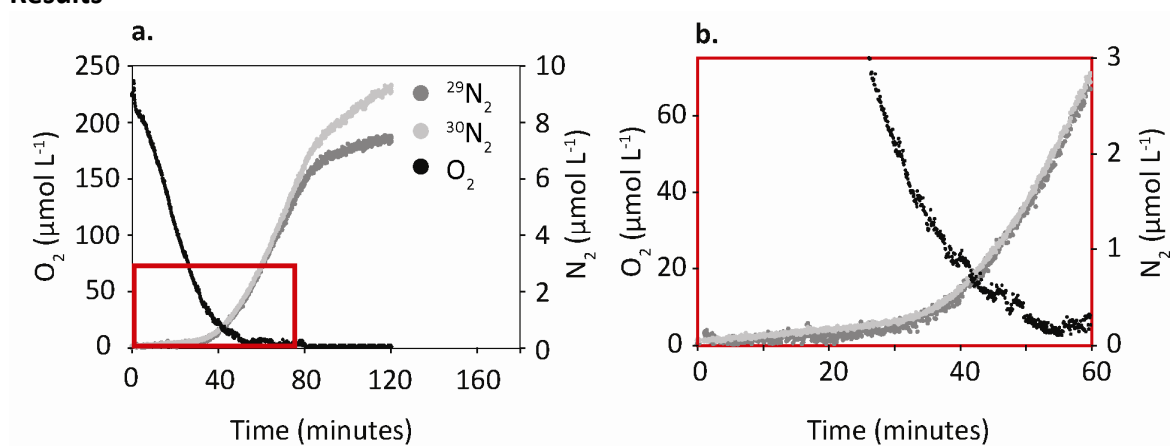


Fig. 1.  $^{29}N_2$  and  $^{30}N_2$  production in a sediment column filled with fresh sediment and kept on a simulated tidal cycle for 3 days before the  $^{15}NO_3^-$  incubation. 3 phases of  $N_2$  production can generally be distinguished during incubations with sediment from the intertidal flat, first, while oxygen is present (a), the second, when oxygen drops below  $30 \mu M$  (b), and the third, when  $^{15}NO_3^-$  starts to become limiting within the sediment core.



*Confirmation of aerobic denitrification* - Sediment from an intertidal flat showed evidence of denitrification while porewater oxygen concentrations were still above 200  $\mu\text{mol L}^{-1}$  (Fig. 1).  $^{29}\text{N}_2$  and  $^{30}\text{N}_2$  production started immediately after porewater had been exchanged for oxidic,  $^{15}\text{NO}_3^-$  labeled seawater. After which,  $^{15}\text{N-N}_2$  production remained linear until oxygen concentrations dropped to around 30  $\mu\text{mol L}^{-1}$  (Fig. 1b). At this point  $^{15}\text{N-N}_2$  production increased and stabilized at the second, linear production rate that was 5-fold higher than the aerobic rate. This rate was maintained when oxygen concentrations dropped to 0.

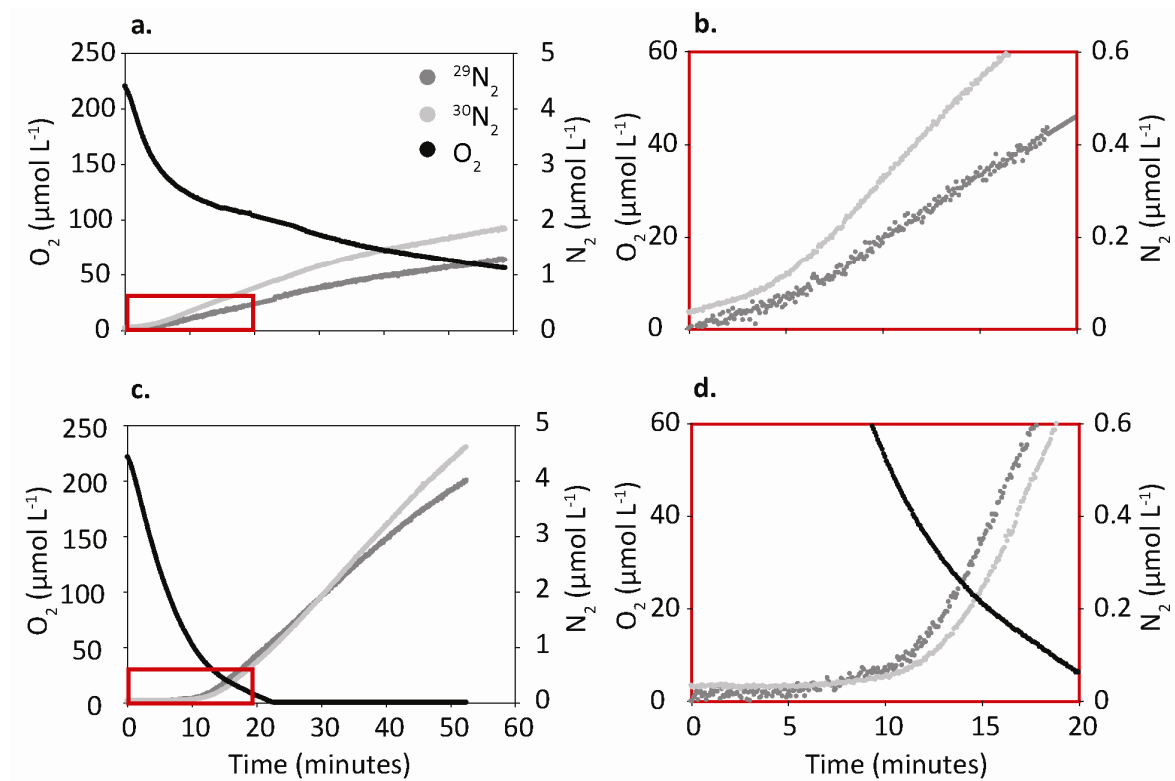


Fig. 2. a+b) The persistence of aerobic denitrification in sediment supplied with aerated seawater on tidal conditions and c+d) the inhibition of aerobic denitrification in sediment supplied with anoxic seawater for 55 days.

*The persistence of aerobic denitrification in the long-term experiment* - After 55 days we investigated the capacity for aerobic denitrification in cores which had been exposed to different oxygen regimes. Within treatment variability in denitrification

rates were remarkably low, however OCR were more variable. Oxygen consumption profiles in the sediment from the anoxic condition were similar to those measured in the initial experiment carried out to confirm the presence of aerobic denitrification (Fig 2a). In contrast changes in oxygen consumption rates and patterns had occurred in the tidal condition; oxygen consumption was linear and similar to the anoxic condition during the initial 10-15 minutes of the incubation. After this OCR dropped significantly (Fig 2c). After 7 days of being replaced on the tidal cycle, oxygen consumption rates in the sediment from the anoxic condition had also dropped significantly. This suggests that less labile organic matter remained within the sediment.

Aerobic denitrification still occurred in the tidal condition (Fig. 2b), where it was higher than in the initial experiment carried out to determine whether aerobic denitrification was present. In contrast, within the sediment from the anoxic condition (Fig. 2d), aerobic denitrification no longer occurred at high oxygen concentrations. A small but non linear increase occurred when oxygen concentrations dropped below 120 $\mu$ M and substantial linear production of  $^{29}\text{N}_2$  and  $^{30}\text{N}_2$  only occurred after oxygen concentrations dropped below 50  $\mu$ M (Fig. 2c), the rate of this anaerobic production matched anaerobic denitrification rates in the initial experiment. We attempted to stimulate aerobic denitrification to restart by repeatedly exposing the sediment to short term oxic-anoxic shifts using filtered seawater and by replacing the sediment columns on a tidal flow regime. Neither of these caused an increase in aerobic denitrification rates.

*Stimulation of aerobic denitrification* - Repeated exposure of a sediment column to the same incubation regime (i.e. exchanging the entire porewater volume with air saturated,  $^{15}\text{NO}_3^-$  amended water and subsequently letting the oxygen be consumed before exchanging the porewater again), increased the magnitude of OCR and anaerobic denitrification rates, but had the greatest effect upon aerobic denitrification. Aerobic denitrification rates increased upon each successive oxic-anoxic shift until rates were almost as high as the anaerobic denitrification rate (Fig 3b). In comparison, the anaerobic denitrification rate only increased slightly upon repeated exposures. The

shape of the  $^{15}\text{N-N}_2$  production profile also changed with multiple oxygen exposures, as did the oxygen consumption profile (Fig 3 a,b). After one exposure, two distinct linear denitrification rates could be observed. After four exposures high denitrification rates were observed at high and low oxygen concentrations, while denitrification rates were slightly lower at intermediate oxygen concentrations (125-25  $\mu\text{M}$ ) (Fig. 3c). Nevertheless upon repeated exposures, when oxygen concentrations were above 50  $\mu\text{M}$  aerobic denitrification rates were consistently higher than during the first exposure

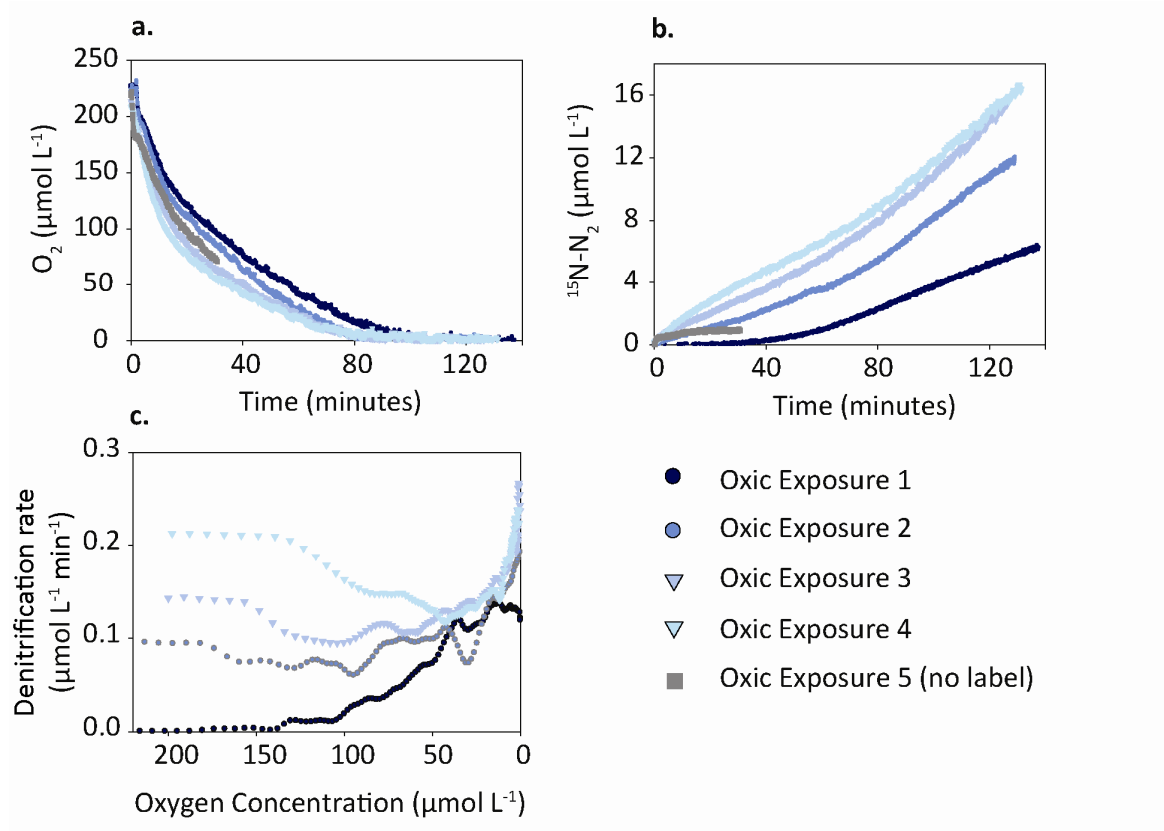


Fig. 3. Stimulation of aerobic denitrification by rapid shifts between oxic and anoxic conditions. a) Oxygen consumption profiles during 5 rapid exposures, b)  $^{15}\text{N-N}_2$  production during the same incubation c) Denitrification rate compared to oxygen concentration for each successive exposure to oxygen

*The likelihood of anoxic microsites* – To test whether aerobic denitrification rates were purely the result of anaerobic denitrification occurring within anoxic microsites, we calculated how much of the sediment column would have to be anoxic to support the measured rates (Fig. 4a). This calculation assumed that the rate of denitrification

within the microsites was the same as the maximal anaerobic denitrification rate measured upon sediment anoxia. Subsequently, we could calculate what the oxygen concentration must have been in the rest of the sediment column to account for the measured bulk oxygen concentration (Fig. 4b). This revealed that if the volume of anoxic microsites were large enough to support the denitrification rates, then for the majority of the incubations oxygen would have been oversaturated (in respect to air equilibration values) within the rest of the porewater.

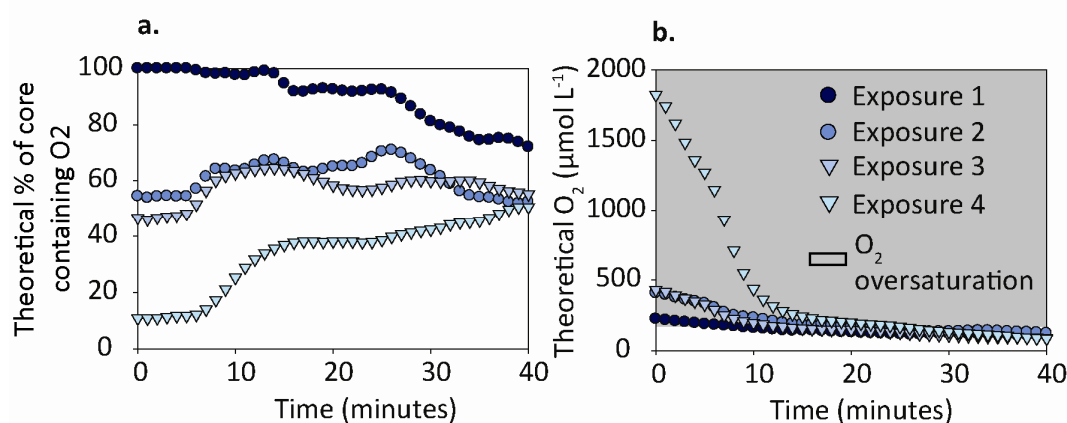


Fig 4. a) Theoretical oxygen concentrations within the sediment if anoxic microsites were wholly responsible for the denitrification rates shown in Fig. 2c. b) Oxygen concentration required in the remainder of the core to give the bulk O<sub>2</sub> concentrations seen in Fig. 2a. The grey part of panel b represents oxygen oversaturation values for seawater.

## Discussion

*Oxygen fluctuations select for aerobic denitrification* - We demonstrated that aerobic denitrification occurs in permeable intertidal sediments from the Wadden Sea by simultaneously measuring oxygen and the production of <sup>15</sup>N-N<sub>2</sub> (Fig. 1). The observation of aerobic denitrification in permeable sediments is consistent with previous studies (Rao et al., 2007; Gao et al., 2010), which have suggested that dynamic fluctuations in oxygen within the sediment stimulate aerobic denitrification. Therefore we were interested in whether the aerobic denitrification rates could be enhanced or inhibited by exposure to different oxygen regimes.

In sediment which had been flushed with oxygenated porewater on a tidal cycle for 55 days, linear production of  $^{15}\text{N-N}_2$  occurred immediately upon addition of air-saturated porewater containing  $^{15}\text{NO}_3^-$  (Fig. 2b), indicating that aerobic denitrification was still occurring within the sediment. In contrast, in sediment that was supplied with anoxic water for 55 days, there was a lag in production of  $^{15}\text{N-N}_2$  upon addition of air-saturated porewater (Fig. 2d).  $^{15}\text{N-N}_2$  was only produced when oxygen concentrations dropped below  $50 \mu\text{mol L}^{-1}$  and furthermore, production of  $^{15}\text{N-N}_2$  did not become linear until oxygen dropped below  $20 \mu\text{mol L}^{-1}$ . Therefore, in the sediment which had been kept anoxic, it appeared that aerobic denitrification was severely limited, even though an active denitrifying community still existed, as exemplified by high anaerobic denitrification rates (Fig. 2c). Upon successive exposures to oxygenated, filtered seawater, we could not induce aerobic production of  $^{15}\text{N-N}_2$  to restart. The inhibition of aerobic denitrification within the sediment cores kept anoxic, but not within the sediment kept on a tidal cycle provides strong evidence that the observed production of  $^{15}\text{N-N}_2$  in the presence of oxygen was not purely due to the presence of anoxic microsites.

The lack of aerobic denitrification in the sediments we kept anoxic supports evidence that alternations between oxic and anoxic conditions are required to select a community which can denitrify aerobically (Patureau et al., 2000). Our results resemble those of studies carried out on bacterial isolates, where the ability to denitrify aerobically degraded when cultures were not exposed to fluctuating oxygen conditions (Robertson et al., 1995).

*Rapid oxygen fluctuations stimulate aerobic denitrification* - When fresh Wadden Sea sediment was exposed to rapid shifts between oxic and anoxic conditions, we witnessed an increase in aerobic  $^{15}\text{N-N}_2$  production rates (Fig. 3b). Repeated shifts quickly led to aerobic denitrification rates reaching a similar magnitude to anaerobic denitrification rates. Combined with the linear  $^{15}\text{N-N}_2$  production this provides strong evidence that aerobic denitrification was stimulated within the sediment by oxygen

fluctuations, rather than resulting from an increase in presence of anoxic microsites, or “dead zones” caused by preferential porewater flow.

Modelling of permeable flows within sediments has revealed that porewater flow follows preferential paths. Therefore within the sediment “dead-zones” occur in which there is no porewater flow (Matyka et al., 2008; Narsilio et al., 2009). It could be argued that with successive porewater exchanges, the build up of isolated “dead-ends” might have occurred and therefore that the increasing  $^{15}\text{N-N}_2$  production was not due to the stimulation of aerobic denitrification but rather the build up of anoxic zones within the sediment. This hypothesis is not supported by the data for several reasons; for anoxic “dead zones” to have a visible impact on rates,  $^{15}\text{NO}_3^-$  would have to diffuse into the zones and  $^{29}\text{N}_2$  and  $^{30}\text{N}_2$  would have to diffuse out into the surrounding pore-waters to be measured. While the steep gradient caused by exchanging the porewater might make this diffusion relatively fast, the diffusional distance from the centre of the spot to the outside would also become larger as the dead ends increased in volume, making it unlikely that we would have observed linear  $^{15}\text{N-N}_2$  production.

Furthermore, by the 4<sup>th</sup> exposure of the sediment to oxygen (Fig. 3a,b) denitrification rates at high oxygen concentrations (>150  $\mu\text{M}$ ) were 89% of the anaerobic denitrification rate. For anaerobic denitrification in anoxic “dead zones” to be responsible for the rates observed then a large volume of the sediment that would have had to be anoxic (Fig. 4a). This conflicts with the high oxygen concentrations measured in the bulk porewater; if part of the sediment were anoxic, then the only way to obtain the measured oxygen values would have been if parts of the porewater were almost 10-fold oversaturated with oxygen (Fig. 4b). As cores were kept in the dark and therefore no photosynthesis was occurring, this is unlikely.

We can also rule out that anoxic microenvironments within the sediment were responsible for the apparent stimulation of aerobic denitrification with successive oxic-anoxic phases. Anoxic microenvironments in sediments form around “hotspots” of organic material such as buried faecal pellets which have large particle sizes, rapid oxygen consumption rates and slow internal diffusivity (Jahnke, 1985). While these

spots are likely to occur within the sediment and are likely to be responsible for the high rates of apparently aerobic denitrification at very low oxygen concentrations ( $< 20 \mu\text{mol L}^{-1}$ ), they would represent fixed spots within the sediment core. New hotspots would not form with successive incubations and therefore could not be responsible for the increase in aerobic denitrification rates with successive incubations. Such hotspots however were likely responsible for the non-linear production of  $^{15}\text{N-N}_2$  at low oxygen concentrations in the sediments kept anoxic for 55 days (Fig. 2d).

The evidence provided here supports previous reports of aerobic denitrification in permeable sediments (Rao et al., 2008; Gao et al., 2010). Furthermore, it indicates that shifts between oxic and anoxic conditions, which occur regularly in permeable sediments, stimulate aerobic denitrification. Often in culture studies, there is a lag between the onset of anoxia and the start of denitrification (Baumann et al., 1996), no such lag between anoxia and the onset of anaerobic denitrification occurs in these sediments (Fig. 1). This indicates that part of the community is primed to denitrify and likely expresses denitrification genes constitutively, a property that has been identified in other denitrifiers that thrive in microaerobic environments (Patureau et al., 1996; Miyahara et al., 2010). Chen and Strous (2013), hypothesised that when switches between oxic and anoxia occur rapidly, it is favourable to continue to use the denitrification pathway to use any overflow of electrons from aerobic respiration. The successive increases in aerobic denitrification suggest that as oxygen continues to fluctuate within the sediment, more of the sediment community continue denitrifying when oxic conditions are re-established. The dip in denitrification rates at intermediate oxygen concentrations (Fig. 3c) also supports this theory, as at this point there would be less overflow of electrons to feed into the denitrification pathway. This coordinated expression and activity of the denitrification enzymes increases fitness during rapid transitions from oxic to anoxic conditions (Bergaust et al. 2008). The ability to either enhance or “switch off” aerobic denitrification within environmental sediment samples offers intriguing possibilities for future work investigating the molecular basis of this process.

## References

- Baumann, B., Snozzi, M., Zehnder, A.J.B., and vanderMeer, J.R. (1996) Dynamics of denitrification activity of *Paracoccus denitrificans* in continuous culture during aerobic-anaerobic changes. *Journal of Bacteriology* **178**: 4367-4374.
- Billerbeck, M., Werner, U., Bosselmann, K., Walpersdorf, E., and Huettel, M. (2006a) Nutrient release from an exposed intertidal sand flat. *Marine Ecology-Progress Series* **316**: 35-51.
- Billerbeck, M., Werner, U., Polerecky, L., Walpersdorf, E., de Beer, D., and Huettel, M. (2006b) Surficial and deep pore water circulation governs spatial and temporal scales of nutrient recycling in intertidal sand flat sediment. *Marine Ecology-Progress Series* **326**: 61-76.
- Bonin, P., and Gilewicz, M. (1991) A direct demonstration of co-respiration of oxygen and nitrogen oxides by *Pseudomonas nautica* - some spectral and kinetic properties of the respiratory components *Fems Microbiology Letters* **80**: 183-188.
- Chen, F., Xia, Q., and Ju, L.K. (2003) Aerobic denitrification of *Pseudomonas aeruginosa* monitored by online NAD(P)H fluorescence. *Applied and Environmental Microbiology* **69**: 6715-6722.
- Chen, J.W., and Strous, M. (2013) Denitrification and aerobic respiration, hybrid electron transport chains and co-evolution. *Biochimica Et Biophysica Acta-Bioenergetics* **1827**: 136-144.
- Codispoti, L.A., Brandes, J.A., Christensen, J.P., Devol, A.H., Naqvi, S.W.A., Paerl, H.W., and Yoshinari, T. (2001) The oceanic fixed nitrogen and nitrous oxide budgets: Moving targets as we enter the anthropocene? *Scientia Marina* **65**: 85-105.
- Cook, P.L.M., Wenzhofer, F., Glud, R.N., Janssen, F., and Huettel, M. (2007) Benthic solute exchange and carbon mineralization in two shallow subtidal sandy sediments: Effect of advective pore-water exchange. *Limnology and Oceanography* **52**: 1943-1963.
- de Beer, D., Wenzhofer, F., Ferdelman, T.G., Boehme, S.E., Huettel, M., van Beusekom, J.E.E. et al. (2005) Transport and mineralization rates in North Sea sandy intertidal sediments, Sylt-Romo Basin, Wadden Sea. *Limnology and Oceanography* **50**: 113-127.
- Frette, L., Gejlsbjerg, B., and Westermann, P. (1997) Aerobic denitrifiers isolated from an alternating activated sludge system. *Fems Microbiology Ecology* **24**: 363-370.
- Gao, H., Schreiber, F., Collins, G., Jensen, M.M., Kostka, J.E., Lavik, G. et al. (2010) Aerobic denitrification in permeable Wadden Sea sediments. *Isme Journal* **4**: 417-426.
- Gao, H., Matyka, M., Liu, B., Khalili, A., Kostka, J.E., Collins, G. et al. (2012) Intensive and extensive nitrogen loss from intertidal permeable sediments of the Wadden Sea. *Limnology and Oceanography* **57**: 185-198.
- Huang, H.K., and Tseng, S.K. (2001) Nitrate reduction by *Citrobacter diversus* under aerobic environment. *Applied Microbiology and Biotechnology* **55**: 90-94.
- Huettel, M., Roy, H., Precht, E., and Ehrenhauss, S. (2003) Hydrodynamical impact on biogeochemical processes in aquatic sediments. *Hydrobiologia* **494**: 231-236.



Jahnke, R. (1985) A model of microenvironments in deep-sea sediments - formation and effects on porewater profiles. *Limnology and Oceanography* **30**: 956-965.

Kim, M., Jeong, S.-Y., Yoon, S.J., Cho, S.J., Kim, Y.H., Kim, M.J. et al. (2008) Aerobic Denitrification of *Pseudomonas putida* AD-21 at Different C/N Ratios. *Journal of Bioscience and Bioengineering* **106**: 498-502.

Lloyd, D., Boddy, L., and Davies, K.J.P. (1987) Persistence of bacterial denitrification capacity under aerobic condition - the rule rather than the exception. *Fems Microbiology Ecology* **45**: 185-190.

Matyka, M., Khalili, A., and Koza, Z. (2008) Tortuosity-porosity relation in porous media flow. *Physical Review E* **78**: 026306.

Miyahara, M., Kim, S.-W., Fushinobu, S., Takaki, K., Yamada, T., Watanabe, A. et al. (2010) Potential of Aerobic Denitrification by *Pseudomonas stutzeri* TR2 To Reduce Nitrous Oxide Emissions from Wastewater Treatment Plants. *Applied and Environmental Microbiology* **76**: 4619-4625.

Moir, J.W.B., and Wood, N.J. (2001) Nitrate and nitrite transport in bacteria. *Cellular and Molecular Life Sciences* **58**: 215-224.

Narsilio, G.A., Buzzi, O., Fityus, S., Yun, T.S., and Smith, D.W. (2009) Upscaling of Navier-Stokes equations in porous media: Theoretical, numerical and experimental approach. *Computers and Geotechnics* **36**: 1200-1206.

Patureau, D., Bernet, N., and Moletta, R. (1996) Effect of oxygen on denitrification in continuous chemostat culture with *Comamonas* sp SGLY2. *Journal of Industrial Microbiology* **16**: 124-128.

Patureau, D., Davison, J., Bernet, N., and Moletta, R. (1994) Denitrification under various aeration conditions in *Comamonas* sp. strain SGLY2. *Fems Microbiology Ecology* **14**: 71-78.

Patureau, D., Zumstein, E., Delgenes, J.P., and Moletta, R. (2000) Aerobic denitrifiers isolated from diverse natural and managed ecosystems. *Microbial Ecology* **39**: 145-152.

Patureau, D., Godon, J.J., Dabert, P., Bouchez, T., Bernet, N., Delgenes, J.P., and Moletta, R. (1998) *Microvirgula aerodenitrificans* gen. nov., sp. nov., a new Gram-negative bacterium exhibiting co-respiration of oxygen and nitrogen oxides up to oxygen-saturated conditions. *International Journal of Systematic Bacteriology* **48**: 775-782.

Pomowski, A., Zumft, W.G., Kroneck, P.M.H., and Einsle, O. (2011) N<sub>2</sub>O binding at a [4Cu:2S] copper-sulphur cluster in nitrous oxide reductase. *Nature* **477**: 234-U143.

Rao, A.M.F., McCarthy, M.J., Gardner, W.S., and Jahnke, R.A. (2007) Respiration and denitrification in permeable continental shelf deposits on the South Atlantic Bight: Rates of carbon and nitrogen cycling from sediment column experiments. *Continental Shelf Research* **27**: 1801-1819.

Rao, A.M.F., McCarthy, M.J., Gardner, W.S., and Jahnke, R.A. (2008) Respiration and denitrification in permeable continental shelf deposits on the South Atlantic Bight: N<sub>2</sub>: Ar and isotope pairing measurements in sediment column experiments. *Continental Shelf Research* **28**: 602-613.

Robertson, L.A., and Kuenen, J.G. (1984a) Aerobic denitrification - old wine in new bottles. *Antonie Van Leeuwenhoek Journal of Microbiology* **50**: 525-544.

Robertson, L.A., and Kuenen, J.G. (1984b) Aerobic denitrification - a controversy revived. *Archives of Microbiology* **139**: 351-354.

Robertson, L.A., and Kuenen, J.G. (1988) Heterotrophic nitrification in *Thiosphaera pantotropha* - oxygen uptake and enzyme studies. *Journal of General Microbiology* **134**: 857-863.

Robertson, L.A., Dalsgaard, T., Revsbech, N.P., and Kuenen, J.G. (1995) Confirmation of aerobic denitrification in batch cultures, using gas-chromatography and N15 mass spectrometry. *Fems Microbiology Ecology* **18**: 113-119.

Zumft, W.G. (1997) Cell biology and molecular basis of denitrification. *Microbiology and Molecular Biology Reviews* **61**: 533-616.

## Chapter VI

### High nitrous oxide emissions from eutrophied coastal sands

Hannah K. Marchant<sup>1\*</sup>, Moritz Holtappels<sup>1</sup>, Gaute Lavik<sup>1</sup>, Frank Schreiber<sup>1,2,3</sup>, Regina Vahrenhorst<sup>4</sup>,  
Marc Strous<sup>1,4</sup>, Marcel M.M. Kuypers<sup>1</sup>, Halina E. Tegetmeyer<sup>1,4</sup>

<sup>1</sup>Max Planck Institute for Marine Microbiology, Celsiusstrasse 1, 28359 Bremen, Germany

<sup>2</sup>Department of Environmental Microbiology, Eawag - Swiss Federal Institute of Aquatic Science and Technology, Dübendorf, Switzerland

<sup>3</sup>Department of Environmental Systems Sciences, Eidgenössische Technische Hochschule, Zurich, Switzerland

<sup>4</sup>Institute for Genome Research and Systems Biology, Center for Biotechnology, Bielefeld University, Universitätsstraße 27, D-33615 Bielefeld, Germany

\*Corresponding author: hmarchan@mpi-bremen.de, tel: +49421-2028630, fax: +49421-2028790

#### Author Contributions:

H.K.M, G.L., F.S., H.E.T. and M.M.M.K designed experiments, H.K.M., and F.S., performed experiments and analysed data. H.K.M. and M.H. modeled air-sea fluxes. H.E.T. performed metagenomic and transcriptomic field and lab work, R.V. processed sequencing data and H.E.T., R.V. and M.S. analysed metagenomic and transcriptomic data. H.K.M., G.L., M.S. and M.M.M.K., and H.E.T. wrote the manuscript with contributions of all co-authors

**In revision after submission to *Nature***

### **Acknowledgements**

We want to thank the crew of the Doris von Ochtum and the Otzum. P. Stief for assistance with GC measurements and E. Robertson and L. Messer for assistance with field work. Ines Kattelman and Rafael Szczepanowski assisted with DNA and RNA sequencing. Christina Ander is thanked for assistance with transcriptome data processing. This work was financially supported by the Max Planck Society, the ERC Starting Grant MASEM (to R.V. and M.S.), and a Grant from the Federal State of North Rhine-Westphalia (to H.E.T.)

Coastal oceans receive large amounts of anthropogenic fixed nitrogen (N), most of which is denitrified in the sediment before reaching the open ocean<sup>3</sup>. Although benthic denitrification can produce nitrous oxide (N<sub>2</sub>O)<sup>4</sup>, coastal sediments are currently not considered as a significant source of this potent greenhouse<sup>5</sup> and ozone-depleting gas<sup>6</sup>. Here we show that eutrophied permeable coastal sandy sediments from the world's largest tidal flat system, the Wadden Sea, release high amounts of N<sub>2</sub>O to the overlying waters and atmosphere. Combined chemical analyses, isotopic incubations, microsensors measurements and metagenomic analyses revealed that benthic denitrification is the main source of N<sub>2</sub>O, with individual steps of the denitrifying pathway being carried out by different members of the microbial community. This metabolic specialization<sup>7</sup> separates microbial N<sub>2</sub>O formation and consumption temporally and spatially, leading to increased concentrations in the porewater. Advective pore water flow subsequently transports up to 3 μmol N<sub>2</sub>O m<sup>-2</sup> h<sup>-1</sup> to the water column leading to in situ saturations of ~160%. If our results can be extrapolated to the other sandy sediments that cover most of the coastal zone<sup>8</sup>, denitrification in coastal sediments may currently contribute 10- 40 % to the global oceanic N<sub>2</sub>O emissions. Future increases in N<sub>2</sub>O emissions can be expected as anthropogenic N inputs increasingly eutrophy the coastal buffer zone.

Increasing coastal eutrophication is a result of drastic increases in fertilizer use, as well as a tripling in atmospheric deposition of fixed nitrogen<sup>9</sup> of which ~20% enters coastal seas<sup>10</sup>. Accordingly, nitrate inputs into the world's largest inter-tidal area, the Wadden Sea, have increased 8-fold since the 1930's (Fig. 1). Benthic denitrification is the main pathway for nitrate removal in coastal systems such as the Wadden Sea, removing a substantial proportion of anthropogenic inputs as dinitrogen gas (N<sub>2</sub>)<sup>11</sup>. However, the final product of denitrification is not always N<sub>2</sub>; incomplete denitrification produces N<sub>2</sub>O, which has a potential warming factor 310 times higher than carbon dioxide<sup>5</sup> and is the most important present day contributor to ozone-depletion<sup>6</sup>.

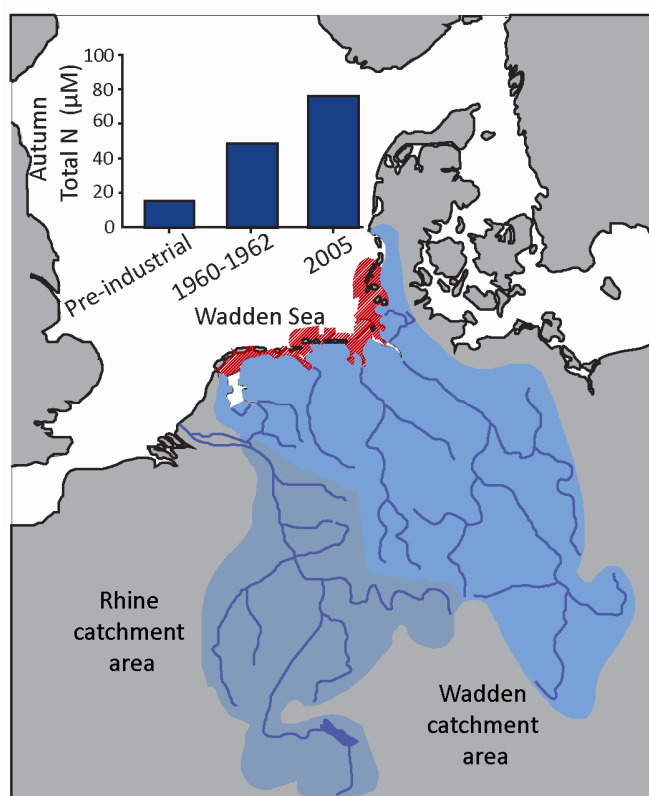


**Figure 1. The Wadden Sea catchment area and changes in water column nitrogen concentration due to industrialization.** The rivers IJssel, Elbe, Eid, Ems and Weser all discharge directly into the Wadden Sea, while nutrients from the Rhine and Meuse reach the Wadden via the continental coastal current. Increases in agriculture have led to increases of riverine TN loading resulting in an eight-fold increase in fixed N concentrations in the Wadden Sea waters during autumn<sup>1,2</sup>.

Extensive surveys of N<sub>2</sub>O saturations are available for European estuaries and open waters, although these rarely consider the processes responsible for N<sub>2</sub>O emissions<sup>12,13</sup>. N<sub>2</sub>O concentrations in marine waters generally decrease with distance from the coast, i.e. they are high in estuaries, substantial in coastal waters (on average 116 % in the German Bight) and lower in open waters (103% in the central North Sea), correlating well with N-loading. N<sub>2</sub>O formation in coastal waters is generally attributed to sedimentary denitrification in estuaries and to water column nitrification in marine systems. So far, few, water column N<sub>2</sub>O measurements exist from intertidal regions such as the Wadden Sea. Added to this, most sedimentary N<sub>2</sub>O emission studies within intertidal regions have focused on muddy sediments<sup>14,15</sup>.

Muddy, diffusion controlled marine sediments, apart from in areas heavily polluted with sewage<sup>16</sup>, are considered a sink for N<sub>2</sub>O rather than a source<sup>4</sup>. While N<sub>2</sub>O is frequently observed in the porewater of muddy sediment, it is subsequently consumed during diffusion limited transport from the production layer to the sediment surface<sup>17</sup>. In

contrast, N<sub>2</sub>O transport in permeable sandy sediment is controlled by pore water advection, which exceeds the speed of diffusion by several orders of magnitude<sup>18</sup>. Permeable sediments are also exposed to frequent oxygen fluctuations<sup>19</sup>, that cause transient accumulation of N<sub>2</sub>O in denitrifier cultures<sup>20</sup>. These oxygen fluctuations combined with high denitrification rates<sup>11</sup> make permeable sediments a likely, but so far overlooked source of N<sub>2</sub>O.

To investigate N<sub>2</sub>O emissions, we measured water column NO<sub>x</sub> (nitrate and nitrite) and N<sub>2</sub>O concentrations directly above an intertidal permeable sand flat in the Wadden Sea. Water column N<sub>2</sub>O was on average  $156 \pm 3.9$  % over-saturated and neither NO<sub>x</sub> nor N<sub>2</sub>O varied significantly with depth or tidal duration. This is the highest saturation measured so far in the North Sea, the previous highest saturation was at a station close to the Wadden Sea barrier islands, which may have been influenced by water from the region<sup>21</sup>. Based on the water column concentration of N<sub>2</sub>O we calculated a sea-air flux of  $1.10 - 1.50 \mu\text{mol m}^{-2} \text{h}^{-1}$  using two different parameterizations of air-sea gas exchange (supplementary methods).

To confirm that the source of N<sub>2</sub>O was within Wadden Sea sediments, we measured N<sub>2</sub>O concentrations at a tidal inlet. Water from the North Sea enters the Wadden Sea through inlets as the tide rises, mixing the two water bodies before water is returned to the North Sea with the outgoing tide, resulting in an average flushing time of 4 days<sup>22</sup>. Strong tidal variations in N<sub>2</sub>O over-saturation were observed (Fig. 2). Water entering the back barrier region at high tide was 3% over-saturated, in accordance with published values for the North Sea<sup>23</sup>. However at low tide, the N<sub>2</sub>O over-saturation was around 10 times higher. Similar water column changes of NO<sub>3</sub><sup>-</sup>, NO<sub>2</sub><sup>-</sup> and ammonium during tidal cycling result from pore water advection within the tidal flat sediment<sup>24</sup>. Therefore we hypothesized that high denitrification in the coarse grained permeable sediments was the source of N<sub>2</sub>O, rather than water column nitrification which would be independent of tidal currents (supplementary discussion).

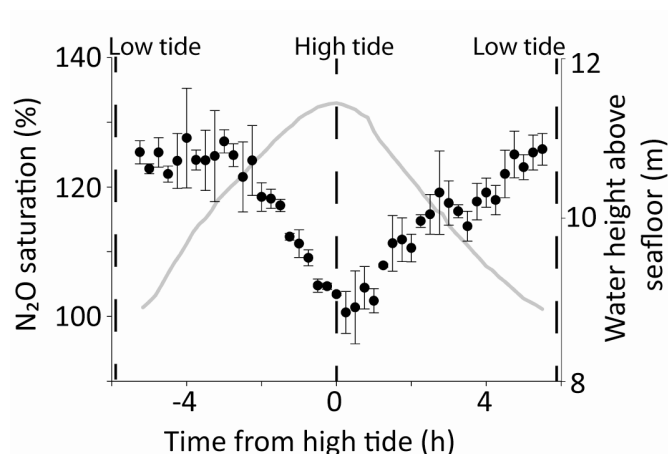


**Figure 2. Tidal changes in N<sub>2</sub>O saturation of surface waters at a tidal inlet to the Wadden Sea.** Surface water was collected over an entire tidal cycle (12 hours) at an inlet between the islands of Langeoog and Spiekeroog (53.44791 'N, 007.418310'E), and compared to air equilibrium values taking temperature and salinity into account. The tidal prism is represented by the grey line. Vertical bars represent SD (n = 3).

Sediment core incubations using <sup>15</sup>N tracers were used to investigate N<sub>2</sub>O formation from nitrification and denitrification in sediment from the intertidal flat region (supplementary methods). The incubations confirmed that N<sub>2</sub>O was formed in the sediment and that denitrification was the source rather than benthic nitrification (supplementary discussion). Previously, aerobic denitrification has been shown to be a result of transient oxygen conditions in these sediments<sup>25</sup>. This could lead to increased N<sub>2</sub>O formation during denitrification<sup>26</sup> as nitrous oxide reductase can be partially deactivated by oxygen<sup>27</sup>. Thus, we also investigated denitrification under oxic conditions.

Incubations revealed that NO<sub>2</sub><sup>-</sup> and N<sub>2</sub>O accumulated transiently in the porewater during denitrification (Figure 3a). When NO<sub>3</sub><sup>-</sup> and subsequently NO<sub>2</sub><sup>-</sup> became limiting (<10 μmol L<sup>-1</sup>), net N<sub>2</sub>O consumption occurred (Figure 3a). Under oxic conditions both N<sub>2</sub>O and N<sub>2</sub> were produced, but N<sub>2</sub> production rates were substantially lower in the oxic phase than in the anoxic phase (63 and 226 μmol N m<sup>-2</sup> h<sup>-1</sup> respectively), while N<sub>2</sub>O rates did not differ significantly (student t test, p = >0.05 df = 31). Therefore the presence of O<sub>2</sub> led to a significantly higher ratio of N<sub>2</sub>O:N<sub>2</sub> production (oxic = 4.3% and anoxic = 0.9%, student t test p < 0.01).



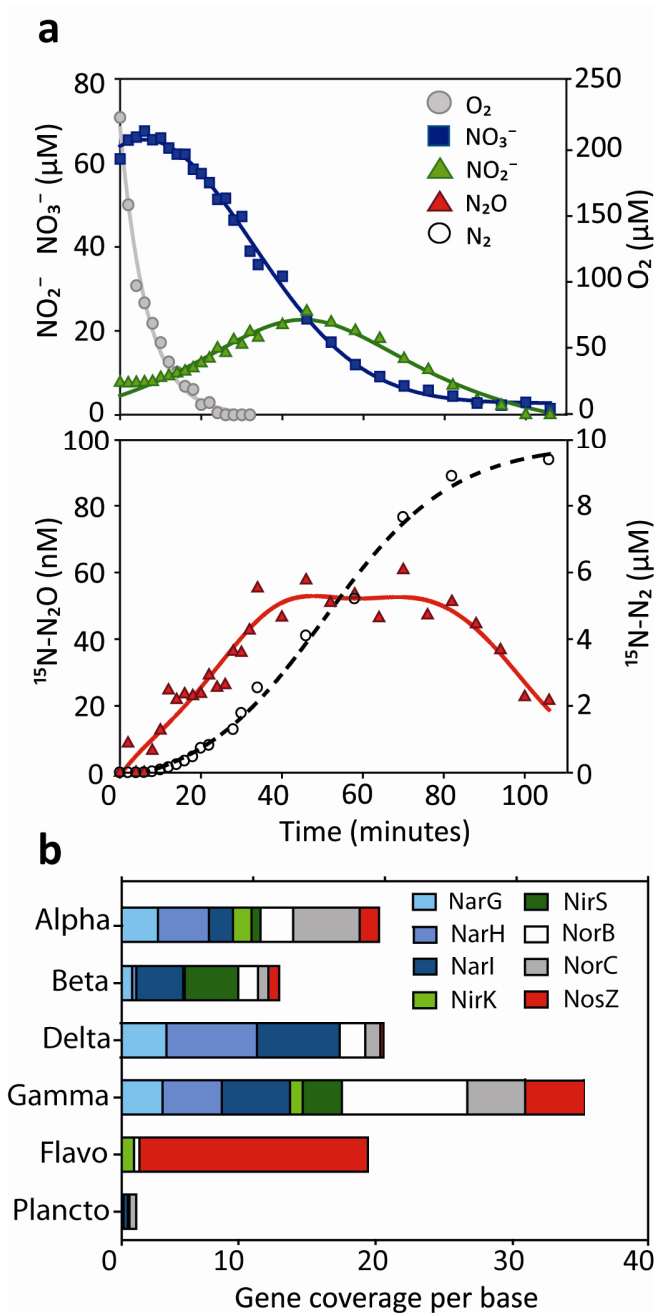


**Figure 3. Metabolic specialization of the microbial community and the resulting accumulation of denitrification intermediates.** (a) Production and consumption of denitrification intermediates in a sediment column incubation started under aerobic conditions and percolated with <sup>15</sup>NO<sub>3</sub><sup>-</sup>. Lines are model polynomial fits. (b) Uneven distribution of functional denitrification genes among the most frequently occurring taxa. “Gene coverage per base” is the sum of bases in the analyzed metagenomes that align to a functional gene, divided by the average length of this functional gene. Taxonomic abbreviations in b refer to, Alphaproteobacteria, Betaproteobacteria, Deltaproteobacteria, Gammaproteobacteria, Flavobacteriia, and Planctomycetes respectively.

These combined results show that high N<sub>2</sub>O concentrations in these sediments can occur because of mismatches between the formation and consumption of N<sub>2</sub>O in the porewater due to the presence of oxygen and nitrate. This mismatch is only resolved when oxygen is fully depleted and NO<sub>3</sub><sup>-</sup> becomes limiting as a substrate. The rates of N<sub>2</sub>O production calculated from the sediment incubations were between 1.5 – 4.3 μmol m<sup>-2</sup> h<sup>-1</sup>, which is in the same range as the areal sea-air flux determined above, and

higher than previously measured in Wadden Sea sediments (Supplementary discussion). Therefore, these rates are sufficient to provide a direct source for the calculated atmospheric flux.

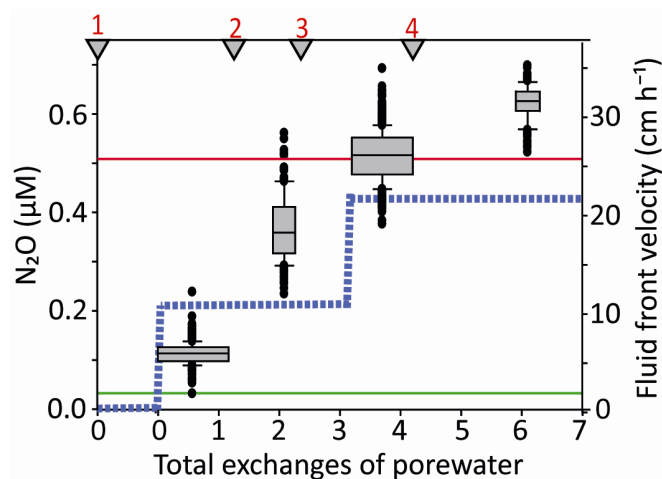


**Figure 4.** The impact of advective pore water flow on N<sub>2</sub>O concentrations in the water column. N<sub>2</sub>O concentrations were measured in the water column overlying a sediment column while aerated seawater amended with 500 µM NO<sub>3</sub><sup>-</sup> was pumped upwards from the bottom of the core at realistic flow velocities (represented by blue dashed line. Red and green lines represent *in situ* flow velocities measured previously in similar sediment<sup>19,28</sup>). The timing of N<sub>2</sub>O appearance within the sediment and subsequently the overlying water correlated with the fluid front velocity. Triangles and associated numbers represent the start of sediment profiles which took 45 minutes to complete (Supplementary fig. 3).

Advective flow in sandy sediments strongly increases transport of solutes and gases such as oxygen and nitrate to and from the water column<sup>29</sup>. We investigated how advective flow affects the N<sub>2</sub>O concentration in the porewaters and water column of a sediment core using N<sub>2</sub>O and O<sub>2</sub> microsensors. Realistic porewater advective flow (11 and 21 cm h<sup>-1</sup>) increased N<sub>2</sub>O concentrations within the sediment (Supplementary Fig. 3), as well as increasing oxygen concentrations, which as discussed previously increases the ratio of N<sub>2</sub>O:N<sub>2</sub> production. N<sub>2</sub>O formed within the sediment was subsequently transported to the overlying water (Fig. 4). Furthermore, increasing the flow velocity increased the flux of N<sub>2</sub>O to the overlying water; this is likely a result of reduced N<sub>2</sub>O consumption due to both increased oxygen concentrations and decreased residence

time of porewaters, which would reduce the time in which accumulating N<sub>2</sub>O could be consumed.

To investigate the organisms responsible for N<sub>2</sub>O formation, we performed metagenomic analyses of the sediment microbial community. Bacteroidetes and Proteobacteria were found to be the two dominant microbial phyla present (Supplementary Table 1) and alignment of metagenomic reads against sequenced genomes indicated that the Flavobacteriial class of Bacteroidetes appeared to be abundant within the sediment (Supplementary Table 2).

Functional genes of the denitrification pathway were unevenly distributed among taxonomic groups (Fig 3b). The genes for nitrate, nitrite and nitric oxide reduction (*narGHI*, *nirK*, *nirS*, *norBC*) were distributed among many different proteobacterial groups. In comparison, *nosZ* reads (the functional gene for nitrous oxide reductase) were more prevalent in the *Flavobacteriia* (odds ratio analysis:  $8.5 \pm 1.7$ ). Likewise, detected transcripts of *nirK* and *nirS* were mostly similar to Proteobacterial nitrite reductase genes, whereas most of the detected *nosZ* transcripts showed highest similarities (77-86%) to known Flavobacteriial *nosZ* genes.

To further explore why *nosZ* encoding sequences were enhanced in the Flavobacteriial community we analyzed the phylogenetic affiliations of the 175 detected *nosZ* sequences in the metagenomes (Supplementary. Fig. 4a-c). This revealed that the majority of Flavobacteriial *nosZ* genes were similar to either *Muricauda ruestringensis* (31 reads; 73-84 % similarity) or *Robiginitalea biformata* (15 reads; 74-85% similarity). *NosZ* is the only functional denitrification gene that *R. biformata* encodes<sup>30</sup>, in fact, no *nirK* or *nirS* encoding reads belonged to either *M. ruestringensis* or *R. biformata*. Taken together, these results suggest that a considerable part of the largely unknown Flavobacteriial population only possesses *nosZ*, and can switch from O<sub>2</sub> to N<sub>2</sub>O respiration if conditions become anoxic. It seems likely that such a specialization on N<sub>2</sub>O respiration results from an adaptation to recurrent production of N<sub>2</sub>O and its accumulation in Wadden Sea sediments. Our molecular results therefore indicate a metabolically specialized<sup>7</sup> denitrifying microbial community within the sediment, the

presence of which could result in a temporal decoupling of N<sub>2</sub>O production and consumption.

The Wadden Sea used to be an oligotrophic system where high concentrations of nitrate rarely accumulated in the water column (Fig. 1)<sup>1</sup>. Today, anthropogenic activity provides a large input of fixed N to the region, stimulating benthic denitrification. While much of the anthropogenic input of bioavailable N is removed by this biocatalytic filter, the supply of oxygen and nitrate to the sediment by advection still exceeds the rate of consumption<sup>11</sup>. Our combined results indicate that under these conditions N<sub>2</sub>O is formed faster than it can be reduced (Fig. 3), resulting in a constant flux to the water column (Fig. 2).

These findings have implications for our understanding of the role of permeable sediments in N<sub>2</sub>O cycling. In contrast to muddy sediments, which are a sink for N<sub>2</sub>O, we show that permeable sediments supplied with nitrate from the water column could account for a large fraction of the oceanic N<sub>2</sub>O production. Recent estimates suggest that 60% of the fixed N input from rivers and atmospheric deposition worldwide is denitrified within coastal sandy sediments (54 Tg)<sup>11</sup>. If, as our results shows 1-4% of this is lost as N<sub>2</sub>O, then permeable sediments could account for 0.54 -2.16 Tg N per year; 10 - 40 % of the global oceanic N<sub>2</sub>O source (5.4 Tg N yr<sup>-1</sup> ~ 11 Tg N yr<sup>-1</sup>)<sup>23</sup>. Permeable marine sediments cover 70% of the continental shelf worldwide<sup>8</sup> and are increasingly subject to eutrophication, therefore they can be expected to become an increasingly important source of N<sub>2</sub>O to the atmosphere.

### **Methods Summary**

Sampling was carried out at the Janssand sand flat, Wadden Sea, Germany. Sea water sampling to determine *in situ* N<sub>2</sub>O concentrations was performed directly above the sand flat and at a tidal inlet. Water samples were collected in 6 ml exetainers (LabCo) and N<sub>2</sub>O concentration was measured on a gas chromatograph with a <sup>63</sup>Ni electron capture detector (Shimadzu GC-8A). Sediment core incubations were carried out in

cores filled with sediment from the upper 5 cm of the sand flat. Prior to sampling the entire porewater volume of the core was exchanged with aerated seawater which had been amended with the appropriate <sup>15</sup>N-labelled compound. At each time point, porewater was sampled passively from the bottom of the core and concentrations of labeled N<sub>2</sub>O and N<sub>2</sub> within the exetainers were determined from a He-equilibrated headspace by gas chromatography-isotope ratio mass spectrometry (VG Optima). Microsensor depth profiles and water column measurements were carried out in a sediment core through which aerated seawater was pumped from the bottom at two fluid flow velocities (11 cm h<sup>-1</sup> and 21 cm h<sup>-1</sup>). Sediment samples for metagenomics were collected on October 24 2009 and on March 23 2010. The extracted DNA was subjected to pyrosequencing on a GS FLX Titanium platform (Roche 454). Metagenomes were analysed by MetaSAMS, MG-RAST, and an analysis pipeline developed in our group. Sediment for metatranscriptomics was collected at 6 points during tidal inundation. After mRNA enrichment, random-primed cDNA libraries were generated and subsequently sequenced using a MiSeq system (Illumina). Generated reads were submitted to DNACLUST (id 98 %) and among the representative sequences from each cluster, *nirK*, *nirS* and *nosZ* transcripts were detected using the automated validation pipeline for functional genes used for the metagenomics (see supplementary material for more detailed methods).

### **Supplementary Information is included with this manuscript**

#### **Data Submission**

The metagenome sequence data sets were submitted to the sequence read archive (<http://trace.ncbi.nlm.nih.gov/Traces/sra/>) under the bioproject PRJNA174601 (Accession: SRP015924). The four sample Accession numbers are SRS365699, SRS365698, SRS365700 and SRS365701. The metatranscriptome sequence data sets were submitted to sra under the bioproject PRJNA198659 (Accession: SRP021900). The

six sample Accession numbers are SRS417277, SRS417279, SRS417280, SRS417281, SRS417282 and SRS417283.

## References

- <sup>1</sup> J. E. E. van Beusekom, *Helgoland Marine Research* **59** (1), 45 (2005).
- <sup>2</sup> H. Postma, *Netherlands Journal of Sea Research* **3** (2), 186 (1966).
- <sup>3</sup> N. Gruber and J. N. Galloway, *Nature* **451** (7176), 293 (2008).
- <sup>4</sup> S. P. Seitzinger and C. Kroeze, *Global Biogeochem. Cycles* **12** (1), 93 (1998).
- <sup>5</sup> L. Y. Stein and Y. L. Yung, *Annu. Rev. Earth Planet. Sci.* **31**, 329 (2003).
- <sup>6</sup> A. R. Ravishankara, John S. Daniel, and Robert W. Portmann, *Science* **326** (5949), 123 (2009).
- <sup>7</sup> D. R. Johnson, F. Goldschmidt, E. E. Lilja, and M. Ackermann, *ISME J* **6** (11), 1985 (2012).
- <sup>8</sup> K. O. Emery, *AAPG Bulletin* **52** (3), 445 (1968).
- <sup>9</sup> R. A. Duce, J. LaRoche, K. Altieri, K. R. Arrigo, A. R. Baker et al., *Science* **320** (5878), 893 (2008).
- <sup>10</sup> F. Dentener, J. Drevet, J. F. Lamarque, I. Bey, B. Eickhout et al., *Glob. Biogeochem. Cycle* **20** (4) (2006).
- <sup>11</sup> H. Gao, M. Matyka, B. Liu, A. Khalili, J.E. Kostka et al., *Limnology and Oceanography* **57** (1), 185 (2012).
- <sup>12</sup> H. W. Bange, S. Rapsomanikis, and M. O. Andreae, *Global Biogeochem. Cycles* **10** (1), 197 (1996).
- <sup>13</sup> Hermann W. Bange, in *Nitrogen in the Marine Environment (2nd Edition)* (Academic Press, San Diego, 2008), pp. 51.
- <sup>14</sup> W. M. Kieskamp, L. Lohse, E. Epping, and W. Helder, *Mar. Ecol.-Prog. Ser.* **72** (1-2), 145 (1991).
- <sup>15</sup> T. Usui, I. Koike, and N. Ogura, *Estuarine, Coastal and Shelf Science* **52** (6), 769 (2001).

- <sup>16</sup> S. P. Seitzinger, M. E. Q. Pilson, and S.W. Nixon, *Science* **222** (4629), 1244 (1983).
- <sup>17</sup> R. L. Meyer, D. E. Allen, and S. Schmidt, *Mar. Chem.* **110** (1-2), 68 (2008).
- <sup>18</sup> M. Huettel, H. Roy, E. Precht, and S. Ehrenhauss, *Hydrobiologia* **494** (1-3), 231 (2003).
- <sup>19</sup> M. Billerbeck, U. Werner, K. Bosselmann, E. Walpersdorf, and M. Huettel, *Mar. Ecol.-Prog. Ser.* **316**, 35 (2006).
- <sup>20</sup> F. Schreiber, P. Wunderlin, K. M. Udert, and G. F. Wells, *Frontiers in Microbiology* **3** (2012).
- <sup>21</sup> C. S. Law and N. J. P. Owens, *Netherlands Journal of Sea Research* **25** (1-2), 65 (1990).
- <sup>22</sup> W. S. Moore, M. Beck, T. Riedel, M. Rutgers van der Loeff, O. Dellwig et al., *Geochimica et Cosmochimica Acta* **75** (21), 6535 (2011).
- <sup>23</sup> H. W. Bange, *Estuarine, Coastal and Shelf Science* **70** (3), 361 (2006).
- <sup>24</sup> M. Grunwald, O. Dellwig, C. Kohlmeier, N. Kowalski, M. Beck et al., *Journal of Sea Research* **64** (3), 199 (2010).
- <sup>25</sup> H. Gao, F. Schreiber, G. Collins, M. M. Jensen, J. E. Kostka et al., *Isme Journal* **4** (3), 417 (2010).
- <sup>26</sup> S. W. A. Naqvi, D. A. Jayakumar, P. V. Narvekar, H. Naik, V. V. S. S. Sarma et al., *Nature* **408** (6810), 346 (2000).
- <sup>27</sup> L. Dendooven and J. M. Anderson, *Soil Biology and Biochemistry* **26** (11), 1501 (1994).
- <sup>28</sup> E. Precht and M. Huettel, *Journal of Sea Research* **51** (2), 93 (2004).
- <sup>29</sup> D. de Beer, F. Wenzhofer, T. G. Ferdelman, S. E. Boehme, M. Huettel et al., *Limnology and Oceanography* **50** (1), 113 (2005).
- <sup>30</sup> H. Oh, S. J. Giovannoni, K. Lee, S. Ferriera, J. Johnson et al., *Journal of Bacteriology* **191** (22), 7144 (2009).

## Supplementary Material

### This file includes:

- 1). Supplementary Methods
- 2). Supplementary Discussion
- 3). Supplementary Figures and Legends
- 4). Supplementary Tables

### 1) Supplementary Methods

#### *Sampling site*

Sampling was carried out at the Janssand sand flat (13 km<sup>2</sup>), which is located in the back barrier area of Spiekeroog Island in the East Frisian Wadden Sea, Germany. The sampling site (53.73515 'N, 007.69913'E) is on the northeastern margin of the flat around 80m upslope from the mean low water line. The flat consists of well sorted silicate sand, with a mean grain size of 176µm, permeability of  $7.2 - 9.5 \times 10^{-12}$ , and porosity of 35% (upper 15cm of sediment)<sup>1,2</sup>. The flat is covered by 1.5 – 2 m of seawater during inundation for 6-8 h and is exposed to air for 6-8 h during low tide, dependent on tidal range.

#### *in situ N<sub>2</sub>O measurements*

*Tidal flat* - On March 21 2011 N<sub>2</sub>O concentrations were determined over an entire tidal inundation period in the water directly above the sand flat. A sampling platform was installed at a height of 120 cm above the sediment surface so as not to disturb pore water advection and samples were collected in triplicate from four water depths as long as the water was deep enough (5, 17, 47, and 80 cm above sediment surface) and stored in 6 ml exetainers (LabCo) prefilled with 200 µl HgCl<sub>2</sub>. A 3ml helium headspace was added to the samples and they were left to equilibrate overnight. The N<sub>2</sub>O concentration was measured by injecting 0.25 ml of headspace into a gas chromatograph with a <sup>63</sup>Ni electron capture detector (Shimadzu GC-8A).



*Tidal inlet* - On May 31 2011 N<sub>2</sub>O concentrations were determined over an entire tidal cycle in surface water samples taken from the main tidal inlet between the islands of Langeoog and Spiekeroog. Samples were collected using the ICBM ship the “Otzum” at 53.44791 'N, 007.418310'E. Whereby surface water collected in a sampling container was subsampled in triplicates into 6ml exetainers (LabCo). N<sub>2</sub>O concentrations were determined as before, and additional data including tidal height was provided by Thomas Badewien from the long term time series station at 53.450100'N, 007.401630'E

#### *Flux calculations*

The air-sea flux of N<sub>2</sub>O was calculated according to Wanninkhof<sup>3</sup> from the product of transfer velocity ( $k$ ) and the difference between N<sub>2</sub>O concentrations measured in the bulk water ( $C_w$ ) and calculated for the air-water interface ( $C_0$ ).

$$F = k(C_w - C_0) \quad (1)$$

The transfer velocity was derived using two parameterizations , referred to hereafter as W92<sup>4</sup> and McG01<sup>5</sup>:

$$k = 0.39 \langle U_{10} \rangle^2 (Sc / 660)^{-0.5} \quad (2)$$

$$k = 3.3 + 0.026 U_{10}^3 (Sc / 660)^{-0.5} \quad (3)$$

The average wind speed at 10m height ( $U_{10}$ ) was set to 9.2 ms<sup>-1</sup> ( $U_{10}$  for European shelves<sup>6</sup>) and the Schmidt number ( $Sc$ ) for N<sub>2</sub>O at in-situ temperatures (6°C) and salinities (31 PSU) was applied<sup>4</sup>.  $C_0$  was calculated from the solubility of N<sub>2</sub>O under in-situ conditions and atmospheric N<sub>2</sub>O concentration of 323 ppbv (IPCC 2007<sup>7</sup>, extrapolated to 2011).

Daily export of N<sub>2</sub>O from the back barrier region to the German Bight was calculated from the difference in concentration between water entering and leaving the tidal flat, using a residual transport of 2.8 x 10<sup>10</sup> L day<sup>-1</sup> (8), export was compared to daily air-sea exchange for a daily inundation region of 44 km<sup>2</sup> (9,10) (supplementary discussion).

### *Sediment Core Incubations*

Pooled and homogenized sediment from the upper 5 cm of the sand flat was used in sediment column incubations. Columns were constructed of PVC tubing (height 22cm, I.D. 10.3 cm) and sealed with rubber stoppers. Inflow and outflow ports were fitted with 2 way valves. The internal face of each rubber stopper was milled with radial grooves to create radially distributed pressure and flow through the columns. To prevent sediment from filling the grooves and obstructing flow, they were covered with a fine mesh filter (500 microns, Hydra-BIOS, Germany). Incubations were carried out using a version of the isotope pairing technique<sup>11</sup> modified to simulate advective flows in permeable sediments. Briefly, the entire porewater volume of the column was exchanged with site seawater amended with <sup>15</sup>NO<sub>3</sub>, at various concentrations (15, 50, 100 or 500 μM) and thereafter subsamples of porewater were collected by opening the bottom valve and letting porewater flow directly into 3 ml exetainers prefilled with 100 μl saturated HgCl<sub>2</sub>. 1.5 ml of porewater was discarded initially at each time point to flush the tubing between the column and the sediment (corresponding to 135 ml per incubation, less than half the porewater contained per core). Sampled porewater was replaced passively from a funnel containing unamended sea water. The oxygen concentration of the porewater at each time point was determined in the exetainer immediately using an O<sub>2</sub> microsensor<sup>12</sup>. Concentrations of labeled N<sub>2</sub>O and N<sub>2</sub> within He-equilibrated headspace in the exetainers was determined by gas chromatography-isotope ratio mass spectrometry (GC-IRMS; VG Optima, Manchester, UK<sup>13</sup>). Nitrite and nitrate were determined using a commercial chemiluminescence NO<sub>x</sub> analyzer after reduction to NO<sup>14</sup>.

### *Rate Determinations*

Denitrification and N<sub>2</sub>O production rates were determined from excess production of <sup>29</sup>N<sub>2</sub> and <sup>30</sup>N<sub>2</sub> or <sup>45</sup>N<sub>2</sub>O and <sup>46</sup>N<sub>2</sub>O respectively according to Nielsen<sup>11</sup>. D<sub>tot</sub> was used for final N-loss determinations<sup>15</sup>.

To calculate areal rates, volumetric rates were integrated to 5cm sediment depth, as previous studies have indicated that at least the upper 5cm of the sediment at the study site are affected by “skin circulation”<sup>1</sup>. In this zone, surficial pore water circulation leads to short residence times of porewater on scales of minutes to hours due to advective transport<sup>16,1</sup>.

#### *Microsensor Incubations*

The dynamics of N<sub>2</sub>O and O<sub>2</sub> were investigated with microsensors within a column covered with a 5cm lense of seawater (I.D. 5.4, sediment height 10cm, total height 20 cm). The column was allowed to become anoxic, after which aerated seawater (amended with 500 μM NO<sub>3</sub><sup>-</sup>) was pumped from the bottom of the core at varying fluid flow velocities (11 cm h<sup>-1</sup> and 21 cm h<sup>-1</sup>). Once the fluid front went through the entire sediment core, repeated porewater profiles in the top 22 mm of the sediment and water column were carried out with N<sub>2</sub>O and O<sub>2</sub> microsensors, constructed as previously described<sup>12,17,18</sup>.

#### *Metagenomics*

*Sediment sampling* - Sediment was collected from the upper Janssand sand flat (53.73519 'N, 007.69914'E) at low tide with a sterile spoon. One sample was collected on October 24 2009 (0-5 cm depth), and three samples on March 23 2010 (0-2cm depth). To assess small scale differences, the three March samples were taken from locations approximately 3 m apart. To analyze sequencing bias, two of the three March samples were pooled, and the pool was divided into two samples, named Mar10/1a and Mar10/1b, to be sequenced in separate sequencing runs. Sediment samples were stored at -20°C in 50ml falcon tubes.

*DNA extraction* - Total DNA extraction from sediment samples was done according to Zhou et al<sup>19</sup>. Briefly, to approx. 10 g (approx. 6 ml) of thawed sediment DNA extraction buffer (100mM Tris-HCl, 100mM Na-EDTA, 100mM Na<sub>3</sub>PO<sub>4</sub>, 1.5M NaCl, 1 % [w/v] CTAB,

pH 8.0) was added to a total volume of 20 ml. Lysozyme was added to a final concentration (f.c.) of 3 mg/ml, followed by incubation at 37°C (water bath) for 30min, addition of Proteinase K (f.c. 10mg/ml), and further incubation at 37°C over night. Then, SDS was added (f.c. 1 %), followed by incubation at 65°C for 2 h with gentle end over end inversion from time to time. The sample was then centrifuged at room temperature (RT) for 10 min at 4500 x g. Chloroform extraction of the supernatant was performed three times by adding an equal volume of a chloroform-isoamyl alcohol mixture (24:1), vigorous shaking of the vials by hand for approx. 2 min and centrifugation for 15 min at 4500 x g. DNA was precipitated from the upper phase by adding 0.6 vol of isopropanol and incubation at RT for 1 h. The DNA was pelleted by centrifugation at 4°C for 40 min at 4500 x g. The pellet was washed twice with ice cold 75 % ethanol, air dried and re-suspended in sterile H<sub>2</sub>O. An equal volume of 2x RNase buffer (100mM Tris-HCL, 2mM EDTA, pH 7.5) was added, and RNA was removed by addition of RNase A/T1 Mix (Fermentas, Germany) and incubation at 37°C for 30 min. The RNase treated DNA extracts were purified via ion exchange chromatography (NucleoBond AXG 20, Macherey Nagel, Germany), and DNA integrity was verified via agarose gel electrophoresis.

*Pyrosequencing (454)* - 500ng of purified DNA per sample were used for the preparation of sequencing libraries according to the “Rapid Library Preparation Method Manual” (October 2009/Rev. January 2010) provided by Roche. Two GS FLX Titanium sequencing runs were performed with each of the four libraries loaded on half a sequencing picotiterplate. Samples Oct09 and Mar10/1a were sequenced in the same run and sample Mar10/1b was sequenced together with sample Mar10/2.

The four sequence data sets were submitted to the sequence read archive (<http://trace.ncbi.nlm.nih.gov/Traces/sra/>) under the bioproject PRJNA174601 (Accession: SRP015924). The sample Accession numbers are SRS365699, SRS365698, SRS365700 and SRS365701. Results are summarized in Supplementary Table 4.

*Data analysis* - The sequence data sets were pre-processed by removing identical reads via a CD-hit based algorithm<sup>20,21</sup>. Metagenomes were analysed by MetaSAMS (<http://metasams.cebitec.uni-bielefeld.de>), MG-RAST<sup>22</sup> and via an analysis pipeline that was developed in our group.

*Taxonomy analysis* - For taxonomy analysis, a reference database was generated by selecting a sequence subset of universally distributed protein orthologs from the FIGfam data base<sup>23</sup> (<ftp://ftp.theseed.org/FIGfams/>, Release 12). FIGfams were selected which contained ribosomal protein sequences universally distributed among bacteria and archaea/eukaryota (15 small ribosomal subunit proteins and 15 large rSU proteins), as well as FIGfams containing at least 50 archaeal sequences or at least 850 bacterial sequences (these figures refer to the number of genomes that had been sequenced at the time of releasing FIGfam 12 [Sept 1<sup>st</sup> 2009]: approx. 1000 bacterial and 60 archaeal genomes; the selected FIGfams should potentially contain around 85% of the orthologues from these sequenced genomes, to ensure a high enough degree of universality in the distribution of the selected FIGfam orthologues among microorganisms). For Eukaryota, FIGfams containing at least 30 eukaryotic sequences were selected for the collection (30 complete eukaryotic genomes in Sept 2009 according to NCBI Genome Project database). To reduce taxonomic redundancy, based on the taxonomic origin of the sequences in the selected FIGfams, if in a given FIGfam several sequences of strains/variants of the same taxonomic species were present, only the sequence originating from the strain/variant that was present in the greatest number of all selected FIGfams was kept (the total number of sequences of a particular strain/variant in all selected FIGfams was not used as a selection criteria, but rather its presence in the greatest number of FIGfams). The resulting sequence collection contained 65 001 sequences. A blastx search (E-value cutoff  $1e^{-10}$ ) with the metagenomic reads against the generated protein orthologues database was performed, and the reads with a hit were assigned to the respective taxonomic class of the top hit FIGfam sequence. Results are summarized in Supplementary Table. 1. Furthermore, all reads were subjected to a blastn search against the NCBI bacterial

genomes database (downloaded Feb. 2012, e-value cutoff 1e-10, restricted to one hit per read). For all hits in a genome of the Flavobacteriia, the average alignment %identity per base was calculated as follows: [SUM(hit alignment length of a hit \* alignment %id of this hit)]/[SUM(alignment lengths of all hits in the genome)]. Results are summarized in Supplementary Table 2.

*Functional gene detection* - For the detection of functional genes, a collection of selected protein sequences (17 to 294 sequences per collection) for each functional gene of interest was used for a tblastn search against the metagenomic reads (E-value cutoff 0.001). For an automated validation procedure of the reads with a hit in this tblastn search, a gene validation database was set up, by extracting protein sequences from all prokaryotic sequenced genomes available at NCBI (FTP://ftp.ncbi.nlm.nih.gov/genomes/Bacteria), file: all.gbk.tar.gz, downloaded on: 08. Oct. 2010) and removing identical sequences using the uclust software<sup>24</sup> (version 3.0). Additionally, available (putative) protein sequences of the functional genes of interest from uncultured prokaryotes were retrieved from Uniprot and from FunGene (<http://www.uniprot.org> , <http://fungene.cme.msu.edu/index.spr> , download on: 24. Feb. 2011). To decrease redundancy, the retrieved sequences were clustered at 90% identity using the uclust software<sup>24</sup>, and only the seed sequences of the resulting clusters were marked as environmental and added to the gene validation database. All of the protein sequences used for the initial tblastn search of the metagenomes that were hit by a metagenomic sequence, were tagged as functional protein of interest and temporarily to the validation database. The reads with a hit in the initial tblastn search were validated by translating them into the respective amino acid sequences and performing a blastp search (no E-value cutoff) against the validation database including the tagged sequences. Based on prior manual evaluation, a read was considered as “validated” if in this blastp search a hit with a tagged sequence (of the expected functional gene) was among the first 50 hits for this read. Additionally, reads retrieved in the functional genes search of the MG-RAST analysis platform<sup>22</sup>

(<http://metagenomics.anl.gov/> search reference database: M5NR) that were not detected by the automated validation, were added to the collection of the automatically validated reads. All reads in this collection were then manually curated to remove “false positives” of the automatic validation procedure and the MG-RAST analysis. The automated validation procedure yielded reads that were not detected by the search via MG-RAST, and vice versa.

Sequencing coverage per base of a functional gene was calculated as follows: From the reads validated for each gene, first, the sum was calculated of all read bases aligning to a known functional gene (database sequence). Second, of all gene sequences in the database to which a read (partially) aligned, the average gene length was calculated. To obtain gene coverage per base values, the sum of the aligned read bases was divided by the calculated average gene length.

To detect potential *nosZ* primer binding sites in the metagenomes, all validated *nosZ* encoding reads were subjected to a blastn search vs. the currently published *nosZ* primer sequences<sup>25,26</sup>. A potential binding site for a primer was rated as “reliable” if at least the last 5 bases of the 3' end matched, if there were not more than 2 mismatches in the entire primer sequence in total, with not more than one mismatch in a row (except for the last two bases at the 5' end), and if no altering of the melting temperature was to be expected (see supplementary discussion)

*Functional gene analysis* - To investigate the phylogenetic identity of *nirK*, *nirS*, and *nosZ* a blastn search<sup>27</sup> was run with default parameters using the validated *nirK*, *nirS*, and *nosZ* encoding reads as query. The database was the current nucleotide collection (nr/nt) database obtained from NCBI (Nov. 2013). For the generation of a phylogenetic tree, *nirK*, *nirS*, and *nosZ* genes for known taxa were chosen if they were among the top 10 hits of a read, and if the e-value was  $\leq 0.0005$ . Otherwise the top hit sequence (clone/unknown taxon) was selected. The selected reference *nirK*, *nirS*, and *nosZ* sequences, and the selected outgroup sequences for the three phylogenetic trees were

aligned with Muscle<sup>28</sup>. The trees were generated with FastTree<sup>29</sup> and drawn using Dendroscope<sup>30</sup>

Of the total 21 validated *nirK* encoding metagenomic reads, 16 could be aligned via blastn to a reference sequence with an e-value of at least 0.0003. Five reads showed significant similarity to database *NirK* sequences on amino acid sequence level, but no significant hit in a *nirK* (or other nitrite reductase) DNA sequence was obtained. Of the total 55 validated *nirS* encoding metagenomic reads, all could be aligned to a reference sequence with an e-value of at least  $5e^{-11}$ . For 30 reads the e-value was  $< e^{-50}$ , and for 15 reads the e-value was  $< e^{-88}$ . Of the total 175 validated *nosZ* encoding metagenomic reads, 172 could be aligned to a reference sequence with an e-value of at least 0.0005. For 141 reads the e-value was  $\leq e^{-29}$ , for 104 reads the e-value was  $< e^{-49}$ , and for 49 reads the e-value was  $< e^{-79}$ . Three reads showed significant similarity to database *NosZ* sequences on amino acid sequence level, or contained a conserved *NosZ* domain, but no significant hit in a *nosZ* DNA sequence was obtained.

For each season an odds ratio analysis was carried out to determine whether *nosZ* was distributed evenly within the *Flavobacteriia* when compared to all denitrification reads within the Proteobacteria using the following equation:

$$\frac{(\text{number of } \textit{Flavobacteriia} \textit{ nosZ reads} / \text{number of all other denitrifying reads in the } \textit{Flavobacteriia})}{(\text{number Proteobacteria } \textit{nosZ reads} / \text{number of all other denitrifying reads in the Proteobacteria})} \quad (4)$$

### *Metatranscriptomics*

*Sediment sampling-* Sediment was collected from the upper Janssand sand flat (53.73519 'N, 007.69914'E), on March 21<sup>st</sup> 2011, at low tide with a sterile spoon, during inundation with a sediment scoop. Collected sediment was immediately immersed in three volumes of RNA preservation solution (LifeGuard<sup>TM</sup> Soil Preservation Solution, MoBio), and stored at 4°C until RNA extraction. Sampling time points were 06:50 (low tide), 08:50 (late low tide), 10:50 (rising tide), 12:50 (high tide), 14:50 (falling tide) and 16:50 (early low tide).



*RNA extraction* - RNA was extracted using TRI Reagent solution (Ambion). Briefly, RNA preservation solution was removed after 10 min centrifugation, 5 volumes of TRI Reagent solution were added, and 1 volume sterile glass beads (0.1 mm diameter). Cells were lysed by bead beating for 45 sec at 6.5 m/s, followed by 5 min incubation at RT and 10 min centrifugation at 4500 x g and 4°C. From the supernatant, RNA was extracted by adding 200 µl Chloroform per 1 ml of added TRI reagent, vigorous shaking, incubation at RT for 10 min and centrifugation at 12000 x g and 4°C for 15 min. The upper phase was transferred to a fresh tube, and RNA was precipitated on ice for 15 min after adding 500µl of ice cold isopropanol per 1 ml of TRI reagent. Pelleted RNA was washed twice with 75% Ethanol, the pellets were air dried and re-dissolved in TE buffer. rRNA was partially depleted with the MICROBExpress™ Bacterial mRNA Enrichment Kit (Ambion).

*Illumina sequencing* - Six random-primed cDNA libraries were generated (by Vertis Biotechnologie AG, Freising, Germany) for illumina sequencing, one for each sampling time point. For each library enriched mRNA resulting from 2-3 ml sediment sample was used. Briefly, RNA was fragmented by sonication, random primed cDNA was generated, barcoded TruSeq sequencing adapters were ligated to the cDNA fragments, and the library was PCR amplified using a high fidelity DNA polymerase. For sequencing, library fragments of size range 300-550bp were eluted from a preparative agarose gel. The cDNA libraries were sequenced on a MiSeq instrument (2x150 bases paired end sequencing). The sequence data sets were submitted to the sequence read archive (<http://trace.ncbi.nlm.nih.gov/Traces/sra/>) under the bioproject [PRJNA198659](https://www.ncbi.nlm.nih.gov/bioproject/PRJNA198659) ([Accession: SRP021900](https://www.ncbi.nlm.nih.gov/bioproject/PRJNA198659)). The sample Accession numbers are SRS417277, SRS417279, SRS417280, SRS417281, SRS417282 and SRS417283. Results are summarized in Supplementary Table 5.

*Data analysis* - The generated illumina reads were merged if possible, and all reads passing trimming and quality filtering were submitted to DNACLUST<sup>31</sup> (<http://sourceforge.net/projects/dnaclust/> ; id 98%). To detect transcripts of functional

genes, the cluster representatives were submitted to the detection and automated validation pipeline of functional genes used for the metagenome analysis.

## 2) Supplementary Discussion

### *The source and fate of water column N<sub>2</sub>O*

We observed high saturations of N<sub>2</sub>O in the water column above the tidal flat, as well as changes in water column N<sub>2</sub>O saturation at a tidal inlet, which correlated with the tide. We hypothesized that the source of N<sub>2</sub>O was within the coarse grained permeable sediment in the backbarrier region, rather than from water column nitrification, which is often cited as the major source of N<sub>2</sub>O in coastal waters<sup>32</sup>. The discrepancy in N<sub>2</sub>O saturation between water driven onto the flats compared to water leaving the flat (ca. 30 %) provides no evidence for water column nitrification as there are no indicators that this process would vary to any extent between the two zones.

Daily export of N<sub>2</sub>O from the back barrier region to the German Bight was calculated as 84 M day<sup>-1</sup>, whereas daily air-sea exchange for the same area was in the range of 1162 - 2302 M day<sup>-1</sup>. Therefore most of the N<sub>2</sub>O present in the water column in the back barrier region is lost to the atmosphere in the same zone, rather than being exported in the water column to the German Bight.

### *Benthic Nitrification as a potential source of N<sub>2</sub>O*

Benthic nitrification was not observed to be an important source of N<sub>2</sub>O within the sandy sediments of the Wadden Sea. Low rates of N<sub>2</sub>O production are a side product of ammonia oxidation under well oxygenated conditions, with the relative amount produced increasing as oxygen decreases<sup>33</sup>, therefore the changing oxygen conditions in permeable sediments appear to be suitable conditions under which N<sub>2</sub>O may be formed by nitrifiers.

Application of the isotope pairing technique calculations<sup>11</sup> when using incubations amended with <sup>15</sup>NO<sub>3</sub><sup>-</sup> can indicate whether nitrification is a significant process. If nitrification would be significant source, the production of <sup>14</sup>NO<sub>3</sub><sup>-</sup> from <sup>14</sup>NH<sub>4</sub><sup>+</sup> would

dilute the NO<sub>3</sub><sup>-</sup> pool, increasing the ratio of <sup>14/15</sup>NO<sub>3</sub><sup>-</sup> and causing more <sup>29</sup>N<sub>2</sub> production than expected. As such, in the oxic phase of <sup>15</sup>NO<sub>3</sub><sup>-</sup> incubations, the ratio of <sup>29/30</sup>N<sub>2</sub> production was compared to the initial ratio of <sup>14/15</sup>NO<sub>3</sub><sup>-</sup> and gave no indication that nitrification is a significant process in these sediments

To further investigate the possible contribution of nitrification to N<sub>2</sub>O production sediments were incubated with <sup>15</sup>NH<sub>4</sub><sup>+</sup> and <sup>14</sup>NO<sub>2</sub>. These incubations were repeated in October 2011, March, May and July 2012 to ensure that no seasonal changes occurred. Ammonia oxidation rates were low and constant throughout the year (0.22 ± 0.02 mmol N m<sup>3</sup> h<sup>-1</sup>), however, N<sub>2</sub>O formation was always below detection limit.

Metagenomic results supported the finding that ammonia oxidation rates were low. No evidence for bacterial or archaeal *amo* (ammonia monooxygenase, the common marker gene for ammonia oxidizers) was found, neither in 16S or functional genes or in the metagenome or metatranscriptome. Most likely these organisms were present but were below the detection limit of the metagenomic approaches. Still, the lack of detection is consistent with the low ammonia oxidation rates measured experimentally This points to a low abundance of ammonia oxidizers in the oxygenated layers of the Janssand sediment further indicating that ammonia oxidation does not play a significant role in N<sub>2</sub>O formation in the sediment.

#### *Comparison of the incubation method to other measurements from the study site*

The average anaerobic denitrification rates reported here 226 μmol N m<sup>-2</sup> h<sup>-1</sup> (using a modified version of the percolation method) are similar to those reported from both slurry incubations in gas tight bags and whole core percolations from the same study site<sup>34,15</sup> (207 μmol N m<sup>-2</sup> h<sup>-1</sup>, 169-238 μmol N m<sup>-2</sup> h<sup>-1</sup> respectively). Furthermore oxygen consumption rates which were on average 14 mmol m<sup>-2</sup> h<sup>-1</sup>, are similar to those measured *in situ* with microsensors<sup>2</sup> (2-15 m<sup>-2</sup> h<sup>-1</sup>) . Therefore we incubation method used appears to be a good proxy for *in situ* conditions while allowing high resolution sampling.

*Comparison to other N<sub>2</sub>O emission rates from the Wadden Sea.*

The N<sub>2</sub>O production rate that we measured within the sediment (1.5 – 4.3 μmol N m<sup>-2</sup> h<sup>-1</sup>) is above the upper range of previously reported rates from incubations in a similar sandy sediment taken from the Western Wadden Sea where, for the majority of the year effluxes were below 0.1 μmol N<sub>2</sub>O m<sup>-2</sup> h<sup>-1</sup> or were negative, however all previous incubations were carried out under diffusive conditions<sup>35</sup>. Therefore we can conclude that they underestimated the actual flux.

In addition to calculating sediment fluxes, we calculated air-sea fluxes according to two models. Extrapolating these fluxes (1.1 and 1.5 μmol N m<sup>-2</sup> h<sup>-1</sup>) to the entire relevant area of the Wadden Sea (Supplementary table 3) adds at least an additional 10% to the total atmospheric N<sub>2</sub>O flux from the North Sea (which is attributed exclusively to water column nitrification), although the Wadden Sea makes up only 2.6% of the North Sea.

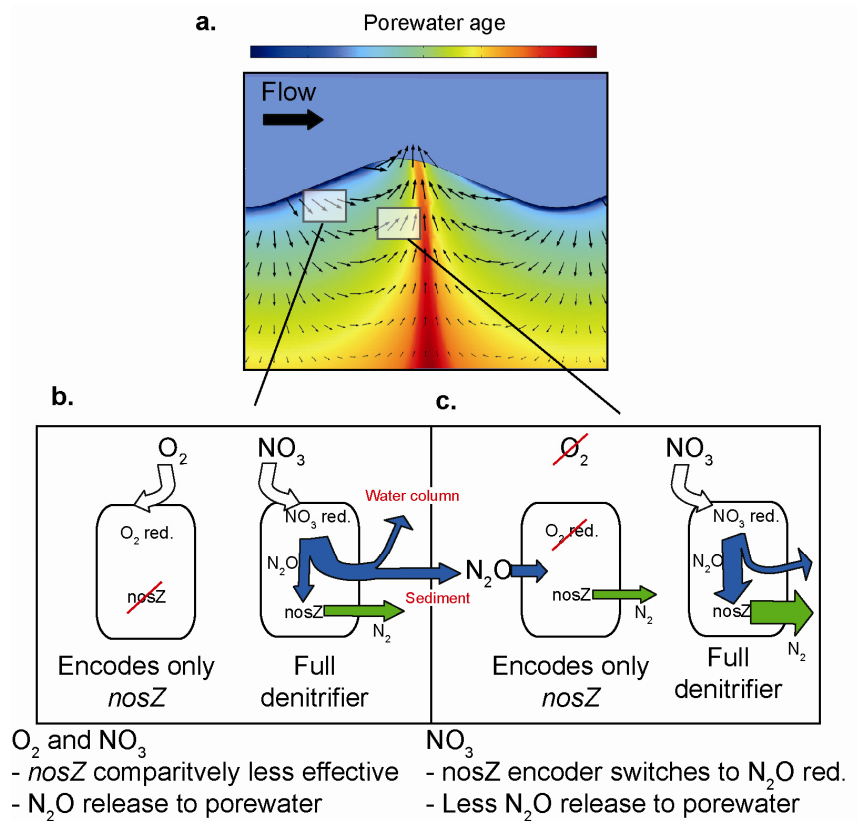
*Novel nosZ gene sequences in the metagenomes*

In 41 of 74 *nosZ* metagenome reads mapping to regions of known *nosZ* primer binding sites, no primer binding sites for reliable amplification were detected, indicating that novel *nosZ* genes are present in the sediment, that would have remained undetected in a PCR based tag sequencing approach, as was recently addressed by Jones et al.<sup>26</sup>.

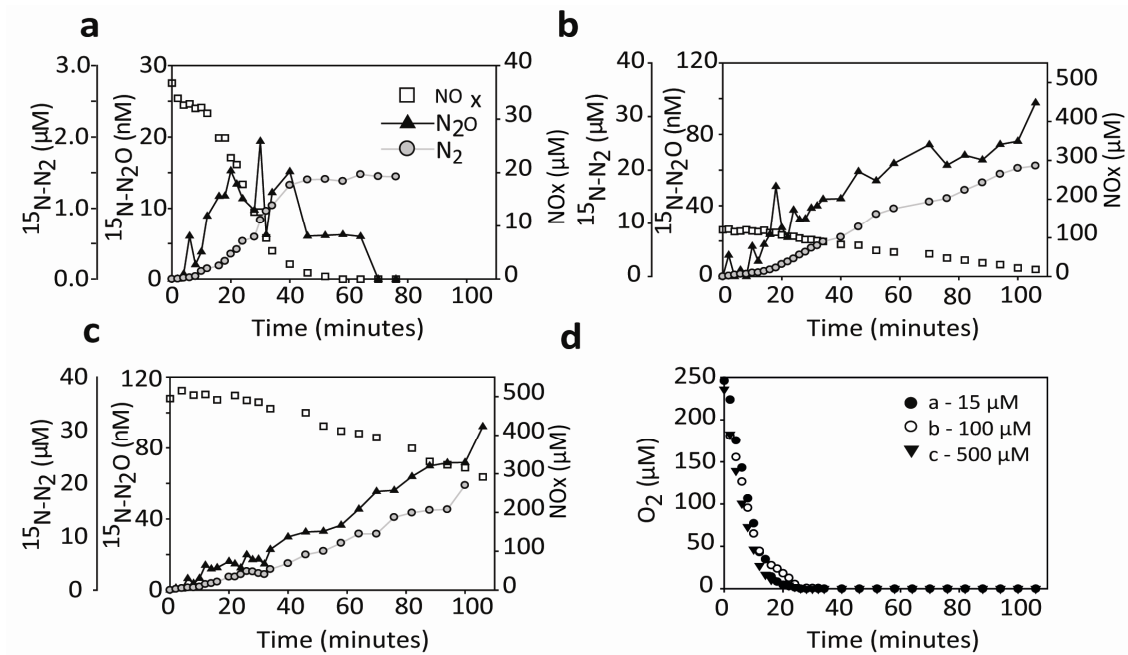
*nosZ reads in the transcriptome*

In each transcriptome data set, except for the high tide sampling point, *nosZ* transcripts were detected.

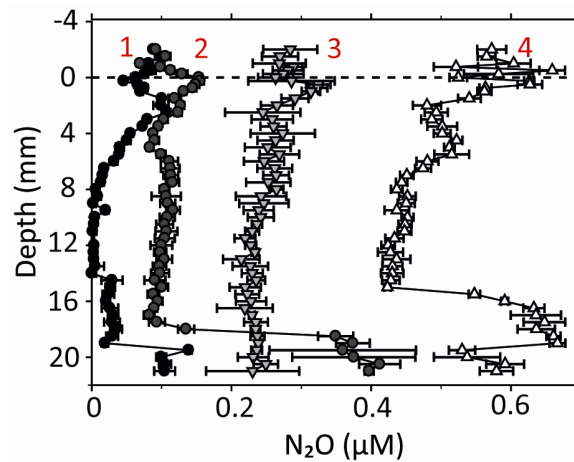
## 3) Supplementary Figures and Legends



**Supplementary Figure 1. Schematic of N<sub>2</sub>O production and emission within permeable sediments.** a) Bottom water flow over rippled sediment topography causes advective transport of water into permeable sediments at velocities more than 3 orders of magnitude higher than diffusion, this supplies both nitrate and oxygen to the sediment down to depths of 5-6 cm (b) Within the sediment, denitrification occurs under oxic conditions, however as N<sub>2</sub>O reductase is more sensitive to oxygen than other denitrification enzymes up to 4% of total nitrate reduction stalls at N<sub>2</sub>O and it not reduced further to N<sub>2</sub>, b) Some porewater travels along shorter advective paths and is flushed out of the sediment, releasing N<sub>2</sub>O to the water column. On longer advection paths oxygen is entirely consumed and the sediment becomes anoxic. Here, a specialized pool of bacteria is able to subsist by the excess respiring N<sub>2</sub>O, however net consumption of N<sub>2</sub>O only occurs when nitrate becomes limiting, in many cases the porewater is returned to the overlying water before this happens, leading to net N<sub>2</sub>O effluxes. Comparatively



**Supplementary Figure 2.** <sup>15</sup>N-N<sub>2</sub>O, <sup>15</sup>N-N<sub>2</sub> and NO<sub>x</sub> concentrations over time in sediment core incubations which were started under oxic conditions with different initial <sup>15</sup>NO<sub>x</sub> concentrations of (a) 15 μM (b) 100 μM and (c) 500 μM. (d) shows the corresponding oxygen concentrations. Note that the scale in panel a differs from b and c. N<sub>2</sub>O accumulation rates did not correlate with the initial concentration of added <sup>15</sup>NO<sub>3</sub><sup>-</sup> (one way anova, p = > 0.05, df = 16)

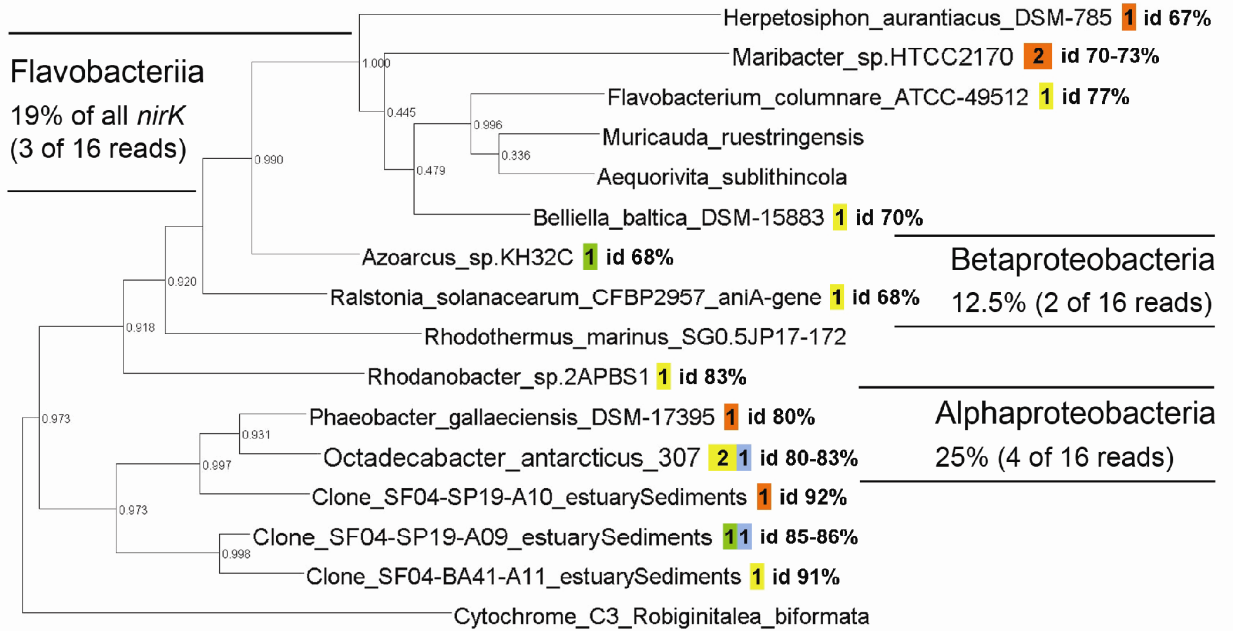


**Supplementary Figure 3.** Depth profiles of N<sub>2</sub>O concentrations within the sediment measured with microsensors under realistic flow velocities, N<sub>2</sub>O concentrations in the overlying water between the profiles are shown in Fig 4. of the main text. The initial profile was carried out while the core was anoxic and subsequent profiles took place while aerated seawater (amended with 500 μM NO<sub>3</sub><sup>-</sup>) was pumped upwards from the bottom of the core. Fluid velocity in the core was 11 cm h<sup>-1</sup> during profile 1 and 2 and 21 cm h<sup>-1</sup> in profile 3 and 4. Therefore each subsequent profile represents a condition in which nitrate supply was increased. See Fig.2 Main Text for exact timing of sediment profiles.

a.

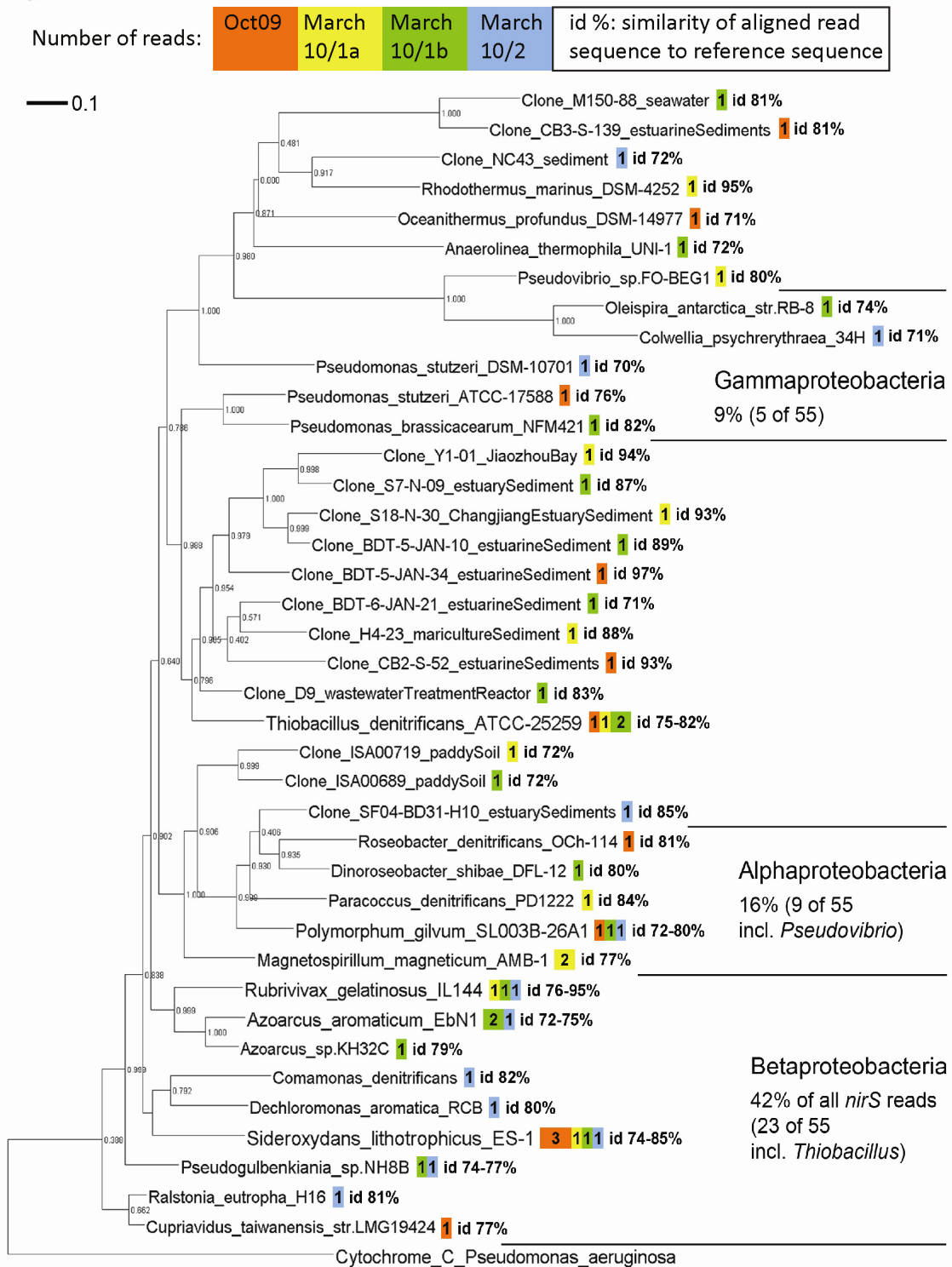
Number of reads: Oct09 March 10/1a March 10/1b March 10/2 id %: similarity of aligned read sequence to reference sequence

█ 0.1





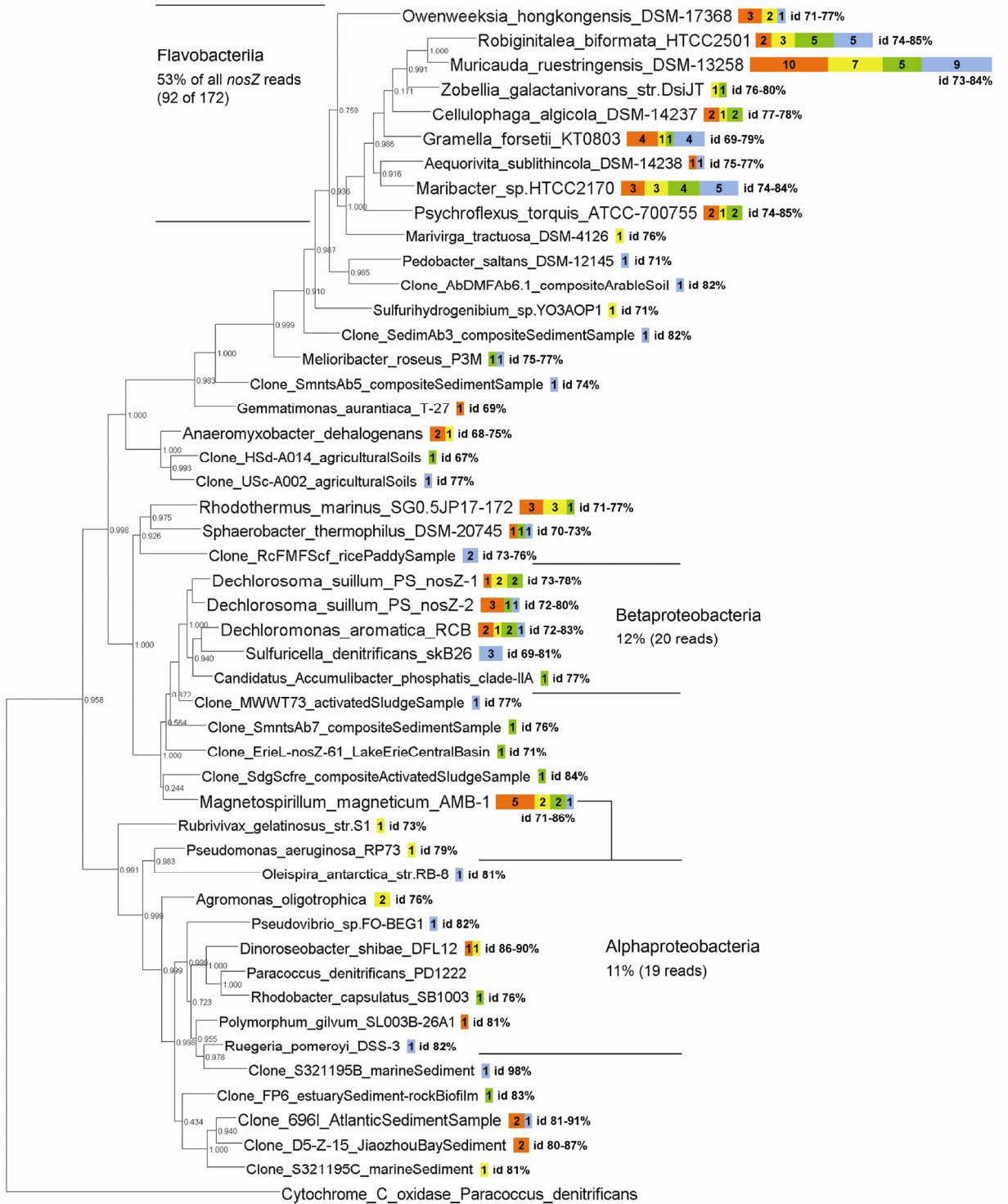
b.



C.

Number of reads: **Oct09** **March 10/1a** **March 10/1b** **March 10/2** **id %: similarity of aligned read sequence to reference sequence**

■ 0.1



**Supplementary Figure 4. Phylogenetic trees of *nirK*, *nirS*, and *nosZ* reads.** The scale bar represents 0.1 nucleotide substitutions per site. Only hits with an e-value of  $\leq 0.0005$  are shown. **a)** Phylogenetic tree of *nirS* database sequences derived from a blastn search of the 55 validated *nirS* encoding reads vs the current (Nov. 2013) nr database. The cytochrome C oxidase gene of *Pseudomonas aeruginosa* is included as outgroup sequence.

**b)** Phylogenetic tree of *nirK* database sequences derived from a blastn search of the 21 validated *nirK* encoding reads vs the current (Nov. 2013) nr database. The *nirK* genes of *Aequorivita sublithicola*, *Muricauda ruestringensis*, and *Rhodothermus marinus* are included as reference sequences, and the cytochrome C gene of *Robiginitalea biformata* HTCC2501 is included as outgroup sequence. **c)**

Phylogenetic tree of *nosZ* database sequences derived from a blastn search of the 175 validated *nosZ* encoding reads vs the current (Nov. 2013) nr database. The *nosZ* and the cytochrome C oxidase genes of *Paracoccus denitrificans* are included as reference and outgroup sequence, respectively.

#### 4) Supplementary Tables

**Supplementary Table 1. Taxonomic distribution of Wadden Sea sediment metagenomes in percent.** \* Indicates that the value is more than 1SD different from the mean. Samples taken in March all showed similar distributions, for example Bacillariophyta were most common followed by Streptophyta, Chordata, Proteobacteria, Bacteroides, Ascomyta/Athropoda and Planctomycetes. October showed the same pattern, except Bacillariophyta were much less common (highlighted in bold), as a result all other percentages were higher, nevertheless they fell within 1.5 SD of the mean.. All sequence reads were submitted to a blastx search against a reference database that was set up from selected FIGfam sequences of widely distributed gene orthologs, to ensure evenly distributed numbers of sequences per taxon. Mar10/1a and 1b are metagenomes from two DNA extracts of the same (homogenized) sediment sample

	Oct-09	Mar10/1 a	Mar10/1 b	Mar10/ 2	Average	±1SD
Bacillariophyta	<b>4.76*</b>	26.4	37.97	39.16	<b>27.07</b>	15.95
Streptophyta	18.49*	15.4	12.3	11.42	<b>14.40</b>	3.21
Chordata	15.74*	13.0	9.98	10	<b>12.18</b>	2.76
Proteobacteria	12.86*	10.8	9.58	9.62	<b>10.70</b>	1.54
Bacteroidetes	12.1*	7.4	7.65	7.72	<b>8.72</b>	2.25
Arthropoda	7.33*	6.1	4.48	4.75	<b>5.66</b>	1.32
Ascomycota	5.78*	5.0	4.62	3.86	<b>4.82</b>	0.80
Planctomycetes	5.18*	3.6	3.16	3.4	<b>3.83</b>	0.92
others	4.06*	3.2	2.85	3.09	<b>3.31</b>	0.53
Eukaryota	2.6*	2.3	1.94*	2.36	<b>2.29</b>	0.27
Acidobacteria	4.13*	2.2	1.89	1.6	<b>2.47</b>	1.14
Nematoda	1.28*	1.4	0.97	0.52*	<b>1.03</b>	0.38
Firmicutes	1.57*	1.0	0.72	0.8	<b>1.03</b>	0.38
Actinobacteria	1.33*	0.8	0.77	0.69	<b>0.90</b>	0.29
Chloroflexi	1.46*	0.8	0.59	0.5	<b>0.83</b>	0.43
Euryarchaeota	1.34*	0.8	0.53	0.51	<b>0.78</b>	0.39

**Supplementary Table 2.** a) results of blastn search vs. NCBI genomes database

Phylum	Class	Hit count on rank species	%
<b>All reads</b>		97.772	100,0
Proteobacteria	Alphaproteobacteria	21.618	22,1
	Betaproteobacteria	12.885	13,2
	Gammaproteobacteria	25.435	26,0
	Delta/Epsilon devisions	8.055	8,2
	Bacteroidetes	12.252	12,5
	Flavobacteriia	10.570	10,8

**b) Flavobacteriia blastn results (>99 hits)**

## i) Ranking by hit count

Species name	NCBI accession	Hit count	Average % identity per base
Maribacter sp. HTCC2170	NC_014472	1.381	80,66
Lacinutrix sp. 5H-3-7-4	NC_015638	1.128	83,33
Cellulophaga algicola DSM 14237	NC_014934	929	81,63
Cellulophaga lytica DSM 7489	NC_015167	887	80,48
Zobellia galactanivorans	NC_015844	720	81,63
Muricauda ruestringensis	NC_015945	615	79,71
Aequorivita sublithincola	NC_018013	491	80,90
Robiginitalea biformata	NC_013222	463	85,33
Gramella forsetii	NC_008571	412	79,92
Croceibacter atlanticus	NC_014230	407	79,96
Zunongwangia profunda	NC_014041	368	79,68
Flavobacterium indicum	NC_017025	318	79,52
Psychroflexus torquis	NC_018721	290	81,29
Persicivirga dokdonensis	NC_020156	256	80,49
Flavobacterium johnsoniae	NC_009441	233	80,60
Krokinobacter sp. 4H-3-7-5	NC_015496	222	81,04
Flavobacterium columnare	NC_016510	203	79,91
Flavobacterium psychrophilum	NC_009613	191	81,09
Myroides odoratus	NZ_CM001437	184	78,70
Owenweeksia hongkongensis	NC_016599	169	82,53
Flavobacterium branchiophilum	NC_016001	152	78,59
Fluviicola taffensis	NC_015321	103	81,67
Capnocytophaga canimorsus	NC_015846	100	78,63

## ii) Ranking by %id

Species name	NCBI accession	Average % identity per base	Hit count
Robiginitalea biformata	NC_013222	85,33	463
Lacinutrix sp. 5H-3-7-4	NC_015638	83,33	1.128
Owenweeksia hongkongensis	NC_016599	82,53	169
Fluviicola taffensis	NC_015321	81,67	103
Cellulophaga algicola DSM 14237	NC_014934	81,63	929

Zobellia galactanivorans	NC_015844	81,63	720
Psychroflexus torquis	NC_018721	81,29	290
Flavobacterium psychrophilum	NC_009613	81,09	191
Krokinobacter sp. 4H-3-7-5	NC_015496	81,04	222
Aequorivita sublithicola	NC_018013	80,90	491
Maribacter sp. HTCC2170	NC_014472	80,66	1.381
Flavobacterium johnsoniae	NC_009441	80,60	233
Persicivirga dokdonensis	NC_020156	80,49	256
Cellulophaga lytica DSM 7489	NC_015167	80,48	887
Croceibacter atlanticus	NC_014230	79,96	407
Gramella forsetii	NC_008571	79,92	412
Flavobacterium columnare	NC_016510	79,91	203
Muricauda ruestringensis	NC_015945	79,71	615
Zunongwangia profunda	NC_014041	79,68	368
Flavobacterium indicum	NC_017025	79,52	318
Myroides odoratus	NZ_CM001437	78,70	184
Capnocytophaga canimorsus	NC_015846	78,63	100
Flavobacterium branchiophilum	NC_016001	78,59	152

**Supplementary Table 3.** Annual N<sub>2</sub>O emissions calculated for the sandy sediment of the Wadden Sea. W92 and McG01 refer to the two parameterizations of air-sea flux used (see supplementary methods)

Geomorphological region of the Wadden Sea	Area (km <sup>2</sup> )	Percentage of sandy permeable sediments (%)	Annual emissions (W92) (x 10 <sup>6</sup> kg N year <sup>-1</sup> )	Annual emissions (McG01) (x 10 <sup>6</sup> kg N year <sup>-1</sup> )
Intertidal flats <sup>1</sup>	4700	93	0.69	0.49
Subtidal flats and gullies	3700	80	1.12	0.80
Offshore area	4900	80	1.49	1.06
Total			3.30	2.36

<sup>1</sup>Calculated for an average inundation period of 10 hours per day

**Supplementary Table 4:** Metagenome 454 pyrosequencing yields after initial quality filtering (data used for analysis)

Sample name	Oct09	Mar10/1a	Mar10/1b	Mar10/2
Mb	280.273	232.433	205.015	232.134
Read number	648,531	555,434	547,915	660,178
Average read length	432	419	374	352

**Supplementary Table 5:** illumina cDNA sequencing results

Sample name	06:50	08:50	10:50	12:50	14:50	16:50
	Low Tide	Late Low Tide	Rising Tide	High Tide	Falling Tide	Early Low Tide
Mb sequenced	84.72	114.91	126.44	112.92	110.73	110.58
Read count	404,183	573,364	648,488	562,189	529,437	534,292
# clusters resulting from DNACLUST	318,485	167,898	164,353	123,425	272,793	338,498

**Supplementary Table 6. a)** Total numbers of blastn hits per data set for data used in construction of phylogenetic trees **b)** GI and accession numbers of the reference sequences in phylogenetic trees

**a.**

	<i>nirK</i>	<i>nirS</i>	<i>nosZ</i>	unaligned
Oct09	5	12	51	3
Mar10/1a	7	12	40	0
Mar10/1b	2	19	37	2
Mar10/2	2	12	44	3

**b.**

Gene	Organism	gi	accession
<b>nirK</b>	Aequorivita sublithicola DSM 14238	390418775	CP003280
	Azoarcus sp. KH32C plasmid pAZKH DNA	358639587	AP012305
	Belliella baltica DSM 15883	390415094	CP003281
	Flavobacterium columnare ATCC 49512	372863588	CP003222
	Herpetosiphon aurantiacus DSM 785	159889572	CP000875
	Maribacter sp. HTCC2170	304420054	CP002157
	Muricauda ruestringensis DSM 13258	343953259	CP002999
	Octadecabacter antarcticus 307	476507773	CP003740
	Phaeobacter gallaeciensis DSM 17395 plasmid pPGA1_262	398659317	CP002977
	Ralstonia solanacearum CFBP2957 plasmid RCFBPv3_mp aniA gene	299073288	FP885907
	Rhodanobacter sp. 2APBS1	459938263	CP003470
	Rhodothermus marinus SG0.5JP17-172	345111121	CP003029
	Uncultured organism clone SF04-BA41-A11 estuary sediments	306488574	GQ454064
	Uncultured organism clone SF04-SP19-A09 estuary sediments	306489214	GQ454384
	Uncultured organism clone SF04-SP19-A10 estuary sediments	306489216	GQ454385
	Outgroup: Cytochrome C	Robiginitalea biformata HTCC2501	257796356
<b>nirS</b>	Anaerolinea thermophila UNI-1	319993263	AP012029
	Azoarcus aromaticum EbN1	56311475	CR555306
	Azoarcus sp. KH32C	358635055	AP012304
	Colwellia psychrerythraea 34H	71143482	CP000083
	Comamonas denitrificans	115383216	DQ865926
	Cupriavidus taiwanensis str. LMG19424	170938221	CU633750
	Dechloromonas aromatica RCB	71845263	CP000089
	Dinoroseobacter shibae DFL 12	157910316	CP000830
	Magnetospirillum magneticum AMB-1	82943940	AP007255
	Oceanithermus profundus DSM 14977	313151615	CP002361
	Oleispira antarctica strain RB-8	508728691	FO203512
	Paracoccus denitrificans PD1222	119372524	CP000489
	Polymorphum gilvum SL003B-26A1	326411376	CP002568
	Pseudogulbenkiania sp. NH8B	345641016	AP012224
	Pseudomonas brassicacearum subsp. brassicacearum NFM421	327374765	CP002585
	Pseudomonas stutzeri ATCC 17588	338799449	CP002881
	Pseudomonas stutzeri DSM 10701	395806679	CP003725



	<i>Pseudovibrio</i> sp. FO-BEG1	359341138	CP003147
	<i>Ralstonia eutropha</i> H16	113528459	AM260480
	<i>Rhodothermus marinus</i> DSM 4252	262333112	CP001807
	<i>Roseobacter denitrificans</i> OCh 114	109453537	CP000362
	<i>Rubrivivax gelatinosus</i> IL144	381376528	AP012320
	<i>Sideroxydans lithotrophicus</i> ES-1	291582584	CP001965
	<i>Thiobacillus denitrificans</i> ATCC 25259	74055513	CP000116
	Uncultured bacterium clone BDT-5-JAN-10 estuarine sediment	500069474	KC614257
	Uncultured bacterium clone BDT-5-JAN-34 estuarine sediment	500069516	KC614278
	Uncultured bacterium clone BDT-6-JAN-21 estuarine sediment	500069584	KC614312
	Uncultured bacterium clone CB2-S-52 estuarine sediments	113202470	DQ675843
	Uncultured bacterium clone CB3-S-139 estuarine sediments	113202732	DQ675974
	Uncultured bacterium clone D9 wastewater treatment reactor	166065006	EU325639
	Uncultured bacterium clone H4-23 mariculture sediment	164606591	EU200619
	Uncultured bacterium clone ISA00689 paddy soil	209486032	FJ204625
	Uncultured bacterium clone ISA00719 paddy soil	209486092	FJ204655
	Uncultured bacterium clone M150-88 seawater	68164641	DQ072184
	Uncultured bacterium clone NC43 sediment	395628703	JX002739
	Uncultured bacterium clone S18-N-30 Changjiang Estuary sediment	356983199	JN177574
	Uncultured bacterium clone S7-N-09 estuary sediment	164374658	EU235750
	Uncultured bacterium clone Y1-01 Jiaozhou Bay	156628387	EU048490
	Uncultured organism clone SF04-BD31-H10 estuary sediments	306488032	GQ453793
	Outgroup: Cytochrome C		
	<i>Pseudomonas aeruginosa</i> UCBPP-PA14	116048575	NC_008463
<b>nosZ</b>	<i>Aequorivita sublithicola</i> DSM 14238	390418775	CP003280
	<i>Agromonas oligotrophica</i> S58	456351576	AP012603
	<i>Anaeromyxobacter dehalogenans</i> 2CP-C	85772941	CP000251
	Candidatus <i>Accumulibacter phosphatis</i> clade IIA str. UW-1	257044187	CP001715
	<i>Cellulophaga algicola</i> DSM 14237	319420253	CP002453
	<i>Dechloromonas aromatica</i> RCB	71845263	CP000089
	<i>Dechlorosoma suillum</i> PS	359353254	CP003153
	<i>Dinoroseobacter shibae</i> DFL-12	157910316	CP000830
	<i>Gemmatimonas aurantiaca</i> T-27	226088597	AP009153
	<i>Gramella forsetii</i> KT0803	117576522	CU207366
	<i>Magnetospirillum magneticum</i> AMB-1	82943940	AP007255
	<i>Maribacter</i> sp. HTCC2170	304420054	CP002157
	<i>Marivirga tractuosa</i> DSM 4126	312940827	CP002349
	<i>Melioribacter roseus</i> P3M	395810495	CP003557
	<i>Muricauda ruestringensis</i> DSM 13258	343953259	CP002999
	<i>Oleispira antarctica</i> strain RB-8	508728691	FO203512
	<i>Owenweeksia hongkongensis</i> DSM 17368	359346608	CP003156
	<i>Pedobacter saltans</i> DSM 12145	324971605	CP002545
	<i>Polymorphum gilvum</i> SL003B-26A1	326411376	CP002568
	Proteobacteria uncultured nosZ clone S321195A	3057076	AF016055
	<i>Pseudomonas aeruginosa</i> RP73	514245605	CP006245
	<i>Pseudovibrio</i> sp. FO-BEG1	359341138	CP003147
	<i>Psychroflexus torquis</i> ATCC 700755	408466736	CP003879
	<i>Rhodobacter capsulatus</i> SB 1003 plasmid pRCB133	294477871	CP001313
	<i>Rhodothermus marinus</i> SG0.5JP17-172	345111121	CP003029

Robiginitalea biformata HTCC2501	257796356	CP001712
Rubrivivax gelatinosus strain S1	260586483	GQ900543
Ruegeria pomeroyi DSS-3 megaplasmid	56680476	CP000032
Sphaerobacter thermophilus DSM 20745	269785296	CP001823
Sulfuricella denitrificans skB26	540592690	AP013066
Sulfurihydrogenibium sp. YO3AOP1	188931022	CP001080
UncultBacterium cloneHSd-A014 agriculturalSoils	376372773	JN882628
Uncultured bacterium 696I AtlanticSedimentSample	4633516	AF119918
Uncultured bacterium clone AbDMFAB6 composite arable soil sample	421953099	JQ514006
Uncultured bacterium clone D5-Z-15 Jiaozhou Bay sediment	226347055	FJ686386
Uncultured bacterium clone FP6 estuary sediment/rock biofilm	83701119	DQ311684
Uncultured bacterium clone MWWT73 activatedSludgeSample	213013193	EU749020
Uncultured bacterium clone RcFMFScf rice paddy sample	422314104	JQ647613
Uncultured bacterium clone SdgScfre composite activated sludge sample	422314034	JQ647578
Uncultured bacterium clone SedimAb3 composite sediment sample	422314438	JQ647780
Uncultured bacterium clone SmntsAb5 composite sediment sample	422314488	JQ647805
Uncultured bacterium clone SmntsAb7 composite sediment sample	422314486	JQ647804
Uncultured bacterium clone USc-A002 agricultural soils	376372771	JN882627
Uncultured eubacterium S321195B marine sediment	3057078	AF016056
Uncultured microorganism clone EriE-nosZ-61 lake Erie central basin	417353496	JX626226
Uncultured Proteobacterium, marine sediment	3057080	AF016057
Zobellia galactanivorans strain DsiJT	339730808	FP476056
Outgroup: Cytochrome C oxidase		
Paracoccus denitrificans PD1222	119372524	CP000489

### Supplementary references

- 1 M. Billerbeck, U. Werner, L. Polerecky, E. Walpersdorf, D. de Beer et al., *Mar. Ecol.-Prog. Ser.* 326, 61 (2006).
- 2 M. Billerbeck, U. Werner, K. Bosselmann, E. Walpersdorf, and M. Huettel, *Mar. Ecol.-Prog. Ser.* 316, 35 (2006).
- 3 R. Wanninkhof, W. E. Asher, D. T. Ho, C. Sweeney, and W. R. McGillis, in *Annual Review of Marine Science (Annual Reviews, Palo Alto, 2009)*, Vol. 1, pp. 213.
- 4 R. Wanninkhof, *J. Geophys. Res.* 97 (C5), 7373 (1992).
- 5 Wade R. McGillis, James B. Edson, Jonathan D. Ware, John W. H. Dacey, Jeffrey E. Hare et al., *Mar. Chem.* 75 (4), 267 (2001).
- 6 Günther Uher, *Estuarine, Coastal and Shelf Science* 70 (3), 338 (2006).
- 7 P. Forster, V. Ramaswamy, P. Artaxo, T. Berntsen, R. Betts et al., in *Climate Change 2007: The Physical Basis. Contribution of Working Group I to the Fourth Assessment Report of the Intergovernmental Panel on Climate Change*, edited by S.

Solomon, D. Qin, M. Manning et al. (Cambridge University Press, Cambridge, UK, and New York, 2007), pp. 129.

8 M. Grunwald, O. Dellwig, M. Beck, J. W. Dippner, J. A. Freund et al., *Estuar. Coast. Shelf Sci.* 81 (4), 445 (2009).

9 B. W. Flemming and R.A. Davis, Jr., *Senckenbergiana Maritima* 24 (1-6), 117 (1994).

10 E. V. Stanev, J. Wolff, H. Burchard, K. Bolding, and G. Flöser, *Ocean Dyn.* 53 (1), 27 (2003).

11 L. P. Nielsen, *Fems Microbiology Ecology* 86 (4), 357 (1992).

12 N. P. Revsbech, *Limnology and Oceanography* 34 (2) (1989).

13 M. Holtappels, Lavik, G., Jensen, M. M., and Kuypers, M. M. M., in *Methods in Enzymology*, edited by Martin G. Klotz (2011), Vol. 486.

14 R. S. Braman and S. A. Hendrix, *Analytical Chemistry* 61 (24), 2715 (1989).

15 H. Gao, M. Matyka, B. Liu, A. Khalili, J.E. Kostka et al., *Limnology and Oceanography* 57 (1), 185 (2012).

16 S. Jansen, E. Walpersdorf, U. Werner, M. Billerbeck, M. E. Bottcher et al., *Ocean Dyn.* 59 (2), 317 (2009).

17 K. Andersen, T. Kjaer, and N. P. Revsbech, *Sensors and Actuators B-Chemical* 81 (1), 42 (2001).

18 F. Schreiber, B. Loeffler, L. Polerecky, M.M.M. Kuypers, and D. de Beer, *ISME J* 3 (11), 1301 (2009).

19 J. Zhou, M. A. Bruns, and J. M. Tiedje, *Applied and Environmental Microbiology* 62 (2), 316 (1996).

20 W. Li and A. Godzik, *Bioinformatics* 22 (13), 1658 (2006).

21 B. Niu, L. Fu, S. Sun, and W. Li, *BMC Bioinformatics* 11, 187 (2010).

22 F. Meyer, D. Paarmann, M. D'Souza, R. Olson, E. M. Glass et al., *BMC Bioinformatics* 9, 386 (2008).

- 23 F. Meyer, R. Overbeek, and A. Rodriguez, *Nucleic Acids Research* 37 (20), 6643 (2009).
- 24 R. C. Edgar, *Bioinformatics* 26 (19), 2460 (2010).
- 25 I. N. Throckback, K. Enwall, A. Jarvis, and S. Hallin, *FEMS Microbiol Ecol* 49 (3), 401 (2004).
- 26 C. M. Jones, D. R. H. Graf, D. Bru, L. Philippot, and S. Hallin, *ISME J* (2012).
- 27 S. F. Altschul, W. Gish, W. Miller, E. W. Myers, and D. J. Lipman, *Journal of Molecular Biology* 215 (3), 403 (1990).
- 28 Robert C. Edgar, *Nucleic Acids Research* 32 (5), 1792 (2004).
- 29 Morgan N. Price, Paramvir S. Dehal, and Adam P. Arkin, *PLoS ONE* 5 (3), e9490 (2010).
- 30 Daniel H. Huson, Daniel C. Richter, Christian Rausch, Tobias DeZulian, Markus Franz et al., *Bmc Bioinformatics* 8 (2007).
- 31 M. Ghodsi, B. Liu, and M. Pop, *Bmc Bioinformatics* 12 (2011).
- 32 H. W. Bange, S. Rapsomanikis, and M. O. Andreae, *Global Biogeochem. Cycles* 10 (1), 197 (1996).
- 33 L. A. Codispoti, *Science* 327 (5971), 1339 (2010).
- 34 H. Gao, F. Schreiber, G. Collins, M. M. Jensen, J. E. Kostka et al., *Isme Journal* 4 (3), 417 (2010).
- 35 W. M. Kieskamp, L. Lohse, E. Epping, and W. Helder, *Mar. Ecol.-Prog. Ser.* 72 (1-2), 145 (1991).

## Chapter VII

### **The impact of ocean acidification on nitrogen cycling in coastal permeable sediments**

**Hannah K. Marchant<sup>1\*</sup>, Tim Ferdelman<sup>1</sup>, Gaute Lavik<sup>1</sup> and Marcel M.M. Kuypers<sup>1</sup>**

<sup>1</sup>Max Planck Institute for Marine Microbiology, Celsiusstrasse 1, 28359 Bremen, Germany

\* Corresponding author: hmarchan@mpi-bremen.de, tel: +49421-2028630, fax: +49421-2028790

Keywords: ocean acidification; permeable sediment; nitrogen cycling; nitrification; denitrification

Author Contributions:

H.K.M., G.L., and M.M.M.K designed research. H.K.M. carried out research, measured samples and analyzed data. H.K.M., T.F., G.L., and M.M.M.K conceived, wrote and edited the manuscript.

**In preparation**

### **Acknowledgements**

Bjoern Rost is thanked for valuable discussion of the experimental set up and results. Felix Raulf and Martin Glas are thanked for their assistance in setting up and running the seawater  $p\text{CO}_2$  manipulation system. Furthermore we are grateful to Gabi Klockgether, Gabi Schüßler, Kirsten Imhoff, and Thomas Max for their technical assistance.

## **Abstract**

Atmospheric carbon dioxide levels continue to rise as a result of anthropogenic emissions, resulting in profound changes in ocean chemistry and reductions in seawater pH. There are indications that ocean acidification will negatively impact nitrification within the oceans, to the extent that pelagic nitrification activity is predicted to drop by 3 - 44% in the coming decades. Nevertheless, little is known about the impact that ocean acidification will have on nitrification and coupled nitrification-denitrification within coastal sediments, which are globally important N-sinks. In a four week experiment we investigated pH scenarios ranging from last glacial maximum to the year 2300. A doubling in  $p\text{CO}_2$  resulted in a 36% decrease in nitrate concentrations in the unfiltered seawater reservoirs; however, there was no subsequent change in the overall benthic denitrification rates in permeable sediments exposed to the seawater. Instead,  $^{15}\text{N}$  stable isotope labeling revealed that there was a stronger coupling of nitrification and denitrification within the permeable sediments exposed to increased  $p\text{CO}_2$  and lower nitrate, when compared to sediments under present day conditions. These results suggest that in future increased benthic nitrification-denitrification could decrease the amount of nitrate recycled from the sediment to the water column. Although coastal sediments play an important role in global N-cycling, this effect has so far not been included in models that predict oceanic responses to ocean acidification.

## Introduction

Carbon dioxide (CO<sub>2</sub>) in the atmosphere has risen significantly since the industrial revolution from 280 to 400 ppm due to the burning of fossil fuels, cement production and changes in land use (Houghton et al. 2001). Atmospheric CO<sub>2</sub> concentrations continue to rise at a rate unprecedented since the Eocene (Zachos et al. 2001), and by 2100 they are expected to exceed 1000 ppm. At least 30% of anthropogenically-produced CO<sub>2</sub> has been absorbed by the surface layer of the oceans (Sabine et al. 2004). This has resulted in a profound change in ocean chemistry, leading to a reduction of 0.1 pH units in surface waters. Continued decreases in pH of up to 0.3 - 0.5 units are predicted by 2100 if CO<sub>2</sub> emissions continue in a “business as usual” scenario (Caldeira and Wickett 2003). While many studies have focused on the impact of a high CO<sub>2</sub> ocean on calcifying organisms, oceanic productivity, and carbon export (e.g. Hutchins et al. 2009; Orr et al. 2005; Passow and Carlson 2012), only a few have examined possible changes in nitrogen cycling (Beman et al. 2011; Huesemann et al. 2002; Levitan et al. 2007).

It has been hypothesized that ocean acidification will have a strong impact on nitrification, the microbial process that mediates the two step oxidation of ammonia to nitrate (Hutchins et al. 2009). Lowered pH has the potential to both positively and negatively influence the extent of nitrification. Nitrifiers are autotrophs, therefore increased CO<sub>2</sub> could stimulate nitrification by lowering the limitations on the RuBisCO enzyme, which evolved under pCO<sub>2</sub> conditions greater than present day levels, and which has a low affinity for CO<sub>2</sub> (Rost et al. 2008). Similar stimulation of CO<sub>2</sub> has been observed in N<sub>2</sub> fixers (Hutchins et al. 2007). Bacterial ammonia oxidizers, however, likely possess carbon concentrating mechanisms that would alleviate this limitation (Badger and Bek 2008; Rost et al. 2008). Furthermore, ammonia oxidizing archaea (which are widespread in oceanic waters), do not use RubisCO and the Calvin-Benson cycle, and therefore, are not subject to CO<sub>2</sub> limitation (Walker et al. 2010).



Nevertheless, current evidence indicates that pelagic nitrification will be negatively impacted by ocean acidification. The availability of  $\text{NH}_3$ , which is thought to be the enzymatic substrate for ammonia oxidizers (Suzuki et al. 1974; Ward 1987), is expected to be reduced by ocean acidification due to shifts in the acid-base equilibrium of the ammonia/ammonium buffer system (by 2100 only 1% of oceanic  $\text{NH}_x$  is expected to be in the form  $\text{NH}_3$  compared to 2% today in 15°C, 35 salinity waters, (Bange 2008)). Initial assessments indicate that marine nitrification is indeed sensitive to ocean acidification, with ammonium oxidation rates decreasing almost linearly from pH 8 to pH 6.5 (with a 40% decrease between pH 8.0 and 7.5) in seawater samples (Huesemann et al. 2002). More recently, in a review of all experiments in which nitrification was measured under different pH's Beman et al. (2011) suggested that nitrification rates in oceanic waters could decrease by 3-44% in the coming decades in response to ocean acidification. Reduced nitrification is likely to shift nutrient ratios within the oceans, increasing the relative importance of  $\text{NH}_4^+$  to  $\text{NO}_3^-$ . A major consequence of this may be shifts in phytoplankton community structure leading to changes in primary productivity and carbon sequestration (Beman et al. 2011; Yool et al. 2007). Decreases in nitrification are also predicted to reduce the flux of nitrate to the sediment, where it supplies denitrification (Blackford and Gilbert 2007). Denitrification in coastal systems represents a globally important sink of nitrate and acts to ameliorate the impacts of anthropogenic inputs of N, which cause eutrophication (Devol 1991; Gao et al. 2012).

Despite the importance of sediments for N-cycling, most previous studies of ocean acidification have focused on the water column. The only study which has investigated nitrification in benthic sediments with respect to ocean acidification found no change in nitrification rates, however the authors neglected the influence that advection might have on the permeable sediments they studied (Kitidis et al. 2011). Moreover, to date no direct measurements exist of the impact of ocean acidification on denitrification and coupled nitrification-denitrification in any marine sediment.

Sandy permeable sediments are characteristic for coastal zones, and are sites of extensive N-loss. For example, some of the highest denitrification rates found in the

marine environment have been recorded in the sand flats of the eutrophic Wadden Sea (Gao et al. 2012; Gao et al. 2010). Substantial biogeochemical cycling is supported in these sediments by advective porewater flow, that supplies nutrient and oxygen rich water to the sediment at speeds more than three orders of magnitude greater than in diffusive sediment (De Beer et al. 2005; Huettel and Gust 1992). Unlike muddy diffusively controlled sediments, changes in the overlying water column are rapidly transmitted to permeable sediments and vice-versa (Chipman et al. 2012). Therefore, any influence of ocean acidification on coupled nitrification-denitrification in permeable sandy sediments will immediately impact nitrogen cycling in coastal zones. To investigate the impact of ocean acidification on sedimentary N-cycling we carried out a four week long experiment using permeable sandy sediments from the intertidal Wadden Sea.

## **Methods**

### ***Sampling Sites***

#### *Sediment*

Sediment was sampled from the Janssand sand flat, which is located in the back barrier area of Spiekeroog Island in the East Frisian Wadden Sea, Germany. The sand flat is located in an intertidal region and is covered by around 2m of seawater during high tide before exposure to the air for 6 – 8 h during low tide in a semi diurnal cycle. The sampling site (53.73515 'N, 007.69913'E) was situated in the upper flat (for more details about the site see (Billerbeck et al. 2006a; Billerbeck et al. 2006b). Sediment from the upper 5cm of the sand flat was collected on October 24 2009 and was pooled and homogenized before being distributed into 12 sediment columns (I.D. 9.3 cm, height 10 cm, stoppers were milled with radial grooves covered with a fine mesh (500 microns, Hydro-BIOS, Germany) to assist homogenous porewater flow). Columns were closed and returned to the Max Planck Institute for Marine Microbiology, Bremen on October 25 2009, at which point they were supplied with unfiltered site seawater from a single

reservoir at 19°C for 7 weeks. Unidirectional fluid flow, simulating the tidal cycle on the sand flat was achieved using peristaltic pumps, which pushed pore fluid upward through each column between in a cycle consisting of 15 min pumping, 15 min no pumping (6 hours), followed by six hours no pumping (2.5 ml min<sup>-1</sup> flow rate).

#### *Seawater*

The seawater (300L) was collected initially from the area of the Janssand sand flat, parallel with sediment collection. Further collections took place on November 12, 2009, November 28, 2009, 13 December, 2009, January 3, 2010, January 15, 2010 and January 24, 2010. Seawater was stored in 10L containers and kept in the dark at 4°C until needed.

#### ***Experimental set up***

The experimental set-up shown in Fig. 1 consisted of four 40 L cylindrical seawater which were kept in the dark and in which  $p\text{CO}_2$  was adjusted before being supplied to sediment columns. Carbonate chemistry in each reservoir was adjusted by bubbling with air of partial pressures of carbon dioxide. Defined concentrations of  $\text{CO}_2$  within the air supply were achieved by mixing  $\text{CO}_2$  from gas cylinders (5%  $\text{CO}_2$  or 2%  $\text{CO}_2$  in synthetic air) with laboratory air scrubbed clean of  $\text{CO}_2$  using an adsorption dryer (K-MT 3-Lab, Domnick Hunter). The  $\text{CO}_2$ -free laboratory air flow was controlled and monitored by mass flow controllers (Brock). The  $\text{CO}_2$  supply was controlled and monitored by rotameters (Purgemaster Durchflussmesser Series A6100, ABB Automation Products GmbH). Reservoirs were refilled using unfiltered seawater from a separate header tank. The replacement rate for each reservoir was 1.87 ml min<sup>-1</sup>, this equated to a replacement of 9% of the  $\text{CO}_2$  equilibrated water each day, which did not affect the reservoir  $p\text{CO}_2$ .

The reservoir water was monitored for pH, DIC, temperature, salinity, nitrate, nitrite and ammonium concentrations throughout the 28 day experiment. pH was measured on the NBS scale with a commercial glass electrode (3-mm tip diameter, InLab 423, Mettler Toledo, Switzerland). DIC was measured by coulometry (UIC, Inc, Model 5012). pH, DIC,

salinity and temperature were used to calculate total alkalinity and  $p\text{CO}_2$  using CO2Sys for excel (Pierrot *et al.*, 2008). See table 1. Nitrate and nitrite within the reservoirs were determined on a chemiluminescence  $\text{NO}_x$  analyzer (Braman and Hendrix, 1989). Ammonium was measured spectrophotometrically.

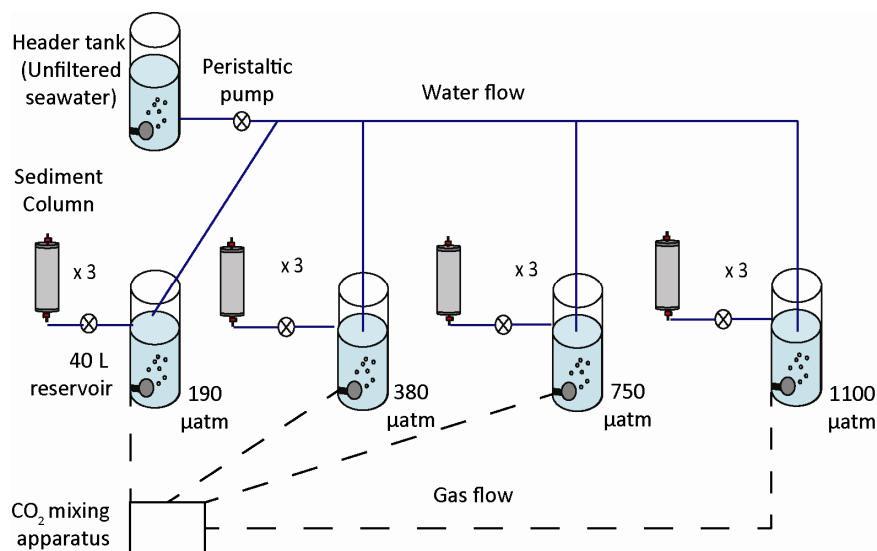


Figure 1. Schematic of experimental set-up.  $p\text{CO}_2$  was adjusted within sediment columns by bubbling seawater supply reservoirs with  $p\text{CO}_2$  adjusted air. This water was pumped unidirectionally through columns on a simulated tidal cycle and discarded upon exiting the column. Water was constantly in reservoirs from a single header tank. All reservoirs and columns were kept in the dark.

### **Denitrification incubations**

On January 5, 2010 and January 8, 2010, control incubations were carried out to determine denitrification rates in each sediment column (see below for details). On January 11, the sediment columns were randomly assigned to one of four  $p\text{CO}_2$  conditions (nominally, 190, 380, 750 and 1200  $\mu\text{atm}$ ) after which denitrification rates were determined once a week in each sediment column. For these measurements, columns were removed from the tidal cycle simulation at the end of a 6 hour “on” cycle. At the same time a 600 ml subsample of seawater from the appropriate reservoir was amended to contain 50  $\mu\text{M}$   $^{15}\text{NO}_3^-$ . The  $^{15}\text{NO}_3^-$  amended seawater was then pumped through the column, which was sufficient to entirely exchange the pore water within the column. After porewater exchange with  $^{15}\text{NO}_3^-$  amended seawater was completed, the

sediment column was closed using a 2-way valve. Subsequently, time point porewater samples were collected by opening the valve and letting porewater flow directly through a sampling port into 6 ml exetainers prefilled with 100  $\mu\text{l}$  saturated  $\text{HgCl}_2$ . Before each sample was collected, 1.5 ml of porewater was discarded to flush the tubing between the column and the sediment. Six samples were taken over 80 minutes. Sampled porewater was replaced passively at the top of the column with unamended sea water. In total 45 ml of seawater was sampled, corresponding to less than a quarter of the total porewater volume. Production of labeled  $\text{N}_2$  within each sample was determined by measurement of isotopes of mass 28 ( $^{14}\text{N}^{14}\text{N}$ ), 29 ( $^{14}\text{N}^{15}\text{N}$ ), 30 ( $^{15}\text{N}^{15}\text{N}$ ), 40 (Ar), using a membrane inlet mass spectrometer (MIMS; GAM200, In Process Instruments).

#### **Denitrification rate determinations**

Denitrification rates (Den) were determined from the slope of  $^{29}\text{N}_2$  and  $^{30}\text{N}_2$  produced over time (referred to hereafter as  $p^{29}\text{N}_2$  and  $p^{30}\text{N}_2$  ( $\mu\text{mol N}_2 \text{ L}^{-1} \text{ h}^{-1}$ )), using the isotope pairing method according to Thamdrup and Dalsgaard (2002):

$$\text{Den} = p^{30}\text{N}_2 (F_N^*) \quad (\text{eq 1})$$

Where  $F_N^*$  is the labeling fraction of nitrate which was calculated from the production of  $^{29}\text{N}_2$  and  $^{30}\text{N}_2$ :

$$F_N^* = 2 / (p^{29}\text{N}_2 / p^{30}\text{N}_2 + 2) \quad (\text{eq 2})$$

The labeling fraction of nitrate ( $F_N$ ) can also be calculated from the initial concentrations of labeled and unlabeled nitrate

$$F_N = {}^{15}\text{NO}_3^- / ({}^{14}\text{NO}_3^- + {}^{15}\text{NO}_3^-) \quad (\text{eq 3})$$

Differences between  $F_N^*$  and  $F_N$  indicate changes in the labeling ratio during the experiment, and can be expressed as:

$$1 - F_N / F_N^* \quad (\text{eq 4})$$

where a value below 0 indicates that a source of  ${}^{14}\text{NO}_3^-$  exists within the sediment column to the  ${}^{14}\text{NO}_3^-$  added in the porewater. Alternatively, negative values may indicate the presence of anammox, but this process has been shown to be insubstantial in the sediments studied here (Gao et al. 2012).

## Results

### *Reservoir carbonate chemistry and nutrient concentrations*

Carbonate chemistry in each of the 4 supply reservoirs remained stable over the course of the experiment (Table 1), with final average  $p\text{CO}_2$  concentrations of 208, 408, 671, and 1131  $\mu\text{atm}$  for the last glacial maximum, present day, year 2100 estimate and year 2300 estimate respectively.

Table 1. Carbonate chemistry in the 4 supply reservoirs over the 28 day experiment. For pH  $n=16$ , for DIC  $n = 5$ ) Other parameters of the seawater were calculated from dissolved inorganic carbon (DIC), temperature, salinity, and pH using the  $\text{CO}_2\text{Sys}$  program ((Pierrot 2006)) ( $n=5$ )

	Nominal $p\text{CO}_2$ ( $\mu\text{atm}$ )	pH (NBS)	DIC ( $\mu\text{mol/kgSW}$ )	TA ( $\mu\text{mol/kgSW}$ )	$p\text{CO}_2$ ( $\mu\text{atm}$ )
Last Glacial Maximum	190	8,42 ( $\pm 0,02$ )	2016 ( $\pm 51$ )	2508 ( $\pm 33$ )	<b>208 (<math>\pm 18</math>)</b>
Present day	380	8,21 ( $\pm 0,02$ )	2308 ( $\pm 123$ )	2597 ( $\pm 75$ )	<b>408 (<math>\pm 16</math>)</b>
Year 2100 estimate	750	8,02 ( $\pm 0,02$ )	2399 ( $\pm 106$ )	2589 ( $\pm 51$ )	<b>671 (<math>\pm 50</math>)</b>
Year 2300 estimate	1100	7,83 ( $\pm 0,02$ )	2529 ( $\pm 115$ )	2576 ( $\pm 62$ )	<b>1131 (<math>\pm 80</math>)</b>

Ammonium varied between 0  $\mu\text{M}$  and 3.5  $\mu\text{M}$ , however no significant differences between time points or reservoirs were observed during the experiment. Nitrite was not detected in the reservoirs at any time point. In contrast, nitrate concentrations within the reservoirs varied significantly, both over time and between  $p\text{CO}_2$  conditions. Nitrate concentrations were always greatest when seawater was fresh and concentrations dropped over time in all reservoirs until the header tank was refilled with freshly collected seawater (Fig. 2a). More importantly, there was a clear correlation between the  $p\text{CO}_2$  of the reservoirs and nitrate concentrations within them (Fig. 2a and 2b). In relation to the reservoir containing seawater at present day  $p\text{CO}_2$ , nitrate concentrations were always greater within the Last Glacial Maximum condition, and lower in the year 2300 condition.

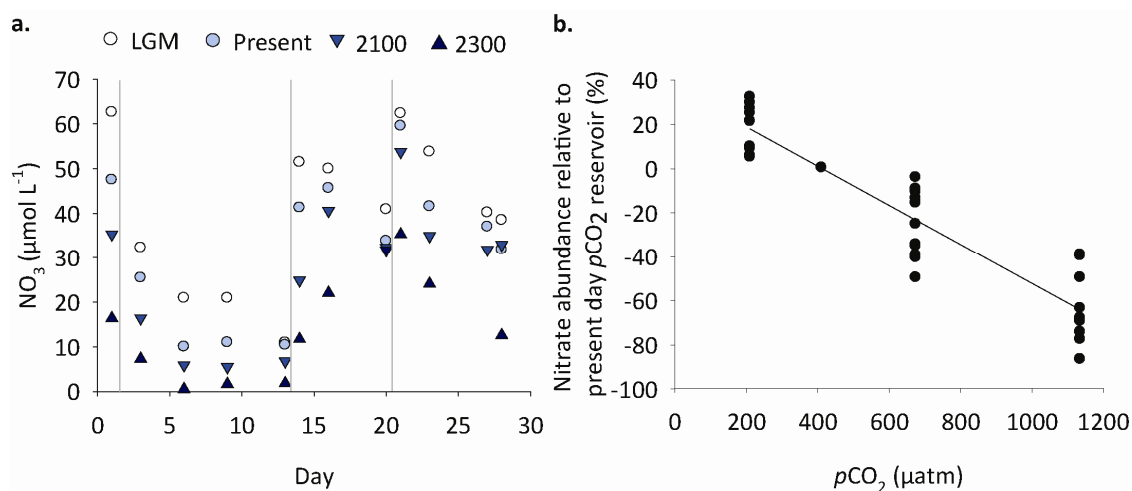


Figure. 2. a) Nitrate concentrations in each reservoir over time, grey line indicates new seawater collection. b) Mean reservoir nitrate abundance relative to the present day  $p\text{CO}_2$  reservoir. Error bars are  $\pm\text{SD}$ ,  $n = 12$ . Linear regression,  $n = 50$ ,  $r^2 = 0.778$ ,  $p = <0.001$ .

### ***Benthic denitrification rates***

Benthic denitrification rates were determined in all sediment columns before the start of the experiment and once a week thereafter. The same amount of  $^{15}\text{NO}_3^-$  was added to each incubation ( $50 \mu\text{mol L}^{-1}$ ), therefore the  $^{15}\text{N}$ -labelling percentage differed in each incubation as a result of the variation in  $^{14}\text{NO}_3^-$  between the seawater reservoirs from which water was sub-sampled prior to the incubation. Oxygen was consumed rapidly within the first 20 to 30 minutes of the incubation, during which time some  $^{29+30}\text{N}_2$  production occurred. Denitrification rates were calculated from linear slopes of  $^{29+30}\text{N}_2$  production after oxygen had been fully consumed. Average rates of denitrification were  $54 (\pm 19)$ ,  $34 (\pm 14)$ ,  $39 (\pm 16)$  and  $37 (\pm 15) \mu\text{mol L}^{-1}$  for the LGM, present day, year 2100 and year 2300, respectively (Fig. 3). No significant changes in denitrification rates were observed when the conditions were compared on a weekly basis (1 way ANOVA,  $p = >0.1$ ). When rates were compared over the entire four weeks of the experiment, denitrification rates were slightly greater under Last Glacial Maximum conditions than the other conditions (based on 1-way ANOVA and Tukey's HSD  $p = <0.05$ ).

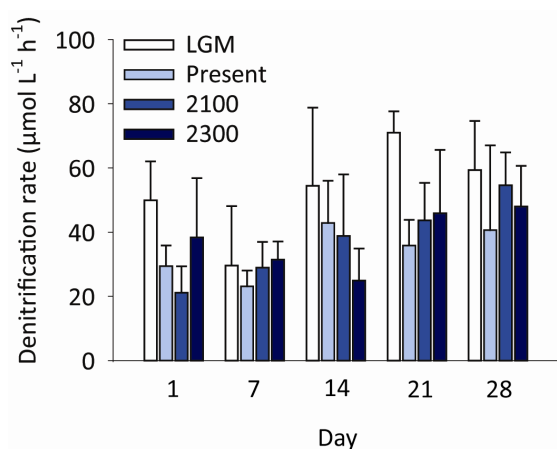


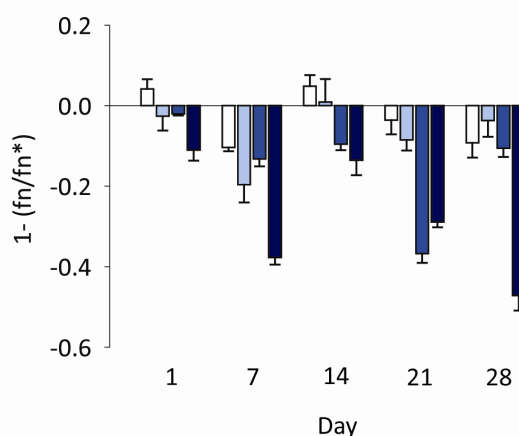
Figure 3. Average denitrification rates in each condition. Error bars are SD, n = 3

### Coupled nitrification-denitrification

The relative importance of benthic coupled nitrification-denitrification to overall denitrification rates can be estimated from differences in the known labeling percentage at the beginning of incubations ( $F_n$ ) and the apparent labeling percentage calculated from the ratio of  $^{29}\text{N}_2$  and  $^{30}\text{N}_2$  production  $F_n^*$ . An  $F_n^*$  value lower than  $F_n$ ,

i.e.  $1-(F_n/F_n^*)$  is negative, indicates that a source of  $^{14}\text{N}$  other than the  $^{14}\text{NO}_3^-$  present in the initial seawater must be present during the incubation. On days 1 and 14 in the LGM condition  $1-(F_n/F_n^*)$  was positive, but the high background concentrations of  $^{14}\text{NO}_3^-$  in the LGM condition, led to low  $^{15}\text{N}$ -labelling percentages (< 50%). Low labelling percentages produce greater errors in the isotope pairing method, and therefore we cannot conclude that the  $F_n^*$  values differed from  $F_n$ . At all other time points  $1-(F_n/F_n^*)$  was negative. The negative values were more pronounced in the high  $p\text{CO}_2$  conditions, throughout the entire experiment (Fig. 4).

Figure 4. Comparison of the labeling ratio of produced  $\text{N}_2$  ( $F_n^*$ ) and the labeling ratio of added  $\text{NO}_3^-$  ( $F_n$ ). Negative values indicate an additional source of  $^{14}\text{NO}_3^-$  was present in the incubations. Error bars are SD, n = 3





## Discussion

### *Water column nitrate*

The most dramatic result observed during this study was not within the sediment, but rather the effect of pH on the nitrate concentrations within the unfiltered seawater reservoirs that supplied the sediment. All the reservoirs were supplied with water from the same header tank, which was periodically refilled with fresh seawater, this was responsible for some of the changes observed in nitrate concentrations, i.e. the trend seen in Fig. 2a for nitrate concentrations to drop over time as seawater aged in the header tank. A more intriguing observation was that, at any given time point, nitrate concentrations in the  $p\text{CO}_2$  adjusted reservoirs differed (Fig. 2b). Nitrate concentrations in the Last Glacial Maximum reservoir were always greater than present day conditions, while nitrate concentrations in the future condition were lower. The response was linear; a doubling in  $p\text{CO}_2$  led to a decrease in nitrate concentrations of 36% (Fig. 2b). Intriguingly, no concurrent change in ammonium concentrations was observed in the reservoirs.

It is unlikely that nitrate concentrations in the reservoirs were directly affected by changes in seawater pH, as nitrate speciation is insensitive to the moderate changes we induced in pH and carbonate chemistry (Zeebe 2001). We can therefore attribute the alterations in nitrate concentrations of the seawater reservoir to biological activity. The seawater reservoirs were kept in the dark; therefore changes in primary production are unlikely to have affected nitrate concentrations. Nevertheless, we cannot rule out that changes in N-uptake by phototrophic or other autotrophic organisms may have occurred, however we can only speculate as to which organisms may have been responsible for this. Diatoms can store nitrate intracellularly (Lomstein et al. 1990), and may have been induced to take up more nitrate in response to the light limited conditions (Kamp et al. 2011). Alternatively, many autotrophs use the Calvin-Benson

cycle to fix CO<sub>2</sub> and are possibly limited by the low affinity of RubisCO for CO<sub>2</sub> (Hutchins et al. 2009; Riebesell et al. 2007). High CO<sub>2</sub> conditions may have stimulated increased respiration by non-photosynthetic autotrophs (Kusian and Bowien 1997) and therefore increased nitrate uptake in these organisms.

Rather than changes in N-uptake, a change in nitrification rates could account for the different nitrate concentrations within the seawater reservoirs. The activity of chemolithoautotrophic nitrifiers is optimal in pH ranges of 7 to 8.5 and beyond this nitrification and growth is inhibited by free NH<sub>3</sub> and nitrous acid toxicity (Canfield et al. 2005), however the pH levels within this study did not extend outside of these optimal ranges. An inhibition in water column nitrification rates may be better explained by a reduction in the available substrate, due to shifts of the ammonia/ammonium buffer system (Bange 2008; Bell et al. 2008). Indeed other studies which have investigated water column nitrification responses to CO<sub>2</sub> have almost all found ocean acidification to be detrimental to nitrification (Beman et al. 2011). Ammonium oxidation rates showed an almost linear decrease from pH 8 to pH 6.5 (with a 40% decrease between pH 8.0 and 7.5) in euphotic and aphotic seawater (Huesemann et al. 2002). Our study used smaller increments of pH change, however the decrease we saw in nitrate concentrations in the reservoirs correlate extremely well with the decreases previously observed in oceanic nitrification rates. The negative correlation between nitrate and *p*CO<sub>2</sub> strongly indicates that N-cycling is affected in seawater by changes in *p*CO<sub>2</sub>. Future studies including direct nitrification experiments and examination of changes in CO<sub>2</sub> and nitrate uptake on a single cell level in natural seawater assemblages are therefore still required.

### ***Benthic denitrification and coupled nitrification-denitrification***

The dramatic changes that we observed in the seawater supply reservoirs in response to different *p*CO<sub>2</sub> conditions were not reflected in denitrification rates within the sediment. Overall, denitrification rates did not change in response to *p*CO<sub>2</sub> (Fig. 3).

This was not unexpected because a direct effect of  $p\text{CO}_2$  or pH on denitrification is not known. However, nitrate supply from the overlying is known to regulate denitrification in muddy diffusive sediments (Seitzinger et al. 2006). Because nitrate inputs varied from one  $p\text{CO}_2$  condition to the next (on average  $37 \mu\text{mol L}^{-1}$  in the LGM condition compared to  $15 \mu\text{mol L}^{-1}$  in the 2300 condition), an effect on benthic denitrification might be expected. Nevertheless, a concentration effect on denitrification rates was not observed. Instead, the main effect of future  $p\text{CO}_2$  conditions was to increase the contribution of benthic  $^{14}\text{NO}_x$  to denitrification, as indicated by the isotope distributions. Production of  $^{29}\text{N}_2$  relative to  $^{30}\text{N}_2$  was higher than expected when compared to the initial labeling percentage and under increasing  $p\text{CO}_2$  the proportion of excess  $^{29}\text{N}_2:^{30}\text{N}_2$  increased substantially (Fig. 4).

Three possible processes could account for the mismatch between labeling percentages: 1) an increase in anammox, which by coupling  $^{14}\text{NH}_4^+$  and  $^{15}\text{NO}_3^-$ , would increase the production of  $^{29}\text{N}_2$  but not  $^{30}\text{N}_2$ . 2) an increase in the release of  $^{14}\text{NO}_3^-$  stored in eukaryotes (Marchant et al. 2013a). 3) an increase in the contribution of  $^{14}\text{NO}_3^-$  from benthic nitrification to denitrification. Previous studies have indicated that anammox is not a substantial process in these sediments (Gao et al. 2012; Marchant et al. 2013b). There is also no evidence that anammox might be stimulated by high  $p\text{CO}_2$  or lowered pH and furthermore anammox bacteria use the acetyl co-a pathway rather than the low affinity RubisCO enzyme to fix  $\text{CO}_2$  (Strous et al. 2006).

The storage of nitrate intracellularly by organisms such as diatoms can play an important role in benthic nitrogen cycling in permeable sediments (Marchant et al., submitted, Stief et al. 2013). Increased nitrate storage in response to lower nitrate concentrations could have led to the negative  $F_N/F_n^*$  values as passive equilibration of intracellular  $^{14}\text{NO}_3^-$  contribution with porewater  $^{15}\text{NO}_3^-$  may have occurred (Dähnke et al. 2012; Sokoll et al. 2012). However, our sediment was kept in the dark for almost 3 months (including pre-incubation time), and diatoms are not predicted to survive in an active state within sediment for such long time periods (Kamp et al. 2011). Moreover, most diatoms have been shown to respire nitrate to ammonium rather than  $\text{N}_2$  (Kamp et

al. 2011). Nevertheless, it is important that future studies examine whether changes in the pool of intracellularly stored nitrate occur, as increases in the proportion of stored nitrate could lead to shifts in the community responsible for in N-loss.

The most likely explanation for the increased  $^{29}\text{N}_2$  production under high  $p\text{CO}_2$  is a closer coupling between benthic nitrification and denitrification. Our observations can be explained by benthic nitrification increasingly contributing  $^{14}\text{NO}_3^-$  to denitrification relative to  $^{14}\text{NO}_3^-$  from the water column. This would indicate that benthic nitrification is not as sensitive to changes in  $p\text{CO}_2$  as has been shown for water column nitrification (Beman et al. 2011). Coastal permeable sediments have large fluctuations in pH over a tidal cycle (De Beer et al. 2005; Jansen et al. 2009). Therefore, unlike the pelagic realm, where pH fluctuations are rare, part of the nitrifying community within the sediment is more likely to be adapted to lowered pH. In fact, Gieseke et al. (2006) have demonstrated before that nitrifiers within sediments may not be as susceptible to changes in pH as those in the pelagic realm. Furthermore, physiological adaptations to low pH have been observed in nitrifiers in soil sediments, where they are known to be able to use urea as an alternative substrate to ammonia (Pommerening-Röser and Koops 2005). If an adapted community in the sediment does exist, then a decrease in nitrification would not be expected (Kitidis et al. 2011). As nitrate inputs from the seawater-supply decreased under higher  $p\text{CO}_2$ , benthic nitrification may have become proportionally more important as a source of  $\text{NO}_3^-$  to denitrification.

### ***Implications for coastal N cycling***

This study has shown that the impact of ocean acidification on permeable sediments cannot easily be determined without taking changes in the pelagic into account. A decrease in water column nitrate under high  $p\text{CO}_2$  conditions caused subtle changes in benthic nitrogen cycling; increasing coupled nitrification-denitrification, but not affecting overall benthic N-loss. In the environment the consequences of this increased coupling would be to limit the  $\text{NO}_3^-$  that escapes from the sediment back to

the water column. In combination with decreased pelagic nitrate concentrations (whether from decreased nitrification or increased uptake by aerobic chemoautotrophs) this could lead to further shifts in the  $\text{NO}_3:\text{NH}_4$  ratio within the water column. Therefore, changes in the source of nitrate for benthic denitrification could exacerbate shifts in the phytoplankton community, as some phytoplankton preferentially take up nitrate rather than ammonium (Beman et al. 2011).

Modelling approaches are often used to predict the response of the oceans to the wide range of changes that may occur as a result of ocean acidification. One such model for the North Sea takes decreases in pelagic nitrification into account (Blackford and Gilbert 2007), so far however, possible changes in pelagic N-uptake and changes in benthic N-cycling have not been considered. To be able to provide future models with enough data, it will be vital to measure nitrification directly in permeable sediments as well as N-uptake in pelagic waters under higher  $p\text{CO}_2$  conditions. While research onto the effects of ocean acidification on N-fixation continues apace, other processes, especially those that occur in the benthos have been overlooked as an important topic in ocean acidification research (Garrard et al. 2013). Changes in the N-inventory in the ocean can have profound effects on other biogeochemical cycles (Yool et al. 2007) and, therefore, must be included in future biogeochemical models.

## References

- Badger, M. R., and E. J. Bek. 2008. Multiple Rubisco forms in proteobacteria: their functional significance in relation to  $\text{CO}_2$  acquisition by the CBB cycle. *Journal of Experimental Botany* **59**: 1525-1541.
- Bange, H. W. 2008. Gaseous Nitrogen Compounds ( $\text{NO}$ ,  $\text{N}_2\text{O}$ ,  $\text{N}_2$ ,  $\text{NH}_3$ ) in the Ocean, p. 51-94. *Nitrogen in the Marine Environment* (2nd Edition). Academic Press.
- Bell, T. G., M. T. Johnson, T. D. Jickells, and P. S. Liss. 2008. Ammonia/ammonium dissociation coefficient in seawater: A significant numerical correction (vol 4, pg 183, 2007). *Environ. Chem.* **5**: 258-U258.
- Beman, J. M. and others 2011. Global declines in oceanic nitrification rates as a consequence of ocean acidification. *Proceedings of the National Academy of Sciences* **108**: 208-213.

- Billerbeck, M., U. Werner, K. Bosselmann, E. Walpersdorf, and M. Huettel. 2006a. Nutrient release from an exposed intertidal sand flat. *Mar. Ecol.-Prog. Ser.* **316**: 35-51.
- Billerbeck, M., U. Werner, L. Polerecky, E. Walpersdorf, D. De Beer, and M. Huettel. 2006b. Surficial and deep pore water circulation governs spatial and temporal scales of nutrient recycling in intertidal sand flat sediment. *Mar. Ecol.-Prog. Ser.* **326**: 61-76.
- Blackford, J. C., and F. J. Gilbert. 2007. pH variability and CO<sub>2</sub> induced acidification in the North Sea. *Journal of Marine Systems* **64**: 229-241.
- Caldeira, K., and M. E. Wickett. 2003. Anthropogenic carbon and ocean pH. *Nature* **425**: 365-365.
- Canfield, D. E., B. Thamdrup, and E. Kristensen. 2005. *Aquatic Geomicrobiology*. Elsevier Academic Press.
- Chipman, L., M. Huettel, and M. Laschet. 2012. Effect of benthic-pelagic coupling on dissolved organic carbon concentrations in permeable sediments and water column in the northeastern Gulf of Mexico. *Continental Shelf Research* **45**: 116-125.
- Dähnke, K., A. Moneta, B. Veuger, K. Soetaert, and J. J. Middelburg. 2012. Balance of assimilative and dissimilative nitrogen processes in a diatom-rich tidal flat sediment. *Biogeosciences* **9**: 4059-4070.
- De Beer, D. and others 2005. Transport and mineralization rates in North Sea sandy intertidal sediments, Sylt-Romo Basin, Wadden Sea. *Limnology and Oceanography* **50**: 113-127.
- Devol, A. H. 1991. Direct measurement of nitrogen gas fluxes from continental-shelf sediments. *Nature* **349**: 319-321.
- Gao, H. and others 2012. Intensive and extensive nitrogen loss from intertidal permeable sediments of the Wadden Sea. *Limnology and Oceanography* **57**: 185-198.
- . 2010. Aerobic denitrification in permeable Wadden Sea sediments. *Isme Journal* **4**: 417-426.
- Garrard, S. and others 2013. Biological impacts of ocean acidification: a postgraduate perspective on research priorities. *Marine Biology* **160**: 1789-1805.
- Gieseke, A., S. Tarre, M. Green, and D. De Beer. 2006. Nitrification in a biofilm at low pH values: Role of in situ microenvironments and acid tolerance. *Applied and Environmental Microbiology* **72**: 4283-4292.
- Houghton, J., Y. Ding , Griggs D.J., Noguer M., Van Der Linden P.J., and X. D. 2001. *Climate Change 2001: The Scientific Basis*. . In IPCC Third Assessment Report: *Climate Change 2001* Cambridge University Press, Cambridge.
- Huesemann, M. H., A. D. Skillman, and E. A. Creelius. 2002. The inhibition of marine nitrification by ocean disposal of carbon dioxide. *Marine Pollution Bulletin* **44**: 142-148.
- Huettel, M., and G. Gust. 1992. Impact of bioroughness on interfacial solute exchange in permeable sediments. *Marine Ecology Progress Series* **89**: 253-267.

- Hutchins, D. A. and others 2007. CO<sub>2</sub> control of Trichodesmium N<sub>2</sub> fixation, photosynthesis, growth rates, and elemental ratios: Implications for past, present, and future ocean biogeochemistry. *Limnology and Oceanography* **52**: 1293-1304.
- Hutchins, D. A., M. R. Mulholland, and F. X. Fu. 2009. Nutrient Cycles and Marine Microbes in a CO<sub>2</sub>-Enriched Ocean. *Oceanography* **22**: 128-145.
- Jansen, S., E. Walpersdorf, U. Werner, M. Billerbeck, M. E. Bottcher, and D. De Beer. 2009. Functioning of intertidal flats inferred from temporal and spatial dynamics of O<sub>2</sub>, H<sub>2</sub>S and pH in their surface sediment. *Ocean Dyn.* **59**: 317-332.
- Kamp, A., D. De Beer, J. L. Nitsch, G. Lavik, and P. Stief. 2011. Diatoms respire nitrate to survive dark and anoxic conditions. *Proceedings of the National Academy of Sciences* **108**: 5649-5654.
- Kitidis, V. and others 2011. Impact of ocean acidification on benthic and water column ammonia oxidation. *Geophysical Research Letters* **38**: L21603.
- Kusian, B., and B. Bowien. 1997. Organization and regulation of cbb CO<sub>2</sub> assimilation genes in autotrophic bacteria. *Fems Microbiol. Rev.* **21**: 135-155.
- Levitan, O. and others 2007. Elevated CO<sub>2</sub> enhances nitrogen fixation and growth in the marine cyanobacterium Trichodesmium. *Global Change Biology* **13**: 531-538.
- Lomstein, E., M. H. Jensen, and J. Sorensen. 1990. Intracellular NH<sub>4</sub><sup>+</sup> and NO<sub>3</sub><sup>-</sup> pools associated with deposited phytoplankton in a marine sediment (Aarhus Bight, Denmark). *Marine Ecology Progress Series* **61**: 97-105.
- Marchant, H., G. Lavik, M. Holtappels, and M. M. Kuypers. 2013a. The fate of nitrate in intertidal permeable sediments. *PloS one* **Submitted**.
- Marchant, H. and others 2013b. Nitrous oxide emissions from coastal sands due to anthropogenic nitrogen input. *Nature Geoscience* **In revision**.
- Orr, J. C. and others 2005. Anthropogenic ocean acidification over the twenty-first century and its impact on calcifying organisms. *Nature* **437**: 681-686.
- Passow, U., and C. A. Carlson. 2012. The biological pump in a high CO<sub>2</sub> world. *Marine Ecology Progress Series* **470**: 249-271.
- Pierrot, D. E. L., and D. W. R. Wallace. 2006. MS Excel Program Developed for CO<sub>2</sub> System Calculations. ORNL/CDIAC-IOS.
- Pommerening-Röser, A., and H.-P. Koops. 2005. Environmental pH as an important factor for the distribution of urease positive ammonia-oxidizing bacteria. *Microbiological Research* **160**: 27-35.
- Riebesell, U. and others 2007. Enhanced biological carbon consumption in a high CO<sub>2</sub> ocean. *Nature* **450**: 545-U510.
- Rost, B., I. Zondervan, and D. Wolf-Gladrow. 2008. Sensitivity of phytoplankton to future changes in ocean carbonate chemistry: current knowledge, contradictions and research directions. *Mar. Ecol.-Prog. Ser.* **373**: 227-237.
- Sabine, C. L. and others 2004. The oceanic sink for anthropogenic CO<sub>2</sub>. *Science* **305**: 367-371.
- Seitzinger, S. and others 2006. Denitrification across landscapes and waterscapes: a synthesis. *Ecol Appl* **16**: 2064-2090.

- Sokoll, S. and others 2012. Benthic nitrogen loss in the arabian sea off pakistan. *Frontiers in microbiology* **3**: 395-395.
- Stief, P., A. Kamp, and D. De Beer. 2013. Role of diatoms in the spatial-temporal distribution of intracellular nitrate in intertidal sediment. *PloS one* **8**: e73257-e73257.
- Strous, M. and others 2006. Deciphering the evolution and metabolism of an anammox bacterium from a community genome. *Nature* **440**: 790-794.
- Suzuki, I., U. Dular, and S. C. Kwok. 1974. Ammonia or Ammonium Ion as Substrate for Oxidation by *Nitrosomonas europaea* Cells and Extracts. *Journal of Bacteriology* **120**: 556-558.
- Thamdrup, B., and T. Dalsgaard. 2002. Production of N<sub>2</sub> through anaerobic ammonium oxidation coupled to nitrate reduction in marine sediments. *Applied and Environmental Microbiology* **68**: 1312-1318.
- Walker, C. B. and others 2010. *Nitrosopumilus maritimus* genome reveals unique mechanisms for nitrification and autotrophy in globally distributed marine crenarchaea. *Proc. Natl. Acad. Sci. U. S. A.* **107**: 8818-8823.
- Ward, B. B. 1987. Kinetic-studies on ammonia and methane oxidation by *Nitrosococcus oceanus*. *Archives of Microbiology* **147**: 126-133.
- Yool, A., A. P. Martin, C. Fernandez, and D. R. Clark. 2007. The significance of nitrification for oceanic new production. *Nature* **447**: 999-1002.
- Zachos, J., M. Pagani, L. Sloan, E. Thomas, and K. Billups. 2001. Trends, rhythms, and aberrations in global climate 65 Ma to present. *Science* **292**: 686-693.
- Zeebe, R. E. A. W.-G. 2001. *CO<sub>2</sub> in Seawater: Equilibrium, Kinetics, Isotopes*. Elsevier.



## Chapter VIII

### **Going with the flow: Why we cannot neglect the importance of the coastal sand filter in the anthropocene**

**Hannah K. Marchant<sup>1\*</sup>, Moritz Holtappels<sup>1</sup> and Marcel M.M. Kuypers<sup>1</sup>**

<sup>1</sup>Max Planck Institute for Marine Microbiology, Celsiusstrasse 1, 28359 Bremen, Germany

\* Corresponding author: hmarchan@mpi-bremen.de, tel: +49421-2028630, fax: +49421-2028790

Keywords: advection; anthropogenic change; bioreactor; microbial community; nitrogen cycling; permeable sediment;

Author Contributions:

H.K.M., M.H. and M.M.M.K. conceived wrote and edited the manuscript

**In preparation for: *Nature Reviews Microbiology***

**Abstract**

Sandy, permeable sediments characterize most of the coastal zone and 70% of the continental shelves, however benthic microbial ecology and biogeochemical cycling has focused almost exclusively on muddy diffusive sediments. While it has been recognized for over a decade that microbiology in sandy sediments is controlled by distinctly different factors from muds, chiefly due to the effects of advective transport, they are still under-represented in our understanding of the benthic environment. In this opinion piece we argue that despite the ingrained paradigms and methodological problems which have stymied work on sandy sediments, it is no longer appropriate to treat all sediments as if they were muddy. Instead we show that by thinking about sands as a biocatalytic filter with a mosaic of active microbial element cycling we can begin to understand how these sediments catalyze the removal of organic matter and nitrate. To date we know that these sediments are sites of intense microbial and biogeochemical activity, however the consequences of this activity are poorly understood. From organic matter removal, to N-loss, to the discovery of new microbial potential we still have a lot to learn. Perhaps most importantly, the extent to which the microbial community of the coastal filter can buffer the open ocean from anthropogenic impacts is still an open question.

### **The common perception of marine sediments**

Marine sediments harbor more microorganisms than any other environment on our planet and play a key role in many global element cycles. Hence it is not surprising that the microbiology of marine sediments has received a lot of attention over the last decades and even centuries. Most of these studies have focused on fine grained, cohesive sediments that are found in regions with reduced bottom water current velocities such as the deep sea, or in estuaries and upwelling regions with high primary production. Fine grained sediments are often rich in organic carbon, particularly in regions that receive a substantial organic matter load and are characterized by a stable redox zonation with depth (Jorgensen, 1977; Froelich et al., 1979; Sorensen et al., 1979; Canfield et al., 1993a; Thamdrup et al., 1994), which is accompanied by a similar zonation in microbial communities (Sorensen and Jørgensen, 1987; Jorgensen and Revsbech, 1989). This zonation is caused by microbial respiration in combination with diffusion limited transport of electron acceptors. Electron acceptor limitation forces microorganisms inhabiting these diffusive sediments to switch from oxygen respiration in the surface to nitrate, manganese (IV), iron (III), and sulfate-respiration and finally fermentation and methanogenesis at depth. Often the zones where oxygen and nitrate respiration occurs are no more than a few mm thick in these sediments (Canfield et al., 1993b).

### **Neglected importance of permeable sediments**

In contrast to fine grained sediments, coarse grained sediments have received relatively little attention by microbiologists and biogeochemists. As coarse grained sediments are typically organic matter poor (Keil et al., 1994), they were considered to have little microbial activity and their contribution to overall carbon mineralization was neglected (Boudreau et al., 2001). This appeared to be confirmed by early experiments, in which incubations were carried out under diffusive conditions, leading to low respiration and

mineralization estimates (Lohse et al., 1993). However, coarse grained sediments are permeable and therefore allow advective porewater flow. This completely changes the governing conditions in the sediment, removing the transport limitations that control microbial activity in diffusive sediments. In fact, the low organic matter content of these sediments is misleading, and rather than indicating a system in which little microbial activity occurs is a result of high turnover and an active and diverse microbial community (Boudreau et al., 2001).

Although coastal areas are dominated by coarse grained sediments (Emery, 1968), microbial community structure, diversity, rates of organic matter mineralization and nutrient cycling are still understudied in these sediments. One of the reasons that studies are scarce is that the highly dynamic nature of porewater transport in permeable sediments strongly complicates estimation of exchange rates of chemical compounds between sediments and bottom water. Many in-situ approaches to measure benthic fluxes such as benthic chamber incubations and O<sub>2</sub>-microsensor profiles do not account for advective porewater flow, or change flow conditions to the extent that results are no longer relevant (Janssen et al., 2005).

Figure 1 shows the few studies which explicitly take into account coarse grained sediments. Those that have been carried out are biased towards a few sites around the world, in particular the temperate intertidal sand flats of the Wadden Sea, which are easily accessible and where sampling and in-situ measurements are facilitated (for examples see (Huettel and Rusch, 2000; de Beer et al., 2005; Billerbeck et al., 2006a; Werner et al., 2006; Jansen et al., 2009; Gao et al., 2012). Observations of the intertidal are hard to extrapolate to the subtidal as the alternation between exposure of sand flats during low tide and inundation during high tide creates a specific porewater flow regime, different from the subtidal driving forces of porewater flow (Billerbeck et al., 2006b).

Since most permeable sediments are found in subtidal areas there is a substantial lack of knowledge about the regulation of microbial processes and their contribution to global budgets of carbon and nitrogen turnover. Most strikingly, no

studies have been carried out within the Arctic, which contributes 20% of the world's continental shelf area (Macdonald et al., 1998). The Arctic Ocean is a site of high primary productivity as well as receiving almost 10% of the total global river discharge (Holmes et al., 2001). Therefore this region currently represents a major gap in our understanding of global sediments. The arctic ecosystem is changing rapidly (Wassmann et al., 2011), therefore to ensure that we understand the biogeochemical transformations that occur in the sediments of the arctic future studies must take sediment permeability into account or risk underestimating fluxes.

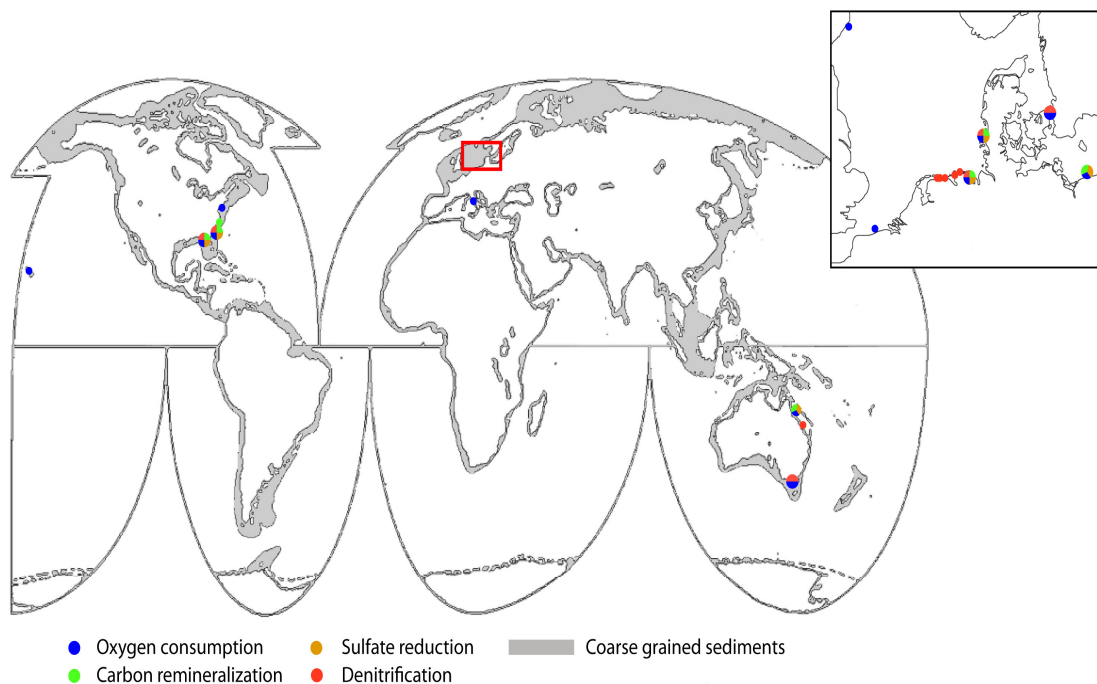


Figure 1. The global distribution of coarse grained permeable sediments on continental shelves (adapted from Emery, 1968). Marked are areas where studies have been undertaken in which the permeable nature of sediments has been explicitly taken into account and experiments designed accordingly. The inlay represents the North Sea, including the Wadden sea, where the vast majority of research has taken place so far.

### The role of permeable sediments in removal of anthropogenic N input

Anthropogenic activities, namely fertilizer use and fossil fuel burning have more than doubled the level of fixed nitrogen (N) in the environment, such that, on land humans

now supply more N than biological nitrogen fixation (Galloway et al., 2004). Worldwide, coastal seas receive a significant amount of this N through riverine run off (48 Tg N yr<sup>-1</sup>, (Boyer et al., 2006)) or atmospheric deposition (Duce et al., 2008). Coastal seas act as a buffer, protecting the open ocean from the impact of anthropogenically derived N, most of which is denitrified in sediments (Gruber and Galloway, 2008). The biocatalytic nature of permeable sediments in coastal eutrophied regions filters and removes large amounts of N inputs from the terrestrial system and acts as a reactor for the remineralization of large amounts of the organic matter produced by enhanced primary production (Cook et al., 2006; Gao et al., 2012). Yet the extent to which coastal permeable sediments can continue to remove N in the face of growing loads is unknown.

One place in which we are beginning to understand the role of permeable sediments is the Wadden Sea, a UNESCO world heritage site, dominated, like most coastal seas by permeable sandy sediments. Today riverine agricultural run-off dominates N inputs into the Wadden as it acts as a catchment area for a large part of Europe, including the rivers Rhine and Elbe (Deek et al., 2012). Despite this, the Wadden provides a well studied example of how coastal areas have changed in the last 100 years. Since the industrial revolution N loads from rivers have increased by a factor of eight and atmospheric deposition has doubled (van Beusekom, 2005). In the past, a complex 3D habitat existed in the Wadden Sea, in which seagrass was the main source of primary production and structure was provided by native oyster banks and reef forming polychaetes (Lotze et al., 2005). Today however, it is characterized by high primary and secondary production dominated by green algae, polychaetes and invasive invertebrate species. The decline of seagrass indicates poor ecosystem health, which can largely be attributed to the direct and indirect effects of eutrophication (Burkholder et al., 2007 and references therein)

Therefore, the Wadden Sea no longer represents a pristine ecosystem, yet, despite the large N-inputs, there has not been a concurrent rise in N exported to the open ocean. This is attributed to benthic denitrification in the permeable sands, which

occurs at some of highest rates ever recorded in the marine environment (Gao et al., 2012). In contrast, denitrification rates are lower within similar sediments from more pristine coastal sediments in the Australia (Evrard et al., 2012). The coastal environment from that study could be seen as a proxy for the Wadden Sea ecosystem before the industrial revolution. Therefore we suggest that permeable sediments are inherently adaptable and have the capability to deal with increasing organic and inorganic loads, a property which is likely a result of advective pore water flow.

### **Drivers and consequences of advective porewater flow**

Advective porewater transport has historically been a field of hydrogeology, used to describe subsurface groundwater flow in aquifers. Interactions between open water flow and porewater flow through underlying permeable bedforms as found in rivers and coastal waters were first described by Webb and Theodore (1968) and Thibodeaux and Boyle (1987). In the 1990's Huettel and Gust (1992), Rutherford et al. (1993) and Shum and Sundby (1996) started to investigate advective porewater flow in light of benthic organic matter turnover. They showed that porewater flow accelerates solute transport into the sediment by more than two orders of magnitude compared to molecular diffusion (Huettel et al., 2003) and that particulate matter is effectively filtered by permeable sands (Huettel et al., 1996). Subsequently it was found that advective porewater flow can increase oxic respiration (de Beer et al., 2005) and denitrification rates (Gao et al., 2012) by a factor of 10. This is a result of advective transport, which allows efficient transport of compounds at even low concentrations, whereas diffusive transport depends on concentration gradients.

Classical measurements of porewater concentrations of electron acceptors and donors are therefore inappropriate proxies for the activity of the microbial community in permeable sediments unless the flow velocity is considered. Furthermore, the common concept of intense element redox cycling between oxidized and reduced sediment layers becomes obsolete under advective flows. Because solute transport is

flow directed, trajectories of advective porewater flow start and end in the water column (Figure 2). The various electron acceptors are successively reduced on their way through the sediment and will not be re-oxidized until they are released directly into the oxenic water column. The depth oriented and bidirectionally coupled redox zones in cohesive sediments turn into flow oriented and unidirectionally coupled redox zones in advective sediments (Figure 2).

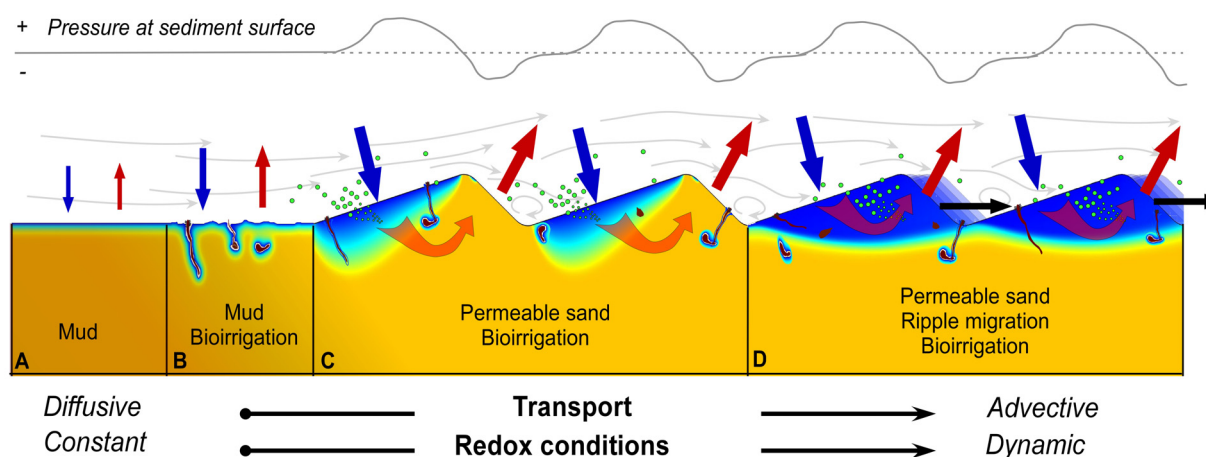


Figure 2: Different forms of mass transport control the exchange of electron acceptors (blue arrows) and reduced compounds (red arrows) between the water column and sediment, causing different penetration depths of electron acceptors (blue color denotes high concentrations). (A) In laminated muddy sediments transport is diffusion limited and directed along concentration gradients. Oxidized and reduced solutes are transported across the same surface and may interact (redox cycling). Where macrofauna is absent the perturbation is minimal and a stable redox zonation is established. (B) Macrofauna burrows enlarge the available surface area for diffusive mass transport. Advective ventilation of the burrows (bioirrigation) and macrofauna respiration increase the mass transport. Burrowing activity (bioturbation) causes less stable redox conditions. (C) In permeable sand, mass transport is dominated by porewater advection and is aligned with the porewater flow field. Here, the obstruction of the flow by a ripple causes sites of high and low pressure at the stoss and lee side, respectively. Fluxes of oxidized and reduced solutes are increased and appear separately at the high and low pressure sites. Variable bottom water flow induces variable porewater flow which leads to highly dynamic redox conditions. (D) Ripples migrate (black arrow) with sediment grains being eroded at the stoss side and deposited at the lee side. This goes along with the release of porewater (stoss side) and the trapping of bottom water (lee side). At increasing migration velocities, pressure gradients change too fast for an effective net transport of porewater at depth causing the separation of well flushed ripple sediment from underlying reduced sediments.

This phenomenon can be observed on intertidal sand flats where gravity driven porewater flow causes the efflux and accumulation of sulphide rich waters in troughs of larger ripples shortly after exposure of the sand flat (Jansen et al., 2009). On a smaller scale the same phenomenon is indicated by different sediment colors of ripple troughs



and crests that reflect different redox conditions along the sediment surface (Huettel et al., 1998). Here, water enters the sediment at the slope of the ripple and leaves the sediment behind the ripple crest. A further consequence of the fast and flow directed solute transport is that microbial processes in the sediment depend directly on the chemical composition of the injected bottom water, whereas the recycling loops in diffusion limited sediments cause a delayed and attenuated response which evens out any short term fluctuations of bottom water properties.

Porewater flow is induced and directed by pressure gradients that occur on several temporal and spatial scales. The numerous driving forces of porewater flow were recently reviewed by Santos et al. (2012). The most wide spread drivers of porewater flow, which are not confined to land-ocean transition areas are bioirrigation and the interaction between bottom water flow and seabed topography. Advective transport by bioirrigation (i.e. the fauna induced flushing of benthic burrows with overlying bottom water) takes place on centimeter scales, varies within seconds to minutes and significantly enhances the exchange of chemical compounds between water column and sediments, whether in permeable or diffusion limited sediment (Aller, 1988; Kristensen, 1988). In diffusion limited sediments the burrows significantly enlarge the redox active surface layer (Figure 2), which can result in a several fold increase of denitrification rates (Pelegri et al., 1994), and increases the total benthic oxygen uptake by a factor of 2 (Glud, 2008). In permeable sediments, bioirrigation causes advective porewater transport in the adjacent sediments which is forced by species and behavior specific fluid pumping (Meysman et al., 2007; Volkenborn et al., 2010).

Bioirrigation is behaviorally triggered and depends on the abundance of infauna, but it does not directly dependent on the hydrodynamics of the bottom water. In contrast, the other wide spread driving force for porewater flow arises from the interaction between bottom water hydrodynamics and seabed topography (Thibodeaux and Boyle, 1987). Obstruction of bottom water flow by topographic features such as ripples or dunes cause pressure gradients along the sediment surface, which induce a transport of porewater through the permeable sediment from locations of high pressure

to those of low pressure (Figure 2). The pressure gradients depend on the flow velocity of the bottom water and the shape and dimensions of the topographic feature. The resulting porewater flow depends on the pressure gradients and the permeability of the sediment (Darcy's law).

### **The effect of sediment transport**

Sediment ripples and dunes migrate when surface sediments are resuspended and redistributed. These so called morphodynamics are again tightly coupled to the bottom water hydrodynamics and the sediment composition, which in turn determine the availability of electron acceptors and the amount of particulate organic matter that is retained. The induced porewater transport creates an environment of highly dynamic redox conditions. At low bottom water current velocities, sediment transport is minimized and the seabed morphology does not change with time. At these times the permeable sediment acts to continuously filter the bottom water and retains organic particulate matter (Huettel et al., 1996; Huettel and Rusch, 2000). As the bottom water velocities increase, ripples and dunes start to migrate (Li and Amos, 1999) and an increasing fraction of the sediment is redistributed during which accumulated particles and dissolved compounds are being washed out. The higher the rate of sediment redistribution, the shorter the filtration time and the higher the frequency of filter wash outs, while bottom water and porewater composition become more similar. A special case exists where high ripple migration velocities decrease the porewater residence time in the ripple to such an extent that the entire ripple stays oxic (Figure 2). Along with the high ripple migration velocities a continuously fast change of the pressure field along the sediment surface prevents effective porewater transport between the deep sediment and the overlying ripples (Precht et al., 2004). The consequence is the formation of two distinct sediment domains: the anoxic diffusion limited deep sediment and the oxic fast migrating ripple.

In summary, it can be expected that the ratio of particulate organic carbon to electron acceptors in permeable sediments is strongly affected by the rate of sediment redistribution. It becomes apparent that micro-organisms face redox conditions that are highly variable in time and space and potentially shape microbial communities that are very distinct from those found in diffusion limited sediments under steady state conditions.

### **Abundance and spatial distribution of microbial communities**

For many years it was assumed that decreased surface area, lower organic content and higher predation pressure all contributed to low cell counts in coarse-grained sediments in comparison to cohesive sediments (Rusch et al., 2003). This helped to maintain the idea that sandy sediments were a desert compared to organic-rich cohesive sediments. However, like many of our previous assumptions, this idea was overturned by application of methods modified with sands in mind.

The publication of the first extensive description of the microbial community structure of coastal sandy sediments (Musat et al., 2006), revealed that cell counts are  $10^9$ ; the same order of magnitude as cohesive sediments. However unlike cohesive sediments, these microbes were firmly attached to sand grains, requiring stronger detachment procedures to allow correct counts. Diversity and function within these sediments have mainly been investigated using 16s rRNA analyses (both low resolution community fingerprinting (Böer et al., 2009b) clone libraries and next generation sequencing (Gobet et al., 2012)), FISH for abundance and identification (Musat et al., 2006; Gittel et al., 2008), specific gene analysis (mainly for SRB, Amo and NosZ (Scala and Kerkhof, 1999; Mills et al., 2008)), and extracellular enzyme activity (Arnosti et al., 2009; Böer et al., 2009a). These have identified that the abundant groups in sandy sediments appear to be Bacteroidetes, Gammaproteobacteria, Deltaproteobacteria, Alphaproteobacteria and Planctomycetes (Rusch et al., 2003; Hunter et al., 2006).

Furthermore the community within the sediment is partitioned into two distinctive groups, those in the porewater, which strongly reflect the overlying water community and make up as little as 0.2% of the overall cell abundance (Rusch et al., 2003; Gobet et al., 2012), and those which are attached to sand grains. Therefore as awareness of the importance of permeable sediments has grown and studies have increased, it has become possible to begin to describe the major spatial and temporal gradients of the microbial communities which inhabit them (Fig. 3).

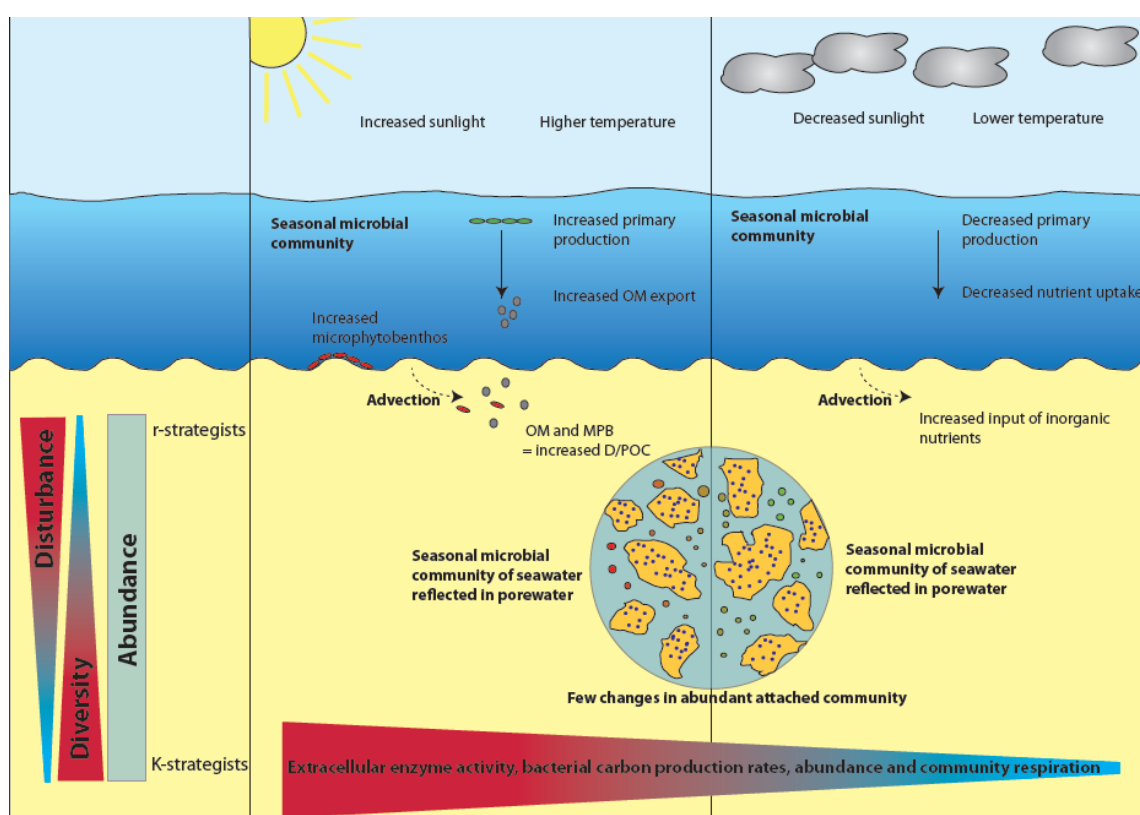


Figure 3. Factors structuring microbial communities within sandy sediments. a) Depth related changes, b and c) Seasonal changes between summer and winter respectively and d) Seasonal changes within the porewater and attached community.

While overall abundance and biomass of microbes does not tend to change with depth, diversity does increase, it has been hypothesized that this is a result of increasing physico-chemical stability with depth, in which slow growing specialists have time to adapt to niches. In contrast diversity is lower in the top layer which is subject to strong

temporal variations, allowing fast growing r-strategists dominate. This is demonstrated by the high abundance of *Gammaproteobacteria* in the upper layers of permeable sediments (Mills et al., 2008), which respond rapidly to the input of growth substrates such as buried phytodetritus, with no lag phase, suggesting that they are poised and prepared to exploit changes in conditions caused by phytoplankton blooms or storm events (Gihring et al., 2009).

What becomes apparent from the knowledge we have gained about microbial communities in permeable sediments is that the dynamic physico-chemical environment, dominated by advection, increased light and mixing with the surface layer provides a very different habitat than redox stratified cohesive sediments. This is not to say however that the same patterns are always found in sands, and the paucity of data makes any generalization tentative. For example depth related changes in bacterial abundance and exo-enzymatic activity appear to be unusual and unlikely within the advectively influenced layers of permeable sediments (Rusch et al., 2003; Musat et al., 2006; Misić and Harriague, 2007; Gittel et al., 2008), nevertheless they have been observed (Böer et al., 2009a), and the factors which drive these inconsistent observations will remain elusive until more studies are undertaken.

### **Temporal changes in microbial communities**

Temporal changes can also be identified in the communities within permeable sediments. Extracellular enzyme activity, bacterial carbon production rates, abundance and community respiration are all generally higher in summer, although this is often not reflected in biomass (Böer et al., 2009a; Böer et al., 2009b). Community changes are also observed (Gobet et al., 2012). The extent of our knowledge so far suggests the main factors controlling seasonal changes - all though by no extent the only factors - appear to be temperature, particulate/dissolved organic carbon inputs (P/DOC), and, porewater exchange with the overlying water (Scala and Kerkhof, 1999). Of these controls on

temporal variability, other than temperature, all are directly related to the permeable nature of sands.

P/DOC inputs in sandy sediments are dependent on the primary production occurring in the overlying water. Much of the organic matter generated during phytoplankton blooms settles on the sea floor in shallow coastal waters, and is then buried or transported by advection in to the sediment (Gihring et al., 2009). This leads to increases in POC and DOC, but also to changes in the available substrates, creating new niches. Although this situation is complicated somewhat by the relationship between the flushing of sandy sediments by higher winds and waves during winter seasons, which can lead to increases in P/DOC in the sediment that are temporally separated from phytoplankton blooms (Chipman et al., 2012).

Furthermore sandy sediments also support higher benthic primary production than muds, as light attenuation is lower in the overlying water column and silica based sediments refract more light (Grippio et al., 2010). The enhanced benthic microalgal community controls nutrient cycling by supplying new OM, therefore structuring the community (Jahnke et al., 2000). Seasonal changes are also related to the identity of microbes in the overlying water column, porewater communities reflect temporal succession in the water column due to advection, providing a “seed bank” to the more abundant, active and stable attached community.

### **Functional groups: appearance and activity under variable redox conditions**

So although sandy sediments are not redox stratified until below the advective layer, there are many open questions about the structure of sand communities. Are functional groups mixed homogenously in the sand? Is there spatial structuring dependent on substrate, or is the reality a mixture of the two? Instead of redox stratification, it may be better to describe permeable sediments as a “microbial mosaic”.

Oxygen dynamics are one of the most important parameters which structure sandy sediments. In the subtidal 3 layers can be defined, a surface layer which is

constantly oxic, a transition zone which is subject to oxic and anoxic conditions and a deep anoxic zone. The oxic and transition zone are the most intriguing of these, it has been hypothesized that in this area, there is a mosaic of strict anaerobes and strict aerobes, and that parts of this community become temporarily active or inactive depending on porewater biogeochemistry (Rusch et al., 2009). Overall, studies have identified microbes with the potential for aerobic heterotrophy, chemoorganotrophy, including fermentation and chemoautotrophy in layers of sediment which are exposed to both high and low oxygen. For example sulfate reducing bacteria and facultative anaerobes such as dissimilatory nitrate reducers have been observed in oxic zones of sandy sediments (Gaidos et al., 2011)

The mosaic structure of permeable sediments is highlighted by observations of sulfate reducing bacteria. One of the first indications that permeable sediment communities do not conform to the classical zonation pattern by redox potential came from direct observations. The presence of “black spots” of sulfate reduction in otherwise oxic sandy sediments of the Wadden (Freitag et al., 2003), led the authors to conclude that a “total loss of the otherwise predominant oxic and suboxic surface and subsurface zones” had occurred. Functional analysis showed that within these zones, diversity of specialized sulfide tolerant microbial communities were no different from the surrounding sediment; however there may have been a reduced functional aerobic diversity. Sulfate reducing bacteria (SRB), have been identified in the upper oxic and transitional zones of permeable sediments, contributing up to 17% of the community (Ishii et al., 2004; Mussmann et al., 2005; Musat et al., 2006; Gittel et al., 2008), furthermore the sulfate reducing community that is exposed to oxygen is capable of carrying out sulfate reduction almost immediately upon anoxic conditions being established within the sediment (Billerbeck et al., 2006b; Werner et al., 2006), indicating that they are an active and thriving community. SRB have been shown to have multiple strategies to cope with oxygen exposure, including the ability to switch between nitrate and sulfate as electron acceptors, oxygen reduction with a variety of electron donors to re-establish local anoxic conditions, and expression of protective enzymes such as

catalase and superoxide dismutase (see Dolla et al., 2006 for review). Cultivation of SRB has revealed that ecologically important SRB from permeable sediments have many of these adaptations. So far however, neither sulfate reduction in the presence of oxygen, nor oxygen reduction coupled to growth has been identified in SRB from these sites (Wieringa et al., 2000).

### **Denitrifiers**

In contrast to sulfate reduction, denitrification in the presence of oxygen has been observed in intertidal (Gao et al., 2010) and subtidal permeable sediments (Rao et al., 2008). *NirK*, *NirG* and *NosZ* detection points to a diverse and abundant denitrifying community which occur within zones frequently exposed to oxygen (Scala and Kerkhof, 2000; Mills et al., 2008), and which are actively involved in the processing of phytodetritus (Gihring et al., 2009). What must still be investigated in greater detail is the extent to which anaerobic respirations occur in the presence of oxygen within these sediments, which microbes are switching their respiration in response to oxygen, or in the case of the strict anaerobes, whether there is a cost to inactivity in the presence of oxygen. Interestingly, not all functional groups appear to be able to exploit the transitional oxic zone, so far as we can tell, methanogenesis and the anaerobic oxidation of methane with sulfate seem to be restricted only to the deep, constantly anoxic layer. What we can conclude however, is that permeable sediments, especially those within the intertidal zone, represent a diverse and interesting environment in which many novel and unique microbial pathways and strategies can be identified.

### **Microenvironments in permeable sediments**

Despite their lack of redox stratification, spatial differentiation still occurs in sands; communities are not homogenous and functional groups of microbes are not fully mixed. At a coarse level at least two distinct communities exist in sandy sediments – a



stable abundant biofilm community attached to sand grains, and a more transient community within the porewater. In fact, heterogeneity most likely exists at a number of scales which have not yet been studied (Fig. 4). Coarse grained sediments consist primarily of silicate sand grains, but can also contain Mn oxides, Fe hydr(oxid)es (Huettel et al., 1998), and particulate organic matter in the form of buried marine snow, microphytobenthos and fecal pellets (Gihring et al., 2009). Each of these provide a different habitat with regard to substrate, electron donor and acceptor, and therefore could be host to a specific microbial community. Furthermore the redox capacity of Mn oxides and Fe hydr(oxid)es will change if grains are physically redistributed and moved between oxic and anoxic sediment layers or during changes in oxygen penetration depth such as those observed in the intertidal (Jansen et al., 2009).

Further microenvironments are created by the small scale variability of porewater flow in the sediment. Model studies suggest that the flow velocity in the pore space of randomly distributed grains can differ significantly across a spatial distance of several grain diameters (Matyka et al., 2008; Hyman et al., 2012). This and biofilm formation at the level of single grains may create gradients in oxygen and other dissolved compounds, thus creating microenvironments with distinct microbial communities.

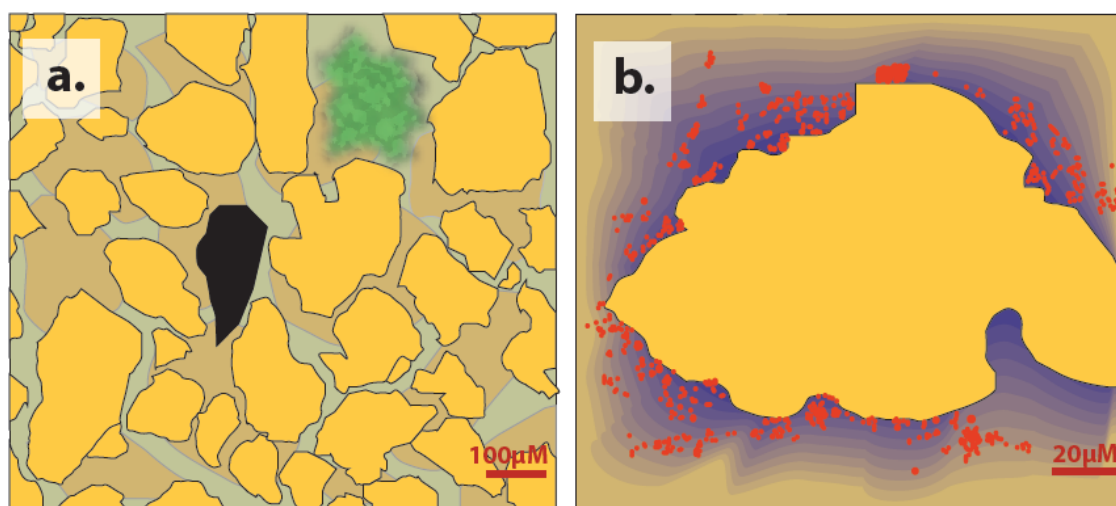


Figure 4. Microenvironments in permeable sediments. a) Different microenvironments in sediments formed by substrate/attachment surface, e.g. Sand grains, organic matter particles, manganese or iron (hydr)oxides. b) Microenvironments due to biofilm formation on surfaces e.g. oxygen gradients.

**Box 1. Lessons from bioreactors**

Our knowledge of the microbial ecology and biogeochemistry of permeable sediments is still to a large extent a black box, where the understanding gained from diffusive fine grained sediments is limited in its application. Can therefore, another field of study, namely bioreactor technology provide us with insights?

At the most basic level, permeable sediments resemble bioreactors in that the low carbon concentrations present in sands do not reflect low microbial activity, but high turnover rates; similar to “complex, non-linear bioreactors” (Santos et al., 2011). This is a rather simplistic approximation of bioreactor technology, which comprises its own deep and established research field, supporting a multimillion dollar industry (in 2011, the global membrane bioreactor market alone was worth an estimated \$746 million). In fact, the biocatalytic activity of permeable sediments, especially those in the intertidal, is representative of facets from a number of different bioreactor technologies. A consideration of these similarities may inspire and guide the growing field of permeable sediment research.

**Sand filters:** The most obvious systems to compare permeable sands to are bioreactors which encompass sands themselves, such as sand filters, which have been used for domestic wastewater treatment for over a hundred years (Healy et al., 2007). In these, wastewater which is percolated through sand, during which time large amounts of ammonium and organic matter can be removed. Efficiencies depend on the retention of bacteria, which is affected by grain size, hydraulic loading rate and adsorption of bacteria onto the sands (Kristian Stevik et al., 2004). All of these are factors which are likely also to affect biogeochemical cycling rates in natural permeable sands, and therefore give us a clear starting point when considering why some sands act differently from others. Sand filters however, have the disadvantage of rarely achieving reducing conditions

while a carbon source is still available, leading to nitrate production rather than  $N_2$ . Therefore, in a clear parallel to the situation on permeable sand flats, modified sand filters often involve a recirculation of water to an anoxic zone in which fresh organic matter is added, increasing N loss through denitrification, although so far this has had limited success in basic sand filters. Another problem with these basic filters is that they become clogged with bacteria, a phenomena which has been observed in natural sediments when excess EPS reduces permeability (Zetsche et al., 2012).

**Moving bed reactors:** This problem is solved in Moving Bed Reactors (Fig. 5) in which filtrate flows in an upward direction through a filter bed (such as sand) which is continuously moving downward, where it is removed and washed before being returned to the top of the bed (e.g. Puempel et al., 2003). In permeable sediments a similar effect is achieved through ripple movement and sediment reworking at high current velocities or bioturbation, which keep pore spaces open, maintaining permeability

**Aerobic-anaerobic bioreactors:** These reactors can be designed in a number of different ways, but in general are optimized to take advantage of both aerobic and anaerobic digestions, by either temporal or spatial separation of oxic and anoxic periods (Chan et al., 2009). Low energy consumption, low sludge production, high simplicity and the vast potential of resource recovery has made them extremely popular. Similar to permeable sediments, the enrichment of microbes capable of unusual processes such as aerobic denitrification can be stimulated by the frequent oscillations in oxygen in these bioreactors (Yao et al., 2012).

Although this is by no means an exhaustive account of the similarities between the biogeochemical cycling in permeable sediments and bioreactors, hopefully it has highlighted the links between the two research fields. It has long been recognized that permeable sediments resemble bioreactors, therefore the next logical step is to use bioreactor research as a map to future permeable sediment research.

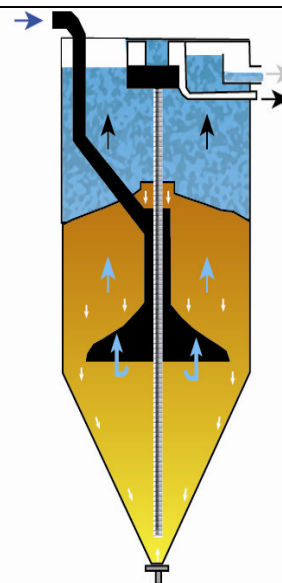


Fig 5. Schema of a moving bed sand filter. Water for treatment enters through the pipe on the left and flows upward through the sand. The sand itself is moving downwards continuously, where it is removed from the sand bed and washed before being released back on top. The sand acts as a filter, removing impurities from the water, the sand is cleaned by the scouring action created by forcing the dirty sand through the central pipe.

## Conclusions

Permeable sediments are still vastly under represented in studies of microbial benthic ecology. However, the ubiquity of permeable sediments in coastal regions means that further research is vital. In the face of growing anthropogenic loads and changing coastal ecosystems we need to understand how the microbial communities of permeable sediments function and interact with their environment. Hopefully in this piece we have highlighted those areas in which knowledge is still sparse.

An interdisciplinary approach is required to achieve a better understanding of role of microbes in the coastal filter. This must be based on the recognition that there are stark differences between diffusion controlled muds and permeable sandy environments. The path which further microbial ecology research takes will be shaped by improved knowledge of the physical environment that exists within permeable sediments; such as the inputs of oxygen, organic and inorganic substrates as well as observations of temporal and spatial variability at macro and microscales. There is the opportunity to learn a lot about this field in a short time by constant reappraisal of methods which have been designed with muddy sediments in mind and by inclusion of the lessons learned from the analogous field of bioreactors.

Hopefully the combination of these approaches in well studied eutrophied permeable sediments such as the Wadden Sea, more pristine environments such as those in Australia, as well as those which are likely to be subject to growing anthropogenic changes in the future such as the Arctic, will allow us to progress in permeable sediment research and enable us to truly make predictions about their role in global cycling.

## References

Aller, R.C. (1988) Benthic fauna and biogeochemical processes in marine sediments: the role of burrow structures. *Scope* **33**: 301-338.

Arnosti, C., Ziervogel, K., Ocampo, L., and Ghobrial, S. (2009) Enzyme activities in the water column and in shallow permeable sediments from the northeastern Gulf of Mexico. *Estuarine, Coastal and Shelf Science* **84**: 202-208.

Billerbeck, M., Werner, U., Bosselmann, K., Walpersdorf, E., and Huettel, M. (2006a) Nutrient release from an exposed intertidal sand flat. *Marine Ecology-Progress Series* **316**: 35-51.

Billerbeck, M., Werner, U., Polerecky, L., Walpersdorf, E., de Beer, D., and Huettel, M. (2006b) Surficial and deep pore water circulation governs spatial and temporal scales of nutrient recycling in intertidal sand flat sediment. *Marine Ecology-Progress Series* **326**: 61-76.

Böer, S.I., Arnosti, C., van Beusekom, J.E.E., and Boetius, A. (2009a) Temporal variations in microbial activities and carbon turnover in subtidal sandy sediments. *Biogeosciences* **6**: 1149-1165.

Böer, S.I., Hedtkamp, S.I., van Beusekom, J.E., Fuhrman, J.A., Boetius, A., and Ramette, A. (2009b) Time- and sediment depth-related variations in bacterial diversity and community structure in subtidal sands. *Isme J* **3**: 780-791.

Boudreau, B.P., Huettel, M., Forster, S., Jahnke, R.A., McLachlan, A., Middelburg, J.J. et al. (2001) Permeable marine sediments: Overturning an old paradigm. *Eos, Transactions American Geophysical Union* **82**: 133-136.

Boyer, E.W., Howarth, R.W., Galloway, J.N., Dentener, F.J., Green, P.A., and Vörösmarty, C.J. (2006) Riverine nitrogen export from the continents to the coasts. *Global Biogeochem. Cycles* **20**: GB1S91.

Burkholder, J.M., Tomasko, D.A., and Touchette, B.W. (2007) Seagrasses and eutrophication. *Journal of Experimental Marine Biology and Ecology* **350**: 46-72.

Canfield, D.E., Thamdrup, B., and Hansen, J.W. (1993a) The anaerobic degradation of organic matter in Danish coastal sediments: Iron reduction, manganese reduction, and sulfate reduction. *Geochimica et Cosmochimica Acta* **57**: 3867-3883.

Canfield, D.E., Jørgensen, B.B., Fossing, H., Glud, R., Gundersen, J., Ramsing, N.B. et al. (1993b) Pathways of organic-carbon oxidation in 3 continental-margin sediments. *Marine Geology* **113**: 27-40.

Chan, Y.J., Chong, M.F., Law, C.L., and Hassell, D.G. (2009) A review on anaerobic-aerobic treatment of industrial and municipal wastewater. *Chemical Engineering Journal* **155**: 1-18.

Chipman, L., Huettel, M., and Laschet, M. (2012) Effect of benthic-pelagic coupling on dissolved organic carbon concentrations in permeable sediments and water column in the northeastern Gulf of Mexico. *Continental Shelf Research* **45**: 116-125.

Cook, P.L.M., Wenzhofer, F., Rysgaard, S., Galaktionov, O.S., Meysman, F.J.R., Eyre, B.D. et al. (2006) Quantification of denitrification in permeable sediments: Insights

from a two-dimensional simulation analysis and experimental data. *Limnology and Oceanography-Methods* **4**: 294-307.

de Beer, D., Wenzhofer, F., Ferdelman, T.G., Boehme, S.E., Huettel, M., van Beusekom, J.E.E. et al. (2005) Transport and mineralization rates in North Sea sandy intertidal sediments, Sylt-Romo Basin, Wadden Sea. *Limnology and Oceanography* **50**: 113-127.

Deek, A., Emeis, K., and van Beusekom, J. (2012) Nitrogen removal in coastal sediments of the German Wadden Sea. *Biogeochemistry* **108**: 467-483.

Dolla, A., Fournier, M., and Dermoun, Z. (2006) Oxygen defense in sulfate-reducing bacteria. *Journal of Biotechnology* **126**: 87-100.

Duce, R.A., LaRoche, J., Altieri, K., Arrigo, K.R., Baker, A.R., Capone, D.G. et al. (2008) Impacts of Atmospheric Anthropogenic Nitrogen on the Open Ocean. *Science* **320**: 893-897.

Emery, K.O. (1968) Relict sediments on continental shelves of world. *AAPG Bulletin* **52**: 445-464.

Evrard, V., Glud, R., and Cook, P.M. (2012) The kinetics of denitrification in permeable sediments. *Biogeochemistry*: 1-10.

Freitag, T.E., Klenke, T., Krumbein, W.E., Gerdes, G., and Prosser, J.I. (2003) Effect of anoxia and high sulphide concentrations on heterotrophic microbial communities in reduced surface sediments (Black Spots) in sandy intertidal flats of the German Wadden Sea. *Fems Microbiology Ecology* **44**: 291-301.

Froelich, P.N., Klinkhammer, G.P., Bender, M.L., Luedtke, N.A., Heath, G.R., Cullen, D. et al. (1979) Early oxidation of organic matter in pelagic sediments of the eastern equatorial Atlantic: suboxic diagenesis. *Geochimica et Cosmochimica Acta* **43**: 1075-1090.

Gaidos, E., Rusch, A., and Ilardo, M. (2011) Ribosomal tag pyrosequencing of DNA and RNA from benthic coral reef microbiota: community spatial structure, rare members and nitrogen-cycling guilds. *Environmental microbiology* **13**: 1138-1152.

Galloway, J.N., Dentener, F.J., Capone, D.G., Boyer, E.W., Howarth, R.W., Seitzinger, S.P. et al. (2004) Nitrogen Cycles: Past, Present, and Future. *Biogeochemistry* **70**: 153-226.

Gao, H., Schreiber, F., Collins, G., Jensen, M.M., Kostka, J.E., Lavik, G. et al. (2010) Aerobic denitrification in permeable Wadden Sea sediments. *Isme Journal* **4**: 417-426.

Gao, H., Matyka, M., Liu, B., Khalili, A., Kostka, J.E., Collins, G. et al. (2012) Intensive and extensive nitrogen loss from intertidal permeable sediments of the Wadden Sea. *Limnology and Oceanography* **57**: 185-198.

Gihring, T.M., Humphrys, M., Mills, H.J., Huettel, M., and Kostka, J.E. (2009) Identification of phytodetritus-degrading microbial communities in sublittoral Gulf of Mexico sands. *Limnology and Oceanography* **54**: 1073.

Gittel, A., Mußmann, M., Sass, H., Cypionka, H., and Könneke, M. (2008) Identity and abundance of active sulfate-reducing bacteria in deep tidal flat sediments determined by directed cultivation and CARD-FISH analysis. *Environmental Microbiology* **10**: 2645-2658.

Glud, R.N. (2008) Oxygen dynamics of marine sediments. *Marine Biology Research* **4**: 243-289.

Gobet, A., Boer, S.I., Huse, S.M., van Beusekom, J.E.E., Quince, C., Sogin, M.L. et al. (2012) Diversity and dynamics of rare and of resident bacterial populations in coastal sands. *Isme Journal* **6**: 542-553.

Grippo, M.A., Fleeger, J.W., Rabalais, N.N., Condrey, R., and Carman, K.R. (2010) Contribution of phytoplankton and benthic microalgae to inner shelf sediments of the north-central Gulf of Mexico. *Continental Shelf Research* **30**: 456-466.

Gruber, N., and Galloway, J.N. (2008) An Earth-system perspective of the global nitrogen cycle. *Nature* **451**: 293-296.

Healy, M.G., Rodgers, M., and Mulqueen, J. (2007) Treatment of dairy wastewater using constructed wetlands and intermittent sand filters. *Bioresource Technology* **98**: 2268-2281.

Holmes, R.M., Peterson, B.J., Zhulidov, A.V., Gordeev, V.V., Makkaveev, P.N., Stunzhas, P.A. et al. (2001) Nutrient chemistry of the Ob' and Yenisey Rivers, Siberia: Results from June 2000 expedition and evaluation of long-term data sets. *Marine Chemistry* **75**: 219-227.

Huettel, M., and Gust, G. (1992) Impact of Bioroughness on Interfacial Solute Exchange in Permeable Sediments. *Marine Ecology-Progress Series* **89**: 253-267.

Huettel, M., and Rusch, A. (2000) Transport and degradation of phytoplankton in permeable sediment. *Limnology and Oceanography* **45**: 534-549.

Huettel, M., Ziebis, W., and Forster, S. (1996) Flow-Induced Uptake of Particulate Matter in Permeable Sediments. *Limnology and Oceanography* **41**: 309-322.

Huettel, M., Ziebis, W., Forster, S., and Luther lii, G.W. (1998) Advective Transport Affecting Metal and Nutrient Distributions and Interfacial Fluxes in Permeable Sediments. *Geochimica et Cosmochimica Acta* **62**: 613-631.

Huettel, M., Røy, H., Precht, E., and Ehrenhauss, S. (2003) Hydrodynamical impact on biogeochemical processes in aquatic sediments. *Hydrobiologia* **494**: 231-236.

Hunter, E.M., Mills, H.J., and Kostka, J.E. (2006) Microbial Community Diversity Associated with Carbon and Nitrogen Cycling in Permeable Shelf Sediments. *Applied and Environmental Microbiology* **72**: 5689-5701.

Hyman, J.D., Smolarkiewicz, P.K., and Winter, C.L. (2012) Heterogeneities of flow in stochastically generated porous media. *Physical Review E* **86**: 056701.

Ishii, K., Mussmann, M., MacGregor, B.J., and Amann, R. (2004) An improved fluorescence in situ hybridization protocol for the identification of bacteria and archaea in marine sediments. *Fems Microbiology Ecology* **50**: 203-212.

Jahnke, R.A., Nelson, J.R., Marinelli, R.L., and Eckman, J.E. (2000) Benthic flux of biogenic elements on the Southeastern US continental shelf: influence of pore water advective transport and benthic microalgae. *Continental Shelf Research* **20**: 109-127.

Jansen, S., Walpersdorf, E., Werner, U., Billerbeck, M., Bottcher, M.E., and de Beer, D. (2009) Functioning of intertidal flats inferred from temporal and spatial dynamics of O<sub>2</sub>, H<sub>2</sub>S and pH in their surface sediment. *Ocean Dynamics* **59**: 317-332.

Janssen, F., Faerber, P., Huettel, M., Meyer, V., and Witte, U. (2005) Pore-water advection and solute fluxes in permeable marine sediments (I): Calibration and

performance of the novel benthic chamber system Sandy. *Limnology and Oceanography* **50**: 768-778.

Jorgensen, B.B. (1977) The Sulfur Cycle of a Coastal Marine Sediment (Limfjorden, Denmark). *Limnology and Oceanography* **22**: 814-832.

Jorgensen, B.B., and Revsbech, N.P. (1989) Oxygen-Uptake, Bacterial Distribution, and Carbon-Nitrogen-Sulfur Cycling in Sediments from the Baltic Sea North-Sea Transition. *Ophelia* **31**: 29-49.

Keil, R.G., Tsamakis, E., Fuh, C.B., Giddings, J.C., and Hedges, J.I. (1994) Mineralogical and Textural Controls on the Organic Composition of Coastal Marine-Sediments - Hydrodynamic Separation Using Splitt-Fractionation. *Geochimica Et Cosmochimica Acta* **58**: 879-893.

Kristensen, E. (1988) Benthic fauna and biogeochemical processes in marine sediments: microbial activities and fluxes. *Scope* **33**: 275-299.

Kristian Stevik, T., Aa, K., Ausland, G., and Fredrik Hanssen, J. (2004) Retention and removal of pathogenic bacteria in wastewater percolating through porous media: a review. *Water Research* **38**: 1355-1367.

Li, M.Z., and Amos, C.L. (1999) Field observations of bedforms and sediment transport thresholds of fine sand under combined waves and currents. *Marine Geology* **158**: 147-160.

Lohse, L., Malschaert, J.F.P., Slomp, C.P., Helder, W., and van Raaphorst, W. (1993) Nitrogen cycling in North Sea sediments: interaction of denitrification and nitrification in offshore and coastal areas. *Marine Ecology-Progress Series* **101**: 283-283.

Lotze, H., Reise, K., Worm, B., van Beusekom, J., Busch, M., Ehlers, A. et al. (2005) Human transformations of the Wadden Sea ecosystem through time: a synthesis. *Helgoland Marine Research* **59**: 84-95.

Macdonald, R.W., Solomon, S.M., Cranston, R.E., Welch, H.E., Yunker, M.B., and Gobeil, C. (1998) A sediment and organic carbon budget for the Canadian beaufort shelf. *Marine Geology* **144**: 255-273.

Matyka, M., Khalili, A., and Koza, Z. (2008) Tortuosity-porosity relation in porous media flow. *Physical Review E* **78**: 026306.

Meysman, F.J.R., Galaktionov, O.S., Cook, P.L.M., Janssen, F., Huettel, M., and Middelburg, J.J. (2007) Quantifying biologically and physically induced flow and tracer dynamics in permeable sediments. *Biogeosciences* **4**: 627-646.

Mills, H.J., Hunter, E., Humphrys, M., Kerkhof, L., McGuinness, L., Huettel, M., and Kostka, J.E. (2008) Characterization of nitrifying, denitrifying, and overall bacterial communities in permeable marine sediments of the northeastern Gulf of Mexico. *Applied and Environmental Microbiology* **74**: 4440-4453.

Misic, C., and Harriague, A.C. (2007) Enzymatic activity and organic substrates on a sandy beach of the Ligurian Sea (NW Mediterranean) influenced by anthropogenic pressure. *Aquatic Microbial Ecology* **47**: 239-251.

Musat, N., Werner, U., Knittel, K., Kolb, S., Dodenhof, T., van Beusekom, J.E.E. et al. (2006) Microbial community structure of sandy intertidal sediments in the North Sea, Sylt-Romo Basin, Wadden Sea. *Systematic and Applied Microbiology* **29**: 333-348.

Mussmann, M., Ishii, K., Rabus, R., and Amann, R. (2005) Diversity and vertical distribution of cultured and uncultured Deltaproteobacteria in an intertidal mud flat of the Wadden Sea. *Environmental Microbiology* **7**: 405-418.

Pelegri, S.P., Nielsen, L.P., and Blackburn, T.H. (1994) Denitrification in Estuarine Sediment Stimulated by the Irrigation Activity of the Amphipod *Corophium-Volutator*. *Marine Ecology-Progress Series* **105**: 285-290.

Precht, E., Franke, U., Polerecky, L., and Huettel, M. (2004) Oxygen Dynamics in Permeable Sediments with Wave-Driven Pore Water Exchange. *Limnology and Oceanography* **49**: 693-705.

Puempel, T., Macaskie, L.E., Finlay, J.A., Diels, L., and Tsezos, M. (2003) Nickel removal from nickel plating waste water using a biologically active moving-bed sand filter. *Biometals* **16**: 567-581.

Rao, A.M.F., McCarthy, M.J., Gardner, W.S., and Jahnke, R.A. (2008) Respiration and denitrification in permeable continental shelf deposits on the South Atlantic Bight: N<sub>2</sub>: Ar and isotope pairing measurements in sediment column experiments. *Continental Shelf Research* **28**: 602-613.

Rusch, A., Hannides, A.K., and Gaidos, E. (2009) Diverse communities of active Bacteria and Archaea along oxygen gradients in coral reef sediments. *Coral Reefs* **28**: 15-26.

Rusch, A., Huettel, M., Reimers, C.E., Taghon, G.L., and Fuller, C.M. (2003) Activity and distribution of bacterial populations in Middle Atlantic Bight shelf sands. *Fems Microbiology Ecology* **44**: 89-100.

Rutherford, J.C., Latimer, G.J., and Smith, R.K. (1993) Bedform mobility and benthic oxygen uptake. *Water Research* **27**: 1545-1558.

Santos, I.R., Eyre, B.D., and Huettel, M. (2012) The driving forces of porewater and groundwater flow in permeable coastal sediments: A review. *Estuarine, Coastal and Shelf Science* **98**: 1-15.

Santos, I.R., Glud, R.N., Maher, D., Eler, D., and Eyre, B.D. (2011) Diel coral reef acidification driven by porewater advection in permeable carbonate sands, Heron Island, Great Barrier Reef. *Geophysical Research Letters* **38**: L03604.

Scala, D.J., and Kerkhof, L.J. (1999) Diversity of nitrous oxide reductase (nosZ) genes in continental shelf sediments. *Applied and Environmental Microbiology* **65**: 1681-1687.

Scala, D.J., and Kerkhof, L.J. (2000) Horizontal Heterogeneity of Denitrifying Bacterial Communities in Marine Sediments by Terminal Restriction Fragment Length Polymorphism Analysis. *Applied and Environmental Microbiology* **66**: 1980-1986.

Shum, K.T., and Sundby, B. (1996) Organic matter processing in continental shelf sediments - The subtidal pump revisited. *Marine Chemistry* **53**: 81-87.

Sorensen, J., and Jørgensen, B.B. (1987) Early diagenesis in sediments from Danish coastal waters: Microbial activity and Mn-Fe-S geochemistry. *Geochimica et Cosmochimica Acta* **51**: 1583-1590.

Sorensen, J., Jørgensen, B.B., and Revsbech, N.P. (1979) Comparison of oxygen, nitrate, and sulfate respiration in coastal marine sediments. *Microbial Ecology* **5**: 105-115.



Thamdrup, B., Fossing, H., and Jørgensen, B.B. (1994) Manganese, iron, and sulfur cycling in a coastal marine sediment, Aarhus bay, Denmark. *Geochimica Et Cosmochimica Acta* **58**: 5115-5129.

Thibodeaux, L.J., and Boyle, J.D. (1987) Bedform-Generated Convective-Transport in Bottom Sediment. *Nature* **325**: 341-343.

van Beusekom, J.E.E. (2005) A historic perspective on Wadden Sea eutrophication. *Helgoland Marine Research* **59**: 45-54.

Volkenborn, N., Polerecky, L., Wethey, D.S., and Woodin, S.A. (2010) Oscillatory porewater bioadvection in marine sediments induced by hydraulic activities of *Arenicola marina*. *Limnology and Oceanography* **55**: 1231-1247.

Wassmann, P., Duarte, C.M., Agustí, S., and Sejr, M.K. (2011) Footprints of climate change in the Arctic marine ecosystem. *Global Change Biology* **17**: 1235-1249.

Webb, J.E., and Theodor, J. (1968) Irrigation of Submerged Marine Sands through Wave Action. *Nature* **220**: 682-&.

Werner, U., Billerbeck, M., Polerecky, L., Franke, U., Huettel, M., van Beusekom, J.E.E., and de Beer, D. (2006) Spatial and temporal patterns of mineralization rates and oxygen distribution in a permeable intertidal sand flat (Sylt, Germany). *Limnology and Oceanography* **51**: 2549-2563.

Wieringa, E.B.A., Overmann, J., and Cypionka, H. (2000) Detection of abundant sulphate-reducing bacteria in marine oxic sediment layers by a combined cultivation and molecular approach. *Environmental Microbiology* **2**: 417-427.

Yao, S., Ni, J.R., Chen, Q., and Borthwick, A.G.L. (2012) Enrichment and characterization of a bacteria consortium capable of heterotrophic nitrification and aerobic denitrification at low temperature. *Bioresource Technology* **127**: 151-157.

Zetsche, E., Bulling, M.T., and Witte, U. (2012) Permeability of intertidal sandflats: Impact of temporal variability on sediment metabolism. *Continental Shelf Research* **42**: 41-50.



## Chapter IX

### Outlook

#### ***1. Open questions and further research topics***

The work contained in this thesis offers insights into biogeochemical cycling of nitrogen in permeable sediments on temporal and spatial scales. Nevertheless, these results comprise snap-shot studies of a few locations during only a few different seasons. Therefore, this only provides the first step towards a complete understanding of the factors controlling microbial activity and biogeochemical cycling in permeable sediments. This final section, aims to suggest directions for future work, and ways in which we can accomplish a greater understanding of the impact of permeable sediments on global nitrogen cycling.

##### 1.1 Identifying changes within the microbial community during aerobic denitrification

In Chapter V, we showed that aerobic denitrification could be stimulated by rapid changes in oxygen concentrations within the sediment or inhibited by long-term anoxia. However, the members and processes within the sediment which contribute to aerobic denitrification are still somewhat unclear. Molecular work might allow us to further quantify whether aerobic denitrification is indeed the rule, rather than the exception in environments within fluctuating oxygen conditions (Lloyd et al., 1987). Additionally, this will show us why the ability to denitrify aerobically is lost during long term anoxia. For example, composition profiles of denitrifying community in longer term experiments could identify whether oscillations in oxygen select for a community which can denitrify aerobically. If a community change does not occur, but rather, denitrifiers have lost the ability to aerobically denitrify, then community composition data may be of little use. Therefore investigation of the enzymes associated with aerobic denitrification might be more illuminating. mRNA studies during stimulation of aerobic denitrification could

allow us to identify candidates for these enzymes. Furthermore, they may reveal whether denitrifying enzymes really are expressed constitutively in response to rapid oxygen fluctuations (Chen and Strous, 2013).

### 1.2 Solving the nitrification mystery

The results presented in this thesis reveal high but variable nitrification rates in the sub-tidal (Chapter IV) and constantly low rates in the intertidal. This simplification hides a greater anomaly, namely that ammonium consumption budgets in the subtidal were close to balanced, while in the intertidal there was a huge discrepancy between ammonium added (which was rapidly consumed), and the ammonium which could be traced back in any other N-pool ( $^{15}\text{NO}_2^- + ^{15}\text{NO}_3^- + ^{15}\text{N}_2\text{O} + ^{15}\text{N}_2$  recovered < 5 % added  $^{15}\text{NH}_4^+$ ). Understanding the fate of ammonium in the intertidal has the potential to provide us with valuable insights into how and why intertidal sediments differ from subtidal sediments, and, thus, improve our ability to predict rates and activity in permeable sediments.

### 1.3 A greater understanding of the role of eukaryotes

Eukaryotes were shown to play a central role in nitrogen cycling and N-loss in intertidal sand flats in Chapter III. Nevertheless, while we and previous authors have shown that intracellular nitrate storage is substantial in these sediments, we have only cursorily investigated the organisms which may have been responsible. We identified high abundances of diatoms within the sediments from the Janssand sand flat and also found benthic foraminifera, furthermore large numbers of nematodes were observed within the sediment. Both foraminifera and diatoms are known to store and respire nitrate, and nematodes have been shown to harbour bacterial epibionts and endosymbionts that carry out anaerobic metabolisms (Kleiner et al., 2012). In future studies, it would be of great interest to identify which members of the meiofauna

community might be mediating N-cycling and whether they are directly responsible or have an associated bacterial community which respire N.

#### 1.4 Transforming volumetric rate measurements of N-cycling processes into areal estimates

In this thesis and other studies on permeable sediments, areal rates of N-processes were estimated by integrating volumetric rates obtained from percolation or slurry experiments to the *in situ* penetration depth of NO<sub>x</sub>. Strikingly similar rates are obtained whether using the core method of Chapter III and VII, slurry incubations or traditional percolated cores. Likewise, oxygen consumption rates measured *in situ* using microsensors are very close to those reported in this thesis. Debate still exists, however, as to the suitability of these incubations for determining areal rates and how to define penetration depths.

Determining the penetration depth of any solute within permeable sediments is difficult, especially as this depth will differ dependent on the part of a ripple measured. Direct measurements of penetration depth are often problematic; use of the *in situ* microsensor profiler requires a large casing chamber to be placed in close proximity to the sediment, which is likely to change flow patterns. Furthermore repeated microsensor measurements in the same spot might also cause channeling of flow within the sediment. Porewater profiles of sediment cores also have their own limitations, coring must be done extremely carefully, otherwise the permeable nature of the sediment could lead to rapid porewater redistribution, furthermore, due to the rapid rates of turnover within permeable sediments, samples must be taken immediately upon coring.

Beyond sampling issues, estimations of *in situ* areal rates from experimental rate determinations is not straightforward. In Chapter IV, we made a step towards more precise areal rate estimates by defining “effective mean mixing depths” or average solute penetration, using the model of Elliot and Brooks (1997). We combined these depths with both aerobic and anaerobic rates of N-cycling and eventually came to areal

rates which were similar to those from the Wadden Sea, and realistic for the German Bight. However, we still had difficulties simulating realistic  $O_2$  and  $NO_3^-$  penetration depths with the Elliot and Brooks model, possibly as it fails to take ripple migration into account, if this problem can be solved, the next step will be to integrate the apparent kinetics of oxygen consumption, nitrification and denitrification into later models.

Finally, we need to compare the output of all these methods for transforming volumetric rates into areal rates. The more advanced methods provide more precision, but come with the need for a greater investment in sampling effort to determine kinetics, rates and *in situ* measurements of bottom velocity and ripple sizes. However, the simpler method needs far fewer *in situ* measurements and sometimes may be the only option available. Therefore knowing the error involved in the simpler areal rate estimation will be helpful within future work.

### 1.5 Benthic N-fixation in permeable sediments

Benthic N-fixation is mainly associated with macrophytes and vegetated sediments such as salt marshes, coral reefs, seagrass and mangroves (Patriqui and Knowles, 1972; Wiebe et al., 1975; Zuberer and Silver, 1978; Wilkinson and Fay, 1979). However N-fixation also occurs in sediments within microbial mat communities and the sediment itself. In well lit areas (e.g. shallow coastal lagoons and intertidal flats), thick cyanobacterial mats can form on the sediment surface and can fix nitrogen at high rates (Stal et al., 1984). These mats and marine sediments themselves often harbour many other bacteria capable of  $N_2$  fixation (Zehr et al., 1995), such as sulfate reducers (Zehr et al., 1995; Bertics and Ziebis, 2010), methanotrophs and facultative anaerobes (Coyer et al., 1996) and it has been hypothesized that these play an important role in providing N to benthic communities (Herbert, 1999). Supporting this, there is now growing evidence that N-fixation may play an ecological role in deep sea and sub-seafloor sediments (D'Hondt et al., 2004; Dekas et al., 2009)

The extent of benthic N-fixation remains relatively understudied in all benthic sediments, and entirely neglected in permeable sediments. To date, it appears that benthic N-fixation is controlled by a complex interplay of oxygen, dissolved inorganic nitrogen and organic carbon (Fulweiler et al., 2007; Rao and Charette, 2012). Most permeable sediments are replete with fixed N and organic carbon as it is supplied advectively from the water column, and eutrophied permeable sediments are therefore unlikely sites of N-fixation. However, permeable sediments which exist in oligotrophic regions, where nitrate is extremely low, but organic matter is filtered and concentrated from the water column, could be ideal places to investigate heterotrophic N-fixation.

#### 1.6 Coupling the benthic to the pelagic

The role of permeable sediments as “natural bioreactors”, which promote denitrification and the decomposition of material from the overlying water column is now well accepted (Chapter VIII), and coupling of pelagic events such as blooms to enhanced cycling within the sediment is apparent (Chapter III). Less well investigated is the effect of benthic processes on water column processes. Arnosti et al. (2009) provided an intriguing insight into benthic-pelagic coupling by showing that the activity of extracellular enzymes had a broader spectrum and more rapid rates of hydrolysis in the water column above sandy sediments compared to fine grained diffusive sediments. The source of these enzymes appeared to be the sediment itself; advective porewater flow had transported them to the water column. As these enzymes initiate microbial solubilization of high molecular weight organic matter, water column microbial communities may have access to high molecular weight substrates that would be unavailable otherwise. This could lead to more rapid and efficient organic matter processing in the water column. So far pelagic enzymatic studies have been restricted to a few sites; in future studying the influence of the benthic on the pelagic in the form of extracellular enzymes and DOC should allow us to more fully assess the impact of sandy permeable sediments.

### 1.7 Visualization of sediment processes

Methodology improvements have been of vast importance in research into permeable sediments and some of those methods which have had the greatest impact have been those which allow us to visualize processes within the sediment such as porewater transport (Huettel and Gust, 1992). Since then, percolation methods, flume studies and new *in situ* lander technology have enhanced our quantification and understanding of rates and processes within permeable sediments.

Gaps still exist in our knowledge of how microbial activity functions at the microscale within these sediments. Visualization methods are therefore required to give us more information about community structure and microscale solute distribution within undisturbed sediments. Possible methods could include techniques such as resin-fixation/cell staining (Fig. 1), correlative imaging and planar optodes. These will improve our understanding of microniches, diffusive boundaries, organic matter hotspots and redox cycling of manganese and iron particles within sediment as it is reworked and subject to advective flows.



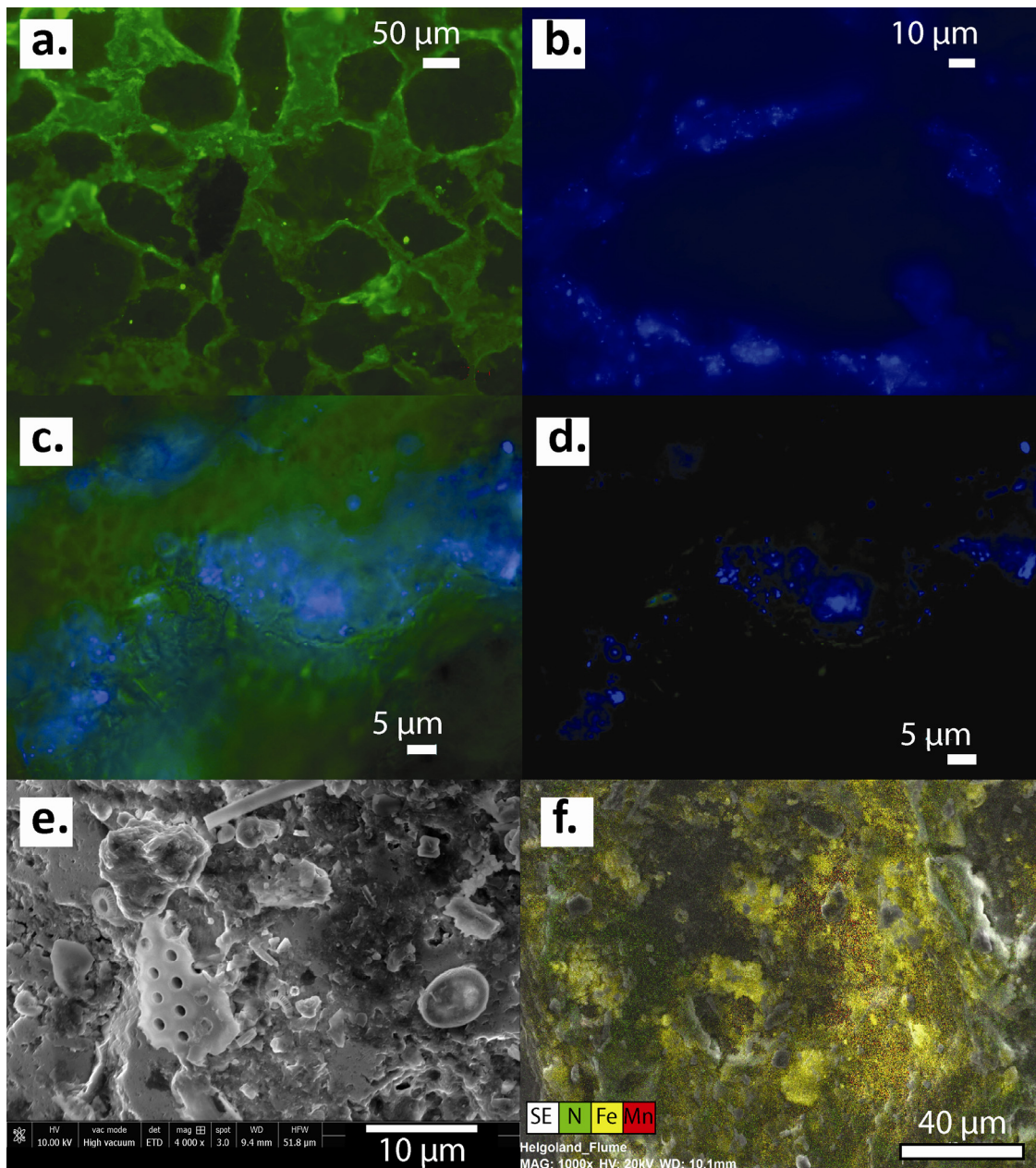


Fig. 1. Different visualization methods of microbial sediment communities a) resin fixed sediment stained with sybrgreen b-d) DAPI staining of resin fixed sediment, c and d are the same sample and show the topography of the sand grain and the stained community respectively. Due to the 3D nature of the sample DAPI stains often look blurry due to the high abundance of microbes stacked on top of each other, therefore confocal imaging is needed e) SEM imaging of a single sand grain, SEM imaging offers advantages in that high magnification can be achieved f) SEM + EDX applied to a different sand grain, this method allows identification of microenvironments such as iron oxide layers (SEM + EDX images courtesy of Jasmine Berg and Sten Littman).

## ***2. Illuminating the factors controlling biogeochemical cycling in permeable sediments***

This section of the outlook briefly introduces and discusses hypotheses regarding biogeochemical cycling in permeable sediments, these have been developed during the work carried out in this thesis and provide a platform for future research. While these hypotheses may not have a simple answer, research into these topics will inform our understanding of the global role of permeable sediments.

### *Hypothesis one: The magnitude of flow has an effect on rates*

Advective porewater flow, caused by bottom water currents, tides or wave pumping is the main driver which distinguishes permeable sediments from fine grained diffusive sediments. However, flow is not always the same, faster bottom water currents for example would enhance the velocity of porewater flow. Does this affect N-cycling and remineralization within permeable sediments and if so are the relationships between flow velocity and rates definable? Answering this question will not only help us understand permeable sediments, but help in the design and interpretation of percolation experiments.

### *Hypothesis two: There is a relationship between grain size and rates*

Grain size effects permeability and therefore also the magnitude of flow within the sediment as well the capacity of the sediment to filter organic matter. Furthermore, as sand grains are the medium to which benthic microorganisms are attached, grain size also determines the surface available for microbes to colonize. Therefore grain size could have multiple effects on rates biogeochemical cycling within sediments ranging from changes in surface area to changes in the availability of organic matter.

### *Hypothesis three: All permeable sediments have the capacity for high rates of biogeochemical cycling, but are ultimately controlled by the type organic matter input*

Permeable sediments filter seawater, not just for organic matter, but theoretically also for microorganisms. Therefore, the water column and all the diversity

contained within it acts as a seedbank for the microbial community in permeable sediments. Hence, the microbial sediment community should be able to adapt over relatively short time scales to exploit the conditions they are exposed to, such as changes in organic matter supply. In Chapter IV we reported the strong correlation between apparent labile organic matter input (measured as oxygen consumption rates) and denitrification within diverse permeable sediments. Many different factors can control organic matter input, including, but not limited to, sediment permeability and the magnitude and type of pelagic primary productivity (e.g. a seagrass versus a phytoplankton dominated system). Furthermore, organic matter inputs can change due to short term events such as storms, on longer seasonal cycles and with growing or lessening eutrophication. By examining the relationships between organic matter inputs and biogeochemical cycling, we will start to be able to predict how different permeable sediments function as biocatalytic filters under different environmental conditions.

## References

- Arnosti, C., Ziervogel, K., Ocampo, L., and Ghobrial, S. (2009) Enzyme activities in the water column and in shallow permeable sediments from the northeastern Gulf of Mexico. *Estuarine, Coastal and Shelf Science* **84**: 202-208.
- Bertics, V.J., and Ziebis, W. (2010) Bioturbation and the role of microniches for sulfate reduction in coastal marine sediments. *Environmental Microbiology* **12**: 3022-3034.
- Chen, J.W., and Strous, M. (2013) Denitrification and aerobic respiration, hybrid electron transport chains and co-evolution. *Biochimica Et Biophysica Acta-Bioenergetics* **1827**: 136-144.
- Coyer, J.A., CabelloPasini, A., Swift, H., and Alberte, R.S. (1996) N<sub>2</sub> fixation in marine heterotrophic bacteria: Dynamics of environmental and molecular regulation. *Proceedings of the National Academy of Sciences of the United States of America* **93**: 3575-3580.
- D'Hondt, S., Jørgensen, B.B., Miller, D.J., Batzke, A., Blake, R., Cragg, B.A. et al. (2004) Distributions of microbial activities in deep subseafloor sediments. *Science* **306**: 2216-2221.
- Dekas, A.E., Poretsky, R.S., and Orphan, V.J. (2009) Deep-Sea Archaea Fix and Share Nitrogen in Methane-Consuming Microbial Consortia. *Science* **326**: 422-426.
- Elliott, A.H., and Brooks, N.H. (1997) Transfer of nonsorbing solutes to a streambed with bed forms; Theory. *Water Resources Research* **33**: 123-136.

Fulweiler, R.W., Nixon, S.W., Buckley, B.A., and Granger, S.L. (2007) Reversal of the net dinitrogen gas flux in coastal marine sediments. *Nature* **448**: 180-182.

Herbert, R.A. (1999) Nitrogen cycling in coastal marine ecosystems. *Fems Microbiology Reviews* **23**: 563-590.

Huettel, M., and Gust, G. (1992) Impact of bioroughness on interfacial solute exchange in permeable sediments. *Marine Ecology Progress Series* **89**: 253-267.

Kleiner, M., Wentrup, C., Lott, C., Teeling, H., Wetzel, S., Young, J. et al. (2012) Metaproteomics of a gutless marine worm and its symbiotic microbial community reveal unusual pathways for carbon and energy use. *Proceedings of the National Academy of Sciences* **109**: 1173-1182.

Lloyd, D., Boddy, L., and Davies, K.J.P. (1987) Persistence of bacterial denitrification capacity under aerobic condition - the rule rather than the exception. *Fems Microbiology Ecology* **45**: 185-190.

Patriqui, D., and Knowles, R. (1972) Nitrogen fixation in rhizosphere of marine angiosperms. *Marine Biology* **16**: 49-8.

Rao, A.M.F., and Charette, M.A. (2012) Benthic Nitrogen Fixation in an Eutrophic Estuary Affected by Groundwater Discharge. *Journal of Coastal Research* **28**: 477-485.

Stal, L.J., Grossberger, S., and Krumbein, W.E. (1984) Nitrogen-fixation associated with the cyanobacterial mat of a marine laminated microbial ecosystem. *Marine Biology* **82**: 217-224.

Wiebe, W.J., Johannes, R.E., and Webb, K.L. (1975) Nitrogen fixation in a coral reef community. *Science* **188**: 257-259.

Wilkinson, C.R., and Fay, P. (1979) Nitrogen fixation in coral reef sponges with symbiotic cyanobacteria. *Nature* **279**: 527-529.

Zehr, J.P., Mellon, M., Braun, S., Litaker, W., Steppe, T., and Paerl, H.W. (1995) Diversity of heterotrophic nitrogen fixation genes in a marine cyanobacterial mat. *Applied and Environmental Microbiology* **61**: 2527-2532.

Zuberer, D.A., and Silver, W.S. (1978) Biological dinitrogen fixation (acetylene-reduction) associated with Florida mangroves. *Applied and Environmental Microbiology* **35**: 567-575.

## List of Publications

### Manuscript 1.

Anammox, denitrification and dissimilatory nitrate reduction to ammonium in the East China Sea sediment (*published*)

G. D. Song, S. M. Liu, H. K. Marchant, M. M. M. Kuypers, G. Lavik

### Manuscript 2.

The fate of nitrate in intertidal permeable sediments (*submitted*)

Hannah K. Marchant, Gaute Lavik, Moritz Holtappels, Marcel M.M. Kuypers

### Manuscript 3.

N-loss due to coupled nitrification-denitrification in subtidal permeable sediments (*in preparation*)

Hannah K. Marchant, Moritz Holtappels, Gaute Lavik, Christian Winter, Marcel M.M. Kuypers

### Manuscript 4.

Stimulation and inhibition of aerobic denitrification in intertidal permeable sediments (*in preparation*)

Hannah K. Marchant, Moritz Holtappels, Soeren Ahmerkamp, Gaute Lavik, Marcel M.M. Kuypers

### Manuscript 5.

High nitrous oxide emissions from eutrophied coastal sands (*in revision*)

Hannah K. Marchant, Moritz Holtappels, Gaute Lavik, Frank Schreiber, Regina Vahrenhorst, Marc Strous, Marcel M.M. Kuypers, Halina E. Tegetmeyer

### Manuscript 6.

The impact of ocean acidification on nitrogen cycling in coastal permeable sediments (*in preparation*)

Hannah K. Marchant, Tim Ferdelman, Gaute Lavik and Marcel M.M. Kuypers

### Manuscript 7.

Going with the flow: Why we cannot neglect the importance of the coastal sand filter in the anthropocene (*in preparation*)

Hannah K. Marchant, Moritz Holtappels and Marcel M.M. Kuypers

## Acknowledgements

What can I say? Firstly, I would like to thank Marcel Kuypers who accepted me as a student, introduced me to the wonderful and at times confusing world of sandy sediments and gave me the freedom to follow my research interests. You have always been available to listen to my worries, discuss science and push me in the direction I needed to go. Without your support, advice and feedback I doubt I would have made it to the end!

Gaute, for your endless patience with my endless questions about data analysis and your skills at keeping the mass spec running through her twilight years (I will restrain myself from writing a small soliloquy to that machine), and also for not questioning some of the questionable set-ups I attached to the MIMS. I am grateful for all your support.

I would also like to thank the whole of the Janssand team, Ole, Theresa, Halina, Ugo, Christy, Anna, Ingrid and everyone else. Our times traveling to the sand flat, working on the sand flat and hanging out on the sand flat were brilliant, and I would happily do it all again, even with the snow and the rain and the dubious “sampling platform”.

To all of the technicians within the Biogeochemistry department, Gabi, Kirsten, Swantje, Daniela, I could not have done this without you, your patience, help and support has been everything I could have wanted. Also, to Sarah, whose help in preparing and analyzing the excessive amount of samples I took was instrumental in me managing to finish somewhat on time...

To the rest of the Biogeochemistry group, I have loved working with you, spending time with you inside and outside the institute and hope we will continue to have many adventures in future. Especially to Tim and Moritz, whose critical reading of my thesis has vastly improved it and gave me the confidence to put the finishing touches to it.

To Ulrike and Ralf, I am indebted to you for your help administrating and organizing my life. The time, stress and panic you have saved me from is incalculable.

Christian, for looking after me on my first real cruise and making sure I was in the right place at the right time... it was fantastic, I am also eternally grateful that you agreed to review my thesis at such short notice.

Obviously I must also thank Corner Office Team, Jessika, Andi, Abdul, Liz, how could I have made it without the laughter, the advice, the ranting and the comfort of such wonderful people?

I also have to thank my friends in Bremen who have not already been mentioned, Tim, Stefan, Judith, Mari, Petra, Renzo and all of those I am sure I have forgotten, you are what makes life good regardless of how work is going. Especially to Morten... where would I be without you?

To Colin Munn, all of this started with you! Your encouragement during my Bachelors and in my application for a Masters was instrumental in giving me the confidence to pursue a career in science. I can never thank you enough for everything you did for me.

And finally, to my family, who supported me unconditionally throughout, forgave me my long absences from home and who have always been there for me

Name: Hannah Marchant..... Datum: 11 Dec 2013.....

Anschrift : Hemmstr, 119, 28215, Bremen.....

## **Erklärung**

Hiermit versichere ich, dass ich

1. die Arbeit ohne unerlaubte fremde Hilfe angefertigt habe,
2. keine anderen als die von mir angegebenen Quellen und Hilfsmittel benutzt habe und
3. die den benutzten Werken wörtlich oder inhaltlich entnommenen Stellen als solche kenntlich gemacht habe.

Bremen, den 11 Dec 2013

-----

(Unterschrift)



**Bremen, 2014**